University of Bath

PHD

Process Intensification of Biofuel Production from Microalgae Applying Magnetic Nanoparticles
(Alternative Format Thesis)

Egesa, Dan

Award date:
2019

Awarding institution:
University of Bath

Link to publication

Alternative formats
If you require this document in an alternative format, please contact:
openaccess@bath.ac.uk

Copyright of this thesis rests with the author. Access is subject to the above licence, if given. If no licence is specified above, original content in this thesis is licensed under the terms of the Creative Commons Attribution-NonCommercial 4.0 International (CC BY-NC-ND 4.0) Licence (https://creativecommons.org/licenses/by-nc-nd/4.0/). Any third-party copyright material present remains the property of its respective owner(s) and is licensed under its existing terms.

Take down policy
If you consider content within Bath's Research Portal to be in breach of UK law, please contact: openaccess@bath.ac.uk with the details. Your claim will be investigated and, where appropriate, the item will be removed from public view as soon as possible.

Download date: 05. May. 2023

Citation for published version:
Egesa, D 2019, 'Process Intensification of Biofuel Production from Microalgae Applying Magnetic Nanoparticles'.

Publication date:
2019

Link to publication

University of Bath

Alternative formats
If you require this document in an alternative format, please contact:
openaccess@bath.ac.uk

General rights
Copyright and moral rights for the publications made accessible in the public portal are retained by the authors and/or other copyright owners and it is a condition of accessing publications that users recognise and abide by the legal requirements associated with these rights.

Take down policy
If you believe that this document breaches copyright please contact us providing details, and we will remove access to the work immediately and investigate your claim.

Download date: 05. Jan. 2021

Process Intensification of Biofuel Production from Microalgae Applying Magnetic Nanoparticles

Dan Egesa

A Thesis Submitted for the Degree of Doctor of Philosophy

University of Bath

Department of Chemical Engineering

May 2019

COPYRIGHT

Attention is drawn to the fact that copyright of this thesis rests with the author. A copy of this thesis/portfolio has been supplied on condition that anyone who consults it understands that they must not copy it or use material from it except as permitted by law or with the consent of the author.

This thesis/portfolio may be made available for consultation within the university library and may be photocopied or lent to other libraries for purposes of consultation with effect from……

Signed on behalf of the department of chemical engineering……..

Acknowledgement

First, I thank GOD for the gift of life, good health and all HIS divine providence without which nothing would be possible.

Secondly, I thank my supervisor Pawel Plucinski for his wise guidance and availability throughout my PhD study. I also thank my second supervisor Christopher J Chuck for the great support and wise guidance he gave me. Furthermore, I thank the technical team for all their support in teaching me the use of different equipment.

Thirdly, I thank the commonwealth scholarship commission for the full funding for my tuition and stipend that I would never have afforded.

Finally, thank my family and friends for their support, encouragement and patience in challenging times.

Abstract

Microalgae are a promising 3rd generation feedstock for biofuel production. However, their harvesting according to literature is uneconomical contributing up to 25% of the total cost of biofuel processing. In addition, the drying and solvent extraction step is energy intensive. Therefore, this research aimed at overcoming these challenges through the application of magnetic nanoparticles (MNPs) for algal separation, catalytic hydrothermal liquefaction and in ionic liquid (IL) lysis of magnetically separated microalgae. The MNPs were synthesized by co-precipitation and used to separate microalgae from culture medium at a separation efficiency of over 95%. The microalgae/MNPs slurry was subjected to HTL and IL treatment in separate experiments. In the HTL process, the microalgae/particle slurry was converted to biocrude oil and a biocrude yield of 37.1 wt.% was achieved in presence of MNPs while microalgae only yielded 23.2%. The percentage areas in the GC-MS chromatogram corresponding to hydrocarbons (HCs) in Zn-ferrite catalysed and uncatalysed biocrude were 46.5% and 19.9% respectively. Heteroatom compounds in the biocrude oil reduced substantially when liquefaction was done in the presence of Zn/Mg ferrites. The MNPs were recovered from solid residue by sonication and recycled. To further reduce N and O content of biocrude, the effect of HTL conditions on yield and biocrude composition was also investigated. HTL under 5 wt.% sulphuric acid reduced the nitrogen content of biocrude by 83 wt.%. In addition, increasing liquefaction time led to a gradual reduction in the N, O and S content of the biocrude. Moreover, HTL under 30 bar hydrogen atmospheres resulted in increased biocrude yield compared to HTL in absence of hydrogen.

ILs were also used for lysis of magnetically separated microalgae to efficiently extract lipids. GC-MS, FT-IR and ^{1}H NMR analyse was done on the extracted lipids. The MNPs were recovered from algal residue by sonication in DI water. TGA analysis of recovered MNPs confirmed absence of algal biomass on the MNPs. These were then recycled to harvest more microalgae at a separation efficiency of 96%. The ILs were also recycled and ^{1}HNMR, mass spectrometry and FT-IR analysis confirmed absence of structural alterations in the recycled IL. Finally, the effect of process conditions on yield of extracted lipids was also investigated. Application of MNPs in magnetic separation of microalgae,

catalytic HTL and IL extraction will potentially reduce the processing cost of biofuels from microalgae. This would result in biofuels being more competitive with petroleum-derived fuels.

Disseminations

Peer Reviewed Journal Articles

Egesa, D., Chuck, C.J. and Plucinski, P., 2017. Multifunctional Role of Magnetic Nanoparticles in Efficient Microalgae Separation and Catalytic Hydrothermal Liquefaction. *ACS Sustainable Chemistry & Engineering*, *6*(1), pp.991-999. This publication is presented as Chapter 3.

Draft manuscripts in Process

Egesa, D and Plucinski, P., A review of microalgae processing for biofuel production. This manuscript is presented as Chapter 2.

Egesa, D., Christopher J Chuck and Plucinski, P., Effect of processing conditions on biocrude oil yield and composition. This manuscript is presented as Chapter 4.

Egesa, D., Christopher J Chuck and Plucinski, P., 2019. Efficient extraction of lipids from magnetically separated microalgae using ionic liquids. To be submitted in the *ACS Sustainable Chemistry & Engineering Journal*. This manuscript is presented as Chapter 5.

Conferences

Egesa, D., and Plucinski, 13-16 May 2018., Multifunctional Role of Magnetic Nanoparticles in Efficient Micro-microalgae Separation and Catalytic Hydrothermal Liquefaction of Microalgae., Presented at the third Green and Sustainable Chemistry Conference in Berlin German. Organised by Elsevier.

Work accepted at these conferences:

Egesa, D., and Plucinski., 11-13th June 2018., Multifunctional Role of Magnetic Nanoparticles in Efficient Micro-microalgae Separation and Catalytic Hydrothermal Liquefaction of Microalgae., 8th International Conference on Algal Biomass, Biofuels and Bio-products., at Seattle Washington U.S.A.

Egesa, D., and Plucinski. December 03-05 2018. Multifunctional Role of Magnetic Nanoparticles in Efficient microalgae Separation and Catalytic Hydrothermal

Liquefaction of Microalgae. Was invited to present as a featured speaker at the 5th Global Nanotechnology Congress and Expo at Valencia, Spain.

Table of Contents

List of figures

Note: Figures starting with S. are in the supporting information of the published paper

List of tables

Note: Tables starting with S. are in the supporting information of the published paper or manuscript.

List of abbreviations

MNPs	Magnetic nanoparticles
SE	Separation efficiency
DI	Deionized water
HTL	Hydrothermal liquefaction
NP	Nanoparticles
ILs	Ionic liquid
FTIR	Fourier-transform infrared spectroscopy
GC-MS	Gas chromatography – mass spectrometry
XRD	X ray diffraction
UV-vis	Ultraviolet visible spectroscopy
HHV	Higher heating value
ER	Energy recovery
SEM	Scanning electron microscopy
TEM	Transmission electron microscopy
TGA	Thermo-gravimetric analysis
ζ	Zeta-potential
FAME	Fatty acid methyl ester
PBH	Photobioreactor
VTB	Vertical tubular reactor
HoTR	Horizontal tubular reactor
HeTR	Helical tubular reactor

Nomenclature

		Units
m	Mass microalgae and magnetic nanoparticles	g
D	Nanoparticle size	nm
ζ	Zeta potential of nanoparticles and microalgae	mV
HHV	High heating value of bio-crude oil	$MJ.kg^{-1}$
Y	Bio-crude yield	wt.%
c	Elemental composition of bio-crude oil	wt.%
T	Reaction temperature	T
P	Pressure of hydrogen and nitrogen in the reactor	bar
t	Separation time and holding time	min

1. Introduction

The background and context of the thesis is given, the structure of the thesis is described, and the aim and objectives of the thesis are given.

1. Introduction

1.1. Context

The ever-increasing global energy demand has encouraged heavy dependence on non-renewable fuels as a major source of energy. This could result in irreversible damage to the environment due to release of toxic chemicals and greenhouse gases into the atmosphere. The global carbondioxide levels are constantly increasing currently standing at 411.8 ppm from 279 ppm in 1750 (CO2-earth, 2019). Atmospheric CO_2 is increasing at a rate of 34 gigatonnes per year (Solomon et al., 2007). In addition, the depletion of fossil fuels is inevitable due to reduction in conventional crude oil production since 2004 when it was at its peak at 74 million barrels per day (Patel et al., 2012). These challenges have encouraged research into alternative sources of clean, renewable and sustainable energy such as biofuels.

Liquid biofuels such as biodiesel are a promising source of clean, renewable and environmentally friendly energy. Biofuels are produced mostly from first generation feedstock like sugarcane, corn and soybean. However, competition between fuel and food for the limited source of food has proved to be a major drawback. Meanwhile, second generation feedstock from non-food sources using energy plants such as Jatropha have been an improvement but these too have limitations due to competition for good quality agricultural land with food crops (Duan and Savage, 2011) and the technology to convert whole energy crops to biofuels has not yet reached commercial scale (Brennan and Owende, 2010). Microalgae are a promising alternative because of their high productivity in comparison to conventional plants, they can be cultivated on large water bodies and on non-arable land hence no competition for fertile agricultural land. In addition, unlike plants, microalgal biomass production can be all year round and is independent of weather conditions (Amaro, Guedes and Malcata, 2011). Furthermore, they are easy to cultivate, grow fast and can easily adapt to various environmental conditions (Safarik et al., 2016). Moreover, their use can lead to a reduction in process costs since microalgae are able to use wastewater, sunlight and CO_2 as nutrient and energy sources (Safarik et al., 2016).

Nevertheless, one of the main challenges of processing biofuels from microalgae is the high cost of microalgae separation from aqueous phase which contributes to about 20 - 30% of the total cost of biomass processing (Safarik et al., 2016). This is partly due to difficult cell separation since microalgae have a slow settling velocity because of their small size (3 - 25 µm in diameter) and low concentration in aqueous medium (0.5 - 2 $g.L^{-1}$); this is magnified by the repulsions between their negatively charged cells (E Molina Grima et al., 2003). Currently, the methods used to harvest microalgae are predominantly very slow, expensive and energy intensive (Uduman et al., 2010). A promising alternative is magnetic separation of microalgae since it is reported to be very economical and that can reduce the cost of microalgae harvesting by 90% (Los-Alamos, 2012). In addition, magnetic separation is easy to manipulate and regenerate, it uses simple devices, and the magnetic field is not destructive to microalgae cells (Prochazkova, Safarik and Branyik, 2013). Magnetic separation relies on electrostatic interaction between positively charged MNPs with microalgae cells that carry an opposite charge. The attached MNPs then respond to an external magnetic force concentrating the algal cells.

The other challenge of biofuel processing from microalgae is the costly solvent extraction (most common extraction technique) of lipids from microalgae (Jasvinder Singh and Gu, 2010; Halim et al., 2012). Solvents present health and safety challenges and solvent extraction is slow and time-consuming, requiring heating the solvent at higher temperatures to increase the extraction efficiency. The use of large quantities of solvents to increase extraction efficiency is also a bottleneck making the process more costly and energy intensive (Medina et al., 1998; Orr et al., 2015). To overcome these challenges, alternative microalgal processing techniques such as hydrothermal liquefaction (HTL) and ionic liquids (ILs) lysis of magnetically separated microalgae were jointly used for the first time in this research.

Due to the difficulties of cultivating lipid rich microalgae and extracting the lipids from microalgae cells, the HTL process is considered as a more viable alternative to produce a biofuel product from microalgae (Duan and Savage, 2010). The HTL process involves use of water as a reactive medium to convert biomass into liquid crude oil under controlled conditions (Rojas-Pérez et al., 2015). In this conversion, the main cellular components

such as lipids, carbohydrates, and proteins are broken down at high temperatures and pressures. This coupled with hydrolytic attack on biomass leads to breakage of biomolecules in the hot compressed water, resulting in the production of a biocrude oil with a reasonably high calorific value (Rojas-Pérez et al., 2015). This process uses the whole microalgae cell and does not require it to overproduce lipid, allowing the use of faster and denser growing strains. Life cycle and techno-economic analysis suggests that the overall HTL process uses less energy than the extraction and transesterification of lipids (Jae-Yon Lee et al., 2010). According to Xu *et al.* (Lixian Xu et al., 2011a), the HTL process uses less than 5% of the total energy needed for complete thermal drying of microalgae in the solvent extraction process.

Some of the major challenges with the HTL process are that it produces a biocrude oil with a high nitrogen and oxygen content and upgrading the biocrude to suitable products such as diesel and kerosene is still a challenge. To this end, effort has been invested in investigating the effect of catalysts and their ability to produce higher-quality products (Dong Zhou et al., 2010; Faeth and Savage, 2016). Magnetite-based nanocatalysts are interesting potential candidates because of ease of separation by magnetic force, hence improving their lifetime and cost-effectiveness. In addition, they have large specific surface areas, less resistance to mass transfer, and high catalytic activity for bio catalysis, photo catalysis, and phase-transfer catalysis (Akia et al., 2014). No study has yet demonstrated the multifunctional role of magnetite-based nanocatalysts in HTL and magnetic separation of microalgae. Therefore, this research seeks to bridge this gap by applying MNPs in both efficient magnetic separation of microalgae as well as in catalytic HTL of microalgae to improve biocrude yield and composition.

The other alternative to the HTL and solvent extraction of lipids is the application of ILs for lysis of magnetically separated microalgae cell walls to efficiently and economically recover lipids from the ruptured cells. ILs are a promising option since many have been proven to solubilise microalgae cell walls under mild conditions and at room temperature (Plechkova and Seddon, 2008; Pinkert et al., 2009; Tadesse and Luque, 2011). They are called ‘green’ designer solvents due to their excellent properties and have many chemical applications (Pinkert et al., 2009). Their properties include: *(i)* they are non-flammable

substances, *(ii)* they have very low vapour pressure and are thermally stable, *(iii)* they are electrochemically and mechanically stable due to their strong ionic interactions, *(iv)* Their solvent properties such as melting point, viscosity and miscibility with other solvents can be tuned by the right design and combination of each ion since they possess discrete anions and cations (Wishart, 2009), *(v)* They are immiscible with water or organic solvents resulting into biphasic systems, *(vi)* They are capable of partially or completely dissolving lignin, cellulose or lingo-cellulosic biomass especially for imidazolium based ILs (Zavrel et al., 2009). This is due to their ability to act as hydrogen bond acceptors with limited capacity to donate hydrogen. They can dissolve biomass because they form hydrogen bonds between the anion and the hydroxyl groups of the cellulose. This results into lysis of the hydrogen bond crosslinking of the polysaccharide (Mazza et al., 2009).

Ionic liquid lysis of microalgae cells improves solvent extraction efficiency by increasing the interfacial surface area of solvent to cellular matrix for mass transfer (Orr et al., 2015). In addition, the use of ILs in wet microalgae biomass results in a reduced energy demand on the system (0.4 MJ kg^{-1}) compared to conventional solvent extraction processes, which consumes 4-9 MJ kg^{-1} (Teixeira, 2012). In this research, magnetically separated microalgae were subjected to IL treatment for cell lysis and lipid recovery using hexane for the first time. Combination of magnetic separation of microalgae and IL extraction of lipids from the separated microalgae can lower the cost of microalgae harvesting and lipid extraction by 90% and 30-50% (Los-Alamos, 2012; Teixeira, 2012). In the literature, IL extraction and magnetic separation have been investigated separately and no study has combined the two processes. This research seeks to bridge this gap as well with the aim of substantially lowering the microalgae processing costs as earlier stated.

1.2. Overall aims and objectives

Some of the main challenges hindering the commercialization of microalgae-based biofuels is the high cost of microalgae separation and lipid extraction and the low yield and quality of biocrude oils from the HTL process. This results in biofuels being more expensive than petroleum derived fuels and of lower standard (HTL biocrude oils) due to presence of large quantities of oxygenated and nitrogenated compounds. Therefore, the overall aim of this research is to intensify the processing of biofuels from microalgae by

applying MNPs for efficient and economical separation of microalgae from aqueous phase and assess the catalytic effect of MNPs on yield and chemical composition of biocrude oil from HTL. The aim will be met through the following objectives:

- Synthesise and characterise MNPs by co-precipitation and apply them in the magnetic separation of microalgae from aqueous phase. Then evaluate the effect of pH, ratio of MNPs to microalgae and separation time on the separation efficiency.
- Investigate the catalytic effect of MNPs on yield and chemical composition of biocrude oil in the microalgae HTL process. Then evaluate the effect of HTL conditions on yield and chemical composition of biocrude oil.
- Recover and recycle MNPs after the HTL process for further microalgae separation and catalytic HTL. Then compare the separation efficiency and biocrude yield for the fresh and recycled MNPs.
- Investigate the effect of ILs on lysis of magnetically separated microalgae and compare the lysis efficiency and lipid yield using different ILs.
- Recover and recycle MNPs after ILs treatment of magnetically separated microalgae and compare the separation efficiency of fresh and recycled MNPs.
- Recover ILs after lysis of magnetically separated microalgae and recycle them. Then compare the lysis efficiency and lipid extraction efficiency using different ILs. Examined the parameter evaluation of the effect of different lysis conditions on the yield of extracted lipids.

1.3. Thesis Structure

This thesis is divided into six Chapters: **Chapter 1** is the introduction section and includes the general introduction, aims and objectives and the thesis structure.

Chapter 2 gives a detailed literature review on microalgae processing starting from algal cultivation. It elaborates the different algal cultivation techniques such as photo-bioreactors and open ponds, then critically analyses the main microalgae separation techniques. It proposes magnetic separation of microalgae as a potential microalgae separation technique and reviews it in detail. It elucidates on the techniques used to synthesise MNPs with major emphasis on chemical methods because they are more

relevant for this research. It then evaluates literature on methods used to extract lipids from microalgae such as mechanical and solvent extraction techniques. It then concludes by discussing literature on the transesterification process that is employed to convert the extracted lipids to biodiesel. It then reviews literature on the hydrothermal liquefaction process (HTL) which is used in this research to convert wet microalgae to biocrude oil. It explains its advantages over the solvent extraction and transesterification route, analyses the different HTL approaches, reviews the effect of process conditions on biocrude yield and briefly describes the major thermal chemical conversion techniques.

Chapter 3 investigates the multifunctional role of MNPs in efficient microalgae separation and catalytic hydrothermal liquefaction of microalgae. It describes the synthesis MNPs, their application in magnetic separation and in catalytic hydrothermal liquefaction of microalgae. It investigates the effect of MNPs on biocrude yield and chemical composition and ends by elaborating on the recovery and recycling of MNPs for further microalgae separation and catalytic HTL of microalgae.

Chapter 4 investigates the effect of HTL process conditions such as holding time, acids and hydrogen gas on the reduction of the oxygen and nitrogen content of biocrude to improve its quality. This was the major challenge of Chapter 3.

Chapter 5 investigates the application ILs for lysis of magnetically separated microalgae cells to extract lipids as a cheaper alternative to solvent extraction. It compares the cell lysis efficiency, yield and extraction efficiency of different ILs. Also compares IL cell lysis efficiency with other cell lysis techniques. Analyses the chemical composition of extracted lipids, microalgae residue, used IL and MNPs. Demonstrates the recycling of MNPs and ILs, investigates their separation and extraction efficiencies respectively, and concludes by optimising the IL extraction conditions such as temperature, treatment time and mass ratio of IL to microalgae.

Chapter 6 presents the summary, conclusions and suggestions for future work.

2. A review of microalgae processing for biofuel production

This review presents the four major areas of microalgae processing for biodiesel production. These include: *(i)* cultivation, *(ii)* harvesting (separation), *(iii)* lipid extraction and *(iv)* transesterification of extracted lipids to biodiesel. It also presents the hydrothermal liquefaction (HTL) of wet microalgae biomass to biocrude oils that can be upgraded to diesel, gasoline or kerosene. The cultivation step reviewed the methods of microalgae cultivation in ponds and photobioreactors. The harvesting step compared current microalgae separation techniques, analysing the advantages and disadvantages of each. The extraction step reviewed the current methods of extraction of microalgae oils. In addition, the transesterification of extracted microalgal oils to biodiesel was also discussed. A gap in literature was identified on the extraction of lipids from magnetically separated microalgae. The review on the HTL process covered the process description, chemistry and the major factors affecting the yield and chemical composition of biocrude. It also analysed the main HTL experimental conditions in literature. Another gap in the literature was identified on the application of magnetically responsive particles for magnetic separation of microalgae as well as catalytic HTL.

2.1. Introduction

The continual combustion of fossil fuels as a major source of energy has had a negative impact on the environment due to increased emission of greenhouse gases such as carbon dioxide. The amount of carbon dioxide in the atmosphere increases annually at a rate of 34 giga-tonnes (Solomon et al., 2007). This has led to increase in global warming because of the greenhouse effect of CO_2 potentially resulting in devastating effects to the environment. The continual utilization of fossil fuels leads to a reduction in their reserves and their end is inevitable. To counteract these negative consequences, governments around the world have invested in alternative sources of biofuels such as biodiesel and bioethanol as a potential replacement for fossil fuels. Biofuel grants and subsidies have been given out especially for corn and sugarcane derived bio-ethanol (Patel et al., 2012). However, production of biofuels using first generation methods has failed to meet carbon dioxide reduction targets and has also led to other social economic challenges. Among these challenges is competition for the limited food sources between fuel and food. While use of non-food energy crops such as Jatropha is an improvement, competition with food crops for the fertile agricultural land is a setback (Duan and Savage, 2010). In addition, first generation biofuels have a low power density, requiring large arable land for cultivation of rape crops. For instance one third of UK land area would be needed to cultivate enough rape crops for biofuels to fuel 30 million cars on the road (Hillman, 2010).

Microalgae is a better-suited candidate to overcome the challenges of first generation (from waste fats and lipids) and second-generation (inedible cultivated energy crops) biofuel feedstock. Compared to green plants, microalgae are more efficient in converting sunlight to chemical energy and they require very small land area for their cultivation with less water for cultivation (Beer et al., 2009). In addition, microalgae grow faster due to their efficiency in photosynthesis, they can double their biomass in 24 hours (Chisti, 2008). They also do not compete for fertile arable land with agricultural crops since they can grow in brackish water and on large water bodies like oceans hence scaling up of microalgae based biofuel systems is easier (Patel et al., 2012). Furthermore, a large proportion of microalgae biomass can be converted to fuel. On average about 30% of

microalgae biomass are lipids and this amount can be increased to 80 wt.% in genetically modified microalgae, while for plants like palm oil, lipids make up only 5% of the total plant biomass (Chisti, 2008; Patel et al., 2012). Also, many different species of microalgae are in existence all over the world, this biodiversity is an advantage since the suitable strains for biofuel production can be easily selected from their local environment (Patel et al., 2012).

This Chapter therefore presents a literature review on microalgae processing for biofuel production basing on their numerous advantages as earlier discussed. It covers the different microalgae cultivation techniques, methods of microalgae harvesting, extraction of lipids from microalgae cells and transesterification of extracted lipids to biodiesel. It further reviews literature on the HTL process, which involves thermochemical conversion of the wet microalgae biomass to bio-crude oil omitting the energy intensive drying and solvent extraction steps. The aim of this review is to compare the different techniques available for microalgae processing and deepen understanding on this subject as well as establish gaps in the literature.

2.2. A typical microalgae processing scheme

Microalgae processing starts with microalgae cultivation usually done in either open ponds or photobioreactors. Then microalgae separation/harvesting follows using methods such as: *(i)* Screening, *(ii)* Flocculation, *(iii)* Sedimentation, *(iv)* Floatation, *(v)* Electrical based methods, *(vi)* Centrifugation and *(vii)* Magnetic separation. After microalgae separation, the processing route that follows usually depends on the final product. There are two major routes; the first route involves solvent extraction of lipids and high value products such: (i) β-carotene, *(ii)* carotenoids, (*iii)* pigments, *(iv)* lycopene, *(v)* Astaxanthin, *(vi)* Phycobiliproteins, *(vii)* steroids, *(viii)* vitamins *(ix)* proteins and *(x)* carbohydrates from the microalgae biomass. The extracted lipids are transesterified to biodiesel and the high value products used in other applications (Figure 2.1).

The second route involves thermochemical conversion of the whole microalgae cell to biofuel through processes such as hydrothermal liquefaction (HTL), pyrolysis or gasification of the microalgae biomass. In the HTL process, wet microalgae biomass with a water content up to 78% is liquefied to biocrude oil under subcritical conditions (300 -

375 °C). The biocrude oil is then upgraded to gasoline, diesel and kerosene. In pyrolysis, the microalgae biomass is heated in absence of oxygen to produce bio-oils, which are also upgraded to gasoline, diesel and kerosene. In gasification, microalgae biomass is converted to syngas, then syngas is catalytically converted to alcohols or to diesel via the Fischer-Tropsch process.

Figure 2.1 presents a schematic illustration of two potential routes for processing of microalgae biomass to biofuels. The green blocks represent microalgae biomass, the pale-yellow blocks represent the solvent extraction routes and orange blocks represent the thermal chemical conversions of the whole microalgae cell to biofuels.

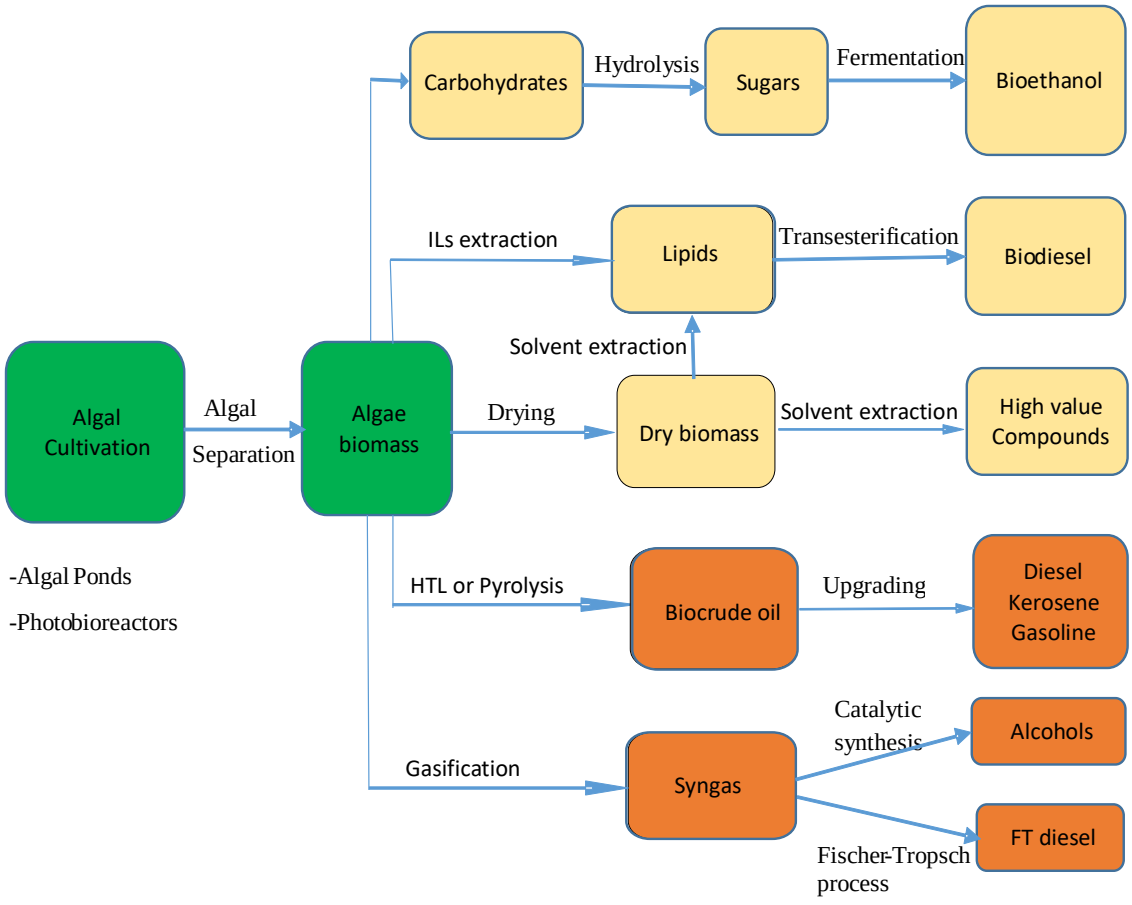

Figure 2. 1. Illustration of a typical algal processing scheme for biodiesel and other essential compounds covering the major areas in this review.

2.3. Microalgae cultivation

Recently, there has been an increasing demand of algal biomass for low cost biofuel production and for recovery of essential compounds like food supplements. This has placed a demand on increased microalgae biomass production. Microalgae biomass production is mainly done in open ponds and has been on a limited scale (hundreds of tonnes) in closed photo-bioreactors (Posten, 2009). This section presents a detailed review on microalgae cultivation in open ponds and photobioreactors.

2.3.1. Microalgae cultivation in open ponds

The schematic illustration of open pond types is presented in Figure 2.2. They are divided into: *(i)* artificial water bodies such as raceway ponds (Figure 2.3) and *(ii)* natural water bodies (Figure 2.4) such as lakes and lagoons (Ugwu, Aoyagi and Uchiyama, 2008; Brennan and Owende, 2010). Artificial ponds can further be classified into: *(i)* circular open ponds and *(ii)* raceways (Masojídek et al., 2009).

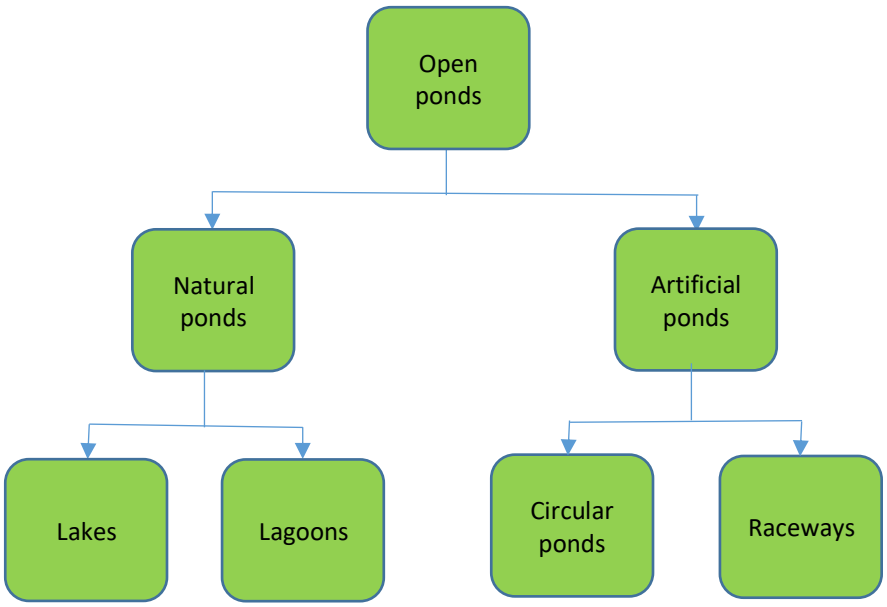

Figure 2. 2. Schematic illustration of open pond systems for microalgae cultivation.

Cultivation of microalgae on industrial scale is mostly done in open ponds because of the low investment and operational costs and ease of operation (Morais et al., 2014). The most

widely used ponds for largescale microalgae cultivation are raceway tanks (Figure 2.3), they are built in a closed loop and the recirculation channels are oval shaped. Their depth is usually between 0.2 to 0.5 m deep and to ensure proper mixing for better algal growth and improved productivity, a paddle wheel is used to stir the medium (Morais et al., 2014).

Figure 2. 3. Spirulina cultivation in a raceway open pond system (Morais et al., 2014).

Figure 2. 4. Microalgae cultivation in an open pond system, photo credit: Christian Fischer (Biofuelwatch, 2017/05).

The materials for construction of raceway ponds can be concrete, membranes or glass fibre and compacted earth with plastic linings have been used too (Ugwu, Aoyagi and

Uchiyama, 2008; Brennan and Owende, 2010; Morais et al., 2014). The microalgae broth and culture medium are fed at the front section of the paddle wheel. Then circulated through the system to the harvesting point behind the paddle wheel (Figure 2.3). To prevent sedimentation of algal biomass the paddlewheel is kept in continuous operation. The carbon dioxide requirements of microalgae come from the surface air and to enhance the intake of carbon dioxide, aerators can be submerged in the culture medium (Terry and Raymond, 1985). Circular ponds have a mechanical stirrer in the centre of the pond to provide mixing of the microalgae culture medium. For efficient mixing, the size of such ponds is currently limited to 10,000 m^2, beyond this, the stirrer can no longer provide a homogenous mixture of the culture medium (Morais et al., 2014). Circular ponds are like the wastewater treatment ponds and are the oldest type of microalgae ponds.

On the other hand, raceways are the cheapest pond systems for large-scale microalgae production, they can be maintained easily, require low power and cleaning is easy (Chisti, 2008). The challenge with open pond systems is that they are prone to contamination therefore only selective microalgae species resistant to contamination can be cultivated in such pond systems. They are also affected by changes in environmental conditions and it is difficult to control parameters such as temperature, light intensity, dissolved oxygen and pH, this has a direct impact on the viability of microalgae cells hence negatively affecting productivity (Harun et al., 2010). Factors such as water loss by evaporation, fluctuations in temperature, limited illumination, limited nutrients, inefficient mixing affect cell viability resulting in reduced yields (Brennan and Owende, 2010).

2.3.2. Microalgae cultivation in photobioreactors (PBH)

Photobioreactors offer numerous advantages over open ponds due to prevention of water loss from evaporation, contamination and competition from invasive microalgae species. They also offer higher areal productivities (Michael A Borowitzka, 1999). The major limitation of using photobioreactors for microalgae cultivation is the high cost (Posten, 2009). Photobioreactors for biofuel purposes should: *(i)* operate on a large scale (in hectares), *(ii)* the cost of construction should be minimal, *(iii)* should be economical in terms of energy demand, *(iv)* should be easy to clean and maintain and *(v)* should have a long life span (Patel et al., 2012). The major constituents within a standard

Photobioreactor are: microalgae, water, nutrients and CO_2 distributed throughout the medium. A good PBR design needs an understanding of the relationship between the various environmental parameters. Such parameters include light penetration into the rector, fluid dynamics and the respective biological responses. Illumination conditions, light to dark cycles and surface to volume ratio are very essential for the productivity of PBRs (Patel et al., 2012). To achieve these important parameters, different PBR geometries have been designed. The most commonly used PBR geometries are: tubular and flat plate reactors (Patel et al., 2012). Tubular reactors are composed of three major types: *(i)* vertical tubular reactors (VTR) (Figure 2.5), *(ii)* horizontal tubular reactor (HoTR) (Figure 2.7) and *(iii)* the helical tubular reactor (HeTR) (Figure 2.10).

2.3.2.1. Vertical tubular reactor (VTR)

The main examples of a vertical tubular reactor are: (i) simple airlift reactor and (ii) the bubble column reactor (Figure 2.6 A and B). It is made of vertical transparent tubing made of polyethylene or glass tubes to permit greater penetration and illumination of light and through which carbon dioxide gas is bubbled at the bottom. This allows for better mixing, efficient removal of oxygen and adequate supply of carbon dioxide.

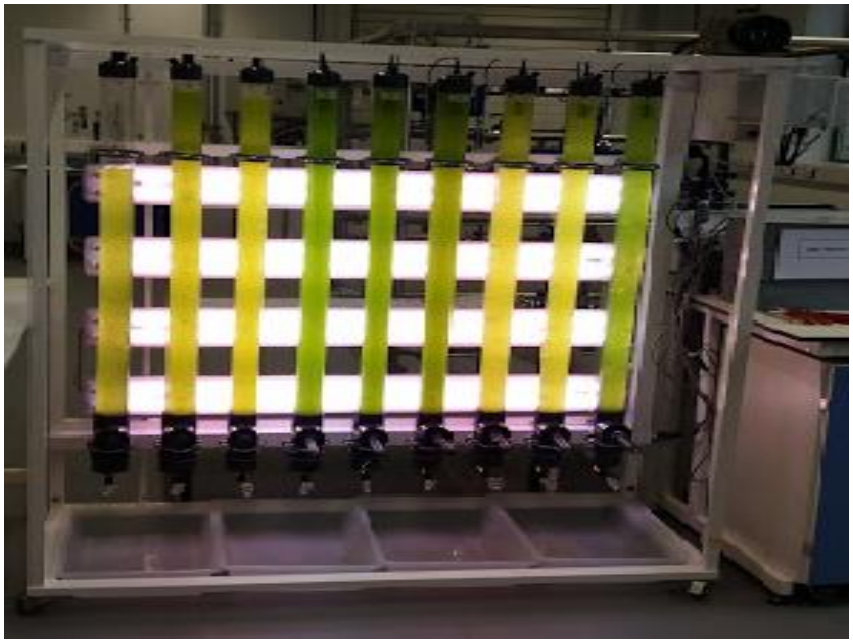

Figure 2. 5. Vertical tubular photobioreactor (photo taken from the undergraduate lab department of Chemical Engineering University of Bath).

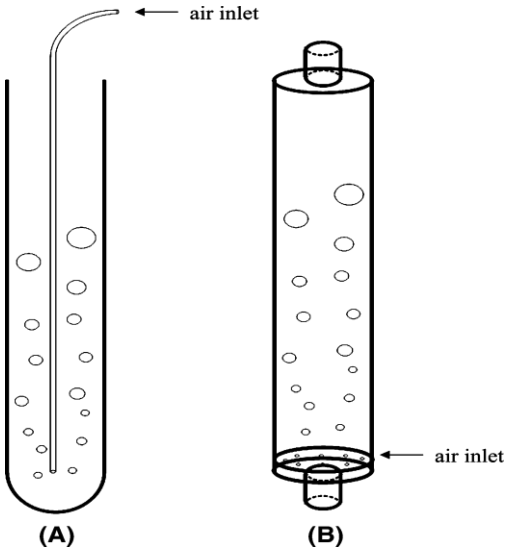

Figure 2. 6. Diagrammatic illustration of the air lift and bubble column reactors (Carvalho, Meireles and Malcata, 2006).

To reduce the cost of construction material for PBRs Cohen (Cohen and Arad, 1989) used polyethylene bags in the cultivation of *Porphyridium sp* and attained cell concentrations of up to 3 times in comparison to those in open ponds. The polyethylene bags were advantageous due to their low cost, high transparency and fine sterility (Carvalho, Meireles and Malcata, 2006). Tredici et al., (1998) further improved on the idea of polyethylene tubular reactors by developing a culture chamber with a thin transparent plastic layer supported by a rigid metal frame forming a vertical panel (Tredici and Zittelli, 1998). Cultivation of microalgae in this way is simple and can be scaled up but there are limitations since the setup is fragile, the materials used are not versatile and the technology is primitive because it uses primitive materials (MA Borowitzka, 1996; Carvalho, Meireles and Malcata, 2006).

2.3.2.2. Horizontal tubular reactors (HoTR)

This type of tubular reactor is made of horizontal transparent tubing with provision for gas transfer systems to facilitate efficient mixing of CO_2 within the culture medium (Figure 2.7 and 2.8). The tubes are positioned at an angle that is adequate for efficient light illumination. These reactors can handle large volumes of culture and they are not prone to contamination. Their only challenge is that in absence of adequate temperature regulation, they can generate heat and reach temperatures of up to 20 ºC in a day, this can

be a short-coming for regular operations (Carvalho, Meireles and Malcata, 2006). A number of horizontal tubular reactors have been reported in literature, for instance Torzillo et al., (1986) reported on a horizontal tubular reactor with a diameter of 14 cm made of Plexiglas with a diaphragm pump to move the culture to A feed tank, gas transfer for this system was in the connection tubes (Torzillo et al., 1986). This reactor had a working capacity of 8 m^3 occupying a land area of 80 m^2 with a maximum productivity of 0.25 g $L^{-1}d^{-1}$ dry mass when Spirulina was used. The major challenge encountered with this reactor was temperature control, however this was overcome by spraying the surface of the tubes with water.

Figure 2. 7. Image of microalgae cultivation in a horizontal tubular photo bioreactor (Aqua, 2019/01/19).

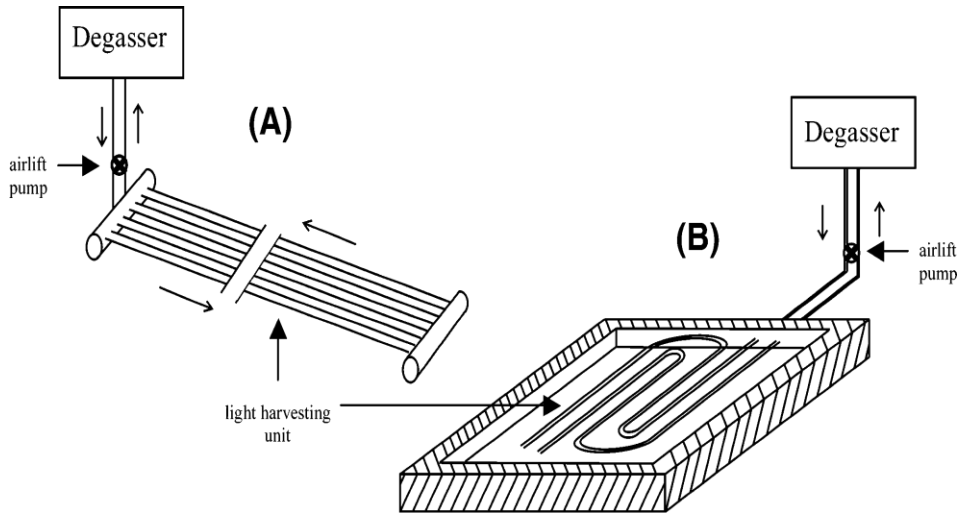

Figure 2. 8. Schematic illustration of a horizontal tubular reactor with a degassing unit and a light harvesting unit with parallel sets of tubes (Carvalho, Meireles and Malcata, 2006).

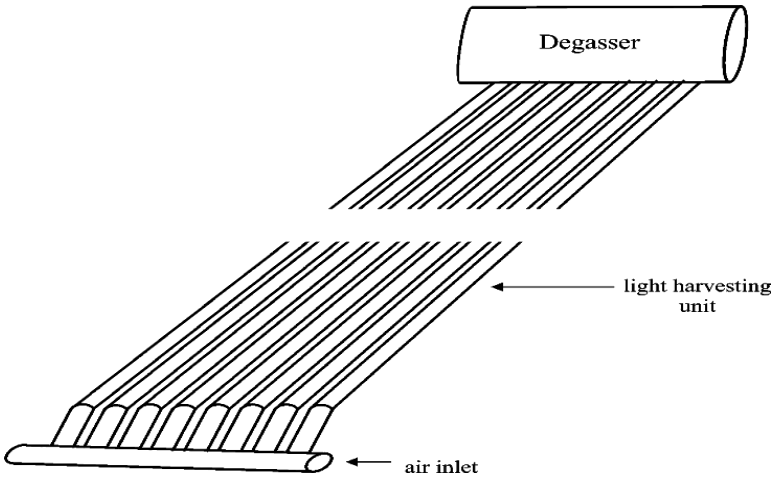

Figure 2. 9. Schematic illustration of a near horizontal tubular reactor with a degassing (Carvalho, Meireles and Malcata, 2006).

In addition, Gudin et al., (1984) reported on a reactor system with a capacity of 7000 L and a productivity of 36 g m^{-2} d^{-1} when *Phorphyridium cruentum* was used. It was composed of 70 L glass vertical tubular reactors connected to a gas exchange unit. Pumping of the culture medium was done mechanically between the light harvesting and the gas exchange units. Temperature control was attained by immersing the culture

medium in water whenever appropriate (Gudin et al., 1984). The major constraint of this reactor was its fragile nature because of the glass tubes and its high cost. A similar configuration of a HoTR with a productivity of 1.5 g $L^{-1}d^{-1}$ with *Spirulina platensis* and 0.32 g $L^{-1}d^{-1}$ with *Isochrysis galbana* was reported by Molina Grima et al., (1994) and Richmond et al., (1993) in which an externally designed unit achieved light illumination. (E Molina Grima et al., 1994) and (Richmond et al., 1993).

Furthermore, Tredici et al., (1998) designed a tubular reactor which was nearly a horizontal tubular reactor referred to as a near horizontal tubular reactor (Figure 2.9) (Tredici and Zittelli, 1998). This consisted of plastic tubes set in parallel and were connected by a PVC pipe on top which acted as a degasser and at the bottom, a pipe with holes was connected to the plastic tubes. Through the bottom pipe, air was injected in each plastic tube which are at angles of 5-7 º in relation to the horizontal plan. Temperature control was achieved by spraying water on the reactor surface. Each parallel tube was 44 m long and in total make up a volume of 4 m^3. With *Nannochloropsis*, a productivity of 0.7 g $L^{-1}d^{-1}$ can be achieved. This reactor system is advantageous since it is easy to scale up, it has a high area to volume ratio and can be controlled with ease. However, this reactor set up suffers from a low rate of gas transfer due to the reactor's huge length and smaller diameter.

2.3.2.3. The helical tubular reactor (HeTR)

The HeTR is made of a flexible plastic tube made in a circular structure, it also has a gas exchanger and a heat exchanger. This type of PBR is advantageous due to easy scale up by simply increasing the number of tubes within the clipid (MA Borowitzka, 1996). This reactor system is not suitable for all algal species since it involves centrifugally pumping the culture medium to the top of the tubing, this action increases shear stress on the algal biomass limiting biomass productivity because of damage caused by the re-circulation pumping. Furthermore, fouling may also take place within the reactor tubing (Michael A Borowitzka, 1999; Carvalho, Meireles and Malcata, 2006).

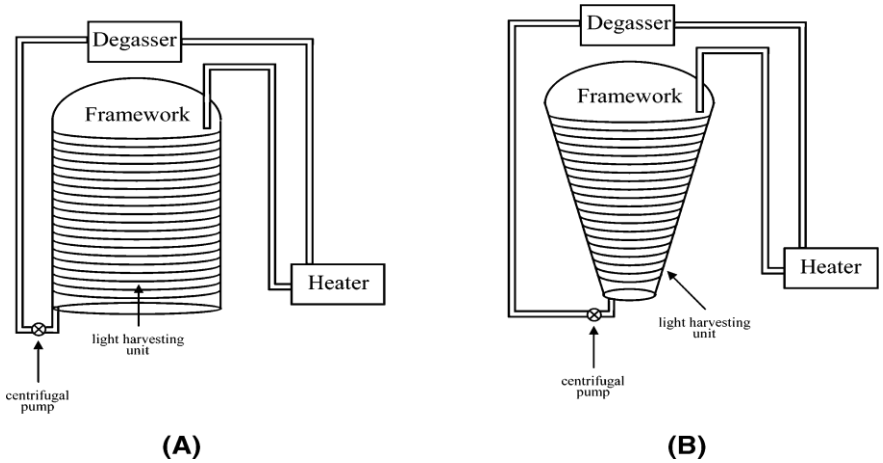

Figure 2. 10. Schematic illustration of helical tubular reactors (Carvalho, Meireles and Malcata, 2006).

Morita et al.,(2000) proposed a helical conical reactor configuration with a light harvesting section made of PVC tubing in a clipided set up as in Figure 2.10 (Morita, Watanabe and Saiki, 2000). It also had a degasser at the top and a heat exchanger. The culture medium was moved from the heat exchanger to the light harvesting section by the pumping action of an air pump done in ascending fashion. The light harvesting section was connected to the degasser at the same level. From the degasser, the culture medium moves to the heat exchanger in a descending course. This system is advantageous because of its high light harvesting efficiency (Carvalho, Meireles and Malcata, 2006).

2.3.3. Hydrodynamics in microalgae cultivation

To achieve high productivity of algal biomass, proper mixing is highly essential in all microalgae cultivation methods. Proper mixing enables efficient heat and mass transfer within the culture medium. It also enables saturation of culture medium with CO_2 and allows uniform concentration of microalgae and nutrients within the medium. Inadequate mixing would result in low biomass concentration due to poor fluid circulation. Poor mixing leads to limited gas exchange within the culture medium, increased shading, light obstruction from the microalgae, poor distribution of nutrients and temperature and increased sedimentation of microalgae. Turbulent flow is appropriate for proper mixing. In raceway ponds, velocities of up to 5 cm s^{-1} are appropriate to eliminate the un-desirable effects of poor mixing (Morais et al., 2014). Different mixing systems are employed in

microalgae cultures depending on the cultivation method. Paddle wheels are used in open ponds to effect turbulence, while in vertical tubular photobioreactors, proper mixing is achieved through the bubbling action of air as an airlift system and in stirred tank photobioreactors, mixing is done using impellers (Ugwu, Aoyagi and Uchiyama, 2008). The highest contribution to the cost of microalgae cultivation systems comes from mixing due to the high energy consumption involved (Ugwu, Aoyagi and Uchiyama, 2008). The cost of mixing in a raceway pond is about 0.07 pounds per Kg of dry weight (DW) while for tubular reactors mixing accounts for 1.27 euros per Kg of DW and in flat panel reactors; it is as high as 3.10 euros per Kg DW (Norsker et al., 2011).

2.4. Microalgae separation techniques

Efficient and cost-effective separation of microalgae from culture medium is essential for downstream processing. Separation of microalgae contributes to 20 - 30% of the total cost of biodiesel production from microalgae (E Molina Grima et al., 2003). Algal cells have a density that is similar to that of the culture medium ranging between 1080-1110 kg m^{-3} and 1030 kg m^{-3} respectively (Patel et al., 2012). This presents major difficulties in microalgae cell separation. In addition, the low concentration of microalgae (0.5 - 5 g L^{-1}) coupled with a negative surface charge of microalgae cells and their small size (2 - 200 µm) are a further hindrance to an efficacious algal separation process (Greenwell et al., 2009). The choice of the microalgae separation method depends on factors like: value of the product to be extracted and the size and density of the microalgae to be separated (Brennan and Owende, 2010). In the following section, current microalgae separation techniques such as: *(i)* screening, *(ii)* flocculation, *(iii)* gravity sedimentation, *(iv)* floatation, *(v)* centrifugations, *(iv)* electrical based methods and *(iv)* magnetic separation are analysed.

2.4.1. Screening (filtration)

Screening is mostly for removal of water, it is usually applied after coagulation and flocculation to improve separation efficiency (Show and Lee, 2013). During screening, the microalgae suspension is introduced through a screen of a specific pore size (for macrofiltration > 10 µm). The efficiency of screening depends on the spacing between screen openings and the size of the cells (Barros et al., 2015; Hee-Jeong Choi, 2015). The

most common screening devises in microalgae harvesting are vibrating screen filters and microstrainers. Microstrainers are revolving filters with fine mesh screens having frequent backwash (Chun-Yen Chen et al., 2011). Microstrainers are advantageous due to simplicity of operation and construction, low investment costs, negligible abrasion since there are no moving parts and achieves high filtration rates (E Molina Grima et al., 2003). It also allows separation of shear sensitive species and high recovery efficiencies are obtained (Vidal-Vidal, Rivas and López-Quintela, 2006). However, screening is disadvantageous because it is not efficient in recovering small bacteria sized microalgae (0.5 µm) while the average size range of microalgae is between 2 and 30 µm, as a result further processing has to be done (Milledge and Heaven, 2013; Barros et al., 2015; Hee-Jeong Choi, 2015). Furthermore, it requires regular maintenance because bacteria and microalgae biofilms form on the mesh or fabric requiring repeated backwashing and hence limiting filtration efficiency (Uduman et al., 2010; Barros et al., 2015). In addition, high operational costs may arise due to clogging or fouling resulting in costs of regular cleaning of membranes, membrane replacement and pumping (Show and Lee, 2013). Filtration equipment for microalgae harvesting can consume between 0.3 to 2 kWh m^{-3} (E Molina Grima et al., 2003). The efficiency of microalgae recovery is between 70-89% if filtration is by tangential flow (Petrusevski et al., 1995).

2.4.2. Chemical Coagulation/ Flocculation

Chemical coagulation is the aggregation of finely divided particles in suspension on to larger aggregates. This is achieved by reducing the repulsive charge between interacting particles through the neutralization action of coagulants. Flocculation is the agglomeration of coagulated particles to form larger flocs that settle to the bottom of the vessel leaving a clear supernatant (Figure 2.11) (Barros et al., 2015). In flocculation high molecular weight cationic polymers are added to the medium to increase the size of the flocs causing them to settle at the bottom (Papazi, Makridis and Divanach, 2010; Barros et al., 2015). This method is considered as a pre-treatment method used to increase concentration of the algal medium by forming flocs before applying other methods like centrifugation and filtration (Patel et al., 2012). The most common flocculants used are aluminium chloride, aluminium sulphate and ferric chloride. When sodium hydroxide is added, the pH of the

culture medium is increased to between 8 - 11, the very high pH is not favourable for microalgae and results in coagulation of the cells in few minutes (Morais et al., 2014). Chemical coagulation/ flocculation has the advantage of being an easy and quick method and there is no energy expenditure. This method has disadvantages in that chemical flocculants may be costly and poisonous to microbial biomass and reprocessing of cultural medium is restricted (Barros et al., 2015).

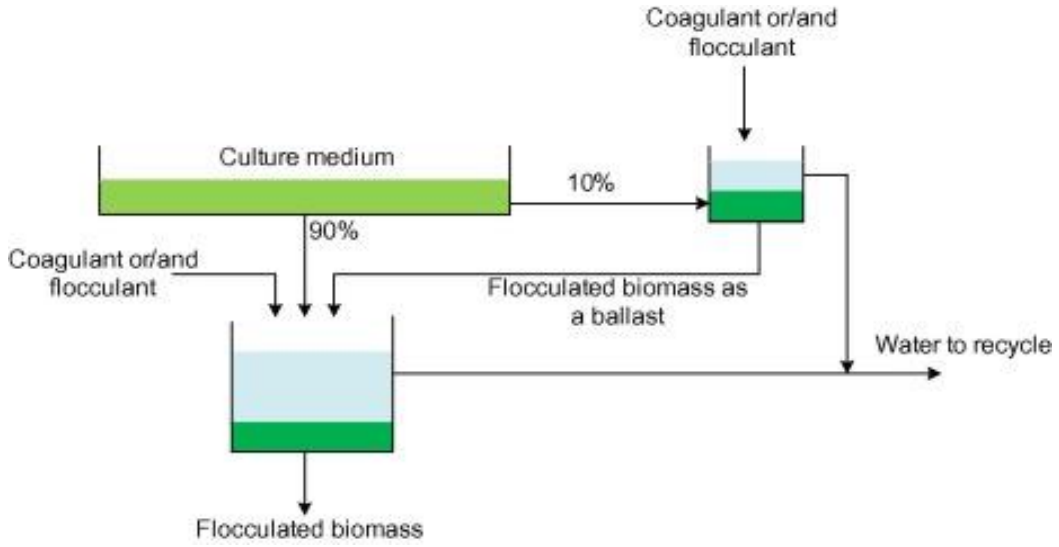

Figure 2. 11. Illustration of microalgae separation by coagulation method (Gorin et al., 2015)

2.4.3. Auto-flocculation

Auto-flocculation is flocculation by increasing pH. This process occurs when carbonate salts are co-precipitated with microalgae cells because of high pH. It is advantageous because it is non-poisonous to microalgal biomass, it is also cost effective and permits culture media reprocessing. Furthermore, there is no use of flocculants and has low energy requirements. However, it is disadvantageous because there is possibility of biological pollution and change in cellular structure (Horiuchi et al., 2003; Barros et al., 2015). Fangjian et al., (2012) reported that auto-flocculation does not work well in recovery of fresh water microalgae, but it is better suited for recovery of marine microalgae, this is possibly because of salts in marine microalgae favouring the process (Fangjian Chen et al., 2012; Barros et al., 2015).

2.4.4. Gravity Sedimentation

Gravity sedimentation is a primitive procedure not applicable to all types of micro-microalgae. The rate of sedimentation is influenced by the density and diameter of the cells. Sedimentation is usually done in sedimentation tanks and it is suitable for microalgae such as cyanobacteria with a cell size greater than 70 µm. To increase its efficiency, it is done in combination with flocculation to increase the sedimentation efficiency (Chun-Yen Chen et al., 2011). Sedimentation is advantageous because it is very energy efficient, easy to use and cost effective (Barros et al., 2015),(Rawat et al., 2011). This method can only be applied in cases where the product is of low value (E Molina Grima et al., 2003; Rawat et al., 2011; Barros et al., 2015). The disadvantages with it is that it takes much time having settling speeds between 0.1 to 2.6 cm h^{-1}, it is therefore not suitable for a large scale continuous separation (SK Choi et al., 2006). In addition, there is possibility of biomass decline, and a reduction in the mass of the algal cake (Barros et al., 2015).

2.4.5. Flotation

Floatation is a separation technique that uses gravity in which the gas bubbles introduced into the microalgae medium provide the necessary force to carry the particle and effect dissociation (Rubio, Souza and Smith, 2002; Barros et al., 2015). Floatation can work effectively on particles with a diameter below 500 µm, it takes place when the gas bubbles interact with microalgae cells after collision (Yoon and Luttrell, 1989). Floatation can be classified as electrolytic, dispersed or dissolved air floatation depending on the bubble size used. Dissolved air floatation (DAF) involves pre-saturation of a water stream with air at excess pressure resulting in reduction in pressure of a water stream and formation of bubbles in the size range of 10 - 100 µm (Uduman et al., 2010). DAF for harvesting of microalgae is influenced by several factors such as hydraulic retention time, the floating rate of particles, the recycling speed and the tank pressure (Chun-Yen Chen et al., 2011). Dispersed air floatation involves formation of bubbles in the size range of 700-1500 µm. Mechanical stirring at high speeds using an air injection device (Rubio, Souza and Smith, 2002) forms the bubbles. Its major advantage is that it is proven applicable on a large scale in combination with flocculants. In addition, there are low space requirements, has

short time of operation and its highly flexible having lower initial equipment costs (Rubio, Souza and Smith, 2002; Hanotu, Bandulasena and Zimmerman, 2012; Barros et al., 2015). Its disadvantages are that it generally requires the use of chemical flocculants and it is unfeasible for marine microalgae harvesting (Barros et al., 2015). Primary microalgae harvesting by floatation or flocculation yields a slurry concentration of between 10 to 20 g L^{-1}, to increase this concentration to between 100 to 200 g L^{-1}, secondary treatment methods like centrifugation or filtration should be applied (Schenk et al., 2008).

2.4.6. Electrical based Processes

Since algal cells carry a negative surface charge, when an electrical field is applied to the cultural medium, the cells are isolated (Rubio, Souza and Smith, 2002; Hanotu, Bandulasena and Zimmerman, 2012; Barros et al., 2015). The hydrogen generated by electrolysis of water carries a positive charge, it attaches to the microalgae flocs which carry a negative surface charge through electrostatic interaction and moves the microalgae cells to the solution surface as illustrated in Figure 2.12 (Morais et al., 2014).

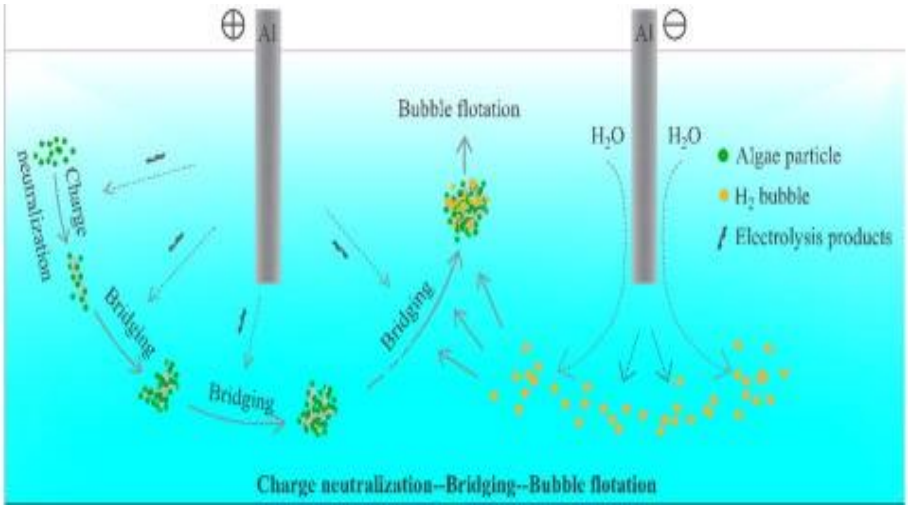

Figure 2. 12. Illustration of electrical method of separation of microalgae from aqueous phase by flotation (Shi et al., 2017)

Electrical methods are environmentally friendly since no pollution occurs (Uduman et al., 2010; Zenouzi et al., 2013; Barros et al., 2015). Also no addition of chemical flocculants is required and are applicable to a wide variety of algal species (Barros et al., 2015). They

are also safe, selective, compatible and versatile (Mollah et al., 2004). However, the disadvantage is that they are not widely applied and they are energy intensive and expensive (Barros et al., 2015).

2.4.7. Centrifugation

Centrifugation entails the application of centrifugal force to effect the separation of microalgae from the culture medium (Figure 2.13). It is the fastest and most expensive harvesting method and it involves high-energy consumption, it is usually applied to high valued products (E Molina Grima et al., 2003; Christenson and Sims, 2011; Rawat et al., 2011; Wenguang Zhou et al., 2013; Barros et al., 2015). It has the following advantages: It is a fast method, high recovery efficiencies are achieved, the disks in the centrifuge can be easily cleaned and sterilized and it is suitable for almost all microalgal species (Barros et al., 2015).

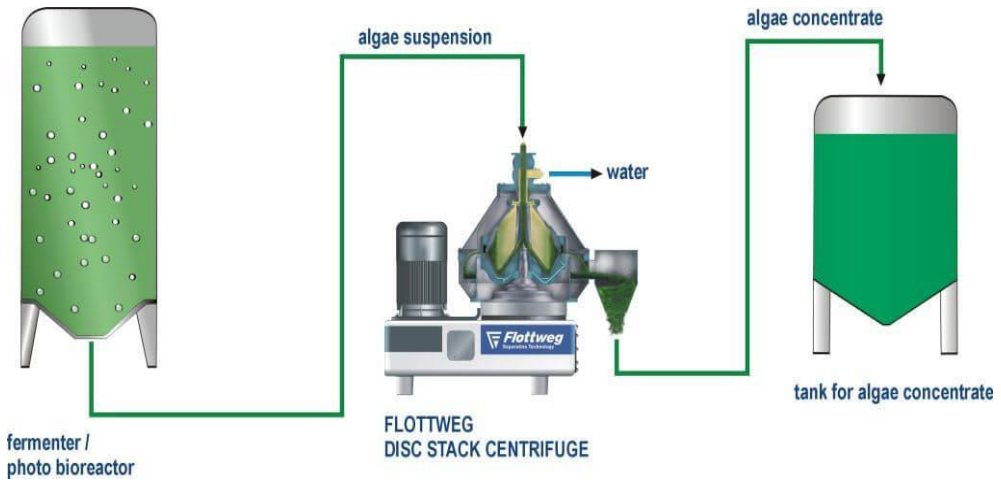

Figure 2. 13. Illustration of a set up for centrifugation of microalgae by a flottweg centrifuge (Flottweg, 2019/01/18).

Centrifugation has the following disadvantages; if it is used for large-scale operation, centrifuges are expensive to maintain, and operation costs are high. In addition, centrifuges are energy intensive requiring an energy input of 3000 kWh per ton of microalgae processed and consume 1 kWh m^{-3} of power (Benemann and Oswald, 1996). Furthermore, centrifugation is only appropriate for separation of high value products therefore it is not suitable for biofuels since they are low value products (Barros et al.,

2015). Also, there is rapid corrosion of equipment due to the effect of the salts within the microalgae culture medium (Pires et al., 2012). Finally, there is a high possibility of cell damage due to the high shear and gravitation forces involved during the operation. Cell damage may lead to contamination especially if high value products are the target product (Barros et al., 2015).

2.4.8. Magnetic separation of microalgae

Magnetic separation of microalgae involves the use of superparamagnetic MNPs for microalgae separation (Figure 2.14). Generally, microalgae cells bear a negative surface negative charge over a wide pH range due to presence of hydroxyl, carboxyl or phosphate groups while magnetic nanoparticles bear a positive surface charge especially under low pH. Therefore, attachment of MNPs to microalgae cells is facilitated by electrostatic interaction between microalgae cells and MNPs and in presence of an external magnetic field, magnetic separation occurs. It is advantageous due to its simplicity of operation, low energy consumption, and low cost (Yavuz et al., 2009; Wang et al., 2015). Industrial application of this method is still lacking since it is still at the experimental level. The surface characteristics of algal cells are essential for the recovery efficiency (Wang et al., 2015). It can be viewed as a single step process since flocculation and separation occur simultaneously (Vandamme, Foubert and Muylaert, 2013). Different MNPs have been investigated for their ability to separate microalgae from culture medium. In some magnetic separation techniques, the surface of MNPs is modified to facilitate the attachment of microalgae to MNPs while in others, no modifiers are used but the attachment of MNPs to microalgae is facilitated by electrostatic interaction. These are discussed in the following sections.

2.4.8.1. Use of MNPs

MNPs synthesised mostly by co-precipitation method have been proven to efficiently separate both fresh water and marine microalgae species (Figure 2.14). In this respect, Hu et al., (2013) reported on the efficient extraction of marine water microalgae *Nannochloropsis maritima* using bare MNPs, the separation efficiency reached 95% at a particle dosage of 120 mg L^{-1}, the separation time was 4 minutes (Hu et al., 2013). In addition, Ling Xu et al., (2011b) separated fresh water microalgae *Botryococcus*

braunii and *Chlorella ellipsoidea* from culture medium using bare MNPs at a separation efficiency of 98% within 1 minute (Ling Xu et al., 2011b).

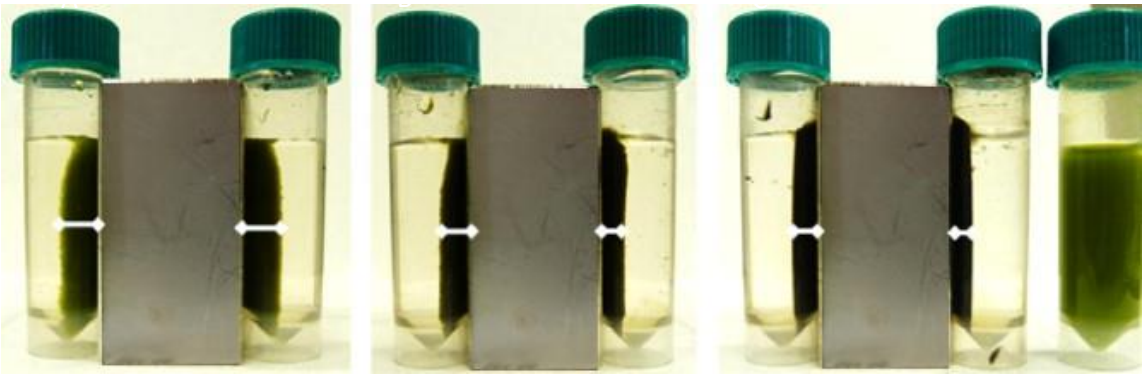

Figure 2. 14. Illustration of magnetic separation of microalgae using MNPs (Cerff et al., 2012).

Furthermore, Prochazkova et al (2013) reported on the use of iron oxide magnetic nanoparticles synthesized by the microwave treatment method to extract *Chlorella vulgaris* from a dilute aqueous solution (Prochazkova, Safarik and Branyik, 2013). A separation efficiency of 95% was achieved when microalgae separation was done in the absence of phosphorous ions from the culture medium at a mass ratio of 3:1 (MNPs to microalgae). The attachment of MNPs on to microalgae cells was facilitated by the electrostatic interaction between microalgae cells and MNPs. This interaction was more evidenced under acidic pH conditions since the surface charge on MNPs is positive in acidic conditions with an isoelectric point around the neutral pH.

2.4.8.2. Use of surface functionalised MNPs

Since microalgae cells bear a negative surface charge, functionalizing the surface of MNPs with positive cationic groups can improve the separation efficiency. Attachment of a polyelectrolyte on the surface of bare MNPs can be done in two ways: *(i)* the ‘‘attached to’’ method and *(ii)* the ‘‘immobilized on’’ method (Lim et al., 2012). The former involves overlaying the microalgae cells with a polymer binder followed by attachment of the bare MNPs. While the later involves surface functionalizing of the bare MNPs with a polyelectrolyte and then attaching the microalgae cells (Wang et al., 2013; Toh et al., 2014b). Comparison of microalgae separation efficiencies for the two approaches under similar conditions revealed that the immobilized-on approach gave better separation

efficiency. This is because the particles have a better distribution and colloidal stability (Lim et al., 2012; Toh et al., 2014b).

Many articles in literature discuss the functionalization of MNPs to improve separation efficiency. For example, Safariki et al., (2016) reported on a method in which magnetic modification of *Chlorella vulgaris* cells could be performed by drying the cells and then thoroughly washing them several times in 0.1 M acetic acid to remove macromolecules. This was then followed by the addition of perchloric acid leading to deposition of MNPs onto the cell surface and formation of magnetically responsive algal cells (Safarik, Sabatkova and Safarikova, 2008; Safarik et al., 2015). Another method was reported by Bitton et al.,(1975) in this approach, magnetic nanoparticles were used in combination with aluminium sulphate for magnetization and separation of A*nabaena* and *Amphanizomenon* cells (Bitton, Fox and Strickland, 1975). Furthermore, Yadidia et al., (1977) reported that the combination of magnetite and ferric chloride can efficiently separate *Scenedesmus obliquus* cells (Yadidia, Abeliovich and Belfort, 1977).

In addition, chitosan has been used successfully for surface modification of MNPs, the linkage between *Chlorella* species and modified MNPs was promoted by simply mixing. The magnetized *Chlorella* cells were separated under low gradient magnetic separation. The MNPs entered cells either passively or through adhesive interaction (Toh et al., 2014a; Toh et al., 2014b; Safarik et al., 2015). Recently, Fakhrullin et al., (2010) described an important process for coating algal cells with MNPs by electrostatic interactions. In this approach, positively charged MNPs were made stale by (poly) allyl amine hydrochloride and used for the magnetization of living *Chlorella pyrenoidosa* cells (Fakhrullin et al., 2010). The single step procedure consisted of dropwise introduction of the aqueous suspension of algal cells into the nanoparticle solution followed by intensive shaking for 10 minutes. Another similar cationic electrolyte called poly (di-allyl-dimethyl ammonium chloride) effectively promoted the attachment of iron oxide nanoparticles onto C*hlorella sp*. through electrostatic interaction (Lim et al., 2012; Toh et al., 2014a; Safarik et al., 2015).

2.4.8.3. Driving force for attachment of MNPs on microalgae

Algal cells carry a negative surface charge over a wide pH range (from pH 2.5 to 11.5) (Hu et al., 2013; Prochazkova et al., 2013; Prochazkova, Safarik and Branyik, 2013; Wang et al., 2013; Wang et al., 2015). This aids in electrostatic interaction between the negatively charged algal cells and the positively charged MNPs. The positive charge on the MNPs originates from the surface modification of MNPs during the synthesis process using poly-cationic polymers such as polyacrylic acid or tetra-methyl ammonium hydroxide or dilute acids (Zhiming Li et al., 2019). The negative surface charge on the microalgae cells comes majorly from the carboxylic (-COOH) and amino ($-NH_2$) functional groups (Pugazhendhi et al., 2019). The amino groups originate from proteins and carboxylic groups from fats or fatty acids which are major components of the cell membrane. In aqueous solutions, a whole range of physical chemical surface interaction such as non-covalent Lifshitz van der Waals forces, acid base interactions and electrostatic interactions occur during adhesion of algal cells to magnetic particles (Bos, Van der Mei and Busscher, 1999; Safarik et al., 2015). In addition, since surfaces carry different surface charges, there is a formation of electric double layers, resulting in the attraction and/or repulsion between surfaces in contact.

There are complex forces of interaction between ions in culture medium, which makes it hard to study and identify the forces responsible for the interaction between microalgae cells and MNPs. This kind of study is best done under model conditions. It has been reported that interfering ions such as Ca^{2+} and Mg^{2+} precipitate under alkaline conditions and bind to cell surfaces (Vandamme et al., 2012; Safarik et al., 2015).

It is also worth noting that ζ-potential measurements of microalgae cells and MNPs have revealed several surface charges depending on the surrounding environment. Due to the presence of hydroxyl, carboxyl, or phosphate groups, micro-microalgae cells maintain predominantly a negative surface charge over a wide pH range (Henderson, Parsons and Jefferson, 2008; Hadjoudja, Deluchat and Baudu, 2010; Lim et al., 2012; Xuezhi Zhang et al., 2012; Safarik et al., 2015). Therefore, the potential separating agents have to be positively charged (Safarik et al., 2015). The surface hydroxyl groups that cover the metal oxide are responsible for ensuring a pH sensitive surface charge of MNPs. Below the

isoelectric point, the surface charge of the metal oxide is positive since it gains protons and above its isoelectric point it loses electrons hence becomes negatively charged (Parks, 1965; Safarik et al., 2015). The electrostatic interaction between positively charged MNPs and negatively charged microalgae cells can be illustrated using Figure 2.15. The negatively charged microalgae cell will attract the positively charged MNPs strongly closer to its surface forming a stern layer. Following the stern layer is a layer of loosely bound ions known as the diffuse layer and beyond the slipping plane, the ions are free from the influence of the central ions and will not move along with it when an external magnetic field is applied.

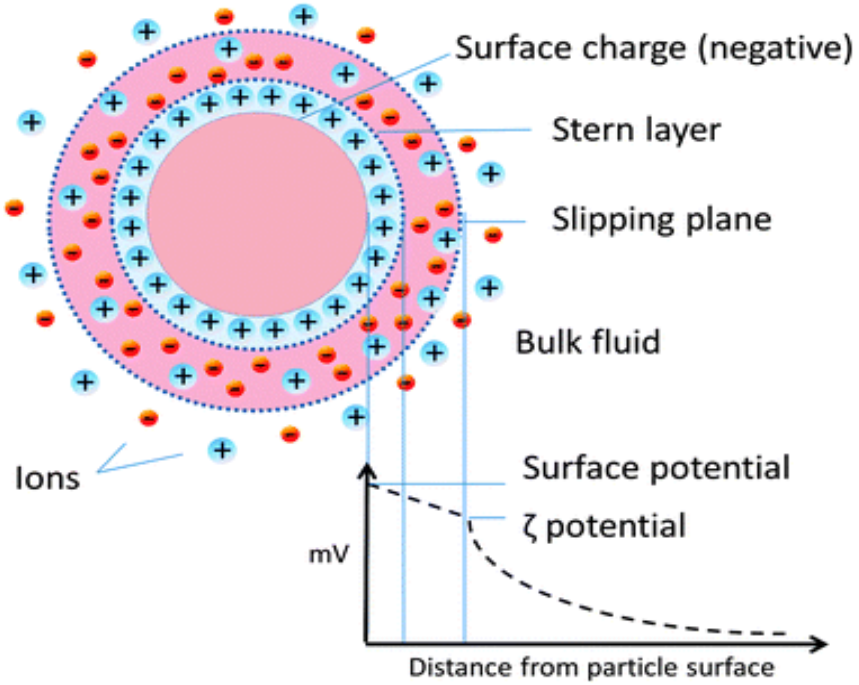

Figure 2. 15. Illustration of electrostatic interaction to effect attachment of MNPs on microalgae cells (Herrada et al., 2014).

Prochazkova et al., (2013) in the harvesting of *Chlorella vulgaris* with MNPs reported that high separation efficiency was achieved under acidic pH due to a very large difference in ζ-potential measurements of the interacting particles. The highest separation efficiency (95%) was registered at pH 4 and at dozes of 800 mg/g of MNPs (Prochazkova, Safarik and Branyik, 2013). On the other hand, it must be emphasized that MNPs-microalgae attachment can also take place under basic conditions even when the surfaces of both cells

and magnetic particles are negatively charged (Prochazkova et al., 2013; Prochazkova, Safarik and Branyik, 2013; Safarik et al., 2015). This type of bonding can be moderated at molecular level through positively charged sections and local attractive electrostatic interactions despite general repulsions (Bos, Van der Mei and Busscher, 1999; Safarik et al., 2015). After microalgae harvesting, the next step in microalgae processing is drying of the harvested microalgae followed by cell lysis, lipid extraction and transesterification of extracted lipids to biodiesel. Before reviewing these steps, it is prudent to first review the synthesis of MNPs.

2.4.8.4. Synthesis of magnetic nanoparticles by co-precipitation

Magnetic nanoparticles can be synthesised using chemical, physical and biological techniques. Chemical techniques include: thermal-decomposition, micro-emulsion, hydrothermal synthesis, sono-chemical synthesis and co-precipitation (Lyon et al., 2004). Emphasis in this review is on the co-precipitation technique because it was employed in this work. Co-precipitation is the most popular chemical method of synthesizing MNPs in literature. This is because it is a more economical and faster technique. In this approach, ferric and ferrous salts are co-precipitated in basic medium followed by stabilization using hydroxide ions (Lyon et al., 2004; Laska et al., 2009). The overall reaction is summarised in equation 2.1:

$$Fe^{2+} + 2\ Fe^{3+} + 8\ OH^{-} \longrightarrow Fe_3O_4 + 4\ H_2O \qquad (2.1)$$

The above reaction is carried out in an oxygen free environment by bubbling through nitrogen gas. Bubbling nitrogen gas through the solution protects magnetite from being oxidized and helps reduce the particle size compared to reactions where nitrogen was not bubbled (Lyon et al., 2004). In an oxygen environment, the magnetite would be oxidized according to equation 2.2:

$$Fe_3O_4 + 0.25\ O_2 + 4.5\ H_2O \longrightarrow 3\ Fe(OH)_3 \qquad (2.2)$$

$$\text{Or } Fe_3O_4 + 0.5\ O_2 \longrightarrow 3\ Fe_2O_3 \qquad (2.3)$$

The above oxidation reaction would adversely affect the physical and chemical properties of magnetite. To prevent oxidation and agglomeration, magnetite is coated with organic or inorganic molecules during the synthesis process (Lyon et al., 2004). An example of

such molecules is tetra-methyl ammonium hydroxide (TMAOH) which acts as a peptizing agent. In the following paragraphs, different co-precipitation approaches to synthesis of MNPs will be critically evaluated.

In the first instance, Kandpal et al. (2014) reported on a method of synthesizing magnetite nanoparticles in which co precipitation was performed with only iron (ii) salts. In this method, the fresh particles synthesised had a size range of 5.65 - 8.16 nm (Kandpal et al., 2014). However, TEM images showed that the size range of particles was between 20 - 22 nm. This increment in particle size could have arisen from particle aggregation. This usually happens in absence of a stabilizing agent.

Secondly, Safari et al. (2013) synthesized nano sized magnetite particles in which the ratio of iron (ii): iron (iii) was 1:2 and the synthesis was under alkaline conditions using ammonium hydroxide at a stirring speed of 600 rpm, for 1 hour, in presence of argon. The ammonium solution was added until the pH was 11. The process was repeated at different temperatures and the particles were washed 5 times with ultra-pure water to eliminate unreacted chemicals then dried under vacuum at 70 °C (Safari and Zarnegar, 2013). The short coming with this method is the high temperature used in drying and storage of nanoparticles. This makes the process energy intensive and uneconomical.

Another co-precipitation method was demonstrated by Santos et al. (2016) in which magnetite nanoparticles were synthesized in an acidic medium at a ratio of iron (III) hexa-chloride: iron (II) tetra-chloride of 2:1 at room temperature in presence of ammonium hydroxide. This was followed by centrifugation of the dispersion and decanting of the magnetic precipitate. These particles had a mean diameter of 10 nm (Santos et al., 2016). The challenge with this method is the centrifugation of the dispersion which makes it an energy intensive technique.

Finally, Salunkhe et al. (2015) elucidated on a co precipitation approach in which the iron oxide nanoparticles were prepared in alkaline conditions using DIPA as the base. The mole ratio of iron (III) hexa-hydrate to Iron (II) tetra hydrate was 2:1, the two solutions were dissolved in a deoxygenated 0.5 M hydrochloric acid solution and the mixture added to 3 M deoxygenated DIPA solution under vigorous stirring for 2 hours. The nanoparticles

formed had an average size of 5.2 - 8.2 nm (Salunkhe et al., 2015). These steps are illustrated in Figure 2.16.

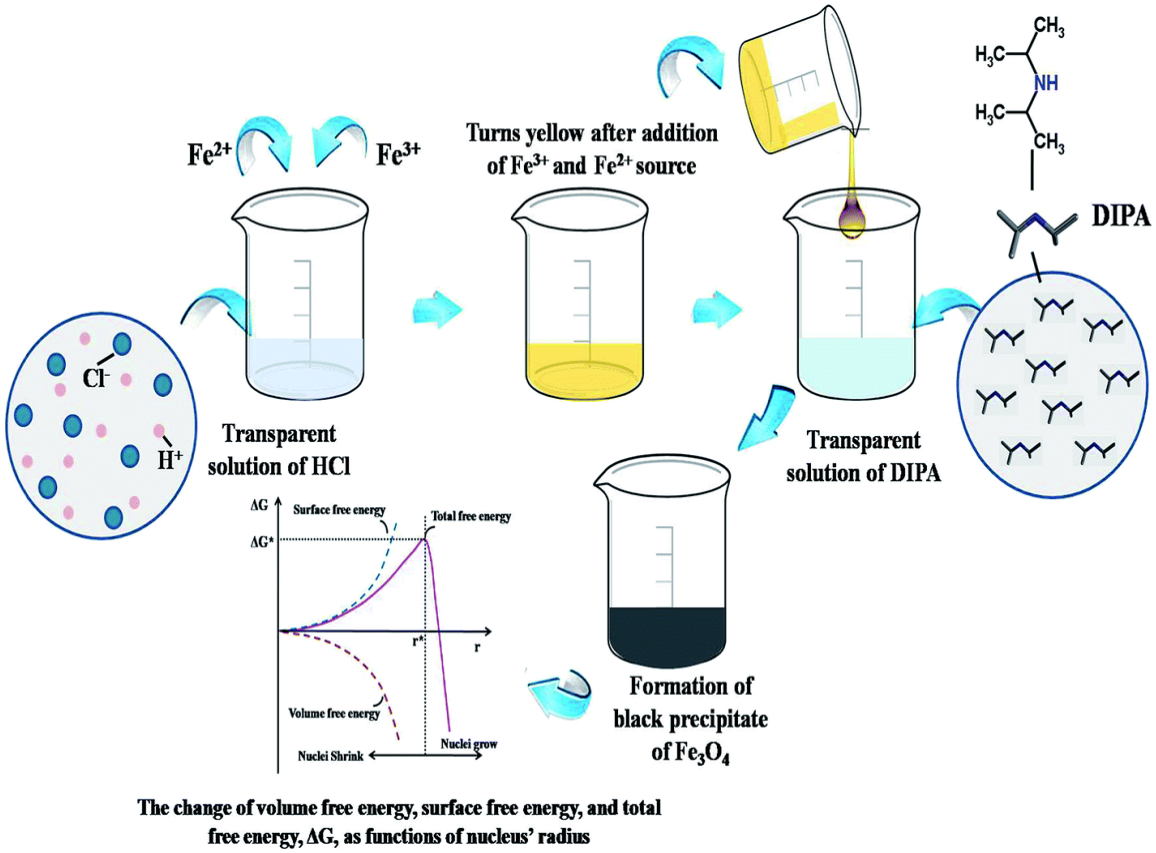

Figure 2. 16: Illustration of Co precipitation method for synthesis of iron oxide nanoparticles taken from (Salunkhe et al., 2015).

Table 2. 1. Summary of major microalgae separation processes in literature

Separation method	Highest Separation efficiency (%)	Energy usage (kWh m^{-3})	Separation cost ($ $m^{-3}day^{-1}$)	Reference
Screening/ Filtration	70-89	2.06	189–442	(Danquah et al., 2009; Uduman et al., 2010; Allnutt and Kessler, 2015)
Flocculation	90	varies	38–89	(Sukenik and Shelef, 1984; Allnutt and Kessler, 2015)
Gravity sedimentation	0.5-1.5	0.1	-	(Shelef, Sukenik and Green, 1984; Semerjian and Ayoub, 2003)
Flotation	90	10–20	38–89	(Sukenik and Shelef, 1984; Feris et al., 2000; Allnutt and Kessler, 2015)
Electrolytic separation	90	High	248–579	(Danquah et al., 2009; Allnutt and Kessler, 2015)
Centrifugation	90	8	207–484	(Heasman et al., 2000; Danquah et al., 2009; Allnutt and Kessler, 2015)
Magnetic separation	100	N/A	0.29 $ kg^{-1}-algal biomass	(Yadidia, Abeliovich and Belfort, 1977; Prochazkova et al., 2013)

2.5. Microalgae drying

Drying of microalgae biomass expels moisture, increases the biomass concentration and conserves the microalgae biomass for storage (Patel et al., 2012). The presence of water acts as a barrier to solvent extraction resulting in lower extraction efficiency (Balasubramanian, Doan and Obbard, 2013). However, if the harvested microalgae is subjected to hydrothermal liquefaction (HTL) or ionic liquid treatment, the drying step can be eliminated because the two process work best with wet microalgae. HTL with a water content of up to 78% and ILs extraction up to 91%. In regions with high temperature and low humidity, drying can be accomplished naturally. Otherwise, dryers or superheated steam is used to speed up the drying process. The most energy intensive process in microalgae lipid extraction is drying, accounting to over 50% of the total energy

requirements (Lardon et al., 2009). This energy requirement is met by burning fossil fuels, therefore a more sustainable way which does not use fossil fuels for drying microalgae is required for large scale biofuel processing (Sander and Murthy, 2010; Patel et al., 2012).

2.6. Extraction of lipids from microalgae

Extraction of microalgae lipids coupled with drying are the most costly and energy intensive steps in the production of biofuel from microalgae (Olkiewicz et al., 2015) (Figure 2.1). Efficient extraction of microalgae lipids is paramount for a sustainable and cost-effective production of biofuels and high value products from microalgae. A suitable extraction technique should minimise the co-extraction of unwanted compounds. All microalgae extraction techniques start with lysis of the cell wall to access the bio-chemical compounds within the cell (Rahul Kapoore et al., 2018). The cell lysis and extraction techniques are majorly divided into mechanical, chemical (solvent extraction), thermochemical, biological and electromagnetic techniques (Rahul Kapoore et al., 2018). Mechanical techniques majorly include bead milling, grinding, mechanical cell press and homogenisers. Chemical techniques include: Bligh and Dyers method (uses chloroform and methanol in a 1:2 mass ratio to extract lipids), extraction by ILs, oxidation, use of nanoparticles, super-critical fluid extraction, use of detergents, chelating agents and osmosis (Rahul Kapoore et al., 2018). For biological extraction, antibiotics, enzymes and phages are used. Techniques such as autoclaving, steam explosion, hydrothermal liquefaction and freeze-drying fall under thermos-chemical extraction. Electromagnetic extraction involves use of microwaves and ultrasound (Rahul Kapoore et al., 2018). In the next section, major extraction techniques such as mechanical extraction, solvent extraction and IL extraction were discussed. Solvent and ILs extractions were discussed in detail because they were applied in this research.

2.6.1. Mechanical extraction techniques

The most used mechanical technique for microalgae cell lysis is bead milling since it can lead to an effective lysis of the cell walls (Rahul Vijay Kapoore, 2014). However, this technique is not effective for the extraction of lipids from certain microalgae species like *Chlorella vulgaris* and *Chlorophyte* because of their small size, they go through

unaffected (Jae-Yon Lee et al., 2010). In addition, there is a problem of overheating and it is not economical for large-scale operations since the maintenance costs are high (Jae-Yon Lee et al., 2010). Furthermore, use of beads complicates the separation process since they have to be removed from the mixture (Gong and Bassi, 2016). Other mechanical methods like cell presses are not effective for microalgae lysis due to the small size of microalgae cells going through without being disrupted (Jae-Yon Lee et al., 2010). Methods like autoclaving and homogenisation would be suitable for microalgae cell lysis due to the low maintenance costs for autoclaves and homogenizers and can disrupt cell walls at room temperature. However, they both are not applicable on industrial scale due to the high energy input and autoclaves are not appropriate for extraction of pigments (Gong and Bassi, 2016).

The microwave method can be scaled up because of: *(i)* reduced solvent usage, *(ii)* effective cell lysis, *(iii)* efficient recovery of bioactive compounds, *(iv)* limited energy input, *(v)* quicker heating and *(vi)* fast reaction time (60 seconds) (Al Hattab, Ghaly and Hammoud, 2015; Rahul Kapoore et al., 2018). The disadvantage with this method is the high maintenance cost and generation of heat. Bath sonication is also a good method for extraction of microalgae lipids since: *(i)* It can be scaled up, *(ii)* no toxic substances are used, *(iii)* the maintenance costs are low, *(iv)* efficient cell wall lysis can be achieved and *(v)* it is a relatively fast method (1-2 hours) (Al Hattab, Ghaly and Hammoud, 2015). Most of the methods discussed so far may not be suitable for a low value product like biodiesel because the energy input and maintenance costs are high.

2.6.2. Solvent extraction

In this section, the possible solvent extraction mechanism, conventional solvent extraction techniques and IL extraction are discussed.

2.6.2.1. Solvent extraction mechanism

According to (Halim, Danquah and Webley, 2012), the mechanism for solvent extraction of lipids is divided into two sections (each with five steps). The upper section (Figure 2.17) illustrates the mechanism for non-polar solvents while the lower section illustrates the mechanism for polar/non polar solvent mixtures. For non-polar solvents, **Step 1.** The organic solvent penetrates through the cell membrane into the cytoplasm.

Step 2. The organic solvent attaches to the neutral lipids via Van der Waals interaction.

Step 3. An organic solvent/lipid complex is formed through the Van der Waals interaction.

Step 4. The complex is driven by a concentration gradient and it diffuses across the cell membrane into the static organic film encircling the cell.

Step 5. The complex moves through the static organic solvent film into the bulk organic solvent.

These steps mark the extraction of neutral lipids from the cell into the bulk non-polar solvent (Halim et al., 2011). The interaction between the organic solvent and the cell wall leads to formation of a static solvent film around the cell wall, this film remains uninterrupted by any movements from the bulk solvent or from mixing (Halim et al., 2011).

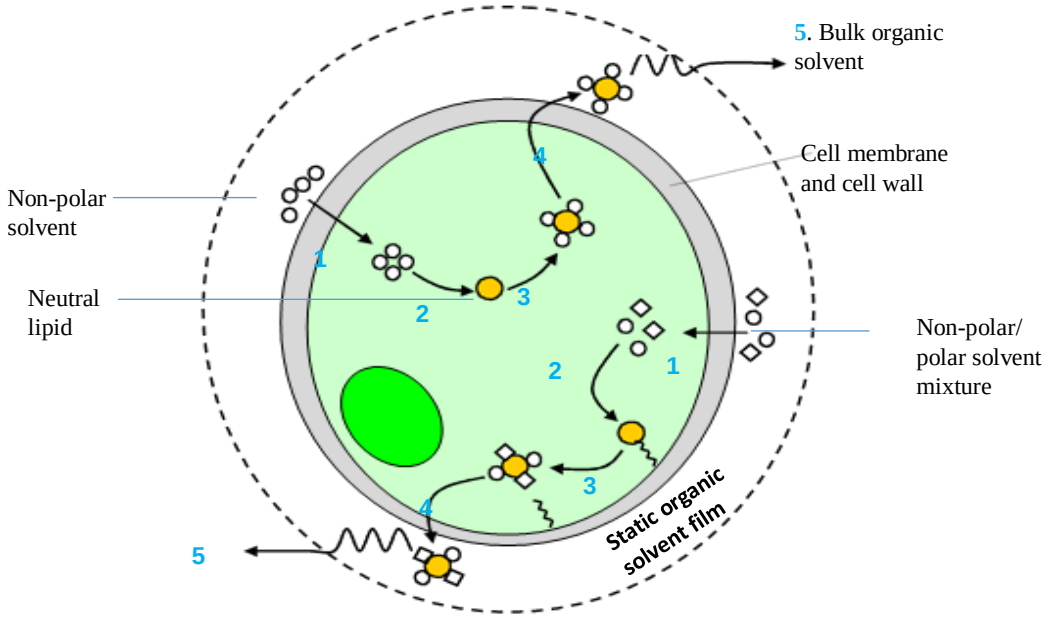

Figure 2. 17. Illustration of a potential extraction pathway of non-polar and polar lipids from microalgae cells using non-polar and polar solvents (Halim et al., 2011).

The lipid protein complexes are part of the cell membrane and are held together by stronger hydrogen bonds. Neutral lipids in the cytoplasm are at times in association with these lipid protein complexes. The weak Van der Waals forces formed between the non-polar solvents and the neutral lipids in the complex are unable to break the strong hydrogen bonds between proteins and lipids in the cell membrane. Therefore, polar solvents like

methanol or isopropanol are used instead. These solvents can disrupt the strong lipid-protein interactions through hydrogen bond formation with the polar lipids in the complex (Kates, 1972). According to (Halim, Danquah and Webley, 2012), the proposed mechanism for the lysis of the hydrogen bonds between lipids and proteins using non-polar/polar solvent mixture involves five steps as illustrated in Figure 2.17 (lower part).

Step 1. Involves the entry of the non-polar/polar solvent mixture into the cytoplasm through the cell membrane.

Step 2. The non-polar/polar solvent mixture then combines with the lipid complex and in the process, the polar organic solvent forms hydrogen bonds with the polar lipids while the non-polar organic solvent interacts with the neutral lipids through van der Waals forces.

Step 3. The stronger hydrogen bonding formed between the polar solvent and the lipid complex displaces the weak associations connecting the lipid complex to the cell membrane. This results in the formation of an organic solvent lipid complex that detaches from the cell membrane.

Step 4. The organic solvent lipid complex then diffuses across the cell membrane into the static solvent film encircling the cell.

Step 5. The solvent lipid complex finally crosses the static solvent film into the bulk organic solvent.

Neutral lipids in microalgae cells can be in form of free globules in the cytoplasm or in association with membrane protein complexes. To ensure complete extraction of all neutral lipids, both polar and non-polar organic solvents are added to the microalgae cells (Halim et al., 2011). One of the challenges with use of polar solvents in combination with non-polar solvents is the co-extraction of polar lipids and other polar compounds like pigments. These compounds act as impurities in the transesterification process thereby lowering the yield of biodiesel. For purposes of extracting lipids for biodiesel production, the use of non-polar solvents like hexane would be suitable as explained earlier.

2.6.2.2. Conventional solvent extraction techniques

Organic solvent extraction is the most used method of extracting lipids from microalgae. One of the most used solvent extraction methods is the Bligh and Dyers method. This method has been found to achieve the highest lipid yield (95%) compared to other

convention solvent extraction methods (Bligh and Dyer, 1959). It involves the use of chloroform, methanol and water in the ratio of 1:2:1.8. The solvents are mixed with the freeze-dried microalgae in the appropriate concentrations then vortexed to form a homogenous phase. Further mixing is done with the same quantity of chloroform giving an overall ratio of chloroform, methanol and water of 2:2:1.8 (Tang, 2014). After mixing, centrifugation is done to separate the chloroform and methanol layers. The chloroform is separated from lipids by distillation.

The Franz von Soxhlet method is also used commonly, it can be scaled up with ease and is cost effective (Soxhlet, 1879). However, when applied to microalgae extraction, it gives low lipid yields, is slow (taking approximately 15 hours) and uses large quantities of toxic solvent. The Soxhlet extraction procedure according to Magdalena et al., (2015) was as follows: *(i)* the freeze-dried algal biomass was ground using a mortar and pestle to form a homogenous powder, *(ii)* The ground biomass was transferred into a round bottom flask and an appropriate amount of hexane was added, *(iii)* The mixture was heated for a specified number of extraction cycles (more than one cycle was used) (Olkiewicz et al., 2015). Solvent extraction can achieve high extraction efficiency of lipids; however, the extraction process uses large quantities of toxic solvents e.g. hexane. In addition, it is an energy intensive process because solvents have to be evaporated and recycled. Furthermore, the process is laborious and can expose the bioactive compounds like pigments to excessive heat, light and oxygen that may alter the structure of the compounds (Rahul Kapoore et al., 2018). Because of the undesirable effects of conventional solvent extraction, alternative green and environmentally friendly extraction techniques like ILs are being developed. In the next section, ILs extraction is explored in detail.

2.6.3. Application of ILs in extraction of microalgae lipids

Ionic liquids are organic salts that contain a relatively larger organic cation paired with a smaller organic or inorganic anion usually with a melting point below 100 °C (Pragya, Pandey and Sahoo, 2013). The cations are usually composed of nitrogen in the ring structure for example imidazolium or pyrimidine. The cation consists of many different functionalities on the side groups (Figure 2.18). The side groups determine the polarity of the ILs. The anions differ ranging from single ions for example Cl^- to complex ones

(Young et al., 2010). Figure 2.17 shows the structures of the most common cationic and anionic ILs.

Structure of the common organic cations in ILs

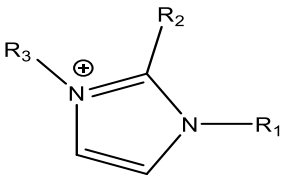

Imidazolium

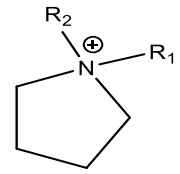

Pyrrolidinium

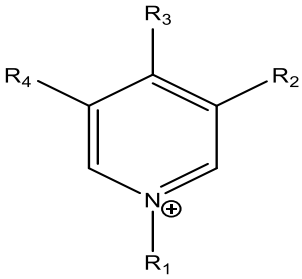

Pyridinium

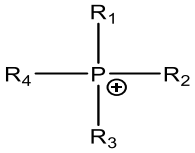

Phosphonium

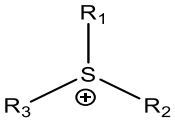

Sulfonium

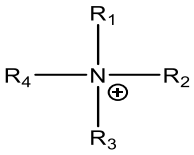

Ammonium

Structure of the common organic anions in ILs

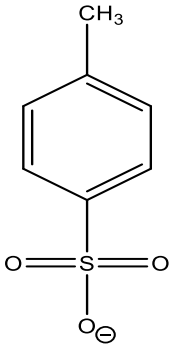

Tosylate

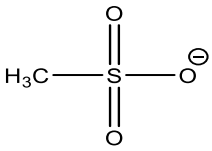

Methanesulfonate

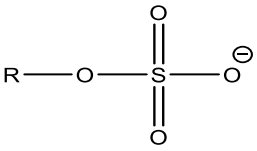

Alkylsulfate

Structure of the common inorganic anions in ILs

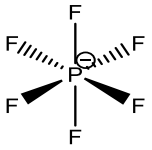

Hexafluoro-phosphate

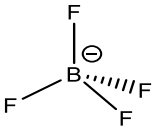

Tetrafluoro-phosphate

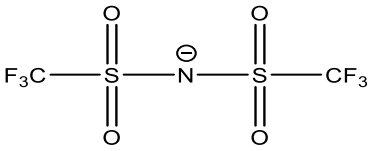

Bis (trifluoromethyl-Sulfonyl) imide

Halides (such as Cl^- and Br^-)

Figure 2. 18. Structures of the common cationic and anionic ionic liquids

2.6.3.1. Properties and applications of ILs

Ionic liquids possess excellent properties that make them suitable for different chemical and biochemical applications. Because of their ionic character, they do not have a considerable vapour pressure (Earle et al., 2006). This makes them resistant to combustion, evaporation and appropriate in vacuum applications. It also gives them a high thermal and mechanical stability as well as a high electrochemical stability. The solvent properties of ionic liquids such as melting point, boiling point, viscosity and miscibility can also be tuned through appropriate ion combinations and through the design of each ion to suite the relevant application such biomass processing (Wishart, 2009). In addition, they also have other fascinating properties like immiscibility with water (hydrophobic ILs) or organic solvents (hydrophilic ILs) resulting in the formation of two-phase systems.

The properties of ILs are highly dependent on the choice of the cation and this determines the stability of the IL (Zhao et al., 2002). While the choice of the anion determines the chemistry and functionality of the IL. Ionic liquids synthesised from strong acidic, oxidizing or reducing compounds can be used repeatedly without breakdown (Zhao et al., 2002; Miao and Chan, 2006). This is advantageous since it enables complete recycling of the IL resulting in a more sustainable and economical application of ILs. Application of ionic liquids in extraction of microalgae lipids is dependent on their ability to dissolve biomass. This is because they can function as hydrogen bond acceptors with a reduced ability to act as hydrogen bond donors. The anion on the IL forms hydrogen bonds with the hydroxyl groups of the cellulose, this results in the lysis of the hydrogen bond cross linkages of the polysaccharide and in the process the biomass is solubilized (Remsing et al., 2006). There are many kinds of ionic liquids. The most common forms are based on dialkylimidazolium, tetraalkylammonium, alkylpyridinium, or tetraalkylphosphonium cations coupled with an inorganic anion (Olivier-Bourbigou and Magna, 2002). Apart from extraction of lipids from microalgae lipids, ILs have numerous applications, for example in separation processes they have been used to extract proteins from biphasic aqueous systems (Pei et al., 2009) and for lipid esterification (Guo et al., 2007).

2.6.3.2. Lysis of microalgae cells using ILs

Owing to their excellent properties as discussed in the previous section, ILs have been used as replacements for hazardous organic solvents in many chemical and biochemical reactions. In microalgae lipid extractions, ILs are used to dissolve the cellulose walls and disrupt the microalgae cellular structure (Sun-A Choi et al., 2014). Teixeira et al., (2012) reported on the application of chloride ILs to dissolve wet microalgae biomass and achieved higher lipid yields than the conventional Bligh and Dyer method (Teixeira, 2012). Wet extractions (in presence of water) using polar ILs eliminates the drying step resulting in an energy efficient and potentially economical extraction process. The use of ILs in wet microalgae extraction results in a reduced energy demand on the system (0.4 MJ kg^{-1}) compared to conventional solvent extraction processes, which consumes 4-9 MJ kg^{-1} (Teixeira, 2012). Polar ILs like 3-methyl-imidazolium methyl hydrogen phosphonate ($[C_2mim]$-$[MeO(H)PO_2]$) could dissolve marine microalgae at room temperature without heating (Fujita et al., 2013).

Kim et al., (2012) reported on the efficient extraction of microalgae lipids using a mixture of ILs [Bmim][CF_3SO_3] (1-Butyl-3-methylimidazolium tri-fluoro-methane-sulfonate) with methanol in a 1:1 volume ratio. Methanol was used to reduce the viscosity of the ILs. (Kim et al., 2012). After dissolving the microalgae biomass in the ILs, the lipid phase floated since it was insoluble in the hydrophilic ILs phase and it separated by centrifugation. The lipid yield from ILs extraction method was compared with that from the Bligh and Dyer's method. It was established that the ILs method gave higher yields (12.5%) compared to 10.6% from the Bligh and Dyer's method while [Emim][$MeSO_4$] (1-Ethyl-3-methylimidazolium methyl sulphate) yielded 11.9% (Kim et al., 2012). They also observed that hydrophilic ILs gave a higher yield of lipids compared to the hydrophobic ILs possibly due to the high solubility of lipids in the hydrophobic ILs. The low lipid yield from the hydrophobic IL was thought to be due to solubility of lipids into the ILs phase resulting in partitioning of lipids between the ILs and methanol phase. Table 2.2 summarises the yields of lipids obtained from application of different ILs for lysis of microalgae cell.

Co-solvents consisting of a hydrophilic IL like [Emim][$MeSO_4$] and methanol have been used at a mass ratio of 1:2 to extract lipids from microalgae (Young et al., 2010). The extracted lipids were auto-partitioned to the hydrophobic or the immiscible phase for ease of recovery after extraction. In this case, where co-solvents were used, it was further proposed that the purpose of polar covalent molecule was for cell wall lysis and improvement in the efficiency of lipid extraction from microalgae biomass (Young et al., 2010).

Table 2. 2. A summary of the lipid yields and some FAME yields from different ILs used in extraction of lipids from microalgae at different treatment conditions

Ionic Liquid	Microalgae	Treatment conditions	Lipid yield wt. %	FAME Yield wt. %	Ref
1-Ethyl-3-methylimidazolium Methyl sulphate [C2mim] [$MeSO_4$]	*Chlorella sp.*	7.4 g IL + 1000 mg of dry microalgae + 8900 mg of methanol at 65 °C for 18 h	8.6		(Young et al., 2010; Orr et al., 2015)
	Duniella sp	7.4 g IL + 1000 mg of dry microalgae + 8900 mg of acetone at 65 °C for 18 h	9.2		(Young et al., 2010; Orr et al., 2015)
	Duniella sp	7.4 mg IL + 1000 mg of dry microalgae + 8900 mg of 2 propanol at 65 °C for 18 h	8.5		(Young et al., 2010; Orr et al., 2015)
1,3dimethylimidazolium methyl phosphate [C1mim] [$MeOPO_3$]	*C. vulgaris*	0.25g microalgae + 2.5 g IL at ambient temperature for 16 hrs + water content 9.1% + mild mixing.	9.0		(Orr et al., 2015)
1-ethyl-3-methylimidazolium ethanoate [C2mim] [O_2CMe]	*C. vulgaris*	0.25g microalgae + 2.5 g IL at ambient temperature for 16 hrs + water content 15.5% mild mixing.	5.0		(Orr et al., 2015)
1-ethyl-3-methylimidazolium ethyl sulphate [C2mim] [$EtSO_4$]	*C. vulgaris*	0.25g microalgae + 2.5 g IL at ambient temperature for 16 hrs + water content 0.3 % mild mixing.	13.0		(Orr et al., 2015)
1-hexyl-3-methylimidazolium chloride 30.6% [C_6mim] Cl	*C. vulgaris*	0.25g microalgae + 2.5 g IL at ambient temperature for 16 hrs + water content 30.6 % mild mixing.	8.0		(Orr et al., 2015)
1-butyl-3-methylpyridinium bromide [C_4mβpy] [Br]	*C. vulgaris*	0.25g microalgae + 2.5 g IL at ambient temperature for 16 hrs + water content 10.9 % mild mixing.	15.0		(Orr et al., 2015)

Di-methyl-ethyl ammonium 2- methoxyethanoate [N0 1 1 2] [$MeOCH_2CO_2$]	*C. vulgaris*	0.25g microalgae + 2.5 g IL at ambient temperature for 16 hrs + water content 0.6 % mild mixing.	14.0		(Orr et al., 2015)
Dimethyl-2-hydroxy-ethyl-4-hydroxyl-butyl-ammonium chloride	*C. vulgaris*	0.25g microalgae + 2.5 g IL at ambient temperature for 16 hrs + water content 0.9% mild mixing.	1.0		(Orr et al., 2015)
Dioctylbutyl-methyl-ammonium chloride [N1 4 8 8] Cl	*C. vulgaris*	0.25g microalgae + 2.5 g IL at ambient temperature for 16 hrs + water content 8.8% mild mixing	15.0		(Orr et al., 2015)
Propyl-ammonium nitrate [N0 0 0 3] [NO_3]	*C. vulgaris*	0.25g microalgae + 2.5 g IL at ambient temperature for 16 hrs + water content 2.0% mild mixing	14.0		(Orr et al., 2015)
Tributylmethylphosphonium methanote [P1 4 4 4] [O_2CH]	*C. vulgaris*	0.25g microalgae + 2.5 g IL at ambient temperature for 16 hrs + water content 0.2% mild mixing	4.0		(Orr et al., 2015)
Tributylmethylphosphonium Propanoate [P1 4 4 4] [O_2CEt]	*C. vulgaris*	0.25g microalgae + 2.5 g IL at ambient temperature for 16 hrs + water content 1.0% mild mixing	25.0		(Orr et al., 2015)
[C_2mim] [NTf_2]	*C. vulgaris*	1.0 g dry microalgae + 9500 mg IL + 9500 mg chloroform 120 °C, 2 h	25.6		(Sun-A Choi et al., 2014)
[C_2mim] [CH_3SO_3]	*C. vulgaris*	1.0 g dry microalgae + 9500 mg IL + 9500 mg chloroform 120 °C, 2 h	16.9		(Sun-A Choi et al., 2014)
[C_2mim] [Et_2PO_4]	*C. vulgaris*	1.0 g dry microalgae + 9500 mg IL + 9500 mg chloroform 120 °C, 2 h	22.2		(Sun-A Choi et al., 2014)
[C_2mim] Cl	*C. vulgaris*	1.0 g dry microalgae + 9500 mg IL + 9500 mg chloroform 120 °C, 2 h	1.7		(Sun-A Choi et al., 2014)
[C_2mim] [Et_2PO_4]	*C. vulgaris*	1.0 g dry microalgae + 19000 mg IL at 120 °C for 2 hours. Then direct transesterification of lipids		24.6	(Sun-A Choi et al., 2014)
[C_4mim] Cl	*C. vulgaris*	1.0 g dry microalgae + 19000 mg IL at 120 °C for 2 hours. Then direct transesterification of lipids		0.037	(Sun-A Choi et al., 2014)
[C_2mim] Cl	*C. vulgaris*	1.0 g dry microalgae + 19000 mg IL at 120 °C for 2 hours. Then direct transesterification of lipids		23.5	(Sun-A Choi et al., 2014)
1-Butyl-3-methyl imidazolium methyl sulphate [Bmim][$MesO_4$]	*C. vulgaris*	5 ml IL + 500 mg dry microalgae at 60 °C. After dissolution added 5 ml of distilled water + 30 ml of n hexane	4.7	0.074	(Kim et al., 2013)
Butyrolactam formate (BTF)	*Chlorella sp*	Ratio of IL: microalgae 10:1 (w/w) at room temperature for 24 hours.	4.5		(Shankar et al., 2017)

	Chlorococcum sp	Ratio of IL: microalgae 10:1 (w/w) at room temperature for 24 hours.	1.3		(Shankar et al., 2017)
Butyrolactam acetate (BTA)	*Chlorella sp*	Ratio of IL: microalgae 10:1 (w/w) at room temperature for 24 hours.	4.2		(Shankar et al., 2017)
	Chlorococcum sp	Ratio of IL: microalgae 10:1 (w/w) at room temperature for 24 hours.	0.82		(Shankar et al., 2017)
Butyrolactam hexanoate (BTH)	*Chlorella sp*	Ratio of IL: microalgae 10:1 (w/w) at room temperature for 24 hours.	7.1		(Shankar et al., 2017)
	Chlorococcum sp	Ratio of IL: microalgae 10:1 (w/w) at room temperature for 24 hours.	2.0		(Shankar et al., 2017)
Caprolactam hexanoate (CPH)	*Chlorella sp*	Ratio of IL: microalgae 10:1 (w/w) at room temperature for 24 hours.	5.6		(Shankar et al., 2017)
	Chlorococcum sp	Ratio of IL: microalgae 10:1 (w/w) at room temperature for 24 hours.	1.7		(Shankar et al., 2017)
Hydrated phosphonium IL $P(CH_2OH)_4Cl$	*N. oculata*	1 g of microalgae + 10-cm^3 IL heated to 100 °C for 24 hrs.	12.8	14.9	(Olkiewicz et al., 2015)
	C. vulgaris	1 g of microalgae + 10-cm^3 IL heated to 100 °C for 24 hrs.	8.1	12.8	(Olkiewicz et al., 2015)

In conclusion, it is evident that imidazolium based ILs are the most used ILs for lysis of microalgae cells and extraction of lipids. It is also evident that some ILs (Table 2.2) can dissolve the cellulose cell walls of microalgae and release lipids and other cellular components at room temperature. This allows for an energy efficient recovery of the extracted lipids. Finally, unlike conventional solvent extraction, the excellent properties of ILs as earlier discussed enable an oil extraction process that is sustainable and less hazardous to the environment.

2.7. Transesterification of extracted lipids to biodiesel

Biodiesels are monoalkyl esters of long chain fatty acids commonly derived from vegetable lipids and animal fats (Pinto et al., 2005). Biodiesel production from extracted microalgae lipids is done by the transesterification process (Robles-Medina et al., 2009). The transesterification process converts the extracted microalgae lipids (triglycerides or

free fatty acids) to the fatty acid methyl esters (biodiesel) which have a lower molecular weight (Rawat et al., 2011) (see reaction 2.4). Transesterification involves a reaction between the triglyceride (fat or lipids) with a short chain alcohol preferably methanol in the presence of a catalysts to produce fatty acid methyl esters and glycerol as a by-product (Reaction 2.4) (Rawat et al., 2011). R_1, R_2 and R_3 represent long chain hydrocarbons or fatty acid chains. The most common fatty acid chains usually include palmitic (C16:0), stearic (C18:0), oleic (C18:1) and linoleic (C18:2). The lipid number for example C18:1 means an 18-carbon chain fatty acid with 1 double bond. Methanol is mainly used in this reaction because it is less costly, more reactive and the fatty acid methyl esters produced from its use are more volatile (Robles-Medina et al., 2009).

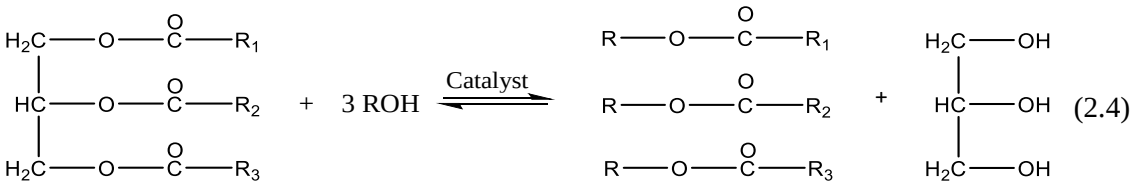

(2.4)

Triglyceride Alcohol Alkyl esters/biodiesel Glycerol

Before the transesterification process, all impurities in the lipids such as water, free fatty acids and phospholipids should be removed because they interfere with the process and lower the yield of biodiesel (Al Hattab, Ghaly and Hammoud, 2015). For example, phospholipids can produce lecithin, an emulsifier, which can be removed in the degumming step by membrane filtration (Van Gerpen and Dvorak, 2002; Dennis YC Leung, Wu and Leung, 2010). For microalgae lipids extracted using hexane such impurities are minimised because they are hydrophilic and cannot be extracted with hexane.

The use of an appropriate catalyst in this reaction can increase the reaction rate and the product yield (Demirbas, 2009). The catalysts used are sometimes acidic, basic or even enzymatic in kind (Rawat et al., 2011). If the extracted lipids contain some free fatty acids, the base catalyst can react with it to produce soap according to reaction 2.5 (saponification).

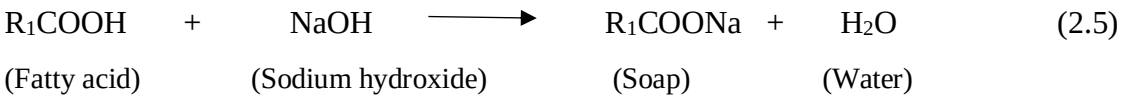

Reaction 2.5 is unwanted because the formation of soap leads to reduction in yield of biodiesel and hinders the separation of esters from glycerol (Halim et al., 2012). It also binds on the catalyst thereby requiring more catalyst for the process and hence increasing the processing costs (Dennis YC Leung, Wu and Leung, 2010). In an alkali catalysed transesterification process, the maximum amount of free fatty acid is 2.5 wt. %. Beyond this amount, a pre-treatment step would be essential for an efficient transesterification process (Center, 2006). The water from the saponification reaction (reaction 2.5) lowers the transesterification reaction rate through hydrolysis of triglycerides to di-glycerides forming more free fatty acids according to reaction 2.6 (Dennis YC Leung, Wu and Leung, 2010).

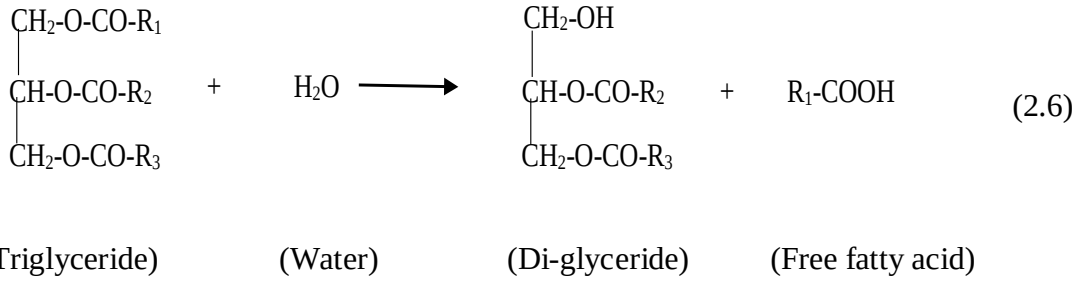

If an acid catalyst is used, the free fatty acids are converted to biodiesel by reaction with an alcohol according to reaction 2.7. Therefore, acid catalysed transesterification is essential for lipids with a high amount of free fatty acids.

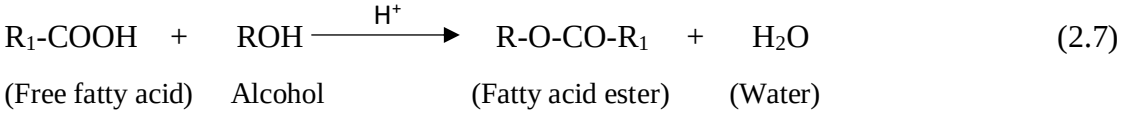

The catalyst used in reaction 2.7 is usually concentrated sulphuric acid, but acid catalysed reactions are slow and the molar ratio of methanol to lipid should be high (up to15). This is the reason why acid catalysed transesterification is rarely used. As mentioned earlier,

three main catalyst types are used in transesterification of lipids to biodiesel: Base, acidic and enzymatic catalysts. These are discussed in the next section.

2.7.1. Base catalysed transesterification

Base catalysed trans-esterification is the most widely used process for biodiesel production (Pragya and Pandey, 2016). Some of the most common catalysts used in base catalysed transesterification include potassium hydroxide, sodium hydroxide and sodium methoxide (Uduman et al., 2010). It is advantageous because the reaction is quick, does not require high temperature and pressure conditions and the conversion rate is high with no intermediate steps (Dennis YC Leung, Wu and Leung, 2010). However, the homogeneous base catalysts are hygroscopic and therefore difficult to store because they absorb water. In addition, when they are mixed with the alcohol reactants, they form water hence greatly affecting the yield (DYC Leung and Guo, 2006) and requiring better handling procedures. Furthermore, some base catalysts are in solid phase and can easily be separated from the product by filtration hence reducing the washing requirement. The high heat of reaction of the metallic base catalysts makes it difficult to control the reaction. Therefore, metallic alkoxides like sodium methoxide in methanol are better alternatives than metal hydroxides such as NaOH and KOH (Pragya and Pandey, 2016). Alkaline alkoxides give high yields in a shorter reaction time. For example according to (Pragya and Pandey, 2016) in 30 minutes of reacting lipids with alkoxides, a biodiesel yield of 98% was achieved. However, presence of water limits their efficiency and this is a hindrance to their application on industrial scale (Schuchardt, Sercheli and Vargas, 1998).

2.7.2. Acid catalysed transesterification

The most commonly used acids for acid catalysed trans-esterification include: sulphuric acid, hydrochloric acid, sulfonic acid and phosphoric acid (Robles-Medina et al., 2009). Acid catalysts can be used together with base catalysts in a two-step process. Feedstock containing large amounts of free fatty acids like waste cooking oil can best be processed using acid catalyst. In the first step, the acid catalysts convert the free fatty acids to methyl esters and in the second step base catalysts convert the remaining triglycerides to methyl esters (Pragya and Pandey, 2016). In converting micro-microalgae lipids to biodiesel, acid catalysts showed a better conversion in comparison to base catalysts. This was reported

by Robles et al. (2009) when transesterification was done on 250 mg of lipid from C*haeotoceros mulleri,* it was established that 10 mg of biodiesel was registered when an acid catalyst was used compared to only 3.3 mg when base catalyst was used (Robles-Medina et al., 2009). The corrosive nature of acid catalysts hinders their application on industrial scale.

2.7.3. Enzyme catalysed transesterification

Enzyme catalysed transesterification has become appealing of recent because it eliminates the undesirable property of soap forming during the reaction. In addition, it is easier to purify the products since the soap is not formed (Dennis YC Leung, Wu and Leung, 2010). The set back with use of enzymes lies in the long reaction time and their high costs. However to reduce the high costs, new enzyme biocatalysts have been developed in recent years (Robles-Medina et al., 2009). The most used enzyme is lipase, it can be found in two types: Extra cellular lipase and intracellular lipase. Extracellular lipases are extracted from living microorganism like C*andida Antarctica* or *Mucor Miehei* and purified while intracellular lipases are inside the cells. Intra and extra cellular lipases can be immobilized before use. This helps to eliminate downstream operations such as enzyme recycling and separation (Robles-Medina et al., 2009).

2.7.3. Factors affecting biodiesel yield

2.7.3.1. Amount of alcohol

The molar ratio of alcohol to triglycerides is one of the major factors that influence the yield of biodiesel in transesterification reactions (DYC Leung and Guo, 2006; Dennis YC Leung, Wu and Leung, 2010). Under ideal conditions, the mole ratio of alcohol to triglycerides is 3:1and this produces 3 moles of fatty acid methyl ester and 1 mole of glycerol. However, in real practice, excess alcohol is used to ensure complete conversion of triglycerides to biodiesel in a shorter time. There is usually increase in biodiesel yield with increase in the ratio of alcohol to triglyceride however, further increase in the alcohol ratio beyond the optimum amount would not increase the yield of triglycerides but will instead increase the cost of recovering alcohol (DYC Leung and Guo, 2006). The molar ratio is also related to the type of catalyst used in the transesterification reaction. When an alkali catalysts is used, the molar ratio of alcohol to triglycerides is usually 6:1 in most

experiments (Bernard Freedman, Butterfield and Pryde, 1986; Yea Zhang et al., 2003). When an acid catalysts is used for transesterification and the amount of free fatty acids in the lipids is high, then the ratio of alcohol to triglycerides of up to 15 to 1 is used (Ali, Hanna and Cuppett, 1995; DYC Leung and Guo, 2006).

2.7.3.2. Reaction temperature

The optimum temperature for transesterification reactions is between 50 ℃ to 60 ℃ subject to the type of lipid used (Ma and Hanna, 1999; DYC Leung and Guo, 2006). If the temperature exceeds the optimum, then the biodiesel yield decreases. This is because a higher temperature favours the saponification of triglycerides to soaps (Eevera, Rajendran and Saradha, 2009). Temperatures above the boiling point of alcohol can result in alcohols leaking out through vaporisation.

2.7.3.4. Reaction time

The rate of conversion of fatty acid esters increases with reaction time (BEHP Freedman, Pryde and Mounts, 1984). Initially the reaction is slow because the alcohol is being dissolved into the lipids. After the dissolution, the reaction rate increases spontaneously and within 90 minutes, the maximum yield is achieved and any further increase in reaction time has no effect on the yield of biodiesel (DYC Leung and Guo, 2006; Alamu et al., 2007).

2.7.3.4. Catalyst loading

The amount of catalyst used has a direct effect on the yield of biodiesel. At low catalyst concentrations, there is low yield of biodiesel. As the catalyst concentration increases, there is a gradual increase in biodiesel yield until the optimum catalyst loading (1.5 wt.%) (Dennis YC Leung, Wu and Leung, 2010). Further increase in catalyst concentration beyond the optimum will result into a slight reduction in yield of biodiesel. The reduction in yield at excess catalyst loading is due to reaction between the triglycerides with the excess catalyst to form soap. The most commonly used catalyst in the transesterification reaction is sodium hydroxide (Dennis YC Leung, Wu and Leung, 2010). But according to Freedman et al., (1984), when sodium hydroxide is mixed with methanol some water is formed and this water causes a hydrolysis reaction leading to breakdown of triglycerides to di-glycerides and fatty acids (BEHP Freedman, Pryde and Mounts, 1984). This reaction

lowers the yield of biodiesel. To overcome this, the alkali catalyst (sodium hydroxide) is first mixed with methanol to form sodium methoxide and then added to the lipid (Dennis YC Leung, Wu and Leung, 2010). Sodium methoxide generally gives higher biodiesel yield compared to sodium hydroxide.

2.8. Hydrothermal liquefaction (HTL) of microalgae

The HTL process is a wet thermochemical conversion process in which biomass is converted to biocrude oil at temperatures ranging between 200-375 °C and pressures between 40 - 200 bars (Peterson et al., 2008). Since wet biomass is used, it eliminates the need for drying microalgae biomass. The HTL process uses less than 5% of the total energy used in the algae drying step of solvent extraction (Zou et al., 2009).

2.8.1. Process description

In the batch HTL process, biomass with a water content of 75 - 95% is introduced into the reactor, which is then tightly closed and pressurised (Figure 2.19A). Pressurizing the reactor prevents blockage of reactor tubes caused by the boiling biomass/water mixture. The pressurised reactor is transferred into a pre-heated furnace for a specified reaction time (Figure 2.19B). A thermocouple connected to a computer records the reaction temperature as a function of time while a pressure gauge connected to the reactor directly records the pressure inside as the reaction proceeds. The products from the HTL process are distributed in the gas phase, an aqueous phase and a solid phase. These will be discussed in detail later.

Figure 2. 19. Images of Batch HTL Reactors: A) A pressurised HTL reactor fitted with a thermocouple and a pressure gauge, B) HTL reactors fitted in a furnace whose temperature was set to 400 ºC (Images taken from the catalytic combustion lab, Department of Chemical Engineering University of Bath).

Most of the research on hydrothermal liquefaction in literature has been carried out in batch reactors (Jazrawi et al., 2013). However, continuous HTL can ensure a more economically feasible process. Most reports in literature are on continuous HTL of lignocellulose and waste biomass as feedstock and few on aquatic biomass such as algae. For example, continuous HTL of hemicellulose recovered from corn cob was performed at 200 $^{\circ}$C for 10 minutes (Makishima et al., 2009). Swine manure was also used in continuous HTL at a reaction temperature of 305 $^{\circ}$C and a residence time of 80 minutes, a bio-crude with a HHV of 31 MJ kg^{-1} was produced and the reactor was operated for 16 hours successfully (Ocfemia, Zhang and Funk, 2006). In addition, continuous HTL of food sludge feedstock has also been carried out in presence of catalysts such as potassium carbonate and zirconium oxide at reaction temperatures of 350 $^{\circ}$C and residence times of 5-10 min in a reactor with volume of 0.1 L (Hammerschmidt et al., 2011). Furthermore, continuous HTL of microalgae in a pilot plant was carried out using Chlorella and Spirulina at biomass loadings of 1-10 wt. %, temperatures of 250-350 $^{\circ}$C, residence time of 3-5 minutes and pressures of 150-200 bar. The maximum bio-crude yield obtained was 41.7 wt. % using chlorella as feedstock, at a solid loading of 10 wt. %, at 350 $^{\circ}$C and 3 minutes residence time (Jazrawi et al., 2013). Fast continuous hydrothermal liquefaction of microalgae in a lab scale reactor has also been reported. The reaction was performed at

300 to 380 °C at a residence time of 0.5 to 4 minutes. The highest bio-crude yield was 38 wt.% at 380 °C and 30 seconds holding time (Patel and Hellgardt, 2015). However, continuous HTL reactors are susceptible to deposition of solid char within the reactor which may result in clogging (Maiella and Brill, 1998). In addition, the biocrude yields are low possibly due to the very short residence time. Furthermore, there was a high oxygen content (10.9 wt.% at 325 °C for 4 minutes) in the bio-crude oil from fast continuous HTL (Patel and Hellgardt, 2015). The high oxygen content lowers the heating value of the biocrude oil.

During the HTL process, water at subcritical state acts as a reactive medium converting biomass into liquid crude oil under controlled conditions (Rojas-Pérez et al., 2015). In this conversion, the main cellular constituents such as lipids, proteins and carbohydrates are broken down into smaller molecules which recombine to form hydrocarbons with a high calorific value (Rojas-Pérez et al., 2015). Due to the high cost involved in extracting microalgae lipids using solvents, the HTL process has recently been considered as a more viable alternative (Andrew Lee et al., 2016). The HTL process uses less energy than extraction and transesterification of lipids (Barreiro et al., 2014; Andrew Lee et al., 2016). It uses less than 5% of the energy needed for complete thermal drying of microalgae in the drying step of solvent extraction (Lixian Xu et al., 2011a). Therefore, the energy intensive drying step is eliminated and it provides avenues for extraction of other compounds within the microalgae biomass (Faeth and Savage, 2016; Harvind Kumar Reddy et al., 2016).

The very high temperature and pressure in the HTL process coupled with hydrolytic attack of biomass leads to breakage of biomolecules in hot compressed water resulting into the production of biocrude oil (Faeth and Savage, 2016). The biocrude oil is mainly recovered from the solid phase using solvents such as dichloromethane, chloroform, acetone and hexane. Under combustion, the biocrude oil produces low sulphur compared to petroleum oils and has a low ash content resulting in less discharge of particulates. However, it may result in high emission of NO_X gases owing to the high amount of nitrogen from proteins and chlorophyll (Barreiro et al., 2013). This is one of the major challenges of microalgae-

based fuels derived from the HTL process. Research is underway to address this challenge through de-nitrogenation of biocrude oils (Costa and De Morais, 2011).

2.8.2. HTL Process Schemes

The most common HTL process schemes consist of three major steps: cultivation, harvesting and microalgae HTL (Figure 2.20A). The other interesting process scheme was proposed by Garcia Alba et al., (2011), it involves four major steps: microalgal cultivation, harvesting, fractionation and microalgae HTL (Figure 2.20B) (Garcia Alba et al., 2011). Fractionation involves microalgae pre-treatment steps such as drying, cell lysis and solvent extraction of high value compounds. Cell lysis techniques such as mechanical or ultrasound techniques can be used before solvent extraction.

After extraction of high value compounds such as proteins, vitamins and pigments, the remaining parts of the cells are subjected to the HTL process to produce biocrude oil, aqueous phase, solid phase and gas phase. Since the aqueous phase is rich in nutrients, it can be recycled back to the algal cultivation step. The fractionation step has an advantage of reducing the nitrogen content of the biocrude if the proteins are extracted as high value co-products (Garcia Alba et al., 2011). It is well known that the high nitrogen content of biocrude arises from the breakdown of protein during the HTL process. Some microalgae species such as Spirulina have a protein content of up to 63%. The fractionation step reduces this high protein content. The major limitation of the fractionation step is the general reduction in the biocrude yield.

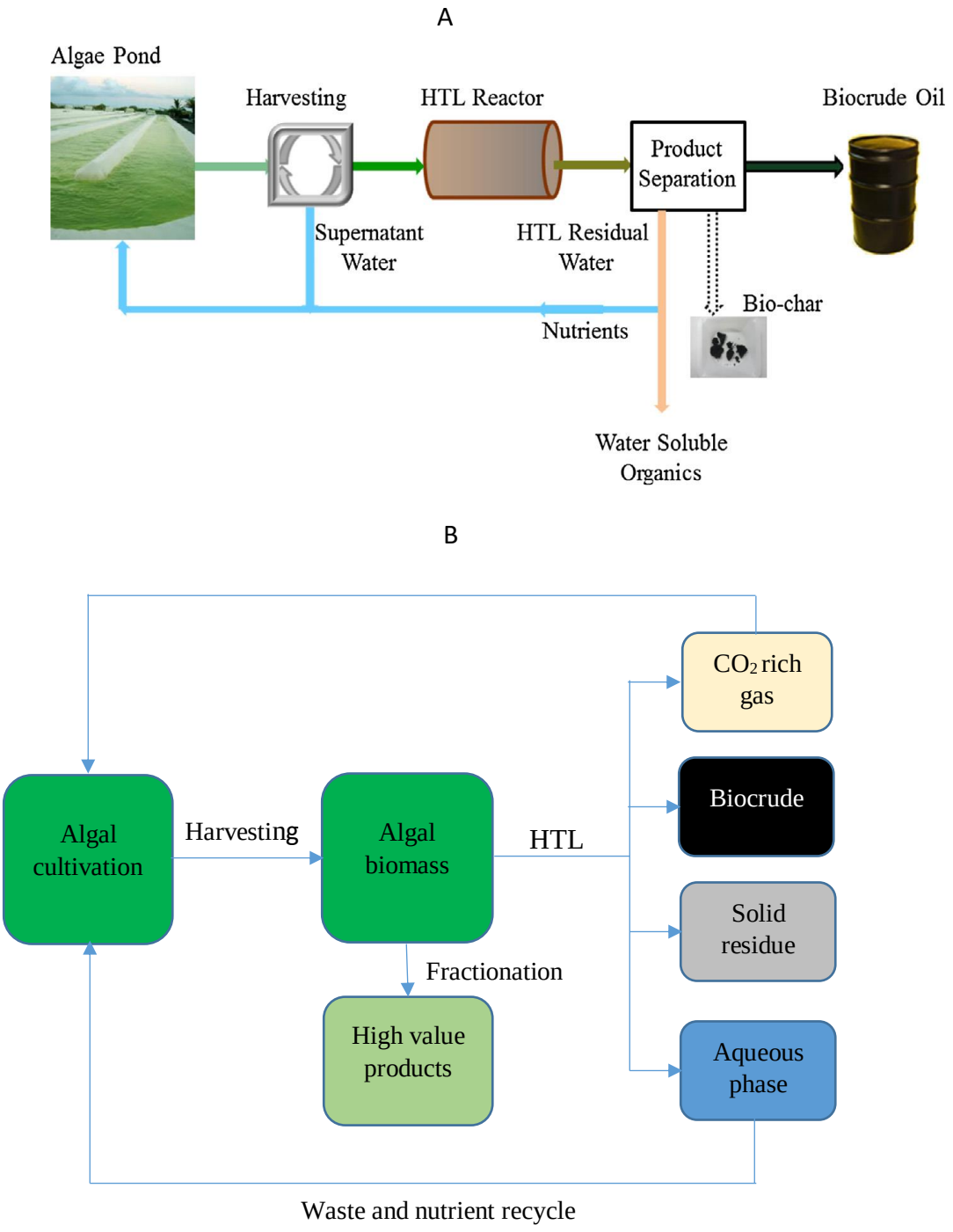

Figure 2. 20. Illustration of the HTL Process from microalgae Harvesting Stage to Biocrude oil Production. A) HTL of whole microalgae cell (Harvind Kumar Reddy et al., 2016), B) HTL of microalgae cell after extraction of essential compounds (adapted from (Garcia Alba et al., 2011).

2.8.3. Chemistry of the HTL process

During the HTL process, hot compressed water is under subcritical state and under such conditions, its properties are different from water at standard conditions (Toor, Rosendahl and Rudolf, 2011). These properties include: *(i)* weakening and reduction in number of hydrogen bonds, *(ii)* There are more ions in solution due to the increase in ionic product of water (10^{-12} compared to 10^{-14} at 25 ºC) leading to increased concentration of H^+ and OH^- ions (Barreiro et al., 2013) and there is promotion of reactions that are catalysed by acids and bases for example hydrolysis reactions, *(iii)* There is also an increase in the solubility of hydrophobic organic compounds due to a reduced permittivity of water (from 78 F m^{-1} at 25 ºC and 1 bar to 14.07 F m^{-1} at 350 ºC and 200 bar) (Barreiro et al., 2013).

The HTL process involves hundreds of concurrent reactions such as decarboxylation of carbohydrates to sugars and breakdown of aldehydes, hydrolysis of fats to fatty acids and breakdown of fatty acids to long chain hydrocarbons, depolymerisation and deamination of proteins and re-polymerisation of the reactive particles into larger compounds (Toor, Rosendahl and Rudolf, 2011). Because of the numerous simultaneous reactions, the HTL reaction mechanism is not yet well elaborated in the literature and the influence of different reaction conditions such as temperature, catalyst type and reaction time are still not well understood. However, it is known that during the HTL process, there is competition between two major reactions: *(i)* hydrolysis and *(ii)* re-polymerization (Garcia Alba et al., 2011; Barreiro et al., 2013).

Hydrolysis takes place at the initial stage of the process when the microalgae are broken down and depolymerised to smaller compounds. Then polymerization of these small and reactive fragments takes place to form biocrude and other compounds in the solid and gas phase (Demirbaş, 2000; Yang et al., 2004; Biller and Ross, 2011). The reduction in biocrude usually observed with increase in reaction temperature or holding time is due to the breakdown of components from the biocrude into other phases like the gas phase (Anastasakis and Ross, 2011). This observation is confirmed by the decrease in biocrude viscosity with increase in holding time and temperature (Tomoaki Minowa et al., 1995). Microalgae conversion mechanisms have been proposed, for example below 250 ºC, most compounds in the biocrude were derived from the liquefaction of lipids and algaenans,

while increasing temperature to between 300-375 ºC promoted the conversion of carbohydrates and proteins (Torri et al., 2012).

During the HTL process, the main microalgae components like lipids, proteins and carbohydrates are decomposed to different compounds. Lipids are composed of glycerol and fatty acid chains. The glycerol is converted to compounds like methanol, ethanol, allyl alcohol, acrolein, propionaldehyde, formaldehydes and gaseous products such as CO, CO_2 and H_2 (Bühler et al., 2002). The fatty acids in the lipids have a higher thermal stability but may be converted to long chain hydrocarbons (Barreiro et al., 2013). Proteins are hydrolysed to amino acids, which undergo decarboxylation to carbonic acid and amines. The amines are then deaminated to ammonia and organic acids. These products are then re-polymerised to long chain hydrocarbons and aromatic compounds such as phenol and hetero aromatics such as indole (Peterson et al., 2008; Barreiro et al., 2013). The products of carbohydrate breakdown are polar water-soluble organic compounds such as organic acids, alcohols, aldehydes and benzene (Peterson et al., 2008; Biller and Ross, 2011; Toor, Rosendahl and Rudolf, 2011; Barreiro et al., 2013). Algaenans are insoluble macropolymers made of hydrocarbons and they are more resistant to chemicals than all other microalgae fractions. During the HTL process, algaenans are converted to hydrocarbons with different chain lengths such as alkanes and alkenes. There is limited data in literature on microalgaenans because their resistance to chemical treatments makes it hard to analyse their chemical behaviour (Torri et al., 2012).

2.8.4. Products from the HTL process

2.8.4.1. Biocrude oil

After HTL, microalgae biomass is degraded into a dark, viscous and energy heavy liquid referred to as biocrude oil (Figure 2.21). The energy content of biocrude oil varies from 70 to 95% (Brown, Duan and Savage, 2010).

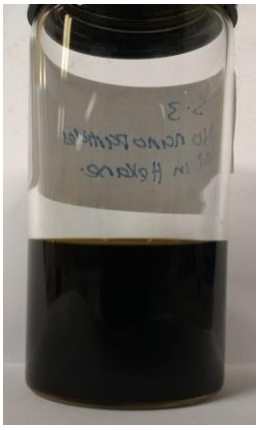

Figure 2. 21. Biocrude oil dissolved in dichloromethane after HTL (photo taken from our lab)

The type of feedstock and processing conditions play a key role in determining the physical and chemical properties of biocrude oil. According to Torri et al. (2012), the compounds in biocrude oil are largely divided into three groups: *(i)* lipid derivatives, *(ii)* protein derivatives and *(iii)* algaenan derivatives (Torri et al., 2012). Lipid derivatives include compounds such as fatty acids and sterols, protein derivatives include peptides and cyclic peptides while heavy insoluble materials are classified under algaenans. Biocrude resembles petroleum crude in nature (Biller and Ross, 2011).

2.8.4.2. Solid residue

Solid residue from HTL is largely composed of ash and a small amount of nitrogen, hydrogen and sulphur (Figure 2.22). The yield of solid residue is mostly below 10 wt.% according to most authors (T Minowa and Sawayama, 1999; Yang et al., 2004). Figure 3.4 shows biomass solid residue after spirulina HTL in the presence of magnetic nanoparticles (MNPS) at 320 ºC for 60 minutes (Egesa, Chuck and Plucinski, 2017).

Figure 2. 22. Solid residue composed of MNPs and microalgae biomass after HTL (photo taken from our lab).

According to Egesa et al., (2017) the elemental composition of solid residue in absence of MNPs at 320 ºC for 60 minutes was: 20.8 wt. % C, 1.8 wt. % H, 0.9 wt. % N, 22.9 wt. % O and 0.2 wt. % S. While in presence of MNPs (mass ratio of MNPs to microalgae of 0.4): 5.1 wt. % C, 0.71 wt. % H, 0.5 wt. % N, 0.18 wt. % S and 14.1 wt. % O (Egesa, Chuck and Plucinski, 2017). Jena et al., (2011) also reported an elemental composition of solid residue after HTL of Spirulina at 350 ºC for 60 minutes as follows: 11.8% C, 1.8% H, 1.4% N and 0.6% S (Jena, Das and Kastner, 2011). In presence of MNPs, fewer elements were observed in the solid residue suggesting a more effective biomass conversion to biocrude oil.

2.8.4.3. Aqueous phase

The aqueous phase is composed of a high of amount organic matter and nutrients. It also has metal ions mostly composed of: ammonium, sodium, potassium, magnesium, CH_3COO^- and phosphate ions (Biller and Ross, 2011; Barreiro et al., 2013). Some studies have demonstrated that microalgae can be successfully grown on the aqueous phase after the HTL process utilizing the nitrogen in this phase for growth, though the growth rate was slower compared to microalgae grown on culture medium (T Minowa and Sawayama, 1999). The carbon source in the aqueous phase is a potential source of carbon for hetero-trophic microalgae (Barreiro et al., 2013).

2.8.4.5. Gas phase

The gaseous phase is largely composed of carbon dioxide (96-99%) and gives a yield of 7.3 – 16.2% (Sofia Raikova et al., 2016b). In the gas phase, hydrogen gas is next to carbondioxide in abundance, other gases in this phase include methane, nitrogen, ethane and ethene (Brown, Duan and Savage, 2010). The concentration of carbondioxide has been reported to decline beyond the supercritical point of water while the concentration of shorter chain hydrocarbons like C_1 and C_2 increases (Barreiro et al., 2013). The amount of CO is reportedly very low suggesting that removal of oxygen during HTL occurs mainly through decarboxylation and not decarbonylation (Garcia Alba et al., 2011). The other possibility is that the CO undergoes the water gas shift reaction to form CO_2 and H_2O (Elliott and Sealock Jr, 1983).

2.8.6. Effect of process conditions on biocrude yield

By controlling experimental conditions, it is possible to increase the yield of biocrude oils from biomass liquefaction. The factors affecting yield of biocrude oil include temperature, reaction time, reactor loading, catalysts, solvents and feedstock composition (Jena, Das and Kastner, 2011; Valdez et al., 2012; MP Caporgno et al., 2016a; Harvind Kumar Reddy et al., 2016). These are discussed in detail in the sections below.

2.8.6.1. Temperature

Temperature is a very essential parameter with a significant effect on the HTL process (Valdez et al., 2012; Hao Li et al., 2014b; MP Caporgno et al., 2016a). The average operating range of temperature in the literature is between 300 - 375 °C (Table 3.1 and Figure 3.5). Increase in biocrude yield occurs when temperature is increased at sub-critical conditions (Zou et al., 2010; Biller and Ross, 2011; Garcia Alba et al., 2011; Jena, Das and Kastner, 2011; Barreiro et al., 2013). Temperature increase beyond the sub-critical/HTL region (Figure 2.23) leads to reduction in oil yield due to increased gasification. Temperature has also been reported to have an effect on the properties of the biocrude oil (Tomoaki Minowa et al., 1995; Garcia Alba et al., 2011). For example an increase in temperature has been shown to lower the oxygen content of the biocrude oil resulting in an increase in the high heating value (HHV) of the biocrude oil (Tomoaki Minowa et al., 1995; Jena, Das and Kastner, 2011). In addition, temperature increase leads

to a higher nitrogen content of the biocrude oil (Barreiro et al., 2013) possibly due to increased break down of proteins. Increase in temperature also leads to increase in the gas yields and reduction in the solid residue yields (Brown, Duan and Savage, 2010; Barreiro et al., 2013).

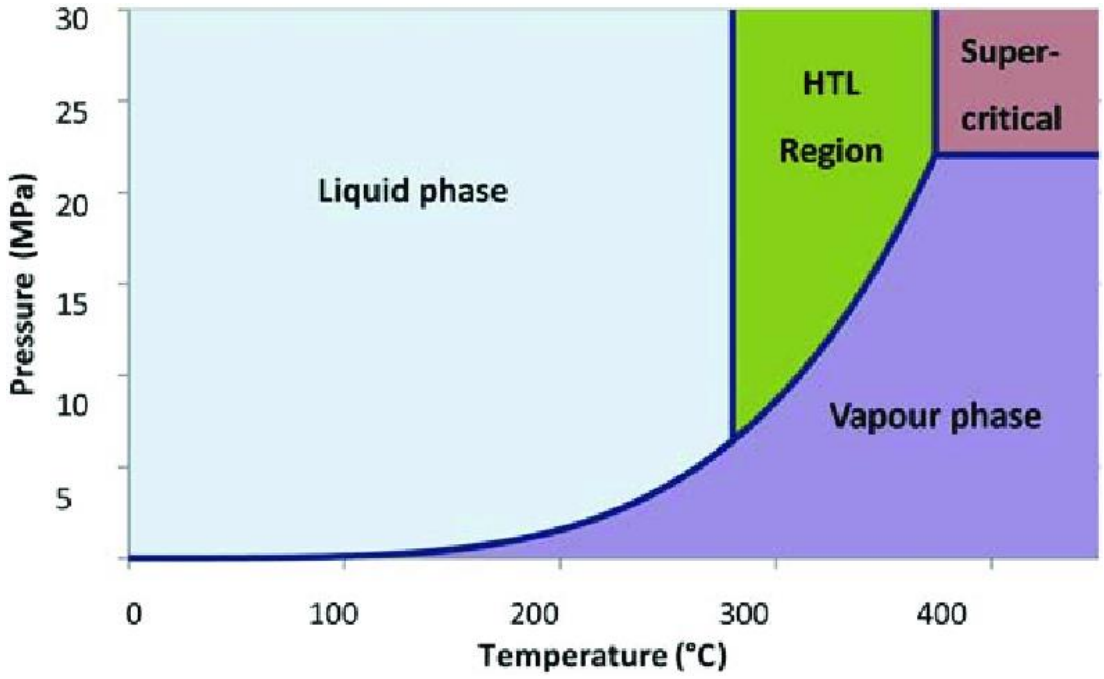

Figure 2. 23. Phase diagram for the HTL process (Wagner, 2016)

Harvind et al., (2016) investigated the effect of temperature on the HTL of *Nannochloropsis gaditana* and *Chlorella sp*. In this investigation, the reactor was charged with 50 ml of microalgae slurry and purged 3 times with nitrogen gas to expel air, initial pressure was maintained at 200 psi, the temperature was increased from 180 °C to 330 °C and the final pressure was recorded at the target temperature. They observed an increment in yield of biocrude oil with increase in temperature for both microalgae species, however further increase in temperature resulted in a decrease in biocrude yield due to increased gasification. It was further observed that though the trend was similar in both microalgae species, the yield of biocrude from *Chlorella species* was smaller due to lower lipid content of the biomass (Harvind Kumar Reddy et al., 2016).

2.8.6.2. Holding time

The holding time is the time at which the final reaction temperature is maintained constant excluding the heating and cooling time. There is an inverse correlation between the reactor holding time and the temperature. A higher reaction temperature requires a shorter holding time to obtain a higher yield of biocrude oil. A lower reaction temperature requires a longer holding time to obtain a higher biocrude oil yield. Optimisation of holding time is paramount for a cost effective HTL process.

2.8.6.3. Reactor Loading

Few reports in literature have investigated the effect of reactor loading on HTL biocrude yield. Faeth et al (2016) investigated the effect of reactor loading on the biocrude yield in a fast HTL process. It was observed that the biocrude yield was highest when the biomass content in the reactor was below 5%. A reduction in biocrude yield was also observed when the water loading of the reactor was increased beyond 60% (Faeth and Savage, 2016). Martin et al. (2016b) however reported that concentrations of solid below 5% could result into a negative energy balance and above 15% may lead to difficulties of feeding biomass into the reactor by pump (Martín Pablo Caporgno et al., 2016b). Therefore, optimisation of reactor loading is essential for a cost effective HTL process and for maximum yield of biocrude oil.

2.8.6.4. Solvent used

Rawel et al. (2015) investigated the effect of solvents such as ethanol, water and methanol on the liquefaction of *Ulva fasciata*. They noted that alcohols act as solvents as well as donating hydrogen to facilitate further transesterification reactions hence increasing the biocrude yield (Rawel Singh, Bhaskar and Balagurumurthy, 2015). The effect of solvents on the biocrude yield was also reported by Matsui et al. (1997). In their investigation, Spirulina was liquefied in the presence of toluene and (Fe $(CO)_5$-S) catalyst for 60 minutes at 350 °C. The lipid yield was 61 wt. % and the lipid fractions had a higher carbon content and a lower oxygen content (Matsui et al., 1997). It is likely that the decomposition of toluene during the HTL process may have contributed to this very high biocrude yield.

2.8.6.5. Effect of catalysts on HTL process

Very recently, a lot of effort has been invested in investigating the effect of catalyst on the efficiency of the HTL process and its ability to produce high quality biocrude oil by lowering the oxygen content in the oil. Some studies have revealed that there is no influence of acid base catalyst on the yield of biocrude oil only sodium hydroxide had an effect of increasing the biocrude yield compared to the normal HTL yield (Biller and Ross, 2011; Jena, Das and Kastner, 2011; Harvind Kumar Reddy et al., 2016). Among the most used HTL catalysts, solid nano catalysts have attracted a lot of attention due to their large chemically active surface area and high chemical and physical stability which are important factors in industrial application (Dong Zhou et al., 2010). The following section will explore some of the solid catalysts so far used in the HTL process.

Matsui et al., (1997) investigated the liquefaction of Spirulina with an iron catalyst (Fe $(CO)_5$-S), the lipid yield increased linearly from 54.4 to 63.7 wt.% as the amount of catalyst increased from 0 to 1.0 mmol at 350 °C for 60. The amount of catalyst used to achieve this yield was 1.0 mmol (Matsui et al., 1997). However, the shortcoming with these catalysts is that their recovery and recycling is a challenge since they are molecularly dispersed. Also, Ni/Al_2O_3 catalysts have been used but with a slight increase in biocrude yield and the catalyst could convert the triglycerides in the biomass to fatty acids and then to alkanes at temperature of 350 °C and pressure of 150-200 bar (Biller, Riley and Ross, 2011). In addition, the biocrude oils were deoxygenated by up to 10 wt.%.

Jena et al. (2009) were among the first to use solid catalysts in HTL process. They used NiO catalyst in the liquefaction of Spirulina and mixed microalgae from an open pond with wastewater at 350 °C, the added catalyst instead decreased the yield of bio crude oils and led to increment in the carbon fraction in the gaseous products (Jena and Das, 2009). NiO is also known to efficiently catalyse gasification reactions (Elliott, 2008). Duan and Savage (2010) were the first to report on the use of common heterogeneous catalysts in hydrothermal liquefaction of *Nannochloropsis sp* (Duan and Savage, 2010). They used three noble metal catalysts supported on carbon (Pd/C, Ru/C, Pt/C), one hydrotreatment catalyst (Sulfided CoMo/γ-Al2O3), one transition metal catalyst supported on silica-alumina (Ni/SiO_2-Al_2O_3) and one zeolite catalyst (Aluminium silicate). It was observed

that Pd/C showed the highest yield of biocrude (close to 60%) compared to all other catalysts tested. The yield from the other catalysts was almost similar in the range of 45 – 50% but higher than the yield of the un-catalysed HTL process. They also noted that the addition of high-pressure hydrogen to the reaction system resulted into a higher yield of biocrude oil in the un-catalysed liquefaction and had no effect on the yield of biocrude on the catalysed liquefaction.

Duan and Savage., (2010) also investigated the effect of catalysts on the elemental composition of biocrude oil. They observed that carbon supported Pt, Pd and Ru increased the H/C molar ratios even in absence of added hydrogen and the presence of Pt, Ni, and CoMo catalysts resulted into biocrude with lower O/C ratios than the biocrude produced in their absence (Duan and Savage, 2010). The results indicated that catalytic deoxygenation or catalytic hydrodeoxygenation took place. Furthermore, it was revealed that the biocrude produced in a catalysed hydrogen environment had a higher heating value than that in an inert environment. Also, Ru/C and Ni/SiO_2- Al_2O_3 produced biocrude with the lowest nitrogen content while Ni/SiO_2-Al_2O_3, Ru/C and CoMo/Al_2O_3 showed activity for sulphur removal.

The challenge with solid catalysts is in their recovery from the catalyst biocrude mixture by means of conventional filtration methods, which are not economically viable. Therefore it is paramount to develop heterogeneous catalysts that can easily be recovered and recycled for continuous thermochemical reactions (Akia et al., 2014). As a result, iron oxide based nanocatalysts are potential candidates because they can be easily separated by magnetic field hence improving their lifetime and cost effectiveness. Furthermore, they have large specific surface areas, less resistance to mass transfer and high catalytic activity for bio catalysis, photo-catalysis, and phase transfer catalysis (Akia et al., 2014). Very few studies have embarked on the application of iron oxide based nanocatalysts in HTL. Iron oxide based nanocatalysts are advantageous since they exhibit high catalytic activity, can be magnetically separated with ease and can be recycled with ease. Research on the use of iron oxide nanocatalysts is still in its infant stages, further investigation on the catalytic effect of iron oxide based nanocatalysts on the yield and chemical composition of biocrude needs to be done. This thesis seeks to bridge this gap

by developing magnetically responsive iron based nanocatalysts that can easily be recovered and recycled.

2.8.6.5.1. Possible HTL catalytic reaction pathway

The HTL process involves hundreds of concurrent and competing reactions (Sofia Raikova et al., 2016b). Some studies have used model compounds to investigate the mechanism of reaction with relation to that specific compound. An example of such studies is the HTL catalytic reaction pathway involving the deoxygenation of stearic acid (a fatty acid) over heterogeneous catalysts at supercritical water conditions. This was proposed by (Watanabe, Iida and Inomata, 2006). The addition of a base catalyst such as potassium hydroxide or sodium hydroxide in a batch reactor at 673 K resulted into monomolecular decarboxylation of stearic acid in supercritical water leading to the production of carbondioxide and C_{17} alkane (Figure 2.24).

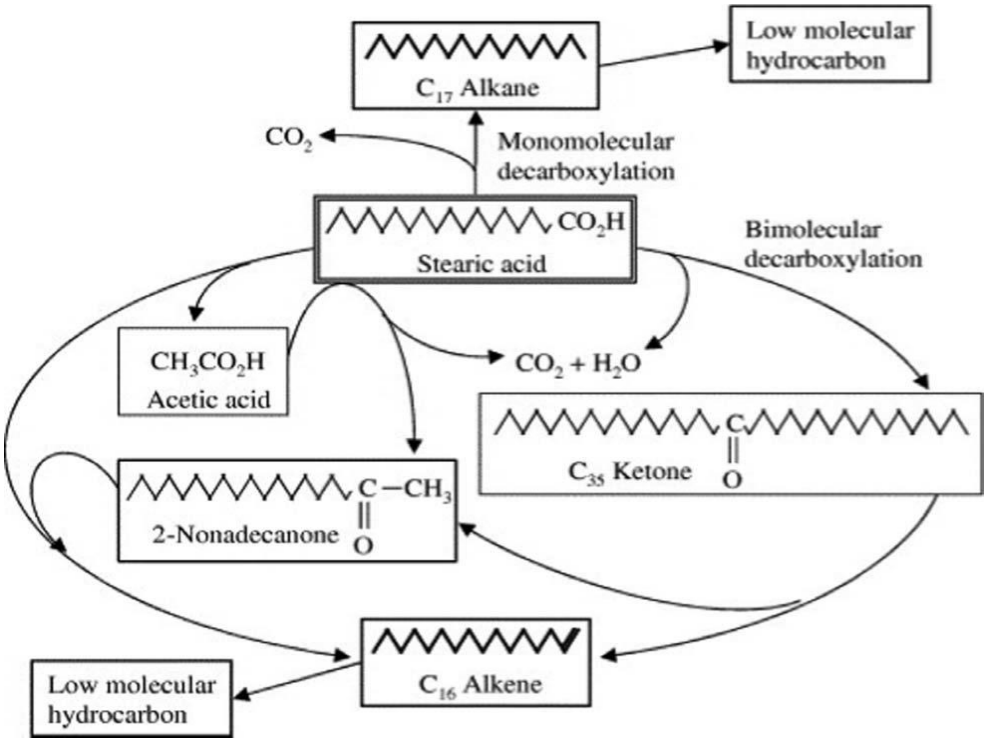

Figure 2. 24. Conversion of stearic acid in supercritical water (Watanabe, Iida and Inomata, 2006)

When using metal oxide catalysts such as CeO_2 and ZrO_2, different bimolecular decarboxylation pathways were proposed (Figure 2.24) resulting into the production of C_{16} alkene either through the direct bimolecular decarboxylation of stearic acid or *via* the breakdown of the intermediate C3 ketone and 2-nonadecanone, which was also present in the product.

2.8.5. HTL conditions in the academic literature

Most HTL experiments in literature are carried out at temperatures between 300 – 375 °C and at liquefaction times of between 5 to 120 minutes. In some processes, catalysts were used to enhance the biocrude yield and improve the biocrude quality through denitrogenation and deoxygenation of biocrude oil. The reactors used are usually below 100 mL some with agitation while others without agitation. It is worth noting that comparing HTL experiments in literature is difficult since they were carried out at different conditions and using different microalgae species whose lipid content and characteristics are different. However, it is useful to give an insight of what different HTL conditions can achieve. Table 2.3 summarises several conditions and yield from HTL of various microalgae species.

Table 2. 3. Summary of microalgae HTL experimental conditions, biocrude yield and nitrogen content of biocrude after HTL of different microalgae species.

Microalgae strain	Lipid (wt.%)	HTL conditions	Yield (wt.%)	N (wt.%)	Reference
Chlorella. pyrenoidosa	<1	280 °C for 120 min, no catalyst	39.4	N/A	(G Yu et al., 2011)
Spirulina	13.1	350 °C for 60 min, toluene and (Fe $(CO)_5$-S) catalyst	61	6.8	(Matsui et al., 1997)
Nannochloropsis sp.	28	350 °C 60 min, no catalyst	39	4.4	(Valdez, Dickinson and Savage, 2011)
Spirulina powder	6	320 °C for 60 min with MNPs	37.1	6.05	(Egesa, Chuck and Plucinski, 2017)
Spirulina powder	6	320 °C for 60 min no catalyst	35.5	7.5	(Egesa, Chuck and Plucinski, 2017)
Botryococcus braunii	50	300 °C for 60 min, Na_2CO_3 (5%)	64	0.7	(Dote et al., 1994)
Dunaliella tertiolecta	22.17	360 °C for 30 min, no catalyst	36.9	N/A	(Zou et al., 2010)
Dunaliella tertiolecta	20.5	300 °C for 5 min, 0, 5 wt.% Na_2CO_3	43.8	NA	(Patil, Tran and Giselrød, 2008)
Nannochloropsis sp.	28	350 °C 60 min, Pd (Pt, Ru)/C	57	NA	(Duan and Savage, 2011)
Nannochloropsis sp.	28	350 °C 60 min CoMo/C-Al_2O_3, zeolite	57	NA	(Duan and Savage, 2011)
Chlorella vulgaris	25	350 °C 60 min, no catalyst	36	5.9	(Biller and Ross, 2011)
Microcystis viridis	-	340 °C 30 min, Na_2CO_3 (5%)	33	7.1	(Yang et al., 2004)
Spirulina platensis	13.1	350 °C 60 min, no catalyst	39.9	6.3	(Jena, Das and Kastner, 2011)
Desmodesmus sp.	10-14	375 °C 5 min, no catalyst	49	6.3	(Garcia Alba et al., 2011)
Porphyridium cruentum	8	350 °C 60 min, Na_2CO_3 (1 mol L^{-1})	27.1	3.2	(Biller and Ross, 2011)

From Table 2.3, the lowest liquefaction temperature was 280 °C while the highest was 375 °C. Most of the experiments were done at 350 °C for 60 minutes. The longest liquefaction time was 120 minutes while the shortest was 5 minutes. It is worth noting that at longer liquefaction times, lower HTL temperatures were used (280 °C) while at shorter liquefaction times, higher temperatures were used for example 375 °C. The highest biocrude yield obtained was 61% from Spirulina liquefaction at 350 °C for 60 minutes.

The Spirulina lipid content was 13.1 wt. % and liquefaction was done in presence of toluene and (Fe $(CO)_5$-S) catalyst. The very high biocrude yields were due to the effect of the catalyst and solvent used in the HTL process. The lowest biocrude yield from Table 2.3 was 27.1%, this was from the liquefaction of *Porphyridium cruentum* at 350 °C for 60 minutes in presence of Na_2CO_3 catalyst. The lipid content in the microalgae was 8 wt. %. This low biocrude yield is possibly due to the low lipid content of the microalgae feedstock. Considerably high biocrude yields (57%) were also registered when typical petroleum upgrading catalysts such as Pd (Pt, Ru)/C and CoMo(C-Al_2O_3) were used in the liquefaction of *Nanochloropsis sp* at 350 °C for 60 minutes. The lipid content in the microalgae was 28 wt. %. This high lipid content may have also contributed to the high yield of biocrude oils.

2.9. Conclusions

Microalgae are a promising feedstock for biofuel production, but several challenges hinder the development of biofuels using their feedstock. Cultivation of microalgae using open ponds or photo-bioreactors is expensive since it requires provision of light, nutrients, pumping carbon dioxide gas and adequate mixing. Therefore, these expenses are reflected in the final biofuel product making it more expensive than petroleum derived fuels. Use of microalgae from wastewater treatment plants may be a solution to reduce the cost of microalgae cultivation. The costly microalgae harvesting step is another challenge hindering the commercialization of biofuels derived from microalgae. The harvesting techniques currently used are expensive and energy intensive. Therefore, development of potentially economical separation techniques such as magnetic separation of microalgae may be a positive step to solving this challenge. The other challenge is the energy intensive lipid extraction step. The drying of microalgae prior to solvent extraction and the evaporation of large quantities of hazardous solvent after extraction consume a lot of energy making the process energy intensive and hazardous. Therefore, use of ionic liquids in wet extraction can be a solution to this challenge since ILs are less hazardous and can solubilise microalgae cells even at room temperature.

In addition, application of thermochemical processing techniques such as hydrothermal liquefaction of microalgae to biocrude oil may be an alternative since the oil extraction

step is avoided. The HTL process is a promising biomass conversion technique since the whole microalgae cell is converted to biocrude oil without the need for lipid extraction and it uses less energy compared to the convention solvent extraction process since there is no need for the drying step. However, it contains many N and O compounds that must be removed to improve the biofuel quality. Development of catalysts for denitrogenation and deoxygenation of biocrude is essential for improvement of the quality of HTL fuels. Addressing these challenges would potentially result in biofuels being more competitive with petroleum-derived fuels in terms of cost.

3. Multifunctional Role of Magnetic Nanoparticles in Efficient Microalgae Separation and Catalytic Hydrothermal Liquefaction

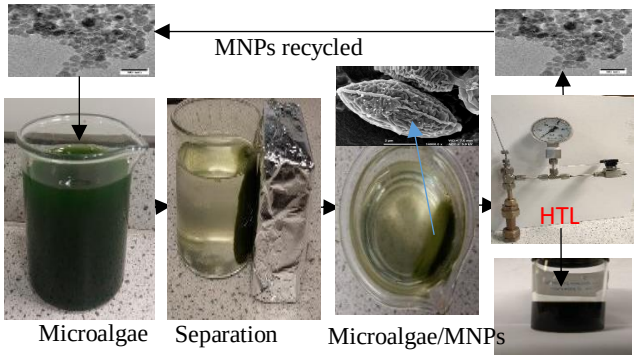

In this Chapter, magnetic nanoparticles (MNPs) were synthesised, characterised and used to separate microalgae from culture medium. The microalgae separation efficiency was optimised at different conditions. The microalgae/particle slurry was subjected to HTL to produce biocrude oil. The catalytic effect of MNPs on biocrude yield and composition was investigated. The MNPs were recycled to harvest more microalgae and to catalyse the HTL process. This Chapter bridged the gap in the literature on HTL of magnetically separated microalgae and it was published in the *ACS Sustainable Chemistry & Engineering* Journal as detailed in the next page.

Statement of authorship

This declaration concerns the article entitled:	Multifunctional Role of Magnetic Nanoparticles in Efficient Microalgae Separation and Catalytic Hydrothermal Liquefaction
Publication status:	Published
Publication details:	Egesa, D., Chuck, C.J. and Plucinski, P., 2017. Multifunctional role of magnetic nanoparticles in efficient microalgae separation and catalytic hydrothermal liquefaction. *ACS Sustainable Chemistry & Engineering*, *6*(1), pp.991-999.
Authorship contributions:	Formulation of ideas and design of methodology done by DE and PP. experiments done by DE and manuscript prepared by DE with the supervision of PP and CJC.
Statement from candidate:	This paper reports on original research I conducted during the period of my higher degree by research candidature.

Signed:  Date: 04/03/2019

Multifunctional Role of Magnetic Nanoparticles in Efficient Microalgae Separation and Catalytic Hydrothermal Liquefaction

Daniel Egesa, Christopher J. Chuck, and Pawel Plucinski*

Centre for Sustainable Chemical Technology, Department of Chemical Engineering, University of Bath, Claverton Down, Bath BA2 7AY, United Kingdom

3.1. Abstract

In this work, the efficiency of extracting microalgae from culture medium using magnetic nanoparticles (MNPs), converting the algal/particle slurry to biocrude using hydrothermal liquefaction (HTL) and successfully recycling the MNPs from the char phase was fully demonstrated for the first time. MNPs were synthesized by co-precipitation and used to extract microalgae from aqueous phase at a separation efficiency (SE) of 99%. The SE was optimized at pH 4. Liquefaction of algal/MNPs slurry gave a biocrude yield of 37.1 wt.% while microalgae only yielded 23.2 wt.%. The percentage area in the GC-MS chromatogram corresponding to hydrocarbons (HC) in Zn-ferrite catalysed and un-catalysed biocrude was 46.5% and 19.9% respectively while the percentage area of heptadecane from Zn-ferrite catalysed and un-catalysed biocrude was 37.8 wt.% and 10 wt.% respectively. Furthermore, the percentage area of heteroatom compounds in biocrude reduced substantially when liquefaction was done in presence of Zn and Mg ferrites. The nanoparticles were recovered from bio-char by sonication and recycled at a SE of 96.1%. Recycling of MNPs for magnetic separation of microalgae and catalytic HTL could lower the cost of microalgae harvesting and improve the yield and quality of biocrude. This could potentially reduce the cost of advanced biofuel processing from microalgae making them more affordable in comparison to petroleum-derived fuels.

3.2. Introduction

The irreversible depletion of fossil fuels and resulting environmental impact from their use has encouraged research into alternative sources of renewable liquid fuels (Yu Chen et al., 2016). Currently, most biofuels are produced from first generation feedstock such as sugarcane, soybean and corn. This is disadvantageous mainly due to competition between fuel and food for the limited food sources. While some non-food sources such as Jatropha are an improvement, these too have disadvantages *e.g.* competition for good quality agricultural land with food crops (Duan and Savage, 2010). One promising alternative is microalgae because of their high productivity, they can be cultivated on large water bodies, with low quality water (Amaro, Guedes and Malcata, 2011) therefore potentially do not compete for fertile agricultural land hence minimal environmental impact on good agricultural land (Barros et al., 2015), (Mata, Martins and Caetano, 2010).

However, one of the major limitations of processing biofuels from microalgae is the high cost of microalgae harvesting (separation) which contributes up to 25% of the overall cost of biomass processing (Safarik et al., 2015). This is in part due to difficult cell separation because of a slow settling velocity of microalgae due to their small size, low concentration and the resulting repulsion between the negatively charged cells.(E Molina Grima et al., 2003) Generally methods currently used to harvest microalgae are extremely slow or expensive and energy intensive (Uduman et al., 2010). A promising alternative is magnetic separation of microalgae because it is easy to manipulate and regenerate, it uses simple devices, it is cost effective and the magnetic field is nondestructive and economical (Prochazkova, Safarik and Branyik, 2013; Wang et al., 2015; Yunfeng Xu, Fu and Zhang, 2017). It was also reported on Los Alamos web site, (Los-Alamos, 2012) that magnetic separation can reduce the cost of microalgae harvesting by 90%. Magnetic separations rely on adsorption of charged magnetic nanoparticles onto microalgae cells which then respond to an external magnetic field concentrating the algal cells.

In this work, microalgae were separated magnetically and subjected to hydrothermal liquefaction (HTL) to produce biocrude oils. The HTL process entails using water as a reactive medium to convert biomass into liquid crude oil under controlled conditions. In this conversion, the main cellular constituents such as lipids, proteins and carbohydrates

are broken down at the high temperatures and pressures. This coupled with hydrolytic attack leads to breakage of biomolecules in hot compressed water resulting into the production of a biocrude oil (Faeth and Savage, 2016) with a reasonably high calorific value (Rojas-Pérez et al., 2015). This process uses the whole microalgae cell and does not require the microalgae to over produce lipid, allowing the use of faster, denser growing strains. Due to the difficulties of cultivating lipid rich microalgae and extracting these lipids from microalgae cells, the HTL process is considered as a more viable alternative to produce a biofuel product from microalgae (Duan and Savage, 2010; Rojas-Pérez et al., 2015). Life cycle and techno economic analysis suggests that the overall HTL process uses less energy than the extraction and transesterification of lipids,(Andrew Lee et al., 2016) though further work is required to increase biocrude yields and quality. To this end, effort has been invested in investigating the effect of catalysts on the HTL process and its ability to produce higher quality products (Dong Zhou et al., 2010).

Among heterogeneous catalysts, solid nanocatalysts have attracted a lot of attention due to their large chemically active surface area and high chemical and physical stability which are important factors in industrial applications (Dong Zhou et al., 2010). One of the key challenges with solid catalysts is in their recovery from the catalyst biocrude mixture by means of filtration methods which are generally not economically viable. Therefore it is paramount to develop heterogeneous catalysts that can easily be recovered and recycled for continuous HTL reactions (Akia et al., 2014). Magnetite based nanocatalysts are interesting potential candidates because they can easily be separated by magnetic force hence improving their lifetime and cost effectiveness. Also, they have large specific surface areas, less resistance to mass transfer and high catalytic activity for bio catalysis, photo catalysis, and phase transfer catalysis (Akia et al., 2014). No study has yet demonstrated the multifunctional role of magnetite based nanocatalysts in HTL and microalgae separation however.

The aim of this research is to potentially lower the processing cost of biofuel from microalgae by optimising microalgae separation efficiency and improving yield and quality of biocrude from microalgae HTL. The objectives are: (*i*) to magnetically separate microalgae from culture medium at a separation efficiency above 95%, (*ii*) to investigate

the catalytic effect of doped MNPs on yield and chemical composition of biocrude and (*iii*) to recycle MNPs for magnetic separation and HTL catalysis. To our knowledge, this is the first time MNPs have been used to play a dual role: harvesting microalgae and catalysing the HTL process. It will also be the first report on recycling MNPs from HTL to further harvest microalgae and catalyse HTL process. Achieving the above objectives could lead to a cost-effective processing of biofuels from microalgae resulting into biofuels being more economically competitive with petroleum derived fuels. As well as a more sustainable approach to biocrude processing since MNPs are easily recycled minimising waste.

3.3. Materials and methods

3.3.1. Synthesis of MNPs and magnetic separation of *S. obliquus*

Ferrite magnetic nanoparticles (MNPs) were synthesized by co-precipitation method (Laska et al., 2009), (Lv et al., 2015). They were then used to separate microalgae from culture medium and separation efficiency (SE) was optimised at different pH and mass ratios of MNPs: microalgae. SE was calculated according to equation 3.1 (Prochazkova et al., 2013).

$$SE = \frac{OB-OA}{OB} \times 100\ (\%) \qquad (3.1)$$

Where: *SE* is the separation efficiency, *OB* is optical density before separation, *OA* is optical density after separation. *Scenedesmus obliquus* was grown in illuminated photobioreactors supplied with CO_2 at pH 8 and temperature 25 °C. Spirulina was purchased from Bulk Powders® and was composed of 63 wt.% protein, 20 wt.% carbohydrates 6wt.% fat and 11% miscellaneous biochemical content. Details of materials and methods of synthesizing MNPs, magnetic separation and microalgae culture composition are in the supporting information (SI).

3.3.2. Hydrothermal liquefaction of microalgae

After magnetic separation, microalgae/MNPs slurry was subjected to HTL at 320 °C for 1 hour according to the method reported by Harvind et al. (2014). The MNPs were recovered from the solid residue by sonication in de-oxygenated and de-ionized water to

remove any attached biomass and then magnetically extracted from the water. Details of HTL procedure and MNP recovery can be found in the supporting information. All experiments were repeated twice. The corresponding values of standard deviation can be found in the respective Figures and Tables.

3.3.3. Biocrude oil Analysis

The percentage yield of HTL products (biocrude and solid residue) was calculated using equation 3.2 (Neveux et al., 2014b). The mass of MNPs was subtracted from the solid residue and the yield of biocrude and solid residue was calculated on an ash and moisture free weight basis using equation 2 below.

$$YP = \frac{WP}{WF - WA - WM} \times 100\ (\%) \qquad (3.2)$$

Where, *YP* is the percentage yield of the product, *WP* is the mass of product (g), *WF* is mass of microalgae fed into the reactor, *WA* and *WM* are ash and moisture content of microalgae. The ash content for the dried Spirulina and *S. obliquus* varied between 16 wt. % to 18 wt. % and 22 wt. % to 25 wt. % and the moisture content was between 8 wt. % to 10 wt. % and 10 wt. % to 12 wt. % respectively. The high heating value (HHV) of biocrude was determined using Dulong's formula (Rojas-Pérez et al., 2015). The energy recovery (ER) for the biocrude was calculated according to equation 3.3 (Neveux et al., 2014a).

$$ER = \frac{(HHVp \times Oil\ Yield)}{(HHVf)} \times 100\ (\%) \qquad (3.3)$$

Where: *ER* is the energy recovery, HHV_p is high heating value of product, and HHV_f is high heating value of feed.

3.3.4. Analytical Techniques

Optical density measurements were done using a UV-Vis Cary series instrument JEM-1200 EX11. Surface morphology and size of MNPs was analysed using a JEM-1200 EX11 TEM instrument at an acceleration voltage of 300 kV. The size distribution of MNPs was determined using image J software. The surface morphology of microalgae cells and the attached MNPs was done on a JEOL JSM 6330F FE-SEM equipment at an acceleration voltage of 2.5 kV. The crystal structure and phase composition of MNPs was characterized on a Bruker D8 Advanced XRD machine operating at 40 kV and 80 mA and a scanning

rate of 0.02°/s in 2θ range from 20° to 70°. Compounds in the biocrude were analysed by GC-MS on an Agilent technologies GC system 7890A with triple axis detector, 5975 network mass selective detector and Agilent JW scientific GC column. Moisture and ash content of microalgae biomass was determined through TGA analysis. TGA runs were done on a TGA 92 Setram equipment. ^{1}HNMR analysis of biocrude was done on a 400 MHz Bruker NMR machine. Elemental composition of biocrude was done in duplicate using a Carlo Earba Flash 2000 elemental analyser.

3.4. Results and discussion

4.4.1. Synthesis and characterization of MNPs

TEM images (Figure S2A) show that magnetite nanoparticles were crystalline, mono dispersed and mostly in the size range of 10-12 nm. The particle size was measured using image J software. Doped MNPs (ferrites) were poly-dispersed with increased particle size mostly ranging between 16 to 18 nm (Figures S2 B, C and D). The increase in particle size with doping is confirmed by XRD results (Figures S4 A, B and C) which show increased intensity and sharpening of peaks with doping. The sharpening of peaks is an indication of increased particle size as a result of doping with Zn and Mg.(Kaur, Jain and Singh, 2015) Reflections which correspond to magnetite nanoparticles were found at 2θ = 30.437°, 35.715°, 43.393°, 53.950° and 57.309° corresponding to the (220), (311), (400), (422), and (511) crystal planes of pure magnetite. These peaks match well with the reported peaks in literature for magnetite (Hariani, Faizal and Setiabudidaya, 2013). The sharpest peaks were from Zn and Mg doped magnetite nanoparticles with the highest (311) at Lin count of 4700, the less intense peaks were for un-doped Fe_3O_4 (311) at 1150 Lin count. Formation of magnetite nanoparticles was also monitored by UV-Vis (Figure S5). From the UV-Vis spectrum hydrolysis of iron ions in presence of ammonium hydroxide resulted into removal of metal-ion complex from solution leading to the disappearance of the peak at 300 nm and to formation of a second broad featureless absorption tail which according to Melo et al. (2013) is due to formation of magnetite and is as a result of transition in band gap of semiconductor materials (Melo et al., 2013).

3.4.2. Magnetic separation of microalgae

The separation efficiency (SE) of *Scenedesmus obliquus* was optimised at different separation times, pH and mass ratios of MNPs to *S. obliquus*. Microalgae SE increased with an increase in separation time (Figure 3.1). SE also increased with increase in mass ratio of MNPs to microalgae (Figure 3.2). This trend is in agreement with the findings of (Prochazkova et al., 2013; Prochazkova, Safarik and Branyik, 2013) in separation of *C.vulgaris* where 90% separation was achieved. Cerff et al. (2012) also observed a similar trend while separating fresh water microalgae *C. reinharditii* and *C. vulgaris* (Cerff et al., 2012). The increase in SE with mass ratio is attributed to presence of more nanoparticles to adsorb onto the microalgae surface resulting in increased magnetic force and a higher SE. The higher the concentration of MNPs, the greater the adsorption hence the stronger the magnetic force resulting in faster separation. Further increase in the concentration of MNPs had no effect on SE. This is presumably because magnetic force is proportional to the volume of the magnetic body, if the volume of the MNPs increases, the magnetic force increases resulting in a better separation. Cells with much less or no MNPs adsorbed will not respond to magnetic force.

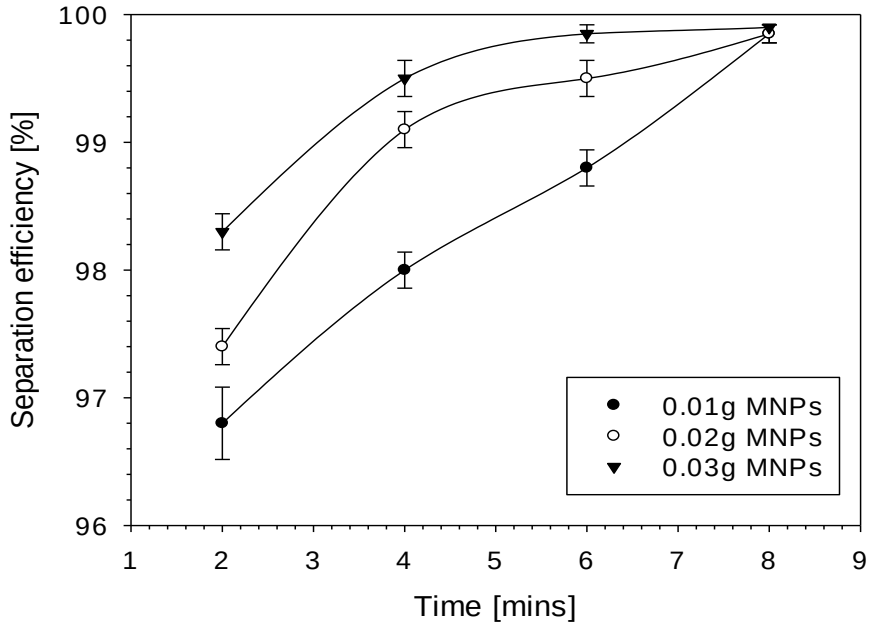

Figure 3. 1. Separation efficiency of *Scenedesmus obliquus* (0.5g L^{-1}, 20 ml, pH4) at varying time intervals and mass ratios of magnetite.

The high SE in acidic pH is attributed to a highly-pronounced deference in ζ-potential (ZP) measurements of the interacting particles (Prochazkova, Safarik and Branyik, 2013; Safarik et al., 2015). The difference in ZP was highest at pH4 (49 mV) and lowest at pH 11(27.9 mV). Micro-algal cells maintain a negative surface charge over a wide pH range and in acidic pH below the isoelectric point, the surface charge of MNPs is positive because they gain protons (Parks, 1965; Safarik et al., 2015). Therefore, there is a higher electrostatic attraction between positively charged MNPs and negatively charged microalgal cells. The difference in ZP of MNPs and microalgal cells was more pronounced in acidic pH (Figure S 6). This led to greater interaction between MNPs and microalgae cells hence a higher SE. The low SE at basic pH is as a result of MNPs gaining electrons above its isoelectric point and hence become negatively charged (Parks, 1965; Safarik et al., 2015). This results in repulsion between microalgae and MNPs hence a lower SE. The limited separation that takes place is due to the attachment between MNPs and microalgae cells at molecular level brought about by restricted electron interactions and positively charged sections within the suspension (Bos, Van der Mei and Busscher, 1999; Safarik et al., 2015).

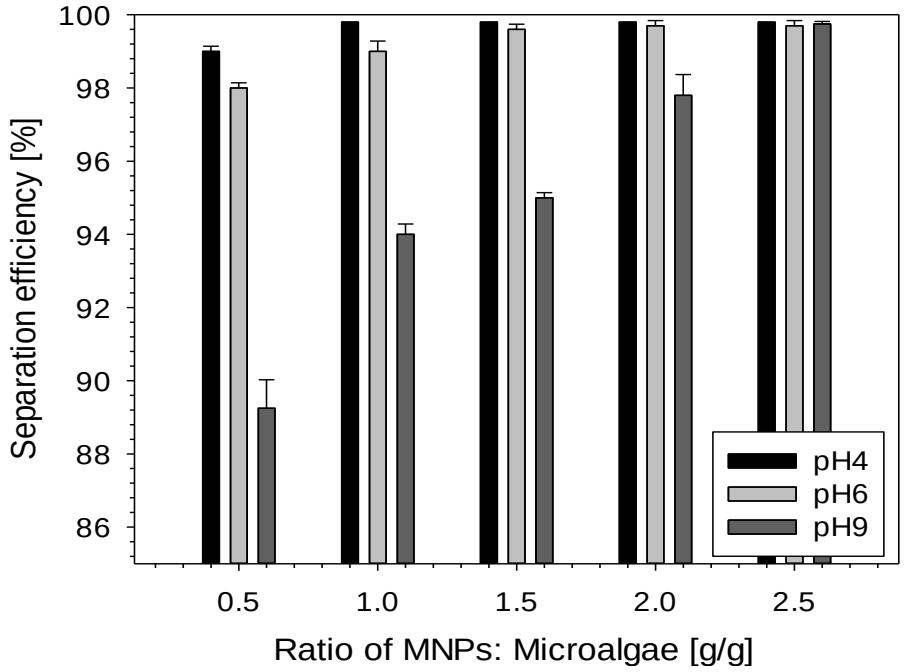

Figure 3. 2. Separation efficiency of *Scenedesmus obliquus* (0.5 g L^{-1}, 20 ml, separation time 4 minutes) at different mass ratios and pH.

3.4.3. Catalytic effect of MNPs on biocrude yield in HTL

The extraction of the microalgae using MNPs leaves an algal/MNPs slurry with a water content of 78 wt. %. This is directly in the range for HTL processing. The effect of the MNPs on the biocrude yield was therefore examined at different mass ratios of MNPs to microalgae (Figure 3.3 A) using both Spirulina and *S. obliquus* strains. Excitingly, biocrude yields were increased substantially on addition of MNPs, with the highest yield (34 wt. %) achieved at a ratio of 0.12, this is in comparison to only 25 wt. % when using Spirulina alone. A number of other studies have demonstrated an increase in yield on using metal catalysts (Rojas-Pérez et al., 2015). The further increase in mass of MNPs did not have any substantial effect on yield. This nonlinear correlation between catalyst loading and biocrude yield has also been reported by Rojas-Perez et al. (2015) while investigating the catalytic effect of magnetite nanoparticles on macroalgae biocrude production (Rojas-Pérez et al., 2015). Also, studies on coal liquefaction by Dadyburjor et al. (1994) found that optimum yields were obtained at low iron oxide catalyst ratios (Dadyburjor et al., 1994). The high biocrude yield at an optimum loading of MNPs can be attributed to an effective distribution of MNPs (catalyst) on the surface of the microalgae cells (Figure S11 D) resulting into maximum exposure of active sites which facilitate increased conversion of algal biomass to biocrude. Additionally, the low yield at higher particle loading can be attributed to increased particle aggregation seen at the algal cell surface (Figure S11 F). This results in loss of catalyst due to a reduction in accessible active sites hence reduced conversion of algal biomass to biocrude. These results show that the yield of biocrude in HTL can be enhanced by an optimum quantity of MNPs.

The yield of the solid residue was lower when Spirulina liquefaction was done in presence of MNPs (Figure 3.3 A). The reduction in solid residue yield has been confirmed by elemental analysis (Table S 3) showing reduction in carbon content of the residue for runs involving MNPs. The reduction in solid residue in presence of MNPs can be attributed to their catalytic effect in favouring the conversion of microalgae biomass into biocrude.

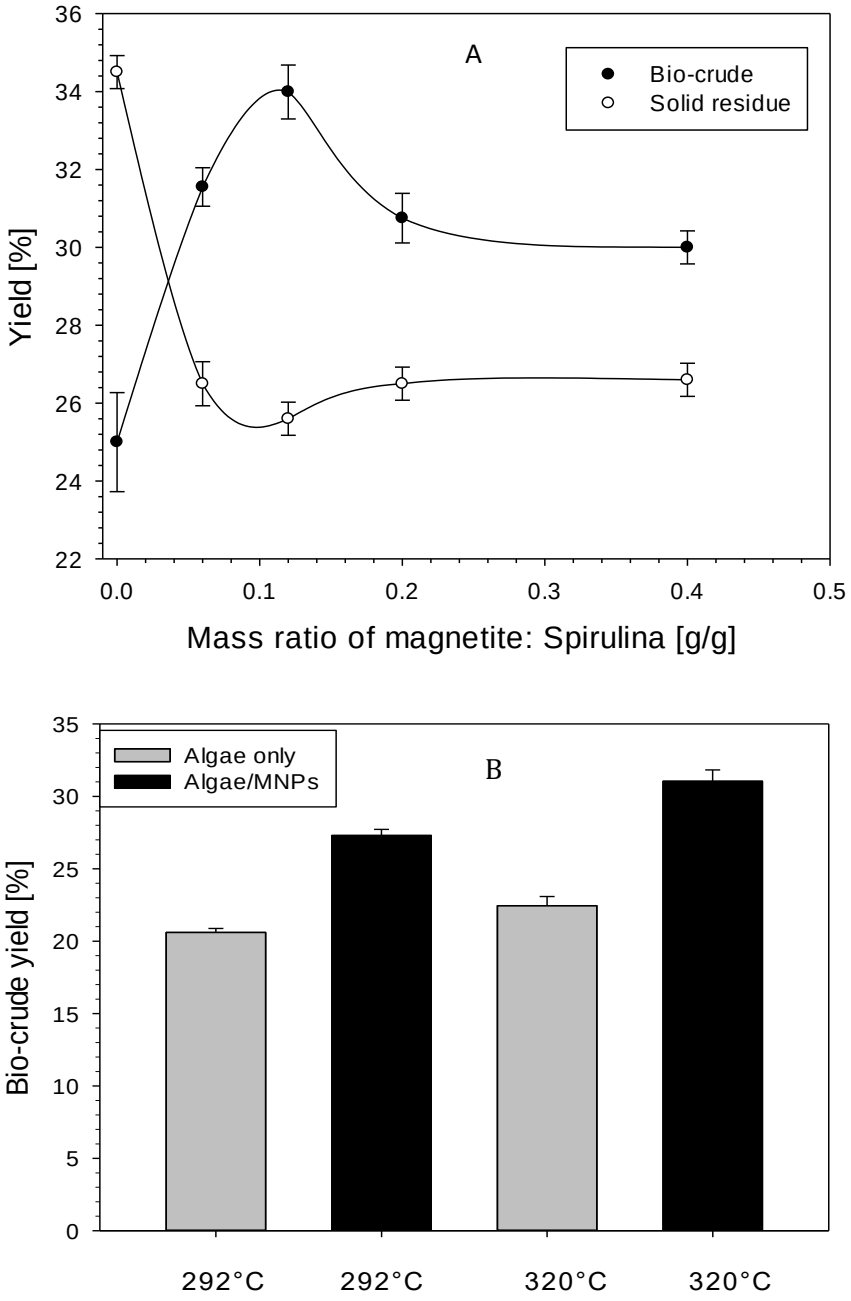

Figure 3. 3. Biocrude yield from microalgae HTL with and without magnetite at 320 °C, P_0 of 50 bar (N2) and P_f of 120 bar for 60 minutes, A) Yield from HTL of Spirulina at different mass ratios of magnetite to Spirulina. B) Yield of biocrude from HTL of *Scenedesmus obliquus* (mass ratio of magnetite: microalgae of 0.4).

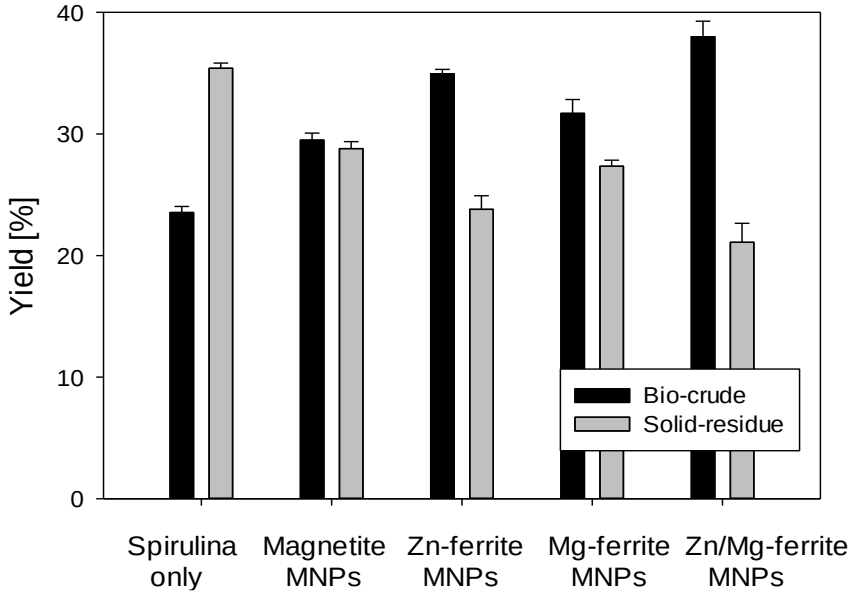

Figure 3. 4. Yield of biocrude and solid residue from HTL of Spirulina biomass in presence of different doped MNPs at 320 °C, for 60 minutes at a mass ratio of MNPs: Spirulina of 0.12.

Liquefaction in absence of MNPs resulted in a higher yield of solid residue (34.5 wt.%) which was translated into a lower yield of biocrude. It seems clear therefore that MNPs are having a catalytic effect on the conversion of the microalgae, favouring biocrude production and reduced solid residue. The detailed catalytic mechanism needs further investigation since the HTL process involves many different reactions. Furthermore, in liquefaction of *S. obliquus* (Figure 3.3B) the presence of MNPs had a similar effect on biocrude yield. The highest biocrude yield of 30.5 wt. % was observed at 320 °C in presence of magnetite while in absence a biocrude yield of 22 wt.% was achieved. All biocrude yields reported greatly exceed the lipid content of the original feed stock. This confirms that other cellular components like proteins and carbohydrates were also converted during the HTL process (Duan and Savage, 2010). Zn and Mg doped ferrite MNPs had an even larger impact on the liquefaction of Spirulina biomass. Doped ferrite MNPs greatly enhanced the yield of biocrude compared to pure magnetite (Figure 3.4). The highest yield (37.1 wt. %) was observed when Zn/Mg/Fe_3O_4 was used giving a 14 wt.% increment in yield in comparison to liquefaction without nanoparticles and an 8% increment in yield compared to pure magnetite.

Also, Zn doped ferrite registered a biocrude increment of 11.5 wt. % compared to liquefaction without MNPs. Doped MNPs also had a substantial effect on reducing the percentage of ash free solid residue, the largest reduction (15.7 wt.%) was observed when Zn/Mg/ferrite was used (Figure 3.4). Liquefaction without MNPs resulted into a higher percentage of solid residue (35.7 wt.), this is reflected in the reduced yield of the biocrude (23.2 wt. %). Similar increases in yield were observed when Mg, Zn, and Fe sulphates were present in the liquefaction of spirulina (Sofia Raikova et al., 2016b). The exact effect of Zn/Mg/ferrites on increasing the biocrude yield is not yet known but what is clear is that they are playing a catalytic role by increasing the biocrude yield. This is possibly due to possession of more active sites enabling higher conversion of biomass to biocrude oil.

This suggests that the use of MNPs can be applied to a range of algal species and a similar increase in HTL yields can be expected. By doping with either Mg or Zn further gains can be made in the biocrude yield. The MNPs play two important roles: separation of microalgae from the culture medium and a catalytic role of increasing the yield of biocrude during the HTL.

3.4.4. Effect of MNPs on chemical composition of the biocrude

To determine the catalytic effect of MNPs on the chemical composition of the biocrude elemental analysis, GCMS and NMR analyses were performed.

3.4.4.1. Elemental composition

The elemental composition of biocrude from Spirulina liquefaction were compared at different mass ratios of MNPs: microalgae and when using different doped ferrite MNPs (Table 3.1). The amount of carbon and hydrogen in the biocrude was much higher than that in the biomass feedstock. The carbon content of the biocrude increased from 46.3% in Spirulina feedstock to 71.9 wt.% in un-catalysed biocrude and to 73 wt. % in catalysed biocrude while the hydrogen content increased from 6.6 wt.% in Spirulina feed stock to 9.2 wt. % in un-catalysed liquefaction. Increasing concentration of MNPs did not have a significant impact on the carbon and hydrogen content of the biocrude. The highest carbon content (73 wt. %) was achieved at a mass ratio of 0.12. This was the most optimum loading of MNPs for the highest possible yield of carbon. This trend is in agreement with the findings of (Sofia Raikova et al., 2016b) on the effect of metal sulphates on Spirulina

liquefaction. A similar range in carbon and hydrogen contents was observed when liquefaction of microalgae was done in presence of Zn and Mg doped ferrite MNPs. Therefore, HTL of micro-microalgae in the presence of MNPs leads to increment in the carbon content of biocrude. The amount of oxygen and nitrogen in the biomass feedstock was also much higher than that in the biocrude. The oxygen content in the biocrude was reduced from 27.7 wt. % in the biomass feedstock to 10 wt. % in biocrude from un-catalysed liquefaction and to 9.4 wt. % in bio lipids from catalysed liquefaction (Table 3.1). Oxygen reduction coupled with an increase in amount of carbon and hydrogen resulted in biocrude having a higher energy density than the microalgae feedstock. The nitrogen content in the biocrude was reduced from 10.3 wt. % in the biomass feedstock to 7.5 wt. % in biocrude from un-catalysed liquefaction and to 6 wt. % in biocrude from catalysed liquefaction. The further reduction in oxygen and nitrogen content of biocrudes in the catalysed liquefaction shows that the presence of MNPs played a major role in de-oxygenation and denitrogenation of the biocrude and can potentially be used as HTL catalysts to improve the quality of the biocrudes.

Table 3. 1. Elemental compositions, HHV, atomic ratios and ER of Spirulina and biocrudes from spirulina liquefaction at different masse ratios of magnetite: microalgae and using different ferrite MNPs. HTL was done at 320 °C for 60 minutes, at P_0 of 50 bar (N2), and P_f of 120 bar.

Ratio Fe_3O_4: microalgae	C (wt. %)	H (wt. %)	N (wt. %)	O (wt. %)	S (wt. %)	N/C* -	H/C* -	O/C* -	HHV (MJ/kg)	ER (%)
Spirulina	46.3±0.06	6.65±0.00	10.3±0.06	27.7±0.03	0.54±0.01	0.19	1.72	0.45	20.3±0.4	0.00
0	71.9±0.06	9.24±0.04	7.50±0.11	10.0± 0.04	0.41±0.03	0.09	1.54	0.10	35.7±0.2	44.0±2.24
0.06	71.9±0.11	8.8±0.120	6.60±0.09	9.4 ±0.04	0.60±0.03	0.08	1.47	0.10	35.3± 0.1	54.9±0.86
0.12	73.0±0.04	9.09±0.09	7.40±0.06	9.4±0.01	0.77±0.03	0.09	1.49	0.10	36.2±0.2	60.8±1.24
0.2	69.3±0.1	8.56±0.06	6.05±0.11	9.8±0.01	0.50±0.02	0.07	1.48	0.14	34.0±0.1	51.5±1.07
0.6	70.7±0.08	8.69±0.05	6.54±0.07	10.7±0.1	0.69±0.00	0.08	1.47	0.11	34.5±0.2	51.0±0.72
Type of MNPs										
Spirulina	46.3±0.06	6.65±0.00	10.3±0.06	27.7±0.03	0.54±0.01	0.23	0.14±0.00	0.60	20.3±0.03	0.00
No MNPs	71.9±0.06	9.24±0.04	7.5±0.11	10.0±0.04	0.41±0.03	0.10	0.13	0.14	35.7±0.03	40.9±0.1
Magnetite	72.6±0.04	9.20±0.09	7.20±0.06	9.40±0.01	0.77±0.03	0.10	0.13	0.13	36.1±0.15	51.7±0.2
Mg ferrite	73.0±0.06	8.64±0.04	7.41±0.01	9.56±0.05	0.53±0.02	0.10	0.12	0.13	35.4±0.03	53.8±0.1
Zn ferrite	72.1±0.15	8.75±0.00	7.58±0.02	10.2±0.00	0.60±0.00	0.11	0.12	0.14	35.1±0.05	60.0±0.1
Mg/Zn ferrite	72.9±0.09	8.74±0.01	7.07±0.04	9.71±0.02	0.60±0.01	0.10	0.12	0.13	35.4±0.05	64.8±0.1

* Molar ratio

Liquefaction in the presence of MNPs led to the highest energy recovery (ER) value of 60.8% at a mass ratio of 0.12 giving an increment of 10.9% in comparison with biocrude from the un-catalysed liquefaction. The high ER at this concentration corresponds well with the high heating value (HHV) at the same concentration. The highest ER was achieved when liquefaction was done in presence of Mg and Zn doped ferrite MNPs. This gave a percentage increment of 23.9% in comparison with the biocrude from the un-catalysed liquefaction. Zn ferrites also gave a high ER of 60%. This shows that Zn and Mg doped ferrite MNPs have a large influence on increasing the ER of the biocrudes.

3.4.4.2. GC-MS Analysis of Biocrude

The identities of the main individual compounds (extracted by hexane) in the biocrude from Spirulina and *Scenedesmus obliquus* liquefaction (Figure 3.5) and their relative percentage areas in the chromatogram after integration were determined. Peaks in the chromatogram with less than 1 wt. % relative area were not considered. The major compounds detected in the biocrude were grouped under hydrocarbons, aromatic hydrocarbons, nitrogen compounds, phenolic compounds, oxygenated compounds, and organic acids. The hydrocarbons (HC) grouping consisted of compounds such as octane, cyclohexane, cyclopropane, hexadecane, heptadecane, and nonyne. In Figure 3.5, biocrude from un-catalysed liquefaction registered the lowest percentage area of hydrocarbons (19.9 wt. %) while biocrude produced in presence of Zn ferrite MNPs registered the highest percentage area (46.5%). Liquefaction in the presence of Mg and Zn ferrite MNPs also gave a high percentage area of HC (36 wt. %).

The increase in hydrocarbon composition in the presence of Zn and Mg ferrite MNPs is an indication of their catalytic role in promoting decomposition of cellular components like lipids, proteins and carbohydrates and the ability to produce hydrocarbons (Duan and Savage, 2010). The hydrocarbons from both biocrudes were largely composed of alkanes with heptadecane as the most predominant. A high percentage of heptadecane (37.8 wt. %) was observed when liquefaction of Spirulina was done in presence of Zn ferrite MNPs. Liquefaction of Spirulina in absence of MNPs registered a low percentage (10 wt. %) of heptadecane in the biocrude.

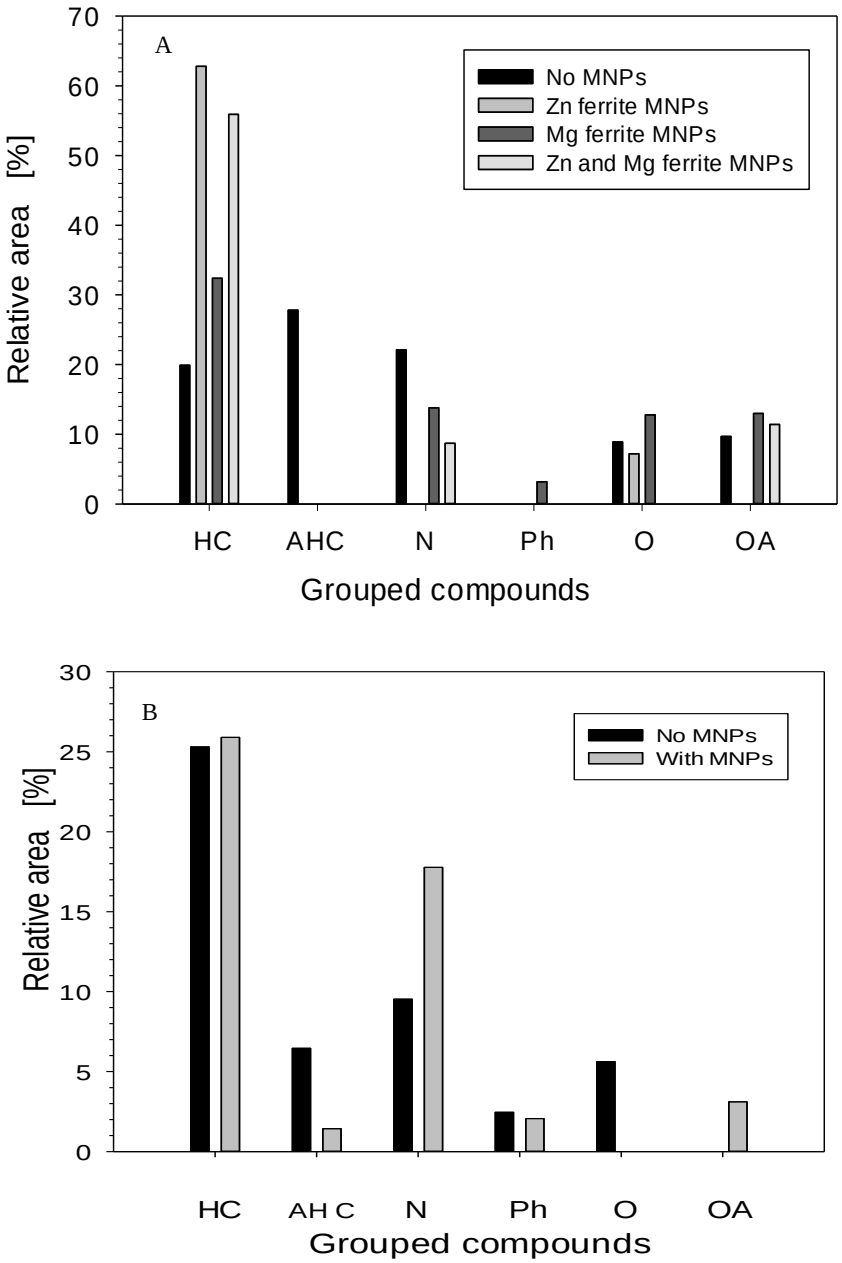

Figure 3. 5. Distribution of major compounds in biocrude after microalgae HTL at 320 °C at P_0 of 50 bar (N2), P_f 120 bar for 60 minutes at ratio of MNPs: microalgae 0.12: A) Spirulina in presence of different MNPs and B), *S. obliquus* in presence of magnetite. HC – hydrocarbons, AHC – aromatic hydrocarbons, N – nitrogen compounds, Ph – phenolics, O – oxygenates, OA – organic acids.

For *Scenedesmus obliquus* biocrude (Figure 3.5B), the percentage of heptadecane in the biocrude was 20 wt. % when liquefaction was done in presence of magnetite and 3.1% when liquefaction was done in absence of magnetite. These results suggest that the catalysts are aiding the deoxygenation of lipids and fatty acids into the hydrocarbon species more effectively than the non-catalysed process. Interestingly, there were more aromatic hydrocarbons (AH) in biocrude from un-catalysed liquefaction. Liquefaction of *Scenedesmus obliquus* in the presence of magnetite led to reduction in AH by 5.03 wt. % while liquefaction of Spirulina in the presence of MNPs led to a 26.8 wt.% reduction in AH. This shows that HTL in presence of MNPs facilitated the catalytic conversion of AH to other compounds within the biocrude.

The grouping of nitrogen compounds included: cyclo-heptylamine, indole, acetamide, 3-pyridinecarbonitrile, butanamide, NN-dimethyl decanamide, isobutyl isothiocyanate, azetidine, benzonitrile and pyrimidine. The un-catalysed biocrude from Spirulina contained more nitrogen compounds (22.1 wt. %) compared to *Scenedesmus obliquus* biocrude (9.5 wt.%). The high percentage of nitrogen compounds in Spirulina biocrude is attributed to its high protein content (63 wt. %). The proteins undergo degradation through different reaction pathways such as deamination, decarboxylation, dehydration, and depolymerisation to form nitrogen compounds (Ross et al., 2010; Shakya et al., 2015). The amino acids from proteins undergo decarboxylation and deamination reactions to form amines, ammonia, carbonic acids, and other organic compounds (Toor, Rosendahl and Rudolf, 2011; Shakya et al., 2015). In Spirulina biocrude, the amount of nitrogen compounds reduced to below 1% after liquefaction with Zn ferrite MNPs while liquefaction with Zn/Mg ferrite led to a decrease of 13.4 wt. %. Elemental analysis results also show a general reduction in the percentage of elemental N in catalysed biocrude. This confirms that Zn and Mg doped ferrite MNPs play a catalytic role in removing nitrogen compounds from biocrude presumably producing more water-soluble species hence improving the biocrude quality.

The grouping of phenolic compounds had only phenol and it was observed in significant quantities in the biocrude from *Scenedesmus obliquus*. The amount of phenol in un-catalysed biocrude was slightly higher than that in catalysed. The percentage of phenol in

un-catalysed and catalysed biocrude from Spirulina liquefaction was below detachable levels only biocrude from Mg ferrite liquefaction (Figure 3.5A) had a percentage of phenolic compounds of up to 3.2 wt. %. Since microalgae biomass do not possess lignin it is possible that phenolic compounds were produced from carbohydrates within the algal biomass (Duan and Savage, 2010; Shakya et al., 2015) having been hydrolysed to glucose which is broken down to furfural and finally condensed to phenols (Barreiro et al., 2014; Shakya et al., 2015). The other grouping included compounds such as propanal and cyclopentan-1-one belonging to aldehydes, ketones and esters. These were grouped under oxygenated compounds. The un-catalysed biocrude from *S. obliquus* had significant quantities of oxygenates (5.6%). However, the biocrude from catalysed *S. obliquus* did not show oxygenates. For Spirulina, the un-catalysed biocrude had more oxygenates (8.9 wt. %) than the uncatalyzed *S. obliquus*. Spirulina biomass liquefied in presence of Zn and Mg ferrite did not show any oxygenates. This agrees with elemental analysis results which revealed a reduction in oxygen when microalgae liquefaction was done in presence of MNPs. Hence confirming that Zn and Mg ferrite MNPs played a catalytic role in deoxygenation of biocrude.

The grouping of organic acids included compounds such as n- hexa-decanoic acid, formic acid, 4-butyl benzoic acid, and propyl phosphonic acid. Liquefaction of *S. obliquus* in presence of ferrite MNPs resulted into increase in organic acids from below 1 wt. % in un-catalysed liquefaction to 3.1 wt.% in catalysed liquefaction. The organic acids were predominantly n-hexadecanoic acid (3.1 wt. %). For biocrude from Spirulina liquefaction the amount of organic acids increased by 3.3 wt. % in Mg ferrite catalysed biocrude. Hydrolysis of fats in microalgae biomass led to formation of fatty acids and fatty acid esters in biocrude (Duan and Savage, 2010; Shakya et al., 2015). Due to the low concentration of tri-glycerides in microalgae biomass, fatty acids in the biocrude may have also arisen from other pathways such as from breakdown of glucose under HTL conditions leading to formation of organic acids such as formic acid, acetic acid, lactic acid *etc.* (Srokol et al., 2004; Shakya et al., 2015). The reduction in the amount of organic acids in Zn ferrite catalysed biocrude was possible due to their catalytic effect in breaking down fatty acids to hydrocarbons as confirmed by the highest yield of hydrocarbons in biocrude from Zn ferrite catalysed liquefaction (Figure 3.5A).

3.4.4.3. NMR Analysis of Biocrude

To further confirm the identity and quantity of functional groups in the biocrudes, the samples were analysed by ^{1}H NMR. All signals relating to the protons in the biocrudes were grouped (Figure 3.6). Large peaks were seen at 0.5 - 1.5 ppm which are characteristic of terminal methyl groups in alkyl chain corresponding to alkanes (Duan and Savage, 2010). The ^{1}H NMR spectra (Figure S10) provided compatible functional group information to GC-MS chromatograph and a comparison of integrated areas in both spectra revealed a similar trend in the quantities and functional groups of corresponding compounds.

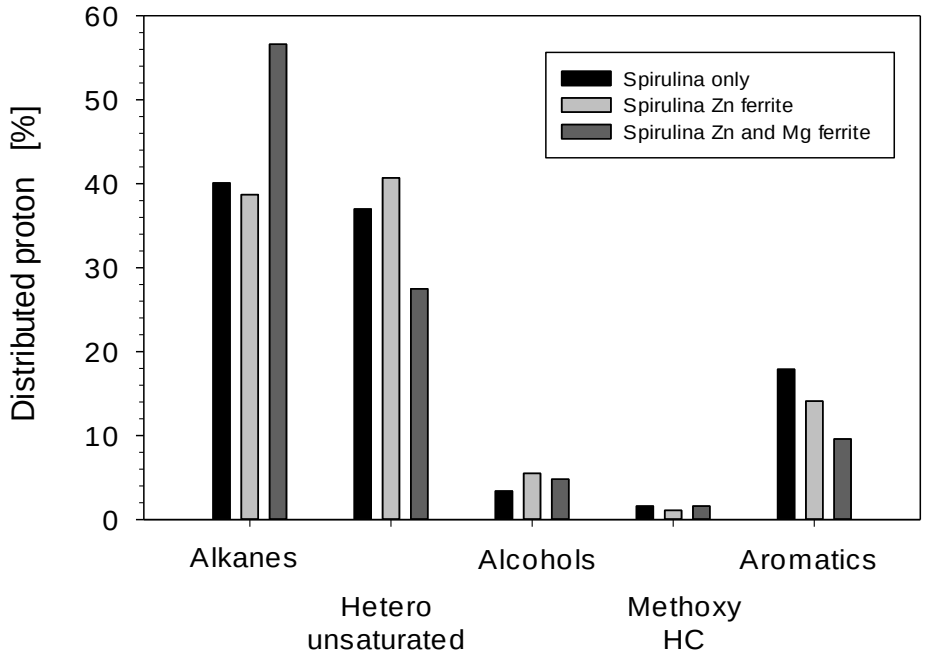

Figure 3. 6. Grouped compounds in ^{1}HNMR spectrum of biocrude from Spirulina liquefied with and without MNPs, liquefaction time 60 minutes at 320 °C.

Like GC-MS, ^{1}H NMR spectra revealed a high percentage of aliphatic functional groups corresponding to alkanes for all the biocrudes. The high percentage of hetero/unsaturated functional groups (1.5 - 3.0 ppm) and aromatics and hetero aromatics (6.0 - 8.5 ppm) in all the biocrudes is due to the large percentage of nitrogenous and oxygenated compounds from the feedstock's high protein (63 wt.%) content.(Dong Zhou et al., 2010) Zn and Mg ferrite derived biocrudes registered the lowest percentage of these functionalities

compared to the other biocrudes revealing a positive impact in reducing hetero/unsaturated and aromatic and hetero aromatic atom functionalities from the biocrudes. The ^{1}H NMR data supports both the GC-MS and elemental analysis, demonstrating increased removal of hetero-atom functionalities from biocrudes using MNPs in HTL. Furthermore, all biocrudes exhibited a low percentage of methoxy and carbohydrate functional groups (4.4 - 6.0 ppm), this is compatible with carbohydrates changing into biocrude in the HTL process (Duan and Savage, 2010).

3.4.5. Recycling of MNPs from HTL

After magnetic separation and HTL, MNPs largely deposited in the solid residue. These were then recovered by sonication as described earlier. The MNPs were then tested for their suitability in harvesting further microalgal cultures. The separation efficiency of fresh and recycled MNPs was compared at pH 9 and mass ratio of MNPs: microalgae of 0.4 g/g. After 18 minutes of separation (Figure 3.7A), recycled MNPs registered a SE of 96.1% compared to 98.4% for fresh ones.

There was a steady increase in the SE for both the fresh and recycled MNPs. However, the kinetics of the recycled MNPs was slightly different from the fresh MNPs in the first 10 minutes, then similar in the last 8 minutes. The difference in kinetics was possibly due to differences in the particle size of the recycled and fresh MNPs. The recycled MNPs underwent aggregation having been through the HTL process. This aggregation may have resulted in increased particle size hence reduced particle distribution on the surface of the microalgae cells compared to the fresh MNPs. This may have led to reduction in separation efficiency for the recycled MNPs because of a reduced adsorption of MNPs onto algae cells hence reduced SE when magnetic force is applied. The effect of leaching was negligible since the leeched MNPs would be recovered when magnetic force is applied.

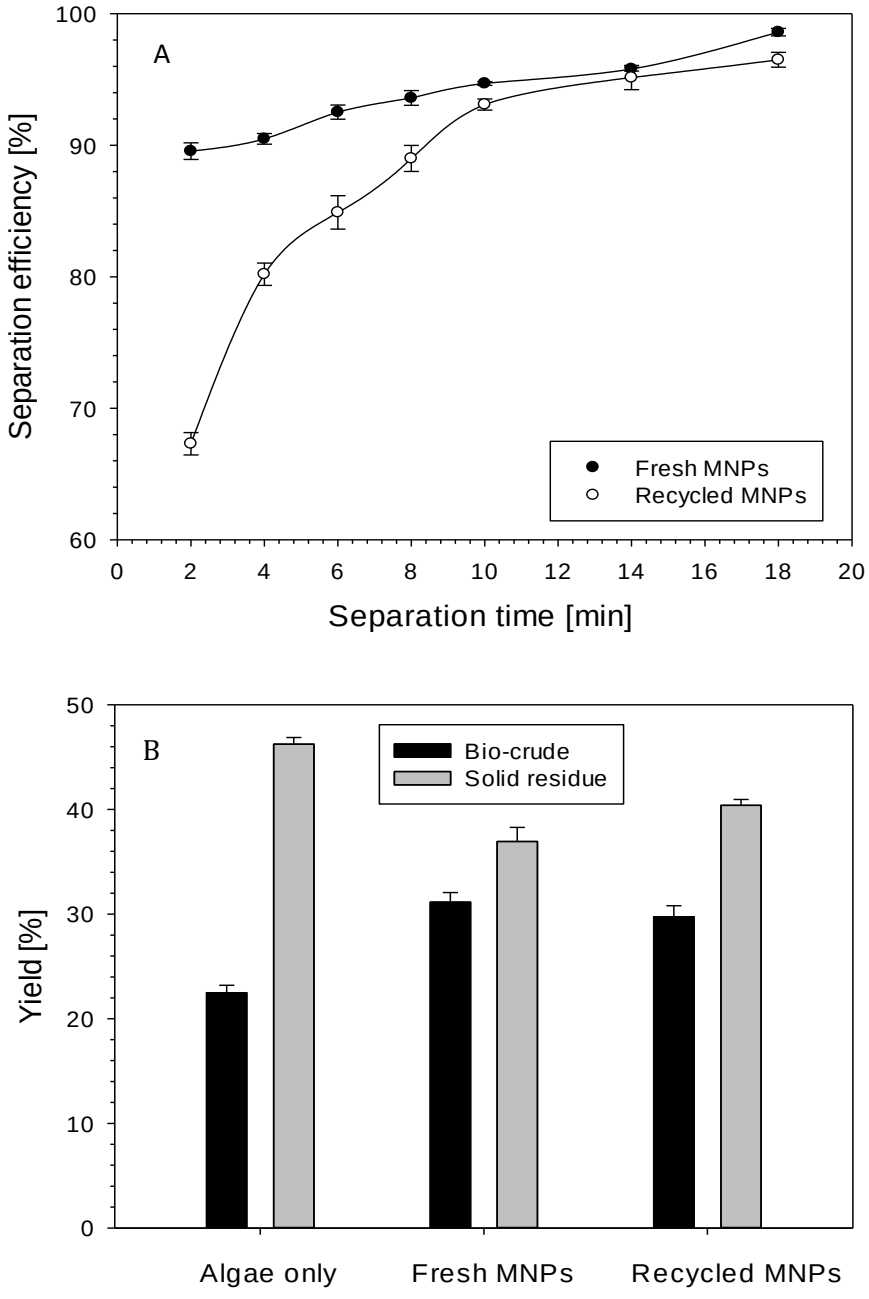

Figure 3. 7. A) Separation efficiency of *S. obliquus* using fresh and recycled MNPs at a mass ratio of MNPs to *S. obliquus* of 0.4, pH 9.0 and separation time of 4 minutes, B) biocrude yield from *S. obliquus* liquefaction in presence of fresh and recycled magnetite nanoparticles at 320 °C for 60 minutes.

The microalgae/recycled MNP slurry was subjected to HTL and the yield of biocrude from re-cycled MNPs was 29 wt. % compared to 30.5 wt.% from fresh MNPs and 22 wt. % from un-catalysed micro-algal liquefaction (Figure 3.7B). These results show that after the HTL process, MNPs can be recycled to efficiently harvest more microalgae and to further catalyse the HTL process. This therefore confirms that MNPs can be applied to both separate microalgae and to catalyse the HTL process hence playing two roles as microalgae harvesting agents and as HTL catalysts.

3.5. Conclusions

In this work, MNPs were synthesised by co-precipitation and used to harvest microalgae at an optimised separation efficiency of 99%. The microalgae/MNPs slurry was then subjected directly to HTL process to investigate the catalytic effect of MNPs on yield and chemical composition of biocrude. It was demonstrated that the yield of biocrude was increased by 13.9 wt. % when HTL of microalgae was done in presence of Zn and Mg doped ferrite MNPs. When Zn doped ferrite MNPs were used in Spirulina liquefaction, GC-MS results revealed that the percentage area of hydrocarbons in the biocrude increased by 26.6% and the percentage area of heptadecane increased by 27.8%. The percentage of hetero atom compounds, nitrogen and oxygen in the biocrude were reduced when HTL was done in the presence of MNPs. This revealed that MNPs did not only play an efficient microalgae separation role but also a catalytic role. Furthermore, MNPs were easily recovered and recycled to harvest more microalgae and to further catalyse the HTL process. It was observed that recycled MNPs were still effective in magnetic separation and HTL catalysis. Using recycled MNPs, a separation efficiency of 96.1% was achieved and the biocrude yield was increased by 7% compared to an increment of 8.7% when fresh MNPs were used in HTL.

Therefore, we have demonstrated for the first time the application of MNPs to harvest microalgae efficiently, to use these then as catalyst in the HTL process which increases yield and quality of biocrude while depositing the MNPs in the solid residue. The MNPs can then easily be recovered and reused in the process. Thus, producing a truly sustainable process culminating in the cost-effective processing of microalgae for biofuel production via the HTL route, potentially enabling a far more efficient route to algal biofuels.

More work is still underway in our group to develop new ferrite catalysts for more efficient de-oxygenation and denitrogenation of biocrude oils.

ASSOCIATED CONTENT

Supporting Information

A list of materials used, methods employed to synthesize magnetic nanoparticles, magnetic separation procedure, procedure for microalgae HTL, bio- crude analysis, TEM images of magnetite, Zn and Mg doped ferrite MNPs, XRD and UV-Vis spectrum of MNPs, graphs of particle size distribution of MNPs, graph of ζ-potential of magnetite and microalgae at different pH, table of elemental composition, HHV and ER of biocrude synthesised with and without MNPs. Table showing the % relative area of major compounds identified from GC-MS spectrum of biocrudes from catalysed and un-catalysed *S. obliquus* and Spirulina liquefaction, GC-MS spectrum of biocrudes from *S. obliquus* and Spirulina liquefaction, graph of grouped compounds from GC-MS spectra of *S. obliquus*, ^{1}H NMR spectrum of biocrudes from catalysed and un-catalysed Spirulina liquefaction, SEM images of microalgae with MNPs attached, pictorial illustration of magnetic separation process, diagrammatic illustration of a potential HTL bio-refinery applying and recycling MNPs, and a graph of biocrude yield using recycled MNPs.

AUTHOR INFORMATION

Corresponding Author

E-mail: P.Plucinski@bath.ac.uk. Phone: +441225786961

Present Addresses

Pawel Plucinski, Department of Chemical Engineering, University of Bath. UK.
Postcode: BA2 7AY

Notes

The authors declare no competing financial interests.

Acknowledgment

Financial support for this research was from the Commonwealth Scholarship Commission UK in form of full Scholarship funding for PhD study of Daniel Egesa.

Supporting Information

Multifunctional Role of Magnetic Nanoparticles in Efficient Microalgae Separation and Catalytic Hydrothermal Liquefaction

Egesa Daniel, Christopher J Chuck, Pawel Plucinski*

Centre for Sustainable Chemical Technology, Department of Chemical Engineering, University of Bath, Bath. United Kingdom. BA2 7AY.

Pages: 14

Figures: 11

Tables: 3

*To whom all correspondence should be addressed. E-mail: P.Plucinski@bath.ac.uk. Phone: +441225786961

Materials

Hexa-hydrate ferrous chloride ($FeCl_3 \cdot 6H_2O$), tetra-hydrate ferrous chloride ($FeCl_2 \cdot 4H_2O$), Ammonium hydroxide (NH_4OH), hydrochloric acid (HCl), sodium hydroxide (NaOH), acetone and ethanol were purchased from fisher scientific UK. Zinc Chloride, Magnesium Chloride hexahydrate, Tetra-methyl ammonium hydroxide, dichloromethane, poly ethylene glycol and pH buffers were purchased from Sigma Aldrich UK. All chemicals used were of analytical grade. All solutions were prepared using de ionized water.

Scenedesmus obliquus was obtained from the undergraduate lab in the department of Chemical Engineering, University of Bath. It was grown in photo bioreactors on culture medium with the following composition in g/L: K_2HPO_4 10.5g, KH_2PO_4 24.6 g, $MgCl_2$ ($7H_2O$) 10.5 g, $NaNO_3$ 35.2 g, NaCl 3.5 g, $CaCl_2$ ($2H_2O$) 3.5g, H_3BO_3 1.6 g, $FeSO_4$ ($7H_2O$) 1.61 g (+ 2.5mL/L H_2SO_4), Na_2EDTA 7.0g, $ZnSO_4$ ($7H_2O$) 1.24 g; $MnCl_2$ ($4H_2O$) 0.2g; MoO_3 0.1 g; $CuSO_4$ ($5H_2O$)0.22 g; Co $(NO_3)2(6H_2O)$ 0.06 g. The microalgae concentration in the culture medium was 0.5g L^{-1}. *Scenedesmus obliquus* had an average composition of protein 56 wt. %, carbohydrates 17 wt. % and lipids 12 wt. % dry weight (Ho, Chen and Chang, 2010).

Methods

Synthesis of magnetite Nanoparticles

Magnetite nanoparticles were synthesized by co-precipitation method. Hexahydrate ferrous chloride ($FeCl_3 \cdot 6H_2O$) 5.4 g and tetra hydrate ferrous chloride ($FeCl_2 \cdot 4H_2O$) 2.0 g was dissolved in 25 cm^3 of an acidic solution (20 mmol hydrochloric acid in DI water). This was then added dropwise to 200 cm^3 of deoxygenated 1.5 molar ammonium hydroxide (NH_4OH) solution with vigorous stirring at 300 rpm for 2 hours. A black precipitate was immediately formed, and it was decanted from the solvent magnetically. The precipitate was then washed with deoxygenated de-ionized (DI) water and ethanol to neutralize residual ions and freeze dried under vacuum conditions for 4 - 6 hours. The dried sample was kept under N_2 to prevent oxidation.

Synthesis of Zn and Mg doped ferrite magnetic nanoparticles

Zn ferrite, Mg ferrite and Zn/Mg ferrite magnetic nanoparticles were synthesized by co-precipitation method (Lv et al., 2015) by dissolving appropriate quantities of the pure powders of hexahydrate ferrous chloride ($FeCl_3.6H_2O$), tetrahydrate ferrous chloride ($FeCl_2 \cdot 4H_2O$), Zinc chloride ($ZnCl_2$) and hydrated magnesium chloride ($MgCl_2 \cdot H_2O$) in de-oxygenated de-ionized water under vigorous stirring in a nitrogen atmosphere. Then 3 ml of modifier (sodium dodecyl benzene sulfonate) was added dropwise under vigorous stirring for 20 minutes. After, NH_4OH solution was added dropwise under vigorous stirring at 400 rpm for 2 hours. The black precipitate was magnetically decanted and washed 3 times with deoxygenated de-ionized water and ethanol to neutralize residual ions, the precipitate was then dried in a vacuum oven at 60 °C for 5 hours and ground in a mortar. The resulting nanoparticle powder was then kept safely for analysis, magnetic separation of microalgae and HTL catalysis.

Magnetic separation of microalgae

Specified quantities of MNPs were crushed, dispersed in 5 ml of deoxygenated DI water, ultra-sonicated for 10 minutes and dispersed in 40 ml of fresh microalgae solution (0.5 g L^{-1}). Magnetic separation was done by placing a magnet beside the beaker containing the microalgae solution (Figure S 7). Microalgae/MNPs slurry was collected on the side of the beaker with the magnet within 1-2 minutes, the absorbance of the supernatant was measured in duplicate at 654 nm by taking 4 ml aliquot after every 2 minutes for 18 minutes. SE was calculated according to method described by Prochazkova et al., (2013). The above procedure was repeated twice to determine the repeatability of the results and to calculate the standard deviation. The effect of gravity and settling ions on the separation efficiency was negligible because of the quick separation time (1-2 minutes) and the method of separation with the magnet on the sides of the beaker. The same observation was made by Prochazkova et al., (2013).

After HTL, MNPs were recovered from bio-char by dispersing the solid residue in 10 ml of deoxygenated de ionized water and sonicated for 5 minutes, in the process the biomass surrounding the nanoparticles floated and MNPs were magnetically recovered and

recycled to further separate microalgae as described in the microalgae magnetic separation procedure above.

Hydrothermal Liquefaction of microalgae

After magnetic separation, the microalgae/MNP slurry was subjected to hydrothermal liquefaction (HTL) at 320 °C for 1 hour. The slurry contained 0.5 g of microalgae dry weight and a specified amount of MNPs with a water content of 78 wt. %. HTL was done according to the method reported by (Harvind K Reddy et al., 2014) The batch reactor was connected to a pressure gauge and had an internal volume of 6.8 ml. The reactor loaded with microalgae/MNP slurry was inserted in a furnace pre-heated to 400 °C. The temperature profile was logged at intervals of 10 seconds using data logging software. The initial and final pressure was read off directly from the pressure gauge. The reactor was cooled to room temperature and the products removed and weighed. The aqueous phase was filtered using a cellulose filter paper and the quantity of dissolved solids was determined gravimetrically. Biocrudes were extracted from the solid phase using dichloromethane (DCM). DCM was separated from the biocrude using a rotary evaporator operated under vacuum at 30 °C at a rotation speed of 30 rpm. The weight of biocrude was measured by subtracting the weight of the glass vial with biocrude from the weight of empty glass vial. The weight of bio-solids was determined by subtracting the weight of dried filter paper with solids from the weight of empty dried filter paper.

Bio Crude oil Analysis

The high heating value of the different biocrude samples was determined using Dulong's formula,(Rojas-Pérez et al., 2015) given by:

$$HHV\ (MJ\ kg^{-1}) = 0.3383C + 1.428(H-O/8) + 0.095S$$

Where: HHV is the high heating value, C, H, O are the wt. % of carbon, hydrogen and oxygen present in the product.

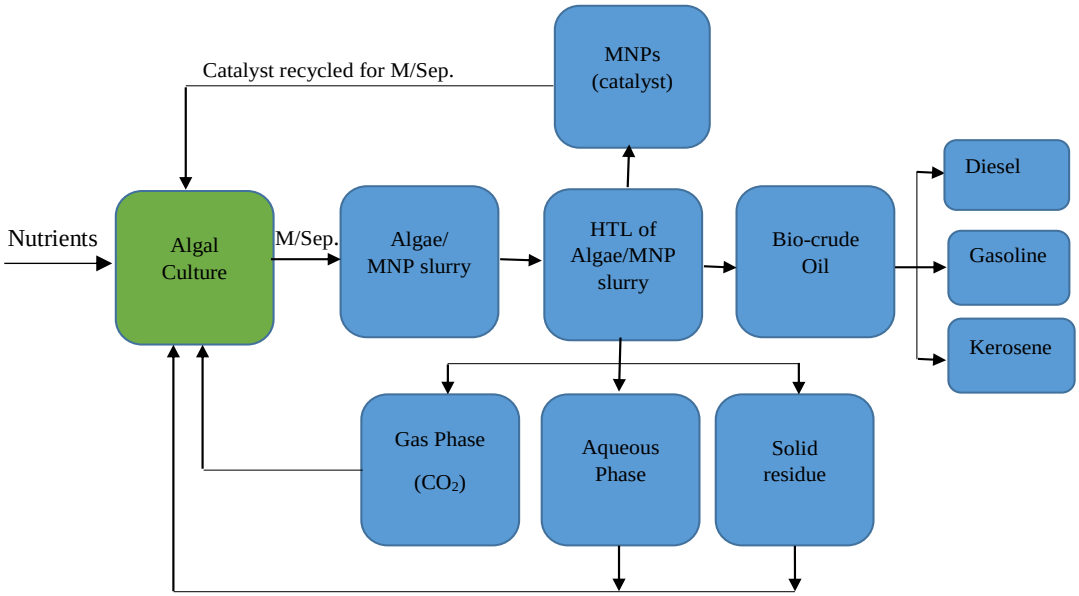

Figure S 1. Illustration of a potential HTL bio-refinery applying and recycling MNPs for magnetic separation of microalgae and as HTL nano-catalysts

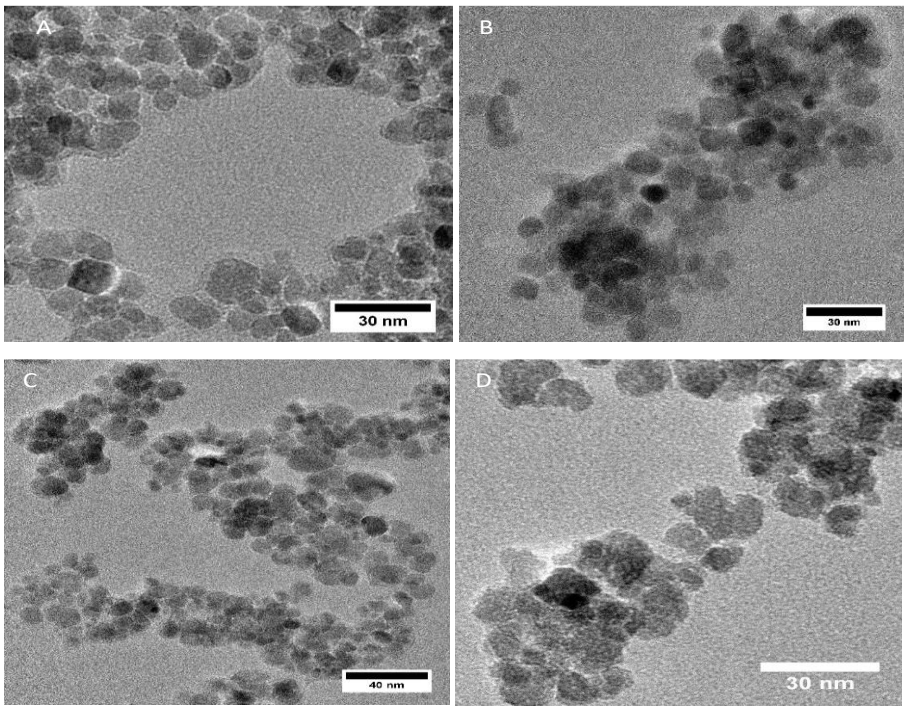

Figure S 2. TEM images of ferrite MNPs synthesized by co-precipitation method: A) un-doped magnetite, B) Zn doped, C) Mg doped and D) Zn and Mg doped ferrite MNPs

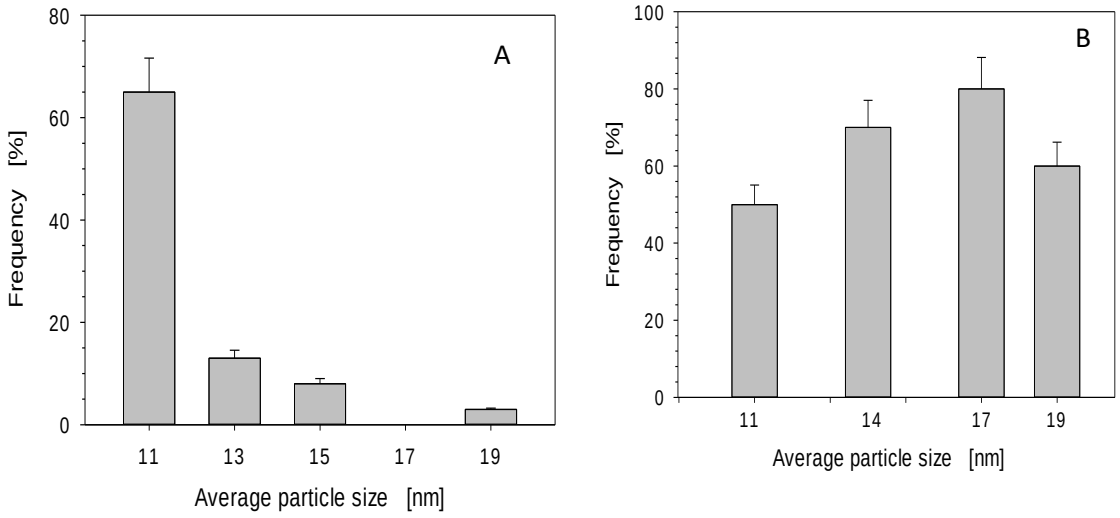

Figure S 3. Particle size distribution of doped and un-doped magnetite nanoparticles: A) of pure Fe_3O_4, B) of Zn/Mg doped Fe_3O_4.

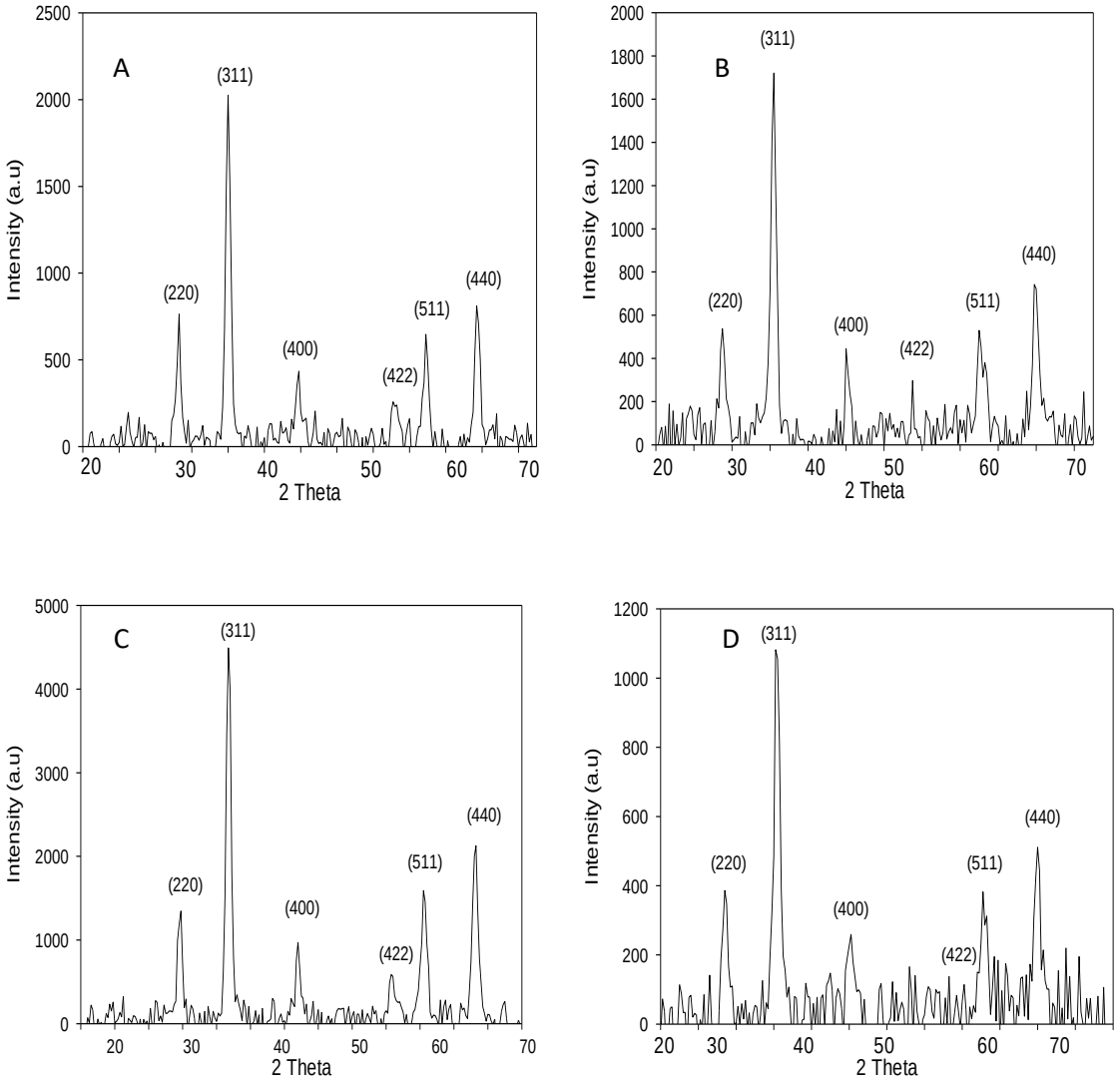

Figure S 4. XRD Spectra of doped and un-doped ferrite magnetic nanoparticles revealing increased peak intensity with doping: A) Zn doped ferrite with the highest peak at 2000 counts, B) Mg doped ferrite with highest peak at 1700 counts, C) Zn/Mg doped ferrite with the highest peak at 4500 Counts, and D) un-doped magnetite with the highest peak at 1150 Lin counts.

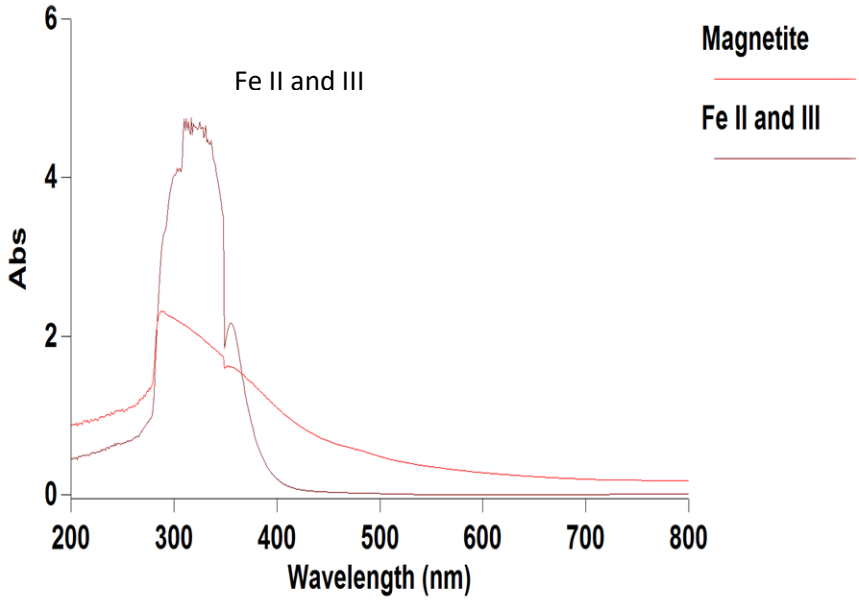

Figure S 5. Comparing UV-Vis spectrum for magnetite (red) and a mixture of iron II and iron III (maroon) from which magnetite was synthesized.

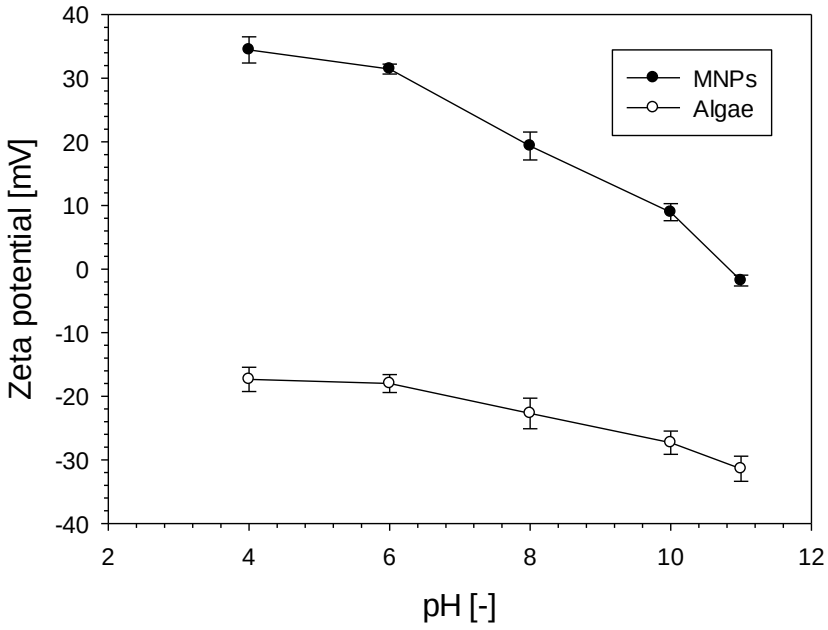

Figure S 6. Zeta potential of Fe_3O_4 nanoparticles and *Scenedesmus obliquus* at different pH values.

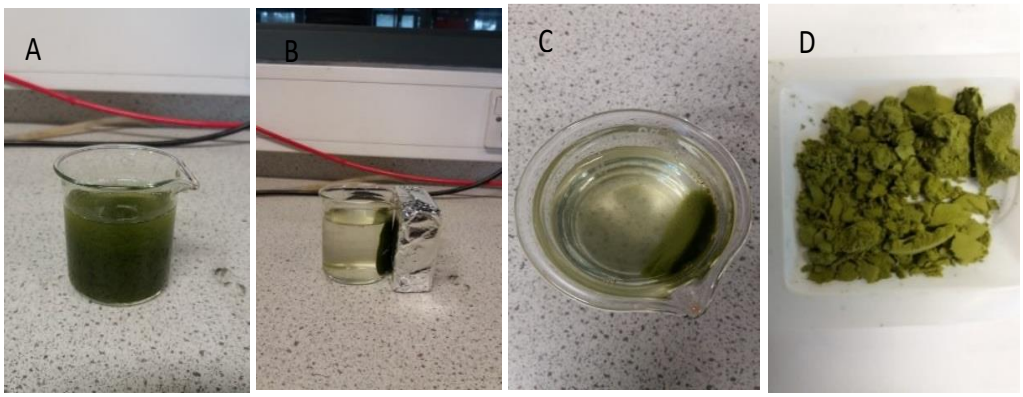

Figure S 7. Illustration of magnetic separation process: A) microalgae/MNPs suspension, B) magnetic separation, C) separated microalgae in solution, D) dried microalgae after magnetic separation.

Table S. 1. Major Compounds identified from GCMS spectrum of bio lipids from *S. Obliquus* HTL in presence and absence of magnetite nanoparticles.

RT(Min)	Compound Name	Relative area (%)	
		S. Obliquus lipid only	*S. obliquus*/magnetite
3.459	Phenol	2.46	2.06
4.363	1,3-diethyl-	3.21	*
4.443	Benzene	6.46	1.43
4.838	2,5-Pyrrolidinedione	2.41	*
5.227	Azetidine	3.14	*
8.78	1H-Indole	6.39	7.71
14.868	Octane	3.08	*
18.771	Cyclohexane	6.34	*
19.12	2-Hexadecene	10.67	5.9
20.745	2-Nonyne	2.09	*
8.654	Benzoxazole	*	3.09
10.096	Benzonitrile	*	1.58
14.868	Heptadecane	3.1	20
16.871	Pyrimidine	*	1.7
22.147	n-Hexadecanoic acid	*	3.11
28.281	N-Methyldodecanamide	*	2.16
29.231	N,N-Dimethyldecanamide	*	1.52
Total		49.35	50.26

** Very small peaks with area less than 1% were left*

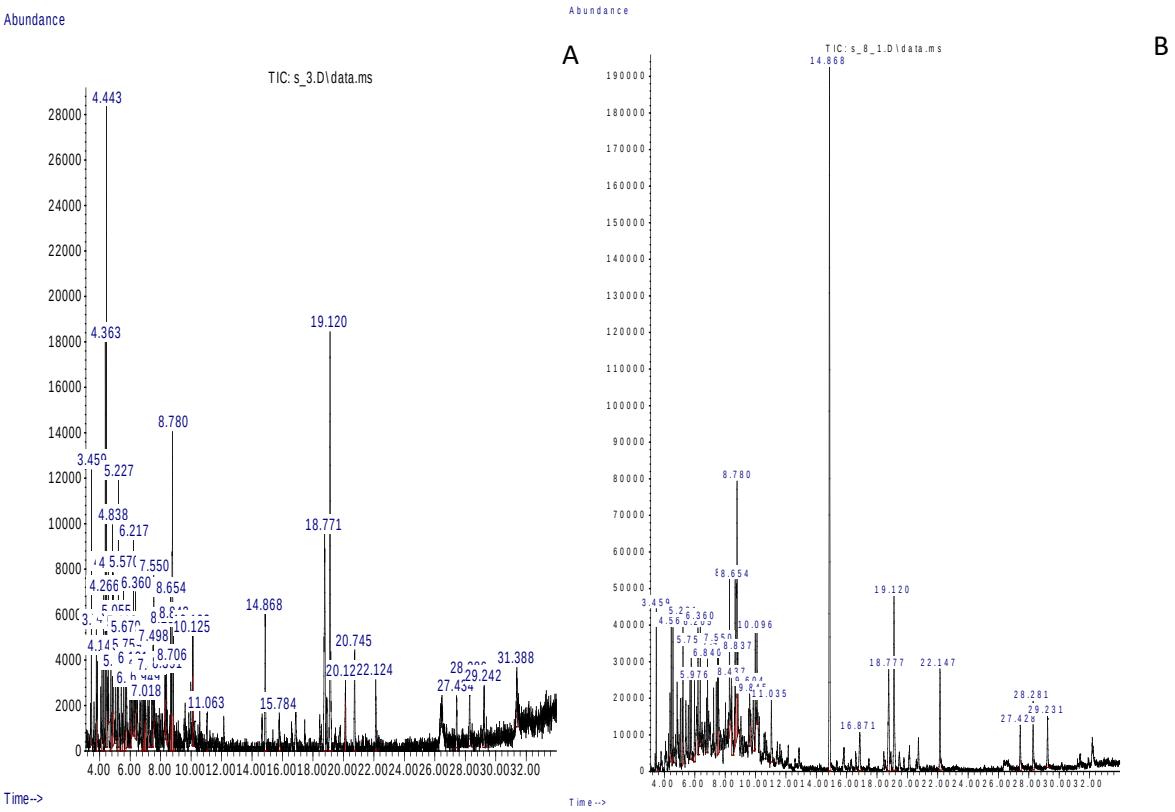

Figure S 8. GC-MS Chromatogram of biocrude samples produced from HTL of *Scenedesmus obliquus* with and without MNPs: A) Pure *S. obliquus*, B) *S. obliquus* in presence of Fe_3O_4 nanoparticles.

Table S. 2. Major Compounds identified from GC-MS Chromatogram of biocrude from Spirulina HTL with and without MNPs

RT(Min)	Compound Name	Relative area (%)			
		Spirulina biocrude	Spirulina/ Zn ferrite	Spirulina/ Mg ferrite	Spirulina/ Zn/Mg ferrite
3.459	Phenol	*	*	3.2	*
4.363	Benzene, 1,3-diethyl-	11.2	*	*	*
4.443	Benzene	16.6	*	*	*
5.221	Cyclo heptylamine	*	*	4.2	*
5.759	1-Hexen-3-yne, 2,5,5-trimethyl-	1.4	*	*	*
7.556	Indole	*	*	4.8	*
8.277	Propyl phosphonic acid	*	*	*	5.8
8.282	2,3,4-Trimethyl-isoxazol-5(2H)-one	*	*	5.9	*
8.780	1H-Indole, 3-methyl-	6.2	*	9.6	8.7
9.982	2-Cyclopenten-1-one	1.7	*	3.4	*
10.090	Acetamide	1.4	*	*	*
14.868	Heptadecane	10	37.8	14.6	23.4
16.865	3-Pyridinecarbonitrile	1.6	*	*	*
16.877	4-Butylbenzoic acid	*	*	3.4	*
18.771	Cyclohexane	3.6	*	*	7.5
18.776	2-Hexadecene	*	8.7	6.3	*
19.108	Cyclopropane	4.9	*	*	*
20.133	Bicyclo[4.1.0]heptan-2-one	*	7.2	3.5	*
20.728	3,7,11-Trimethyl-2,4-dodecadiene	*	*	*	5.1
20.739	Formic acid	*	*	3.1	*
22.124	n-Hexadecanoic acid	9.7	*	6.5	5.6
27.428	Butanamide	3.7	*	*	*
28.292	Propanal	7.2	*	*	*
29.230	N,N-Dimethyldecanamide	6.1	*	*	*
32.189	Isobutyl isothiocyanate	3.1	*	*	*
Total		88.4	70	80	76

** Very small peaks with area less than 1% were left*

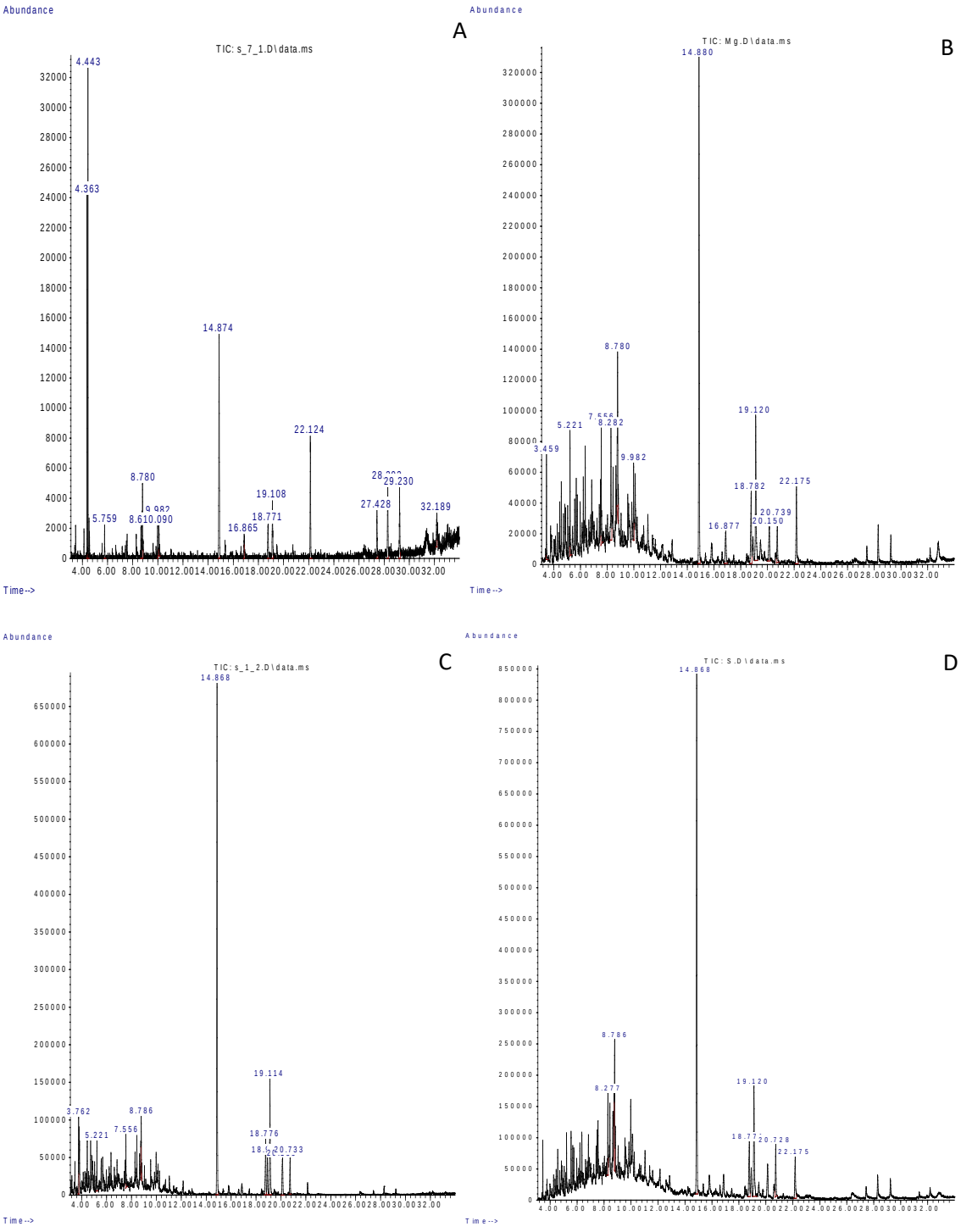

Figure S 9. GCMS Spectrum of biocrude oil samples produced from HTL of spirulina with and without multi metal ferrite nanoparticles: A) Pure Spirulina, B) spirulina in presence of Mg/Fe_3O_4, C) Spirulina in presence of Zn/Fe_3O_4, D) Spirulina in presence of Zn/Mg/Fe_3O_4.

A

DE NMR1

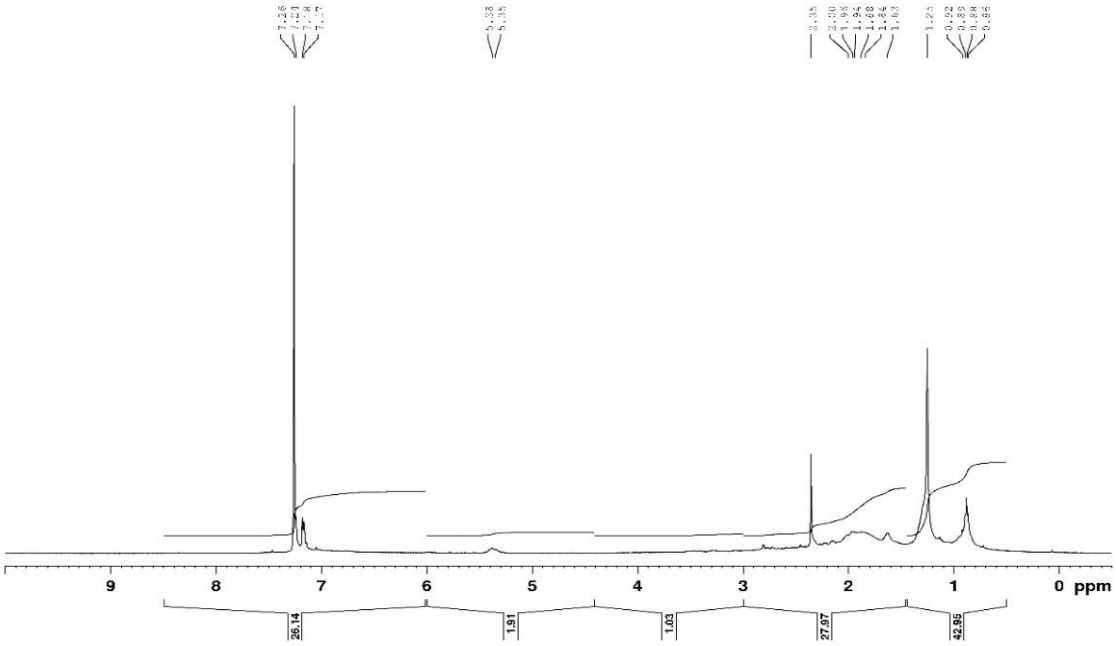

B

DE S.3.1

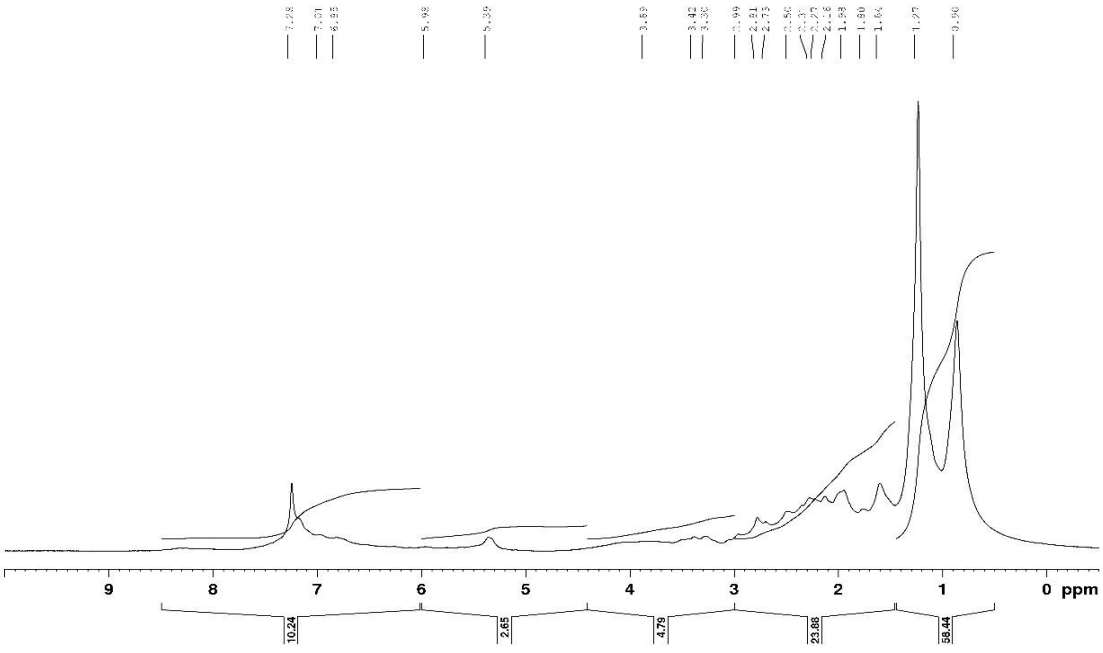

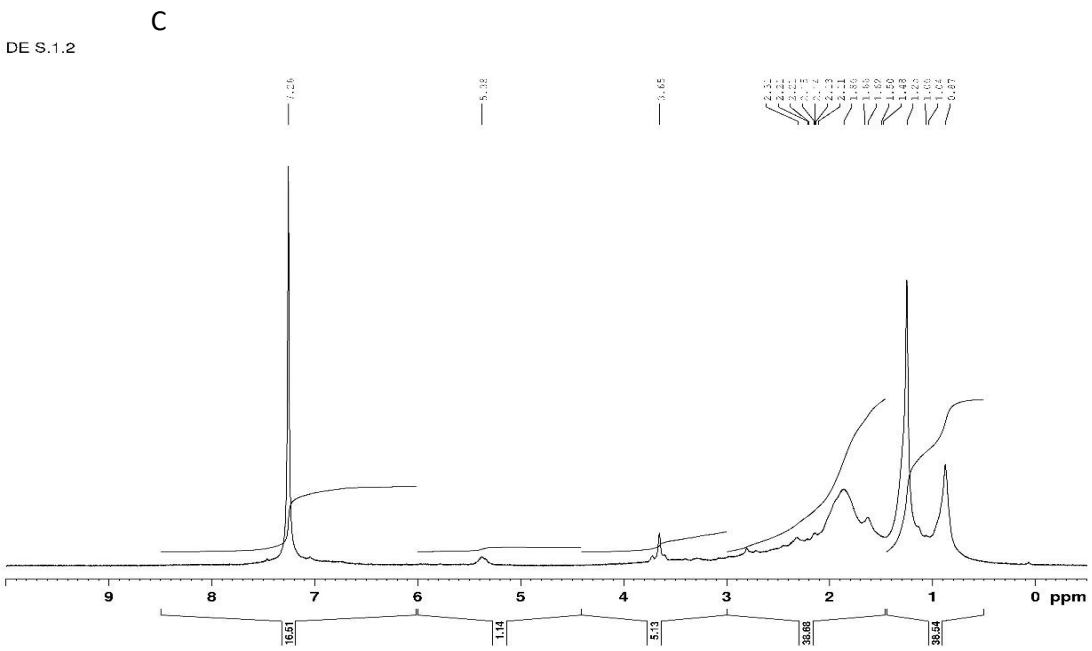

Figure S 10. ^{1}H NMR Spectra of Spirulina biocrude synthesized in presence and absence of MNPs at 320 °C, for 60 minutes at a mass ratio of MNPs: Spirulina of 0.12: A) Biocrude synthesized in absence of nanoparticles, B) biocrude synthesized in presence of Zn/Mg/ ferrite and C) biocrude synthesized in presence of Zn ferrite.

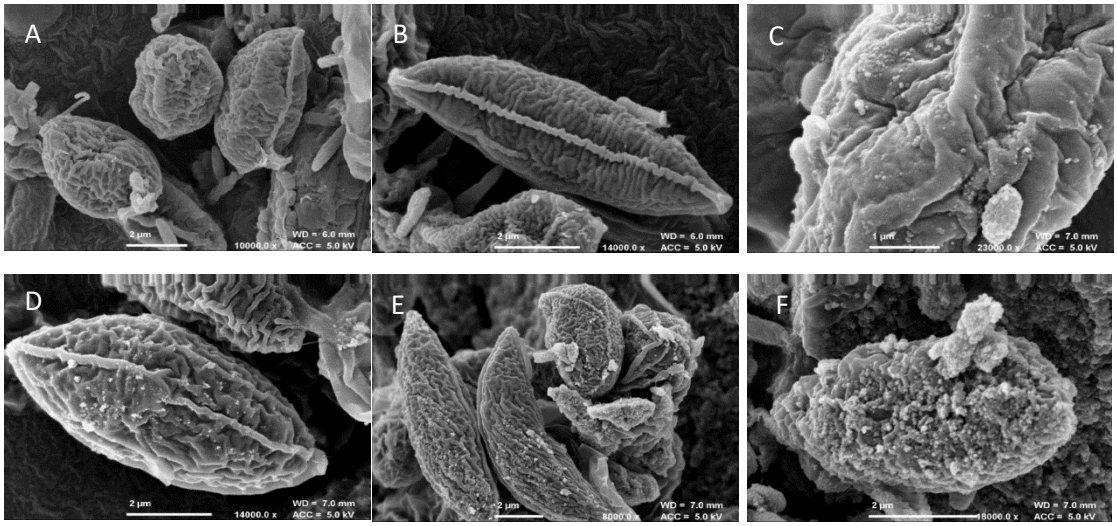

Figure S 11. A, and B, SEM Images of microalgae cells before adding MNPs, C, D, and E SEM Images MNPs adsorbed onto microalgae cells at a lower mass ratio of MNPs to microalgae (0.06 g/g for D), E at a higher mass ratio (0.6)

Table S. 3. Elemental compositions, HHV, atomic ratios and ER of solid residue from spirulina liquefaction at different masse ratios of magnetite: microalgae at 320 °C for 60 minutes, at P_0 of 50 bar (N2), and P_f of 120 bar.

Ratio Fe_3O_4: microalgae	C (wt %)	H (wt %)	N (wt %)	O (wt %)	S (wt %)	N/C* -	H/C* -	O/C* -	HHV (MJ/kg)	ER (%)
0	20.77±0.21	1.81±0.16	0.86±0.06	22.85±0.04	0.22±0.03	0.04	1.045	0.82	5.55±0.16	9.26±0.13
0.06	20.19±0.06	1.94±0.04	0.10±0.01	23.15±0.01	0.31±0.00	0.04	1.15	0.86	5.49±0.25	7.17±0.16
0.2	8.35±0.21	1.34±0.02	0.65±0.00	15.18±0.08	0.24±0.01	0.05	1.55	1.10	2.72±0.09	3.55±0.06
0.4	5.10±0.11	0.71±0.02	0.52±0.00	14.07±0.31	0.18±0.04	0.09	1.66	2.07	0.24±0.00	0.31±0.00

*****Atomic ratios

4. Effect of process conditions on biocrude yield and composition

The previous Chapter presented the multifunctional role of MNPs in efficient microalgae separation and catalytic HTL and the recycling of MNPs after HTL. The MNPs also played a catalytic role in reducing the N and O content and increasing biocrude yield. However, The N and O content remains high. Therefore, the main objective of this Chapter is to reduce the N and O content of biocrude oil by investigating the effects of HTL process conditions on biocrude composition and yield. The microalgae liquefaction was done in presence and absence of MNPs.

4.1. Abstract

Hydrothermal liquefaction (HTL) of microalgae produces a biocrude oil with a high nitrogen and oxygen content that makes it unsuitable for use as a transportation fuel. In the previous Chapter, HTL in presence of MNPs led to reduction in the N, O and S content of biocrude oil and improvement in the high heating value (HHV) and energy recovery (ER) of biocrude. However, the N, O and S content of biocrude is still high and further reductions are needed to improve the fuel quality. Therefore, the aim of research presented in this Chapter is to further reduce the N, O and S content of biocrude oil while maintaining the crude yield. This was done by assessing the impact of processing conditions on biocrude yield and especially on biocrude chemical composition. The processing conditions assessed include holding time, temperature, the presence of hydrogen and 5% formic and sulphuric acids. Increase in holding time resulted in gradual increase in biocrude yield up to an optimum yield of 36.2 wt.% after 60 minutes at 320 ℃ and 32.8 wt. % after 90 minutes at 307 ℃. Increase in holding time also led to gradual increase in carbon and hydrogen content of biocrude and to steady reduction in O, N and S content of biocrude oil. Liquefaction in the presence of 5% sulphuric acid resulted in the highest removal of nitrogen by 83 wt. % and the highest hydrogen content (10.6 wt. %) for all liquefaction experiments done in this work. Sulphuric acid has the disadvantage of corroding equipment. Liquefaction under hydrogen atmosphere resulted in the further removal of oxygenated compounds and increase in hydrocarbons according to the GC-MS and elemental analysis results. The chemical composition of biocrude was analysed using GC-MS and elemental analysis. The MNPs used for microalgae separation and catalytic HTL were characterised using HRTEM, elemental mapping and TGA analysis. Reduction in N, O and S content of biocrude greatly improves the oil quality since these elements impart undesirable properties. High oxygen content reduces the energy value of biocrude oil. Removal of these elements and addition of hydrogen improves the biocrude quality making it more suitable for integration into a fossil oil refinery.

4.2. Introduction

The global carbondioxide levels are continuously increasing at an alarming rate, currently (February 2019) standing at 411.8 ppm from 279 ppm in 1750 (CO2-earth, 2019). This huge increase is largely contributed through the burning of fossil fuels for energy, resulting in high emission of greenhouse gasses. Some of the negative effects of greenhouse gases is increased global warming and environmental pollution. Maintenance of greenhouse gas emissions to a range of 445-490 ppm of CO_2 equivalent would limit the global temperature increase to 2 ºC (Moomaw et al., 2011). To achieve this goal, heavy dependence on fossil fuels as a source of energy should be minimised and replaced with renewable sources of energy such as biofuels. It is estimated that by 2030 biofuels will contribute to 11% of the total global energy demand if a climate change alleviation strategy that maintains CO_2 levels to 450 ppm is implemented (Edenhofer et al., 2011).

Currently, the main feedstock for the production of biofuels is biomass (Jestin-Fleury, 1994). Among the biomass used, microalgae has proved to be more favourable for biofuel production. This is due to their high productivity, high rate of photosynthesis, can grow on non-arable land and on brackish water, no competition between fuel and food for the limited biomass feedstock and they contain large quantities of lipids (up to 80 wt.% with genetic engineering) (Aaronson and Dubinsky, 1982; Christensen et al., 2014; Egesa, Chuck and Plucinski, 2017). The most common method of converting biomass to biofuel is through solvent extraction of lipids and their subsequent transesterification into biodiesel (Umdu, Tuncer and Seker, 2009; Halim et al., 2011). The major setback with this approach is the usage of large amounts of hazardous organic solvents for lipid extraction and the biomass requires drying before extraction leading to an increased energy input to evaporate water and solvent. Other thermochemical conversion techniques such as pyrolysis and gasification have been explored too. The challenge is that they require the use of dry biomass resulting in a considerable increase in energy costs due to the need for drying prior to the conversion step (Zou et al., 2009).

Because of this, a wet biomass conversion technique such as hydrothermal liquefaction (HTL) is more favourable for the production of biofuels from microalgae since the energy intensive drying step with the high costs involved is avoided. The HTL process uses less

than 5% of the total energy needed for biomass drying and can accommodate an microalgae concentration of 5-20% (Lixian Xu et al., 2011a). Through the HTL process biomass is treated at high temperatures (250-400 °C) and pressures (50.7-202.7 bar) to produce a liquid biocrude oil (Huber, Iborra and Corma, 2006). It utilizes the properties of superheated solvents to lower the resistance to mass transfer (Peterson et al., 2008). The process can utilize any type of biomass and biomass with high moisture content. During the HTL process, the complex bio-compounds in the microalgae such proteins, carbohydrates and lipids are broken down into a mixture of chemicals composed mainly of carbon, hydrogen, nitrogen and oxygen (Huber, Iborra and Corma, 2006). Microalgae contains a high protein content which is broken down to nitrogen compounds through the deamination of amino acids (Peterson et al., 2008).

The high nitrogen and oxygen content in biocrude impart undesirable fuel characteristics. For example, a high percentage of nitrogenated compounds in the biofuels results in a high emission of NOx gases into the atmosphere while a high percentage of oxygenated compounds reduces the high heating value and energy recovery of the biofuels. Therefore, the aim of this Chapter is to improve the biofuel quality through denitrogenation and deoxygenation of biocrude in presence of MNPs under different HTL conditions. This will be achieved by liquefying microalgae under different conditions such as hydrogen atmosphere, acids and under different reaction times. The effect of these conditions on elemental composition of biocrude especially on nitrogen, oxygen and sulphur removal and on hydrogen and carbon addition will be investigated. The aim of this research Chapter will be achieved through the following objectives:

(i) Synthesis and characterisation of MNPs to be used in catalytic HTL and magnetic separation of microalgae.

(ii) Investigation of the effect of liquefaction time and temperature on yield and elemental composition of biocrude oil.

(iii) Investigation of the effect of HTL under hydrogen atmosphere on yield and chemical composition of biocrude oil.

(iv) Explore the effect of microalgae liquefaction under 5% formic and sulphuric acid on yield and chemical composition of biocrude oil.

Achieving the above aim and objectives will potentially result in production of better quality biocrude oil that would potentially improve its quality as a transportation fuel.

4.3. Materials, methods and analytical techniques

4.3.1. Materials

Hexahydrate ferrous chloride ($FeCl_3 \cdot 6H_2O$), tetra-hydrate ferrous chloride ($FeCl_2 \cdot 4H_2O$), ammonium hydroxide (NH_4OH), hydrochloric acid (HCl), sodium hydroxide (NaOH), acetone and ethanol were purchased from Fisher scientific UK. Zinc chloride, magnesium chloride hexahydrate, palladium chloride, nickel chloride, cobalt chloride, tetra-methyl ammonium hydroxide, dichloromethane, poly ethylene glycol, sulphuric acid, formic acid and pH buffers were purchased from Sigma Aldrich UK. All chemicals used were of analytical grade. All solutions were prepared using de ionized water. Spirulina was purchased from bulk powders and had the following composition: carbohydrates 20 wt.%, proteins 63 wt.%, fats 6 wt.% and miscellaneous biochemical content 11 wt.%. The ash content of spirulina was between 16-18 wt.% and the moisture content was between 8-12 wt.%.

4.3.2. Methods

4.2.2.1. Synthesis of magnetite nanoparticles

Magnetite nanoparticles were synthesized by co-precipitation method as described in the previous chapter. Hexahydrate ferrous chloride ($FeCl_3 \cdot 6H_2O$) 5.4 g and tetra hydrate ferrous chloride ($FeCl_2 \cdot 4H_2O$) 2.0 g was dissolved in 25 cm^3 of an acidic solution (20 mmol hydrochloric acid in DI water). This was then added dropwise to 200 cm^3 of deoxygenated 1.5 molar ammonium hydroxide (NH_4OH) solution with vigorous stirring at 300 rpm for 2 hours. A black precipitate was immediately formed, and it was magnetically decanted from the solution. The precipitate was then washed with fresh deoxygenated deionized (DI) water and ethanol to neutralize residual ions and freeze dried under vacuum conditions for 4 - 6 hours at -40 °C. The dried sample was kept under N_2 to prevent oxidation.

4.3.2.2. Synthesis of ferrite MNPs

Ferrite magnetic nanoparticles were synthesized using the co-precipitation method (Lv et al., 2015) by dissolving 5.4g of the pure powders of hexahydrate ferrous chloride ($FeCl_3.6H_2O$), 2.0 g of tetrahydrate ferrous chloride ($FeCl_2 \cdot 4H_2O$) and 0.4 g of metal chlorides (Zn, or Mg) in deoxygenated deionized water under vigorous stirring in a nitrogen atmosphere. Then 3 ml of modifier (sodium dodecyl benzene sulfonate) was added dropwise under vigorous stirring for 20 minutes. To reduce the ferrous ions to magnetite nanoparticles, 40 mL of NH_4OH solution (1.5 M) was added dropwise under vigorous stirring at 400 rpm for 2 hours. The black precipitate was magnetically decanted and washed 3 times with deoxygenated de-ionized water and ethanol to neutralize residual ions, the precipitate was then dried in a vacuum oven at 60 °C for 5 hours and ground in a mortar. The resulting nanoparticle powder was then then kept under N_2 atmosphere to prevent oxidation.

Ni and Pd doped ferrites were synthesised according to the method described by (Lyon et al., 2004) by dispersing magnetite nanoparticles (0.5 g) in 75 ml of de-ionised water and then sonicating for 30 minutes. Then nickel chloride or palladium chloride (0.164 g each) were dissolved in an acidic solution containing 100 µl of hydrochloric acid in 10 ml of water and mixed with the magnetite dispersion. Afterwards 25 ml of ethanol was added, and the mixture was stirred for 1 hour under a nitrogen atmosphere. Then 50 ml of 0.04 M sodium borohydride ($NaBH_4$) in water was added dropwise for 30 minutes and the mixture was stirred overnight to complete the reaction. Doped ferrite MNPs were magnetically extracted from the solution, washed with water and ethanol to neutralize residual ions and vacuum dried.

4.3.2.3. Hydrothermal liquefaction of microalgae

The spirulina/MNPs was subjected to hydrothermal liquefaction (HTL) at 307 and 320 °C at varying reaction conditions such as liquefaction time, HTL in presence of hydrogen gas and HTL in presence of 5% formic and sulphuric acid. The mass of microalgae was 0.5 g dry weight and the mass ratio of MNPs to microalgae was 0.12 g/g with a water content of 78 wt.%. HTL was performed according to the method reported by (Harvind K Reddy et al., 2014). The batch reactor was connected to a pressure gauge and had an internal

volume of 6.8 ml. The reactor with its contents was inserted in a furnace pre-heated to 400 °C. The temperature profile was logged at intervals of 10 seconds using data logging software. The initial and final pressure was read off directly from the pressure gauge. After HTL, the reactor was cooled to room temperature and the products removed and weighed. The aqueous phase was filtered using a cellulose filter paper and the quantity of dissolved solids was determined gravimetrically. Biocrudes were extracted from the solid phase using dichloromethane (DCM). DCM was separated from the biocrude using a rotary evaporator operated under vacuum at 30 °C at a rotation speed of 30 rpm. The weight of biocrude was measured by subtracting the weight of the glass vial with biocrude from the weight of empty glass vial. The weight of bio-solids was determined by subtracting the weight of dried filter paper with solids from the weight of empty dried filter paper. Figure 4.1 illustrates the HTL process from the microalgae feed the process and products.

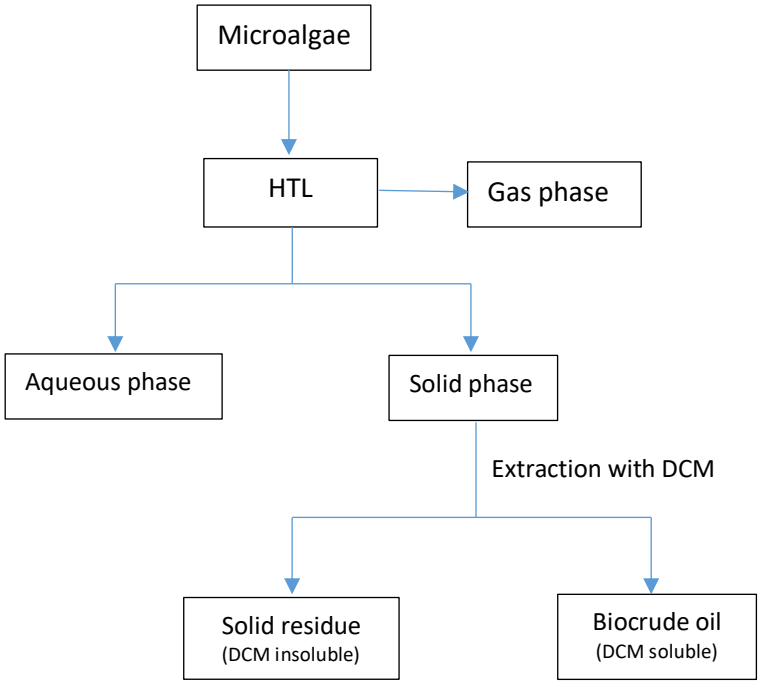

Figure 4. 1. Diagrammatic illustration of the hydrothermal liquefaction process

4.3.2.4. Biocrude oil analysis

The percentage yield of HTL products was determined using equation 4.1 as described in the previous chapter. The biocrude and solid residue was calculated on an ash and moisture free basis.

$$YP = \frac{WP}{WF - WA - WM} \times 100\ (\%) \qquad (4.1)$$

where, *YP* is the percentage yield of the product, *WP* is the mass of product (g), *WF* is mass of microalgae fed into the reactor, W_A and W_M are ash and moisture content of microalgae respectively.

The high heating value (HHV) of biocrude was determined using Dulong's formula see equation 4.2 (Rojas-Pérez et al., 2015).

$$\text{HHV (MJ kg}^{-1}) = 0.3383C + 1.428(H-O/8) + 0.095S, \qquad (4.2)$$

Where: HHV is the high heating value, C, H, O are the wt. % of carbon, hydrogen and oxygen present in the product.

The energy recovery (ER) for the biocrude was calculated according to equation 4.3 (Sofia Raikova et al., 2016b).

$$ER = \frac{(HHVp \times Oil\ Yield)}{(HHVf)} \qquad (4.3)$$

where: *ER* is the energy recovery, HHV_p is high heating value of product, and HHV_f is high heating value of feed.

4.3.3. Analytical techniques

4.3.3.1. HR-TEM and EDS analysis of MNPs

To ascertain the surface morphology, size and particle distribution of MNPs, high-resolution transmission electron microscopy (TEM) was done. TEM samples were prepared by suspending a specified amount of MNPs (0.02 g) into methanol (5 ml), ultra-sonicating it for 10 minutes to dismantle aggregated particles, a drop of MNPs suspension was then placed on carbon coated copper grids, and the solvent could evaporate. The measurements were done on a JEM-1200 EX11 TEM instrument at an acceleration voltage of 300 kV. Energy Dispersive X-Ray Spectroscopy (EDS) and elemental mapping

were also done on the same instrument to establish the extent of distribution of doped MNPs into the matrix of magnetite.

4.3.3.2. GC-MS analysis of biocrude oil

To analyse the compounds in biocrude oil, GC-MS analysis was applied. A GC 3800 was used with an auto-sampler 8400, the syringe size was 10 micro litres. Carrier gas was helium, the column oven initial temperature was 100 °C, holding time was 5 minutes, raised to 250 °C at a rate of 5 °C/min and held for 15 minutes, total time was 35 minutes. The compounds were identified using a mass spectral library software.

4.3.3.3. Elemental analysis of microalgae and biocrude oil

To determine the elemental composition of microalgae and HTL products (biocrude and solid residue) elemental analysis was applied. Samples were sent to OEA Laboratories, in Cornwall, UK. The CHNOS elemental compositions were determined according to the following procedure as received from OEL laboratories:

CHNS Analysis

Samples were analysed for elemental composition for nitrogen, carbon, hydrogen and sulphur using a Thermo model EA1110 elemental analyser, running Xperience EA software, single tube configured for simultaneous CHN or CHNS analysis using a Porapak QS 2 metre separation column. References and samples were weighed to 6 decimal places using a Mettler UMX5 microbalance.

The **EA1110 elemental analyser** was calibrated to reference standards (Acetanilide for CHN or 2,5-Bis(5-tert-butyl-2-benzo-oxazol-2-yl) thiophene (BBOT) for CHNS both traceable to international certified materials). Samples and reference weights were target weight optimised to ensure samples were within the calibration range of the system. Sample results were calculated from the mean of the calibration response of the references. Standard deviations were calculated for the references and reported on the analysis report and were within working specification for the system (typically better than N=0.15, C=0.3, H=0.1 & S=0.3)

Oxygen Analysis

Samples were analysed for elemental composition for oxygen using a Thermo model EA1110 elemental analyser, running Xperience EA software, single tube configured for oxygen analysis using a Molecular Sieve 3A separation column. References and samples were weighed to 6 decimal places using a Mettler UMX5 microbalance. The EA1110 elemental analyser was calibrated to reference standards (acetanilide traceable to international certified materials). Samples and reference weights were target weight optimised to ensure samples were within the calibration range of the system. Sample results were calculated from the mean of the calibration response of the references. Standard deviations were calculated for the references and reported on the analysis report and were within working specification for the system (typically better than O=0.15).

4.4. Results and Discussion

4.4.1. Synthesis and characterization of MNPs

MNPs were synthesised, characterised and used to separate microalgae from the culture medium and to catalyse the HTL process under different process conditions. Their catalytic effect on yield and chemical composition of biocrude oil under different reaction conditions especially their effect on denitrogenation and deoxygenation of biocrude oil was investigated. The nanoparticles synthesised include magnetite (Fe_3O_4), Zn ferrites ($ZnFe_3O_4$), Ni ferrites ($NiFe_3O_4$) and Pd (0) Fe_3O_4 doped MNPs. The magnetic nanoparticles were synthesised by coprecipitation method (Laska et al., 2009) because it is economical, fast, simple and offers good control over particle size, distribution and shape at room temperature and pressure. Most of the characterization techniques on MNPs were presented in Chapter 3. In this chapter, the characterization techniques not covered in the previous Chapters such as elemental mapping, EDS and TGA are presented.

4.4.1.1. HR-TEM analysis of MNPs

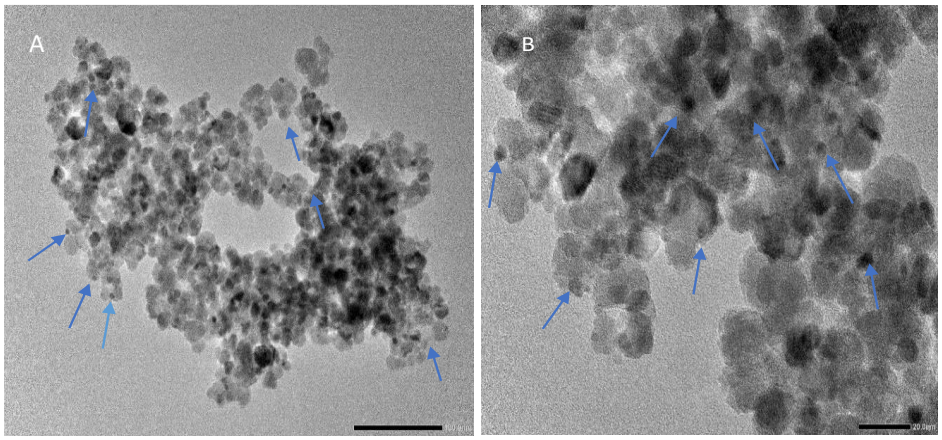

Figure 4. 2. TEM Images of magnetite nanoparticles with attached Pd (0) nanoparticles as indicated by the arrows. A) At lower magnification (scale 100 nm) and B) at higher magnification (scale 20 nm).

The synthesis method of MNPs/Pd (0) nanoparticles was based on the modified procedure described by Lyon et al., (2004). The average particle size of the MNPs was 10-12 nm as stated earlier while the palladium particles on their surfaces were in the range of 2-3 nm. TEM Elemental mapping (Figure 4.2) confirmed the presence of palladium.

4.4.1.2. EDS Elemental mapping

The elemental composition of the synthesized MNPs was also confirmed using EDS as shown in Figure 4.3. The EDS analysis confirmed the presence of Zn, Mg and Ni in the doped samples. The spectra confirmed that synthesized samples contained the doped elements.

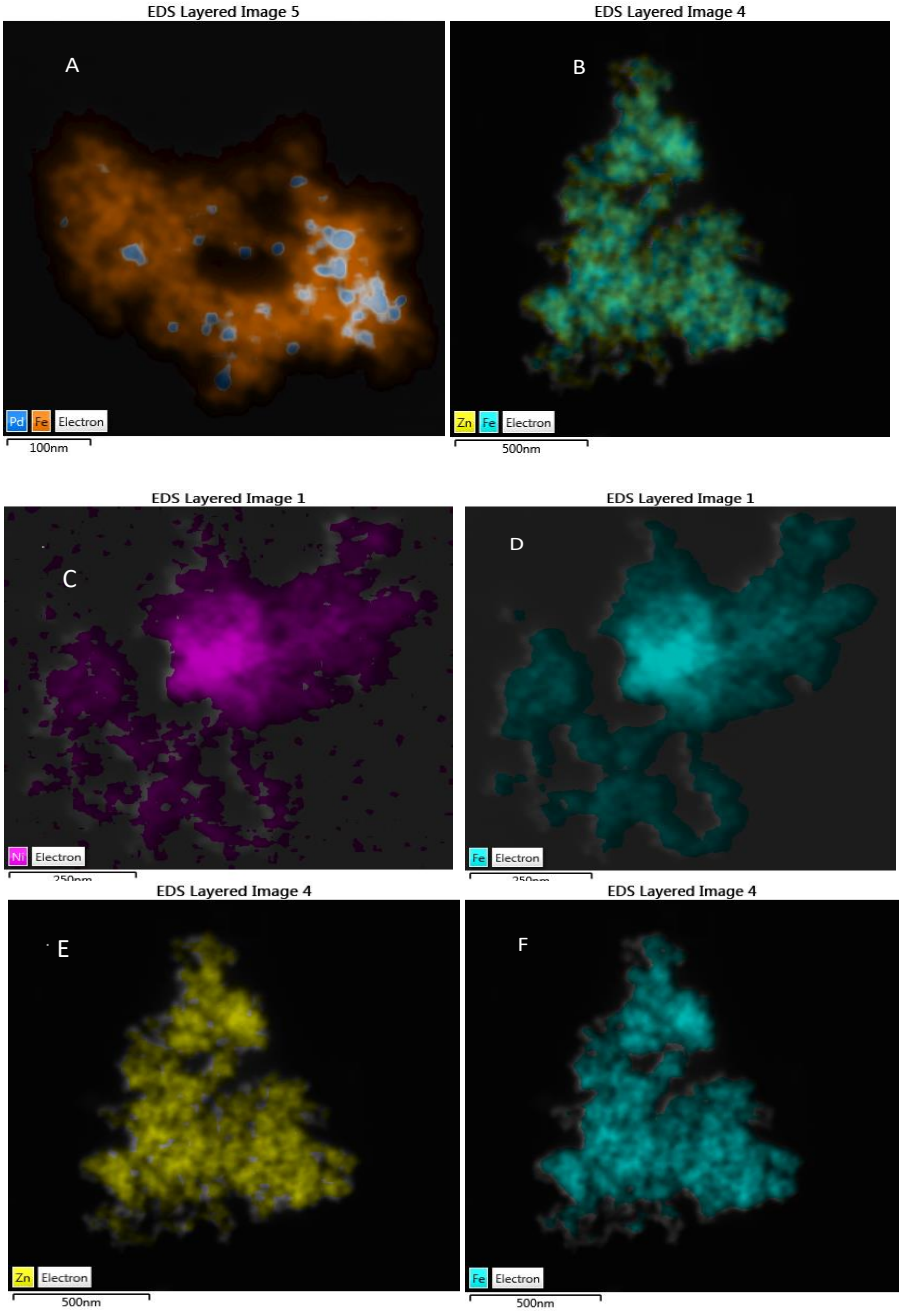

Figure 4. 3. TEM images showing elemental distribution of Pd, Zn and Ni over magnetite nanoparticles.

Based on the above characterisation techniques, it is evident that MNPs were successfully synthesised. The synthesised particles were used to magnetically separate microalgae from culture medium and the separated microalgae/MNPs slurry was subjected to high temperature liquefaction to produce biocrude oil.

4.4.2. Effect of holding time on biocrude yield and composition

The effect of holding time on biocrude yield was investigated at two temperatures (307 ºC and 320 ºC). The purpose of these experiments was to optimise the holding time and to determine its effect on biocrude yield and composition.

4.4.2.1. Effect of holding time on biocrude yield

The holding time is the time during which the maximum temperature during HTL is maintained (excluding the initial heating and final cooling time) (Barreiro et al., 2013). Its effect on biocrude yield was investigated at 307 ℃ and 320 ℃ in presence and absence of MNPs (Figure 4.4). It is evident that there was a steady increase in biocrude yield with holding time in both cases up to the optimum time (60 minutes for HTL at 320 ℃ and 90 minutes for HTL at 307 ℃) then a sharp reduction in biocrude yield with further increase in holding time (Figure 4.4 A and B). The highest biocrude yield after 60 and 90 minutes at 320 ℃ and 307 ℃ respectively shows that these were the most optimum holding times at these temperatures to achieve the highest biocrude yields. Further increase in holding time led to reduction in biocrude yield possibly due to decomposition of biocrude oil into the gas phase in the form of CO_2. This trend is in agreement with the findings of Faeth and Savage.,(2016) who experienced an increasing trend in biocrude yield with holding time up to an optimum time then a reduction in yield with further liquefaction at 320 ℃ (Faeth and Savage, 2016).

According to Barreiro et al.,(2013), the effect of holding time on biocrude yield is closely related to the effect of temperature whereby higher temperature results in a shorter holding time while lower temperature results a longer holding time (Barreiro et al., 2013). Similar findings were observed in this work. At 307 ℃ it took 90 minutes to reach the optimum biocrude yield while at 320 ℃ it took only 60 minutes to reach the optimum biocrude yield (Figure 4.4 C). Christensen et al.,(2014) also observed an increment in biocrude yield with time during HTL of *Phaeodactylum tricornutum* at 325 ℃ for a holding time of 25 minutes after which rapid cooling of reactor contents was done by immersing reactor in water (Christensen et al., 2014). At very high HTL temperatures for example 350 ℃ and above, the effect of holding time on biocrude yield may be minimal since the biomass liquefaction time is too short (10 - 15 minutes).

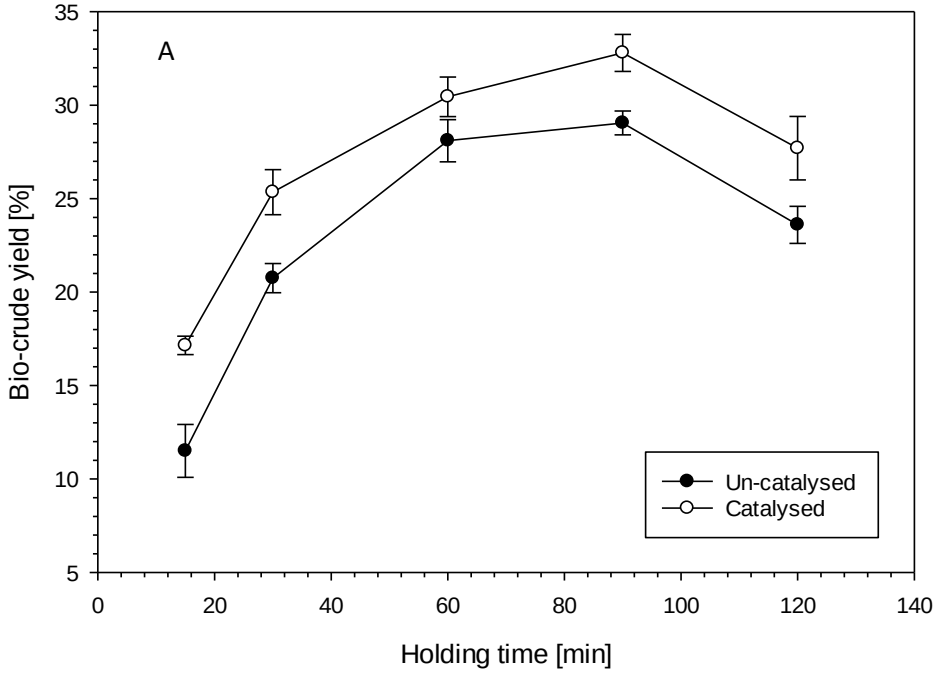
A
Bio-crude yield [%]
Holding time [min]
Un-catalysed
Catalysed
35
30
25
20
15
10
5
0
20
40
60
80
100
120
140

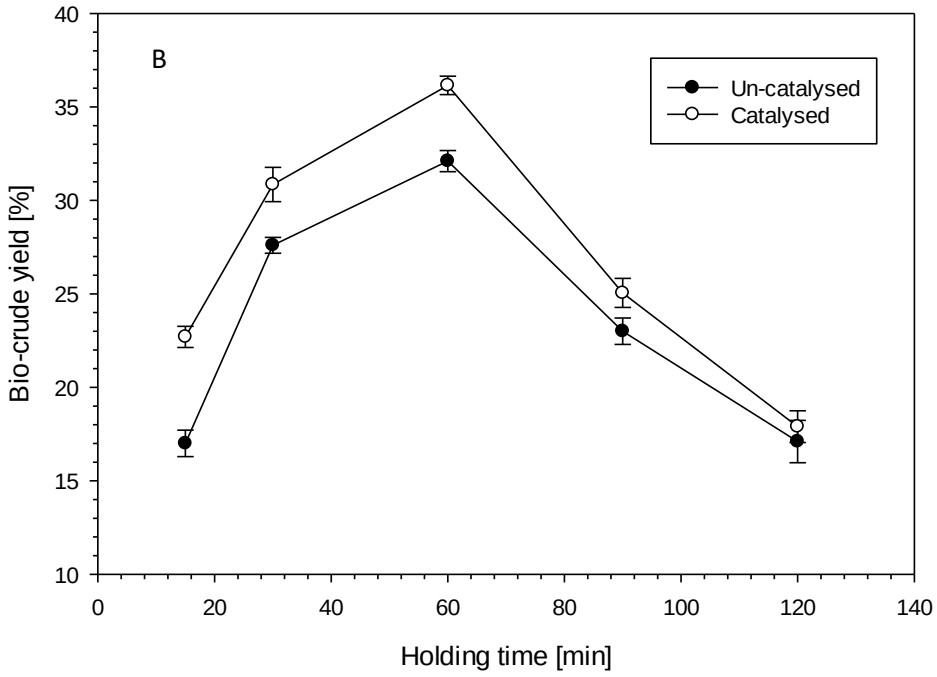
B
Bio-crude yield [%]
Holding time [min]
Un-catalysed
Catalysed
40
35
30
25
20
15
10
0
20
40
60
80
100
120
140

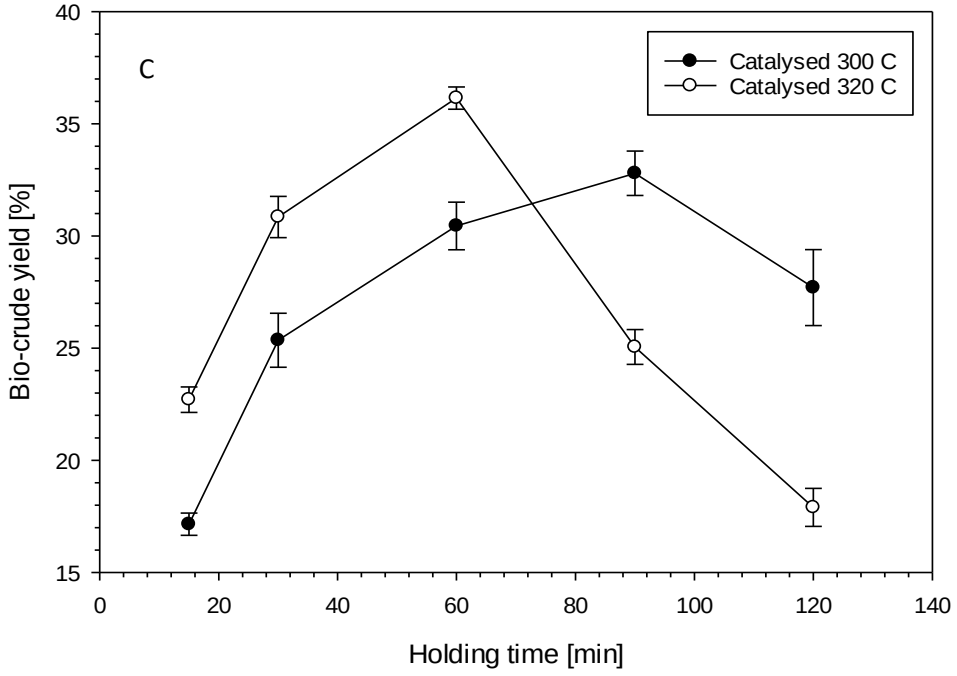

Figure 4. 4. Effect of holding time on yield of biocrude in HTL of Spirulina in presence and absence of MNPs. A) at 307 °C and 90 bar final pressure, B) at 320 °C and 120 bar final pressure and C) in presence of MNPs (Zn ferrites) at 307 °C and 320 °C. Reactor was initially pressurised with 30 bar N_2.

Furthermore, Donghai Xu and Savage., (2015) investigated the effect of reaction time on microalgae HTL and observed a gradual increase in biocrude yield from 10, 30, 45 and finally 60 minutes after which the reactor was cooled (Donghai Xu and Savage, 2015). In this work, HTL in presence of MNPs (Figure 4.4 A, B and C) resulted in higher yields at all liquefaction times compared to liquefaction in absence of MNPs further confirming the catalytic effect of MNPs on biocrude yield.

The increase in biocrude yield with liquefaction time signifies that more carbon was converted to biocrude from the ash free organic solid residue. This is also confirmed by the elemental analysis results (Table 4.1), which show a steady increase in the carbon content of the biocrude with time. The reduction in biocrude yield at higher holding times can be attributed to increased gasification leading to formation of more carbondioxide gas (Donghai Xu and Savage, 2015). Elemental analysis results in Table 4.1 confirm the

reduction in carbon content of biocrude at longer holding time. In conclusion, HTL at 320 ºC for 60 minutes gave the highest yield of biocrude in the shortest liquefaction time. Therefore, these are the most optimum reaction conditions for the highest possible biocrude yield.

4.4.2.2. Effect of liquefaction time on solid residue yield

There was a gradual reduction of solid residue (ash and organic matter after HTL) with time at both reaction temperatures for both the catalysed and uncatalysed liquefaction (Figures 4.5 and 4.6). The elemental analysis results also show a reduction in the carbon content of the solid residue with liquefaction time (Table 4.2). Implying that more biomass was converted to HTL products with time; this is also evidenced by the increase in biocrude yield with liquefaction time in Figure 4.5 suggesting that the reduction in solid residue was due to conversion of biomass to biocrude and other HTL products. The solid residue in the catalysed liquefaction was lower compared to the un-catalysed liquefaction at both reaction temperatures (Figure 4.5 and 4.6). This further confirms that MNPs played a catalytic role in increasing the carbon content of biocrude oil from the solid residue. Chapter 3 discussed in detail the catalytic role of MNPs in microalgae HTL.

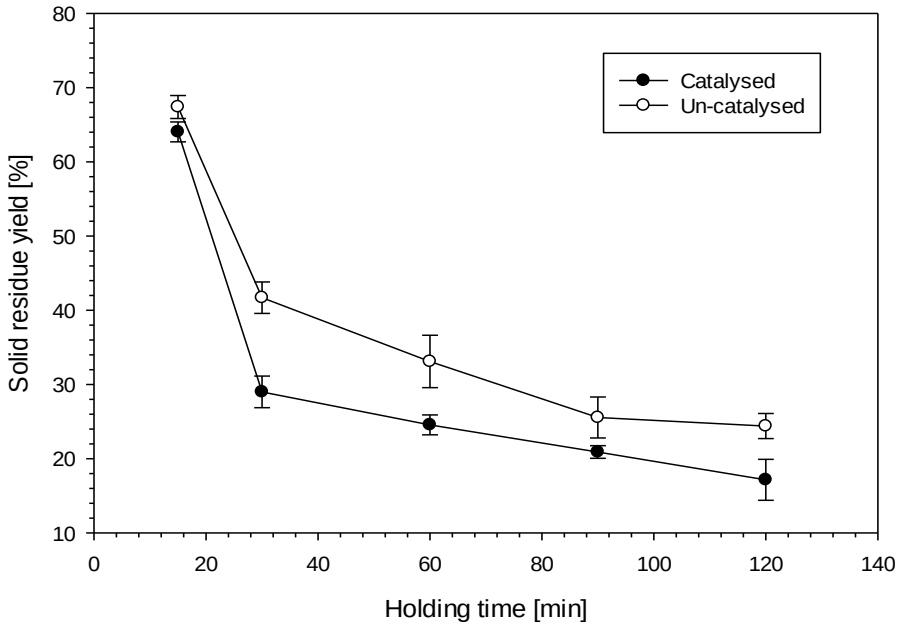

Figure 4. 5. Effect of liquefaction time on yield of solid residue in HTL of Spirulina in presence and absence of Zn ferrite MNPs at 307 °C.

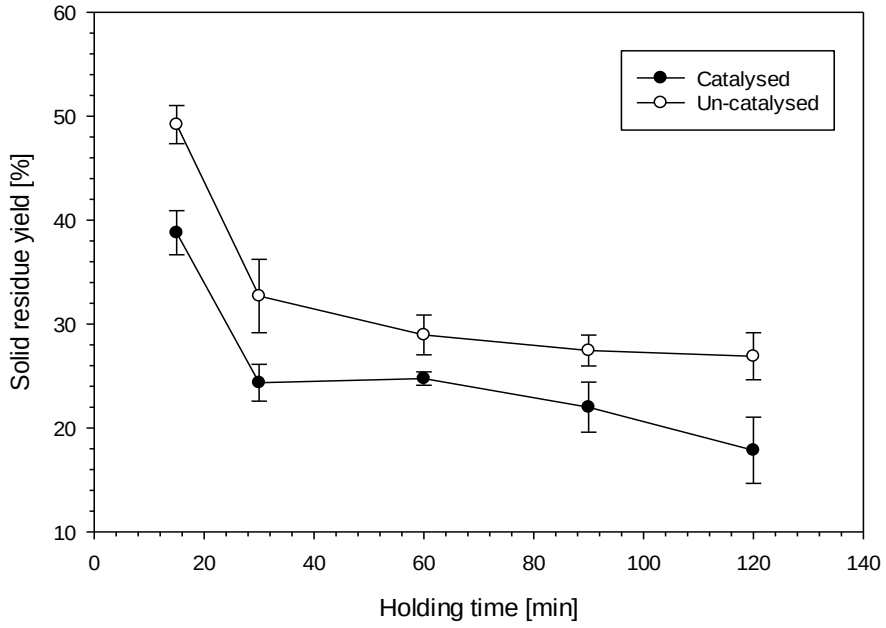

Figure 4. 6. Effect of liquefaction time on yield of solid residue in HTL of Spirulina in presence and absence of Zn ferrite MNPs at 320 °C and 120 bar.

A similar trend in gradual reduction of solid residue amount with reaction time was observed by Garcia Alba et al., (2011) in the liquefaction of *Desmodesmus sp*. for 60 minutes at 200 ℃ and 300 ℃ (Garcia Alba et al., 2011). However, Christensen et al., (2014) in the liquefaction *of Phaeodactylum tricornutum* for 15 minutes observed that reaction time had no effect on the amount of solid residue (Christensen et al., 2014). The difference in results could be due to the shorter liquefaction time used (15 minutes). It is possible that in the short liquefaction time it was not possible to notice considerable changes in the amount of solid residue.

4.4.3. Effect of holding time on biocrude composition

The effect of holding time on biocrude composition was investigated by carrying out elemental and GC-MS analysis on the biocrude produced at different holding times at 307 ºC and 90 bars. This temperature was chosen because it is milder and would potentially result in limited degradation and loss of the biocrude oil at longer holding times.

4.4.3.1. Elemental analysis of biocrude oil

Tables 4.1 and 4.2 show the elemental composition, atomic ratios, high heating values (HHV) and energy recovery (ER) of biocrude oil and solid residue produced at different holding times. The HHV and ER were calculated based of equations 2 and 3 respectively (please see the method section). These give an indication of the energy content of the fuel. Therefore, to improve the fuel energy value and quality, the effect of holding time on the HHV, ER and elemental composition was investigated.

Table 4. 1. Elemental composition, HHV and ER of Biocrude from HTL of Spirulina in presence and absence of Zn ferrite MNPs at 307 °C

HTL Time (min)	C (wt. %)	H (wt. %)	N (wt. %)	O (wt. %)	S (wt. %)	N/C* -	H/C* -	O/C* -	HHV (MJ/kg)	ER (%)
Spirulina	46.3±0.06	6.65±0.00	10.3±0.06	27.7±0.03	0.54±0.01	0.19	1.72	0.45	20.3±0.4	0.00
15	68.90±0.09	8.77±0.08	8.55±0.03	12.06±0.14	0.58±0.08	0.10	1.53	0.13	33.71±0.17	19.1±0.02
30	70.88±0.05	9.24±0.04	6.93±0.01	10.04±0.01	0.55±0.00	0.08	1.54	0.10	35.4±0.03	36.6±0.03
60	72.42±0.04	9.26±0.07	6.97±0.07	9.97±0.13	0.53±0.06	0.08	1.53	0.10	35.98±0.05	48.8±0.03
90	75.52±0.12	9.41±0.06	6.23±0.03	7.54±0.14	0.45±0.00	0.07	1.49	0.07	37.67±0.16	52.3±0.07
120	73.45±0.03	9.42±0.04	5.42±0.01	7.54±0.21	0.40±0.01	0.06	1.54	0.11	37.0±0.00	44.1±0.01
With MNPs										
15	70.88±0.13	8.45±0.02	8.65±0.01	9.51±0.16	0.42±0.03	0.10	1.43	0.10	34.38±0.05	28.0±0.07
30	72.96±0.14	8.64±0.01	7.41±0.11	9.56±0.04	0.40±0.03	0.09	1.42	0.09	35.36±0.05	44.9±0.02
60	75.86±0.06	9.01±0.01	6.91±0.01	7.72±0.07	0.24±0.01	0.08	1.42	0.07	37.17±0.04	55.1±0.04
90	76.21±0.02	9.64±0.06	5.96±0.01	6.88±0.00	0.21±0.00	0.06	1.47	0.06	38.3±0.10	60.8±0.13
120	73.34±0.16	9.54±0.03	5.38±0.00	6.36±0.01	0.10±0.00	0.06	1.56	0.06	37.30±0.02	48.7±0.03

* Atomic ratios

Table 4. 2. Elemental composition, HHV and ER of Solid residue from Spirulina liquefaction in presence and absence of Zn ferrite MNPs at 307 °C

T(min)	C (wt %)	H (wt. %)	N (wt. %)	O (wt. %)	S (wt. %)	N/C*	H/C*	O/C*	HHV (MJ/kg)	ER
60	20.18±0.26	1.93±0.1	0.99±0.02	23.15±0.06	0.305±0.01	0.04	1.15	0.86	5.49±0.25	9.39±0.21
120	11.10±0.01	1.25±0.04	0.67±0.01	13.60±0.05	0.35±0.00	0.05	1.35	0.92	3.15±0.48	4.26±0.01
240	5.04±0.06	0.75±0.01	0.51±0.01	11.11±0.03	0.99±0.01	0.09	1.79	1.65	0.88±0.04	1.14±0.01

* Atomic ratios

From Table 4.1 and Figure 4.8A, the ER of biocrude increased with increase in holding time for both catalysed and uncatalysed microalgae HTL. The highest energy recovery (60.8%) was registered after 90 minutes of liquefaction in presence of MNPs. The ER at the same liquefaction time in absence of MNPs was 53.9% giving a difference of 9.5%. The lowest ER (19.1%) was registered after 15 minutes in absence of MNPs, giving a difference 40.7% in relation to the highest ER. The high ER after 90 minutes corresponds well with the HHV (38.3 MJ/kg) at the same liquefaction time. This gradual increase in ER corresponds to the increase in biocrude yield with liquefaction time. A similar increasing trend in HHV with increasing holding time was observed (Figure 4.7B). The highest being after 90 minutes of liquefaction in presence of MNPs (38.3%). Increase in holding time beyond 90 minutes resulted in reduction in the HHV of biocrude oil. The gradual increase in HHV with time is possibly due to the gradual reduction in oxygen content and a gradual increase in hydrogen content of biocrude oil as evidenced in Table 4.1 and Figure 4.7 B. On the other hand, the reduction in HHV after 90 minutes holding time is possibly due to the reduction in the carbon content of biocrude oil. These results show that increasing liquefaction time in presence of MNPs has a great influence on increasing the ER and HHV of biocrudes.

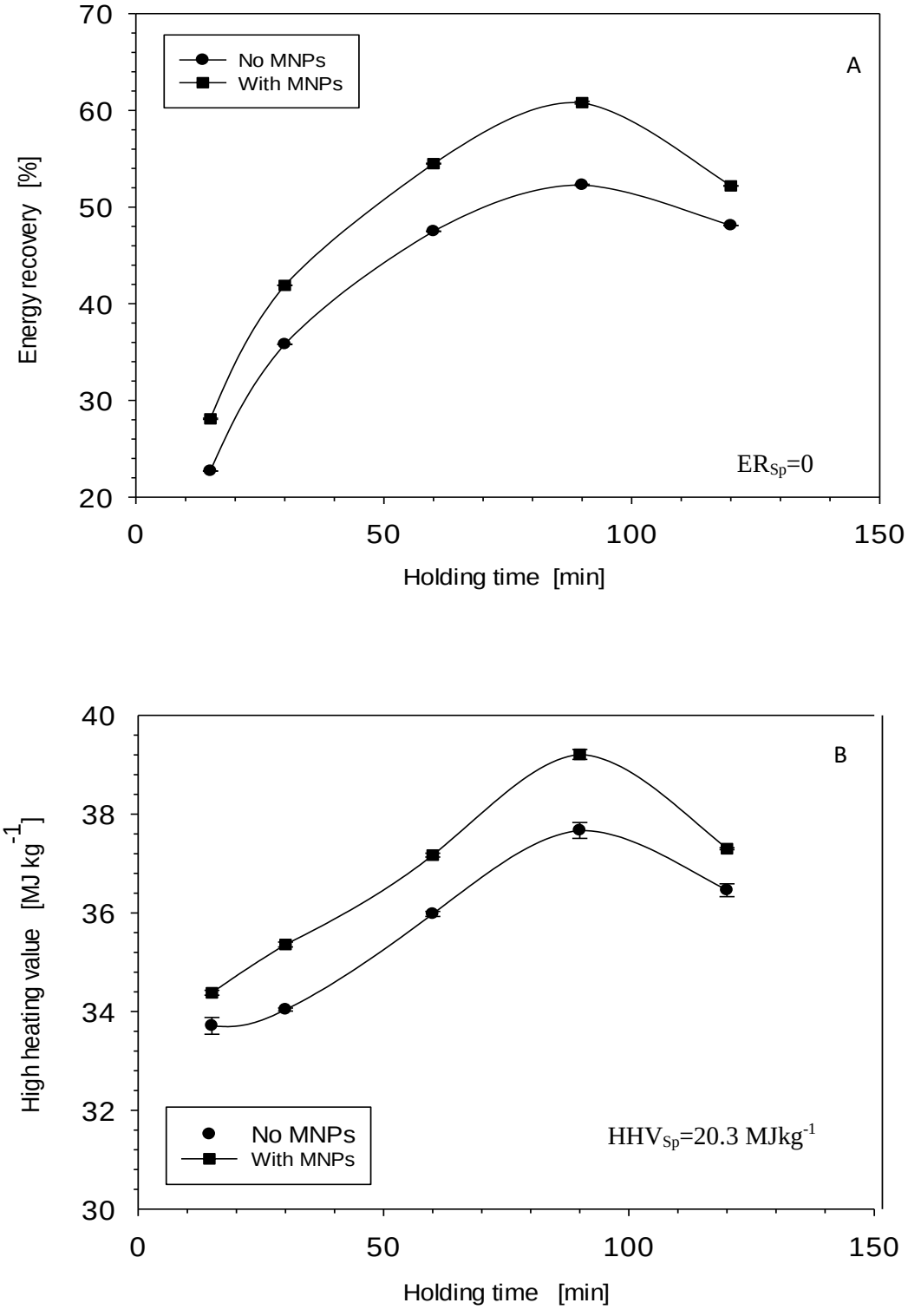

Figure 4. 7. A) ER and B) HHV of biocrude oil at different holding times in presence and absence of MNPs. HHV_{Sp} (high heating value of Spirulina) and ER_{Sp} (energy recovery of Spirulina).

Elemental analysis was also done on the solid residue (Table 4.2) to investigate the trend in HHV, ER and elemental composition at different holding times. The ER and HHV of solid residue reduced gradually with increasing holding time (Table 4.2). Based on equation 4.2 (for calculation of HHV), the decrease in the HHV of solid residue is attributed to the reduction in the C and H content and an increase in S content of solid residue with liquefaction. While the reduction in ER according to equation 4.3 (for calculation of ER) is attributed to the decrease in HHV and yield of the solid residue with time. These results show that increasing holding time leads to the increased decomposition of biomass to release more H and C into the biocrude and allows time for the deposition of more S into the solid phase. This possibly explains the increasing trend of C and H in biocrude oil and its reducing trend in the solid residue with time; and the reducing trend in S content of biocrude oil compared to its increasing trend in solid residue with time.

According to Table 4.2, the C, H, N and O content of solid residue reduced by 15.2, 1.2, 0.5 and 12.1 wt.% respectively and the S content increased by 0.68 wt.% after 240 minutes of HTL. The reduction in C content of solid residue was possibly due to the loss of C into the gas phase in form of CO_2 and the loss of C into the biocrude oil and the aqueous phases. This is confirmed by the increase in the biocrude and aqueous phase yields with increasing holding time (Figure 4.15). The reduction in H content of solid residue was possibly due to its conversion to the biocrude phase as confirmed by the increase in the H content of biocrude oil with time (Table 4.1). The reduction in N content of solid residue was possibly due to its breakdown to ammonia which is dissolved in the aqueous phase (S Raikova et al., 2016a). This is also evidenced by the increase in the aqueous phase yield with time (Figure 4.16). The reduction in O content of solid residue was possibly due to O being lost into the gas phase in form of CO_2. The longer the holding time the more O is lost into the gas phase. According to literature, 98 wt. % of the HTL gas phase is CO_2 (S Raikova et al., 2016a). The increase in S content of the solid residue was due to S being deposited on the compounds in the solid residue (Adjaye, Sharma and Bakhshi, 1992). This is also confirmed by the reduction in S content of biocrude oil with time (Figure 4.13), justifying its increase in the solid residue with time. The next sections present a

detailed discussion of the trends in elemental composition of biocrude oil with holding time.

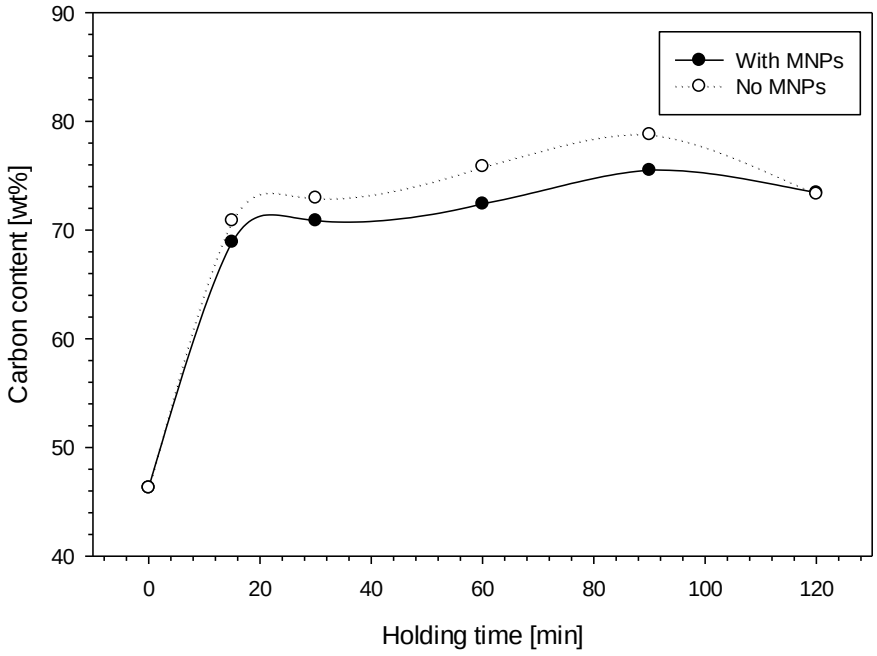

Figure 4. 8. Effect of holding time on Carbon content of biocrude for catalysed and uncatalysed Spirulina liquefaction at 307 °C. 0 holding time corresponds to spirulina biomass before HTL.

The carbon and hydrogen content of the biocrude is higher than that of the biomass feedstock (Tables 4.1, Figures 4.7, and 4.8 respectively). The carbon and hydrogen content of biocrude increased gradually for HTL in presence and absence of MNPs. The carbon content in the catalysed liquefaction (with MNPs) was higher than that in uncatalysed liquefaction (without MNPs) at almost all liquefaction times. The carbon content of biocrude increased from 46.3 wt. % in spirulina feedstock to 75.5wt. % in uncatalysed liquefaction and to 78.8% in catalysed liquefaction after 90 minutes of HTL.

This trend is in agreement with findings of Garcia Alba et al., (2011) in the HTL of *Desmodesmus sp.* at 300 °C and 200 °C where they observed a gradual increase in carbon content of biocrude with increasing liquefaction time. The highest carbon content was 75 wt. % after 60 minutes of HTL at 300 °C (Garcia Alba et al., 2011). Christensen et al., (2014) also observed an increase in carbon content of biocrude with liquefaction time

during HTL of *Phaeodactylum ricornutum*. The highest carbon content was 74.4 % after 15 minutes of HTL at 350 °C (Christensen et al., 2014). The increase in carbon content of biocrude with liquefaction time is potentially due to the breakdown of un-converted carbon in the biomass residue into the biocrude oil. This is confirmed by the elemental analysis results of the solid residue in table 5.2 that confirm reduction in the carbon content of the solid residue with liquefaction. The reduction in carbon content for both catalysed and uncatalysed biocrude observed at longer liquefaction times after 90 minutes could be due to increased loss of carbon into the gas phase in form of carbon dioxide and formation of char (Dong Zhou et al., 2010).

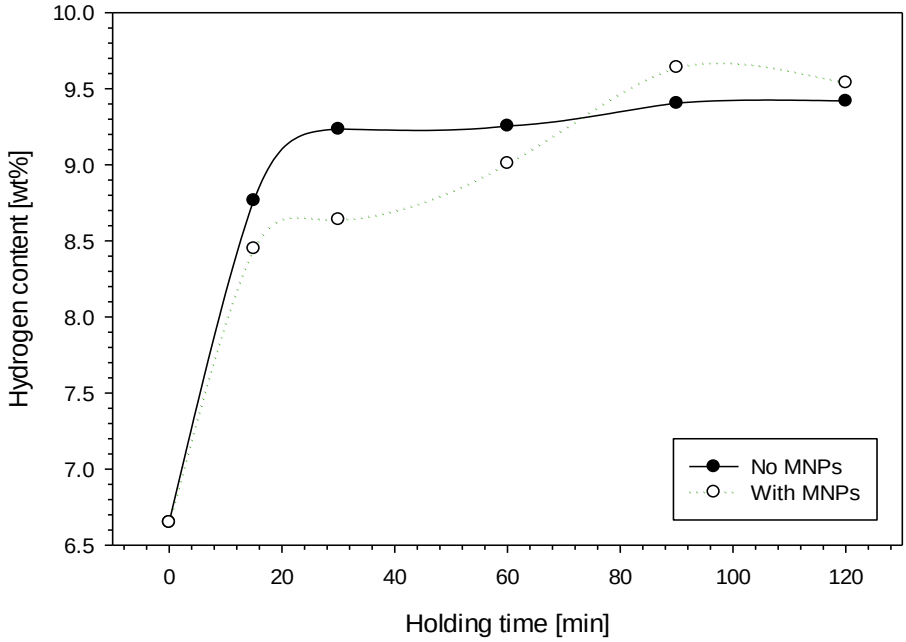

Figure 4. 9. Effect of liquefaction time on Hydrogen content of biocrude for catalysed and un-catalysed Spirulina liquefaction at **307 °C**. The plotted values are mean values with standard deviation (SD) less than 0.17 and *n*=2. See table 4.1 for detailed values of SD.

The hydrogen content increased from 6.65 wt. % in spirulina feedstock to 9.4 wt.% in un-catalysed liquefaction and to 9.6 wt.% in catalysed liquefaction after 90 minutes of HTL. The increase in hydrogen content with liquefaction time for both catalysed and un-catalysed liquefaction was so small showing a negligible effect of liquefaction time (Figure 4.9). A similar trend in hydrogen content with liquefaction time was observed by

Garcia Alba et al., (2011) in microalgae HTL at 200 °C. There was a slight increase in hydrogen content from 9.1 wt. % after 5 minutes to 9.5 wt. % after 30 minutes and then to 9.6 wt. % after 60 minutes while at 300 °C there was a slight reduction from 9.0 wt. % to 8.8 wt. % after 60 minutes of HTL (Garcia Alba et al., 2011). Christensen et al., (2014) also observed a slight increase (from 9.4 % after 5 minutes to 9.5 % after 15 minutes of reaction) in hydrogen content of biocrude during HTL of *P. tricornutum* at 350 °C (Christensen et al., 2014). These result shows that there is no significant effect of liquefaction time on the hydrogen content of biocrude oil.

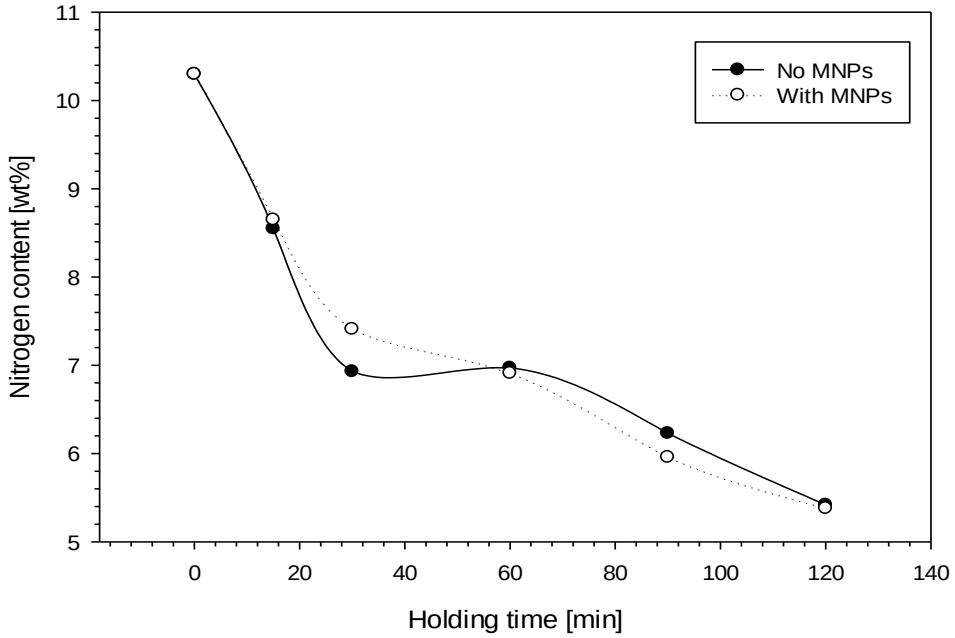

Figure 4. 10. Effect of liquefaction time on Nitrogen content of biocrude for catalysed and un-catalysed Spirulina liquefaction at 307 °C**.** The plotted values are mean values with standard deviation less than 0.17 and *n*=2. See table 4.1 for detailed values of SD.

Simultaneously, there was a general reduction in the nitrogen, oxygen and sulphur content with liquefaction time, for both catalysed and uncatalysed microalgae HTL. The nitrogen, oxygen and sulphur content in the biomass feedstock were much higher than those in the biocrude were. The nitrogen content reduced from 10.3 wt. % in biomass feedstock to 5.3 wt. % and 5.4 wt. % after HTL in presence and absence of MNPs respectively (liquefaction time of 120 minutes) (Figure 4.10). Similar trends in reduction of nitrogen

content of biocrude with liquefaction time are recorded in literature at closely similar conditions (Garcia Alba et al., 2011; Christensen et al., 2014; Donghai Xu and Savage, 2015). From these results, it is evident that liquefaction time had an effect of lowering the nitrogen content of biocrude in both the catalysed and uncatalysed algal HTL. The longer the holding time the lower the nitrogen content. This is possibly due to partitioning of nitrogen into the aqueous phase in form of NH_4^+ ions, the longer the reaction time the more NH_4^+ ions partition into the aqueous phase and hence the lower the nitrogen content in the biocrude oil. This explanation is in agreement with the findings of (Sofia Raikova et al., 2016b) in the HTL of spirulina in presence of metal sulphates where large quantities of NH_4^+ ions were found in the aqueous phase at higher HTL temperatures and longer liquefaction time. It is interesting to note that the nitrogen content is lower than the one reported earlier in Chapter 3 (7.5%) where HTL was done at 320 ºC for 60 minutes, it is also lower than the one reported by Raikova et al., (2015) (6.5%) where microalgae HTL was done at 350 ºC for 60 minutes. This suggests that HTL at lower temperatures (307 ºC) for longer times (90 minutes) can further lower the nitrogen content of biocrude oil and improve its quality.

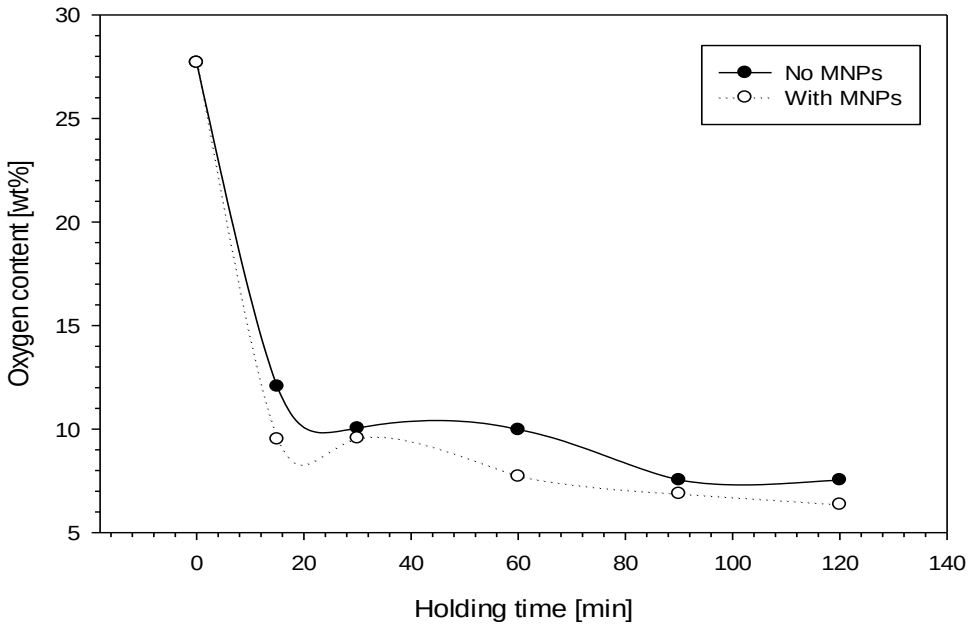

Figure 4. 11. Effect of liquefaction time on oxygen content of biocrude for catalysed and un-catalysed Spirulina liquefaction at 307 °C**.** The plotted values are mean values with standard deviation less than 0.17 and *n*=2. See table 4.1 for detailed values of SD.

Liquefaction time had also a profound impact on lowering the oxygen content of biocrude in both the catalysed and uncatalysed HTL. This effect was more in catalysed HTL (Figure 4.11). The longer the liquefaction time the lower the oxygen content. The oxygen content was reduced from 27.7 wt. % in the microalgae biomass feedstock to 7.5 wt. % in biocrude from uncatalysed liquefaction and to 6.3 wt. % in biocrude from catalysed liquefaction after 120 minutes. Dong Zhou et al., (2010) also reported the reduction in oxygen content with liquefaction time in assessing the effect of reaction conditions on biocrude composition (Dong Zhou et al., 2010). In addition, Christensen et al., (2014) reported on a similar trend in oxygen content of biocrude oil with liquefaction time. They observed a reduction from 11.0 wt. % after 5 minutes of HTL to 9.7 wt. % after 15 minutes of HTL (Christensen et al., 2014). Furthermore, Garcia Alba et al., (2011) observed a similar decrease in oxygen content of biocrude from 22.2 wt. % after 5 minutes of HTL to 17.5 wt. % after 60 minutes at 200 ºC and from 12.3 wt. % after 5 minutes to 10.2 wt. % after 60 minutes of HTL at 300 ºC (Garcia Alba et al., 2011). Moreover, Donghai and Savage., (2015) observed a huge reduction in oxygen content from 27 wt. % in dry microalgae biomass to 17.5 wt. % after 10 minutes of HTL and then to 12.2 wt. % after 60 minutes of HTL (Donghai Xu and Savage, 2015). The reason for the reduction in oxygen content with liquefaction time is possibly due to the loss of oxygen into the gas phase in form of CO_2. The longer the liquefaction time, the more the CO_2 in the gas phase and hence the lower the oxygen content in the biocrude oil. It has been reported by Raikova et al., (2016) that 98% of algal HTL gas phase is CO_2 (Sofia Raikova et al., 2016b). The oxygen content in biodiesel usually ranges between 10-12 wt. % and in crude oil it is between 0 - 2 wt. % depending on the type of crude oil (Biller and Ross, 2011).

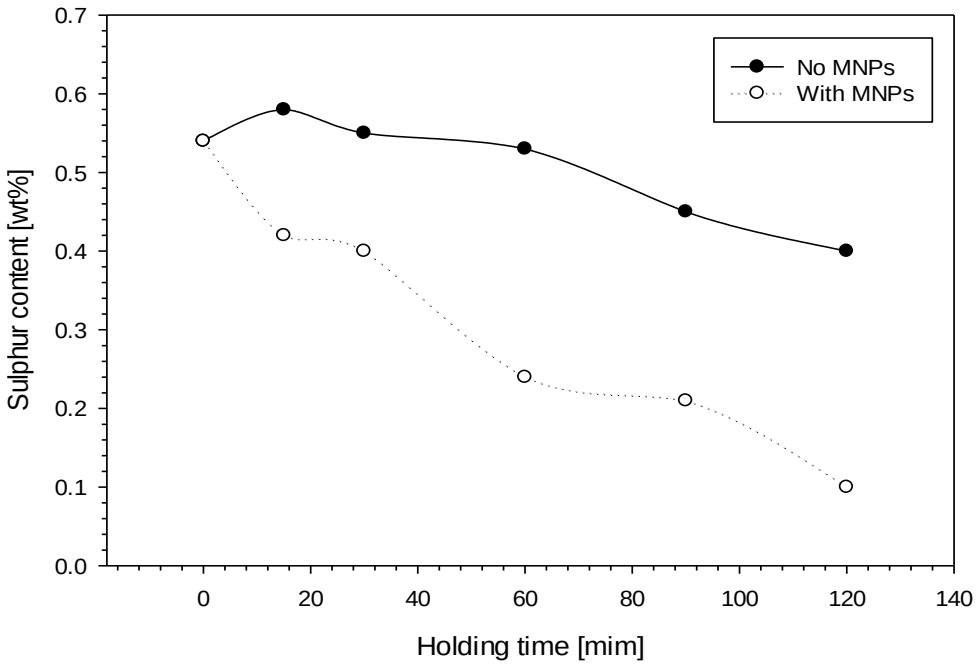

Figure 4. 12. Effect of liquefaction time on Sulphur content of biocrude for catalysed and un-catalysed Spirulina liquefaction at **307°C.** The plotted values are mean values with standard deviation less than 0.17 and *n*=2. See table 4.1 for detailed values of SD.

There was also a gradual reduction in sulphur content of biocrude in the un-catalysed liquefaction and a sharper reduction in the catalysed liquefaction with time (Figure 4.12 and Table 4.1). The sulphur content reduced from 0.54 wt. % in microalgae biomass to 0.4 wt.% in un-catalysed biocrude and to 0.1 wt.% in catalysed biocrude oil after 120 minutes of HTL. The reduction in sulphur content was more pronounced in the biocrude produced in presence of MNPs (Figure 4.12). This shows that MNPs may have played a catalytic role in removing sulphur from the biocrude oil with the greatest removal happening at longer HTL time (120 minutes). The MNPs may have played a catalytic role through catalytic oxidation by acting as oxygen carriers. In this way, they selectively oxidise sulphur compounds in the biocrude oil and the MNPs are regenerated by molecular oxygen (Javadli and De Klerk, 2012). This is a two-step process involving oxidation of sulphur compounds followed by regeneration of the oxygen carrier (MNPs). The mechanism of sulphur remove under HTL conditions needs further investigation. Elemental analysis of solid residue in Table 4.2 shows an increasing trend of sulphur

content with liquefaction time. This confirms that sulphur was deposited in the solid residue with time and the longer the liquefaction time the more sulphur is removed from the biocrude oil. This is in agreement with the findings in literature that shows that during liquefaction sulphur binds on to the compounds in the solid residue (Adjaye, Sharma and Bakhshi, 1992; Huber, Iborra and Corma, 2006; Ramirez, Brown and Rainey, 2015). A similar reducing trend of sulphur was also observed by Donghai et al., (2015) during HTL of microalgae at 350 ºC. They observed a reduction in sulphur content from 0.57 wt. % in dry microalgae biomass to 0.56 wt. % after 10 minutes of HTL and to 0.50 wt. % after 60 minutes of HTL. The liquefaction was done in absence of catalysts (Donghai Xu and Savage, 2015). This possibly explains the slow reduction in sulphur content despite the high HTL temperature used.

In conclusion, increasing algal liquefaction time increases the carbon and hydrogen content of biocrude up to an optimum liquefaction time of 90 minutes. Further increase in liquefaction time leads to reduction in carbon content and no significant effect on the hydrogen content. Increasing liquefaction time leads to reduction in nitrogen, oxygen and sulphur content of biocrude oil for both catalysed and un-catalysed HTL. The best liquefaction time in this experiment for removal of nitrogen, oxygen and sulphur was 120 minutes. This shows that longer liquefaction times are favourable for removal of O, N and S, but this comes at the expense of biocrude yield because at this liquefaction time the yield is lower. Finally, increasing liquefaction time increases the HHV and ER of biocrude provided the optimum liquefaction time is not exceeded.

4.4.3.2. GC-MS ANALYSIS

In addition to elemental analysis, GC-MS analysis was done to compare results and analyse the variation of major compounds with holding time (GC-MS analysis only gives a picture of the most volatile substances). The identities of the main compounds extracted by hexane in the biocrude from spirulina liquefaction and their relative area in the chromatogram after integration were determined. In Table 4.3 and Figure 4.14, the percentage relative area of major compounds in the GC-MS chromatogram for biocrude liquefied at 15, 30, 60, 90 and 120 minutes were compared. Peaks in the chromatogram with relative area less than 2% were not considered. The major compounds in the biocrude

were grouped under hydrocarbons, nitrogen compounds, oxygenated compounds and sulphur compounds. The hydrocarbon grouping consisted of aromatic and aliphatic hydrocarbons, these included compounds like heptadecane, biphenyl, and hexadecene. The nitrogenated compounds consisted of compounds such as indole, N, N dimethyl and pyridine. The oxygenated compounds included fatty acids, aldehydes and ketones, among these were; n-hexadecanoic acid, propanoic acid and benzaldehyde. The amount of sulphur containing compounds was too small to be detected.

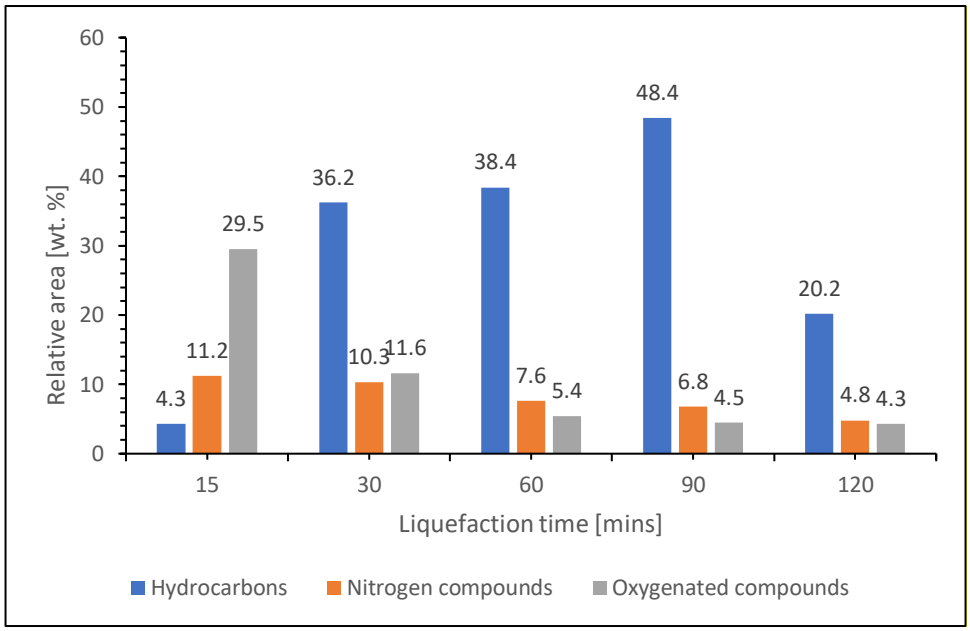

Figure 4. 13. Effect of liquefaction time on biocrude composition. The spirulina was liquefied at 307 °C, initial pressure 0 bar, final pressure 90 bar depending on liquefaction time (internally generated pressure after HTL) at different liquefaction times.

There was a steady increase in the relative area corresponding to hydrocarbons (HC) with liquefaction time (Figure 4.13 and 4.14). The relative area corresponding to HC increased from 4.3 wt. % after 15 minutes to 48.4 wt. % after 90 minutes. Further liquefaction led to a drop in the relative area corresponding to HCs to 20.2 wt. % after 12 minutes. This trend agrees with the elemental analysis results of carbon and hydrogen content that also revealed an increasing trend until 90 minutes and then a decline with increase in liquefaction time. It also agrees with the trend in yield of biocrude that increased steadily with time until 90 minutes and then a decline in yield observed beyond 90 minutes (Figure

4.1 A). Since the largest composition of biocrude is hydrocarbons, this comparison makes sense. This further confirms that the optimum liquefaction time for spirulina HTL at 307 °C is 90 minutes.

Table 4. 3. GC-MS results of major compounds after HTL of Spirulina at different reaction times in absence of MNPs.

RT (min)	Compound name and structure	Relative area (wt.%) at different liquefaction times (min) in absence of MNPs				
		15	30	60	90	120
3.384	Benzaldehyde (C_6H_5CHO)	2.6	*	*	*	*
3.459	Phenol (C_6H_5OH)	2.0	*	2.6	5	3.2
7.55	Indole C_8H_7N	9.1	8.1	6.1	6.8	4.8
8.706	Biphenyl $(C_6H_5)_2$	4.3	4.4	6.5	8.5	4.4
14.851	Heptadecane $CH_3(CH_2)_{15}CH_3$	*	31.8	31.9	31.7	12.7
16.848	Propanoic acid $CH_3CH_2CO_2H$	5.6	*	*	*	*
19.44	Thiourea, N,N'-dimethyl- $C_3H_8N_2S$	2.1	2.2	1.5	*	*
19.097	2-hexadecene $C_{16}H_{32}$	*	*	*	8.2	3.1
22.181	n-Hexadecanoic acid $C_{16}H_{32}O_2$	18.7	11.6	5.4	4.5	4.3
	Others	55.6	41.9	46	35.3	64.7
Total (%)		100	100	100	64.7	32.5

* *Very small peaks with area less than 2% were left*

The percentage relative area in the GC-MS chromatogram corresponding to nitrogen, oxygen and sulphur compounds decreased with liquefaction time. The relative area corresponding to nitrogenated compounds decreased gradually as liquefaction time was increased. The highest relative area corresponding to nitrogenated compounds was registered after 15 minutes of HTL at 11.2 wt. % and the lowest was registered after 120 minutes of HTL at 4.8 wt. %. This trend is also in agreement with the elemental analysis results that show a general a gradual reduction in the nitrogen content of biocrude with

increasing liquefaction. The relative area corresponding to oxygenated compounds in the biocrude also decreased gradually from 28.9 wt. % after 15 minutes of HTL to 7.5 wt. % after 120 minutes of HTL. This agrees with elemental analysis results that show a reduction in the oxygen content of biocrude with increasing liquefaction time. The reduction in oxygen content of biocrude with liquefaction time is due to loss of oxygen into the gas phase in form of CO_2 as explained earlier.

The relative area corresponding to sulphur compounds in the biocrude also decreased from 2.1 wt. % after 15 minutes of HTL to below detection levels after 120 minutes of HTL. This too agrees with elemental analysis results, which showed a reduction in sulphur content with liquefaction time. In summary, increasing liquefaction time favours the decomposition and removal of nitrogen, oxygen and sulphur compounds from biocrude oils.

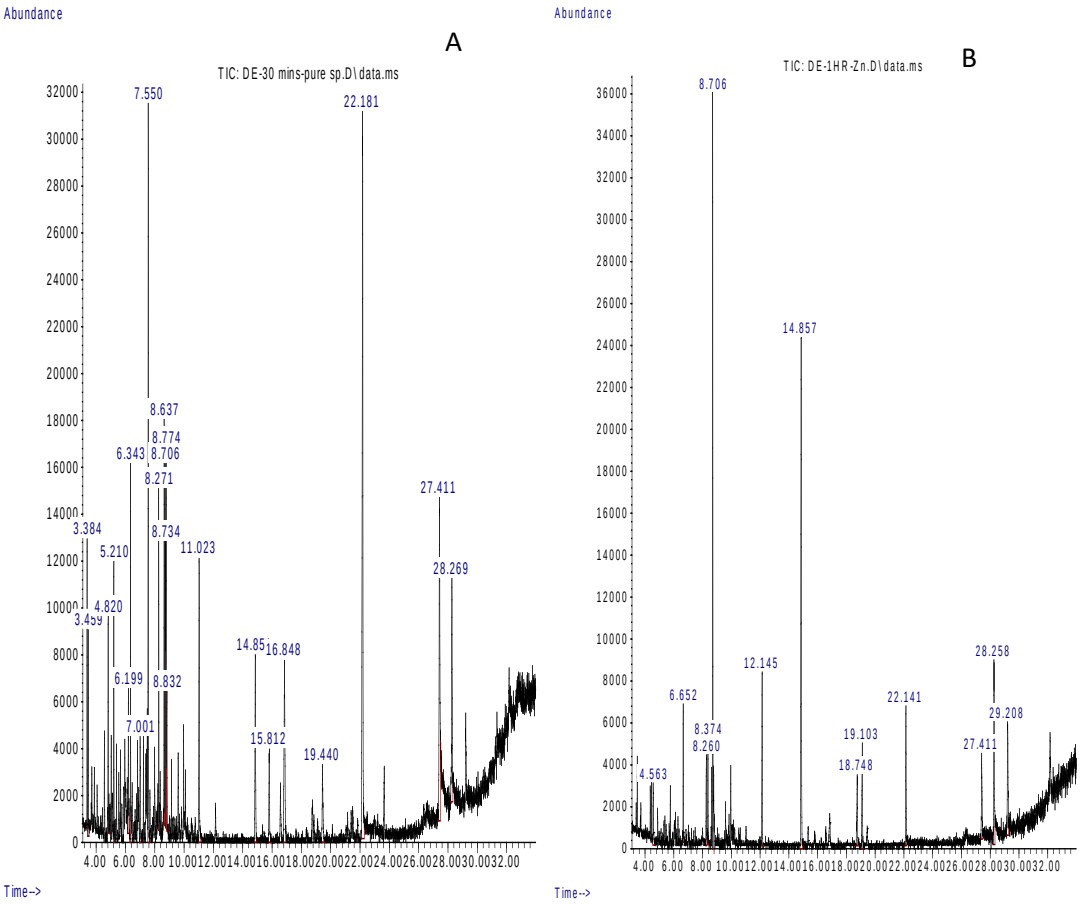

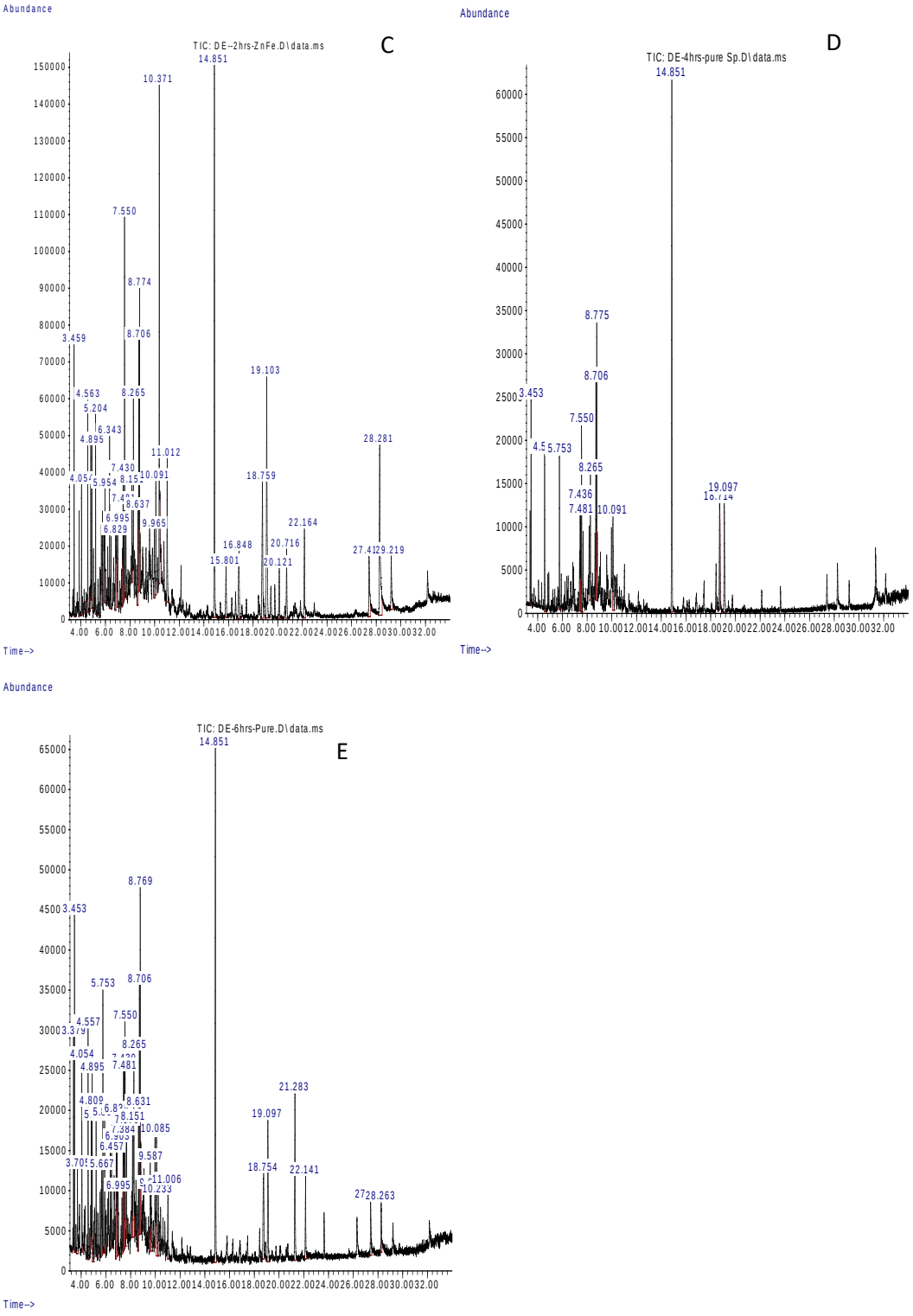

Figure 4. 14. GC-MS Chromatogram for biocrude from Spirulina liquefaction: A, B, C, D, and E correspond to 15, 30, 60, 90 and 120 minutes respectively of HTL in absence of MNPs respectively.

4.4.4. Effect of HTL under hydrogen on biocrude yield and chemical composition

4.3.4.1. Effect of HTL under hydrogen on biocrude yield

Hydrothermal liquefaction was completed under a hydrogen atmosphere to investigate if hydrogenation reactions can occur under HTL conditions. It is well known that hydrogen is used in the petroleum industry to improve the quality of crude oil through removal N, O and S in the form of NH_3, H_2O, and H_2S respectively (Speight, 2015). Successful hydro-treatment of biocrude oil would greatly improve its quality through removal of N, O and S and increase its HHV. Therefore, to determine the effect of hydrogen atmosphere on biocrude yield and composition, the reactor containing microalgae with a water content of 78 wt. % was pressurised with hydrogen gas (30 bar) and HTL was done at different liquefaction times and temperatures in presence and absence of MNPs (Figure 4.16).

Liquefaction in the absence of MNPs resulted in higher biocrude yield compared to liquefaction in presence of MNPs. This is opposed to the results in the previous section where presence of MNPs resulted in higher biocrude yield. The reason for the reduction in biocrude yield is possibly due to hydro-deoxygenation or decarboxylation reactions that result in increased removal of oxygen from oxygenated compounds (aldehydes, ketones, esters and organic acids) in form of H_2O, CO and CO_2. GC-MS analysis of biocrude liquefied in presence of hydrogen shows absence of peaks corresponding to oxygenated compounds (Table 4.5) which are usually present in biocrude liquefied in absence of hydrogen gas (Table 4.3). The presence of MNPs potentially favoured these reactions leading to reduction in biocrude yield. Some reports in literature confirm that HTL in presence of hydrogen gas and catalysts results in a reduction of biocrude yield compared to HTL under hydrogen atmosphere without catalysts. But the biocrude quality is better when HTL is done under hydrogen atmosphere with catalysts possibly because of increased catalytic deoxygenation and denitrogenation of the biocrude oil (Rojas-Pérez et al., 2015; Jinlong Yu et al., 2017). Therefore, the improvement in biocrude quality comes at the expense of the biocrude yield in this case.

There was also a gradual increase in the yield of the aqueous phase (Figure 4.15) with liquefaction time in both catalysed and un-catalysed HTL. The aqueous phase is largely

composed of ammonia originating from the decomposition of proteins during the HTL process (S Raikova et al., 2016a). The solid residue yield reduced with liquefaction time in all cases, which is also consistent with the previous findings (Figure 4.1 A) where HTL was done in absence of hydrogen gas. From these results, it is evident that HTL in presence of hydrogen gas and catalyst can result in lower biocrude yields but with better quality biocrude through oxygen removal and hydrogen addition hence improving the energy content of the biocrude but at the expense of the biocrude yield.

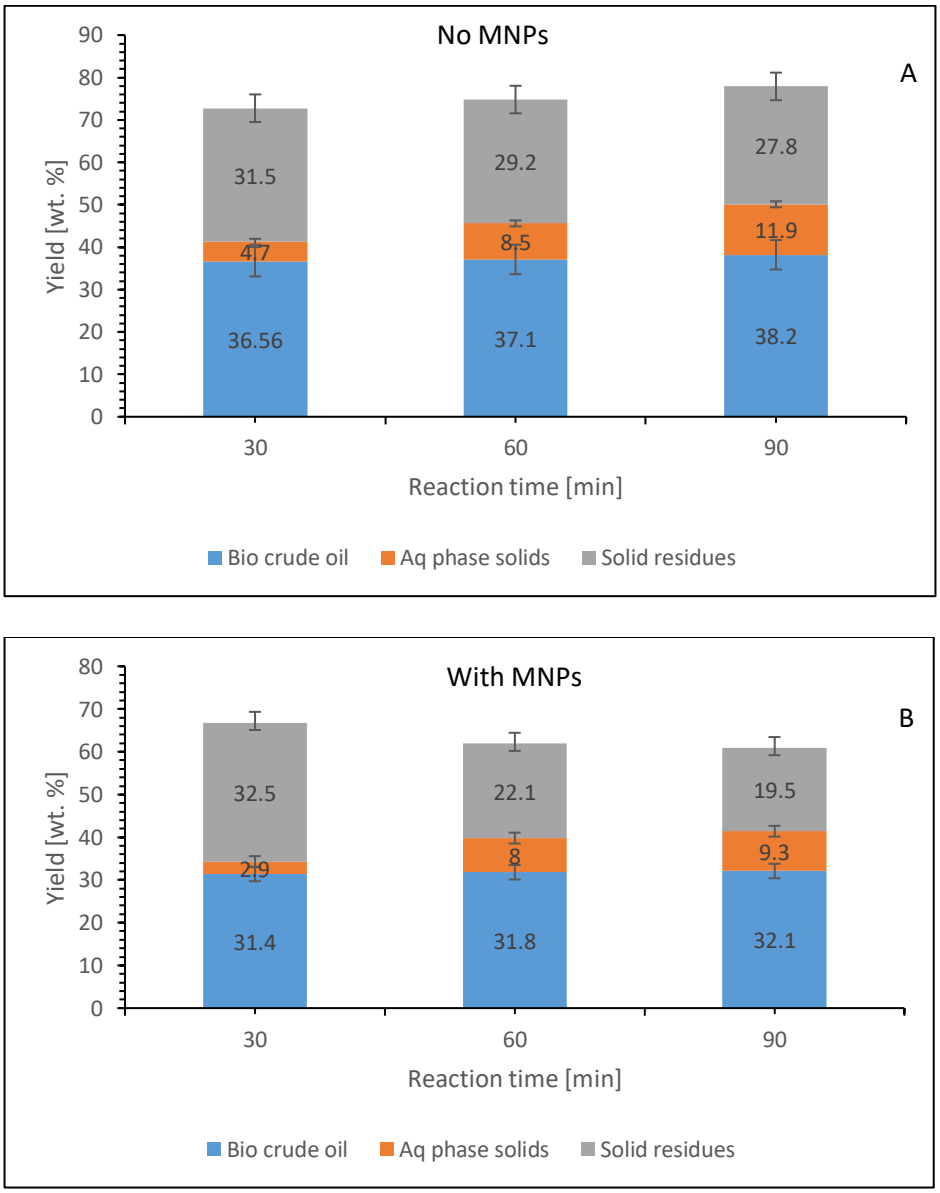

Figure 4. 15. Yield of HTL products after liquefaction of Spirulina at different HTL times at 30 bar hydrogen gas and temperature of 307 °C. A) No MNPs, B) presence of MNPs.

Comparing the biocrude yield in absence of hydrogen gas (under nitrogen gas at initial pressure of 30 bar Figure 4.5) and in presence of 30 bar hydrogen gas (Figure 4.15) at 307 °C, it is evident that the biocrude yield was higher when HTL was done under hydrogen atmosphere than in absence of hydrogen. For the uncatalysed liquefaction in absence of hydrogen gas, the biocrude yield increased from 26 wt. % to 36.6 wt. % in absence and presence of hydrogen gas respectively after 30 minutes holding time. After 60 minutes holding time, it increased from 30 wt. % to 37.1 wt. % in absence and presence of hydrogen gas respectively. While after 90 minutes, it increased from 33 wt. % to 38.2 wt. % in presence and absence of hydrogen gas respectively. On the other hand, for the catalysed liquefaction, the biocrude yield increased from around 20 wt.% to 31.4 wt. % in absence and presence of hydrogen gas respectively after 30 minutes holding time. While after 60 minutes, it increased from 23 wt.% to 31.8 wt.% in absence and presence of hydrogen atmosphere respectively. Moreover, after 90 minutes holding time, it increased from around 25 wt. % to 32.1 wt. % in absences and presence of a hydrogen atmosphere respectively. Hong Yi et al., (2014) observed a similar increasing trend in biocrude yield from 55.6 wt. % to 78.5 wt. % when liquefaction of *Nannochloropsis Salina* was done under 30 bar hydrogen in the presence of Ni-Mo/Al_2O_3 catalyst at 340 °C at a mixing speed of 300 rpm (HongYi Li et al., 2014a). These results show that HTL under a hydrogen atmosphere favours the conversion of microalgal biomass to biocrude oil resulting in increased biocrude yield. This could be due to the increased hydrogenation reactions resulting in the formation of more hydrocarbon compounds (HongYi Li et al., 2014a).

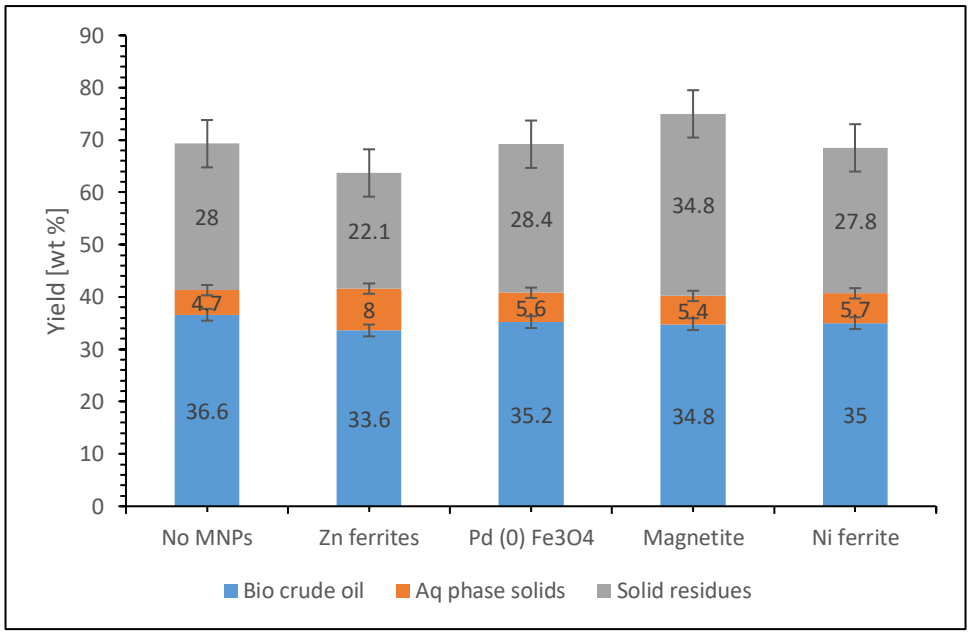

Figure 4. 16. Product yield after HTL of Spirulina in presence of hydrogen gas (30 bar) at 318 °C for 60 minutes and mass ratio of MNPs: spirulina of 0.12.

Liquefaction under hydrogen atmosphere was also compared in the presence of different ferrite MNPs (Figure 4.16) to determine their effect on biocrude yield and elemental composition. The highest biocrude yield (36.6 wt. %) was observed in the sample without MNPs. The lowest biocrude yield (33.6 wt. %) was observed in the sample with Zn/ferrites. As explained earlier, the low yield of biocrude in presence of hydrogen and MNPs is potentially due reactions such as hydrodecarboxylation and hydrodeoxygenation that lead to removal of oxygen from oxygenated compounds such as organic acids and aldehydes in the biocrude, resulting in the liberation of CO_2 gas. The release of oxygen in form of CO_2 into the gas phase and the removal of nitrogen into the aqueous phase in form of ammonia potentially resulted in the reduction of biocrude yield. This can be confirmed by the GC-MS results in Table 4.6 which shows absence of oxygenated compounds when HTL was done in presence of different MNPs under 30 bars of hydrogen.

Furthermore, the increase in the hydrogen content of the biocrude produced in presence of MNPs (9.2 wt. % for Zn/ferrites compared to 9.0 wt. % for spirulina without MNPs) also confirms that hydrogenation was higher when microalgae liquefaction was done in presence of MNPs under hydrogen. This confirms that MNPs played a catalytic role

possibly through hydrodeoxygenation reactions leading to the conversion of oxygenated compounds such as carboxylic acids to hydrocarbons with the release of CO_2. Resulting in reduction in the oxygen content and an increase in hydrogen content of biocrude oil. It is worth noting that hydrogenation may have occurred under a hydrogen atmosphere even in absence of MNPs but at a lower rate since HTL in absence of MNPs under hydrogen also shows absence of oxygenated compounds (Table 4.6).

4.4.4.2. Effect of HTL under H_2 on elemental composition of biocrude oil

The effect of HTL under hydrogen on elemental composition was determined by carrying out liquefaction in presence and absence of MNPs under 30-bar hydrogen and comparing this to elemental composition in absence of hydrogen (Table 4.1). Table 4.4 shows the details of elemental analysis of biocrude liquefied under hydrogen at different liquefaction times in presence and absence of MNPs and Table 4.5 shows elemental analysis for HTL under 30 bar hydrogen in presence of different MNPs.

Table 4. 4. Elemental analysis of biocrude from spirulina liquefaction under 30-bar hydrogen at different liquefaction times in presence and absence of MNPs (Zn ferrites) at 318°C.

HTL time (min)	C (wt. %)	H (wt. %)	N (wt. %)	O (wt. %)	S (wt. %)	HHV	ER
Spirulina	46.27±0.03	6.65±0.04	10.31±0.06	27.69±0.03	0.54±0.01	20.25±0.03	0
Sp-30	74.18±0.03	9.04±0.00	6.85±0.00	8.71±0.01	0.50±0.01	36.51±0.01	65.83±0.01
Sp-60	75.24±0.01	9.19±0.00	6.46±0.00	8.34±0.02	0.37±0.01	37.12±0.00	67.84±0.00
Sp-90	75.50±0.13	9.31±0.00	6.41±0.00	7.60±0.01	0.31±0.01	37.51±0.05	70.58±0.07
Sp/MNPs-30	73.60±0.10	9.15±0.04	6.74±0.01	8.92±0.10	0.47±0.01	36.42±0.01	56.33±0.01
Sp/MNPs-60	73.96±0.00	9.17±0.02	6.60±0.01	8.73±0.03	0.35±0.01	36.58±0.03	57.31±0.04
Sp/MNPs-90	75.04±0.06	9.25±0.01	6.28±0.01	8.18±0.02	0.30±0.01	37.19±0.00	58.80±0.01

*Sp stands for Spirulina biomass

Table 4. 5. Elemental analysis of biocrude from spirulina liquefaction under 30 bar hydrogen using different MNPs at 318°C for 1 hr HTL.

Biocrude	C (wt. %)	H (wt. %)	N (wt. %)	O (wt. %)	S (wt. %)	HHV	ER
Spirulina	46.27±0.03	6.65±0.04	10.31±0.06	27.70±0.03	0.54±0.01	20.25±0.03	0
Sp/No MNPs	74.18±0.03	9.00±0.00	6.85±0.00	8.71±0.01	0.50±0.01	36.45±0.01	65.19±0.01
Sp/Fe_3O_4	73.71±0.04	9.00±0.00	6.91±0.01	9.06±0.01	0.52±0.00	36.22±0.01	62.10±0.02
Sp Ni /Fe_3O_4	73.29±0.04	9.00±0.01	6.97±0.01	8.70±0.03	0.52±0.01	36.14±0.01	62.31±0.01
Sp/Pd/Fe_3O_4	73.45±0.02	9.00±0.00	7.11±0.00	9.38±0.04	0.30±0.01	36.05±0.00	62.52±0.00
Sp/Zn/Fe_3O_4	73.60±0.10	9.15±0.04	6.74±0.01	8.92±0.1	0.47±0.01	36.42±0.01	60.28±0.01

*Sp stands for Spirulina biomass

In Table 4.4, there was a gradual increase in carbon content of biocrude oil when HTL was done in a hydrogen atmosphere (30 bar) for both the catalysed and the uncatalysed liquefaction. The carbon content increased from 46.3 wt. % in Spirulina biomass to 74.2 and 75.5 wt. % in uncatalysed (no MNPs) biocrude after 30- and 90-minutes holding time respectively. In catalysed (with MNPs) biocrude, it increased from 46.3 wt. % in Spirulina biomass to 73.6 and 75 wt. % after 30- and 90-minutes holding time respectively. The low carbon content in catalysed HTL suggests the increased loss of carbon in form of carbondioxide possibly due to hydrodecarboxylation reactions such as the one illustrated in equation 4.4 involving the removal of a carboxyl group from organic acids and the addition of hydrogen to form hydrocarbons.

$$RCOOH \xrightarrow{\text{Catalyst}} RH + CO_2 \qquad (4.4)$$

The reduction in carbon content is consistent with the reduction in biocrude yield when liquefaction was done in presence of hydrogen gas (Figure 4.14). The disappearance of peaks corresponding to oxygenated compounds in the GC-MS chromatogram after HTL in a hydrogen atmosphere (Table 4.5 and Figure 4.17) further suggests the loss of carbon and oxygen in the form of carbondioxide. The peaks corresponding to oxygenates were clearly visible in the GC-MS spectrum of biocrude liquefied in absence of hydrogen (Table 4.3, Figure 4.13 and 4.14). This confirms that hydrodecarboxylation of organic acids which is among the many HTL reactions may have led to their degradation to hydrocarbons releasing CO_2 gas. This is also supported by the high relative area corresponding to hydrocarbons in the GC-MS spectrum of biocrude liquefied under hydrogen atmosphere and the disappearance of peaks corresponding to organic acids such as hexadecanoic acid which were so huge in the GC-MS spectrum of biocrude produced in absence of hydrogen gas. Comparing Table 4.4 to Table 4.1 (where HTL was done in absence of hydrogen), it is evident that the carbon content was generally higher in a hydrogen atmosphere than in a nitrogen atmosphere.

The hydrogen content increased with liquefaction time when HTL was done under hydrogen atmosphere for both catalysed and uncatalysed microalgae HTL (Table 4.4). For uncatalysed HTL, it increased from 6.7 wt. % in Spirulina biomass to 9.0 and 9.3 wt. % in biocrude oil after 30 and 90 minutes of HTL respectively. For liquefaction in presence

of MNPs, it increased from 6.7 wt. % in Spirulina biomass to 9.2 and 9.3 wt. % after 30 and 90 minutes of HTL respectively. A similar increasing trend was observed when HTL was done in absence of hydrogen gas (Table 4.1). A comparison of the hydrogen content of biocrude for HTL in absence and in presence of hydrogen gas (Table 4.4 and 4.1), shows that HTL under hydrogen gas (30 bar) had a slight impact on increasing the hydrogen content of biocrude oil. For catalysed HTL, the hydrogen content increased from 6.7 wt. % in Spirulina biomass to 8.6 and to 9.2 wt. % in absence and in presence of hydrogen gas respectively after 30 minutes of HTL. While for the uncatalysed HTL, the hydrogen content increased from 6.7 wt. % in Spirulina biomass to 9.2 wt. % in absence of hydrogen gas and then reduced slightly to 9.0 wt. % under hydrogen atmosphere for 30 minutes of HTL. This shows HTL under low-pressure hydrogen atmosphere can lead to increase in hydrogen content of biocrude if it is done in presence of MNPs for a shorter holding time (30 minutes).

The nitrogen content also decreased with increase in liquefaction time when HTL was done under a hydrogen atmosphere, for liquefactions in presence and absence of MNPs. The lowest nitrogen content (6.28 wt. %) was observed after 90 minutes of HTL in presence of MNPs while the highest nitrogen content was 6.85 wt. % after 30 minutes of HTL in absence of MNPs and at 10.3 wt. % in Spirulina biomass. A comparison of HTL in absence and HTL in presence of a hydrogen atmosphere (Figure 4.1 and 4.4), shows no significant effect of hydrogen gas on lowering the nitrogen content of biocrude oil. The nitrogen content in biocrude was generally higher when HTL was done under a hydrogen atmosphere but it reduced with increasing holding time. This (and a few other results) does not correspond to what you would expect possibly due to poor dissolution of hydrogen at 30 bars. In these experiments, the main impact on nitrogen content was holding time and not a hydrogen atmosphere. Microalgae liquefaction under low-pressure hydrogen is rare in literature so it is hard to find literature to compare with. Most work involving HTL under hydrogen uses high-pressure hydrogen to upgrade biocrude oil to lighter hydrocarbon fractions.

The oxygen content of biocrude also decreased with liquefaction time when HTL was done under hydrogen atmosphere. For uncatalysed HTL, it decreased from 27.7 wt. % in Spirulina biomass to 8.7 and 7.6 wt. % after 30 and 90 minutes of HTL respectively. While under catalysed HTL, it decreased from 27.7 wt. % in Spirulina biomass to 8.9 and 8.2 wt. % after 30 and 90 minutes of HTL respectively. The oxygen content was generally lower when HTL was done under a hydrogen atmosphere. For example, for HTL in absence of hydrogen gas (Figure 4.1), the oxygen content reduced from 27.7 wt. % in Spirulina biomass to 10.0 and 9.6 wt. % after 30 minutes of liquefaction for uncatalysed and catalysed HTL respectively. While under a hydrogen atmosphere, the oxygen content reduced from 27.7 wt. % in Spirulina biomass to 8.7 and 8.9 wt. % after 30 minutes of liquefaction for uncatalysed and catalysed HTL respectively. This shows that the presence of hydrogen favoured hydrodeoxygenation or deoxygenation reactions resulting in loss of more oxygen at these liquefaction conditions.

There was a general reduction in sulphur content of biocrude oil with increasing liquefaction time for both the catalysed and uncatalysed microalgae HTL. For the uncatalysed liquefaction, the sulphur content decreased from 0.54 wt. % in Spirulina biomass to 0.5 and 0.31 wt. % after 30 and 90 minutes of HTL respectively. While for the catalysed liquefaction, the sulphur content decreased from 0.54 wt. % in Spirulina biomass to 0.47 and 0.3 wt. % after 30 and 90 minutes of HTL respectively. The sulphur content of biocrude was lower when HTL was done in presence of MNPs. (Table 4.5). The effect of HTL in absence and in presence of hydrogen gas was compared and it was observed that the sulphur content of biocrude was slightly higher when HTL was done under hydrogen atmosphere. Suggesting that that low-pressure hydrogen atmosphere suppresses the desulphurisation process.

Liquefaction of microalgae under different MNPs (Zn ferrites, Ni ferrites, Pd (0) ferrites and magnetite) in presence of hydrogen gas was also done (Table 4.5). The aim was to compare their catalytic effect on elemental composition of biocrude especially on denitrogenation. As observed earlier, the carbon content of the biocrude was highest in absence of MNPs. The hydrogen content was highest (9.15 wt.%) in presence of Zn ferrites, suggesting better catalytic effect in hydrogenation reactions. The nitrogen content

was also lowest (6.74 wt.%) with liquefaction under Zn ferrites suggesting better denitrogenation in presence of hydrogen gas. The oxygen content (8.7 wt. %) was lowest under Ni ferrites while the sulphur content (0.3 wt. %) was lowest under Pd (0) ferrites suggesting better de-oxygenation and desulphurization effect respectively. The highest energy recovery and high heating value were obtained in the biocrude liquefied under Ni ferrites due to the slightly lower oxygen content of biocrude. Oxygen content is largely dependent on liquefaction time (Dong Zhou et al., 2010; Biller and Ross, 2011; Christensen et al., 2014).

GC-MS Results

Table 4.6 and Figure 4.16 show the GC-MS results of biocrude oil liquefied in the presence of different MNPs (Ni ferrites, Magnetite and Pd (0) ferrites) under 30 bar hydrogen gas atmospheres. The major peaks in the GC-MS chromatogram were presented in table 4.6. Peaks with relative area below 4 wt. % were not considered. A comparison of compounds from GC-MS analysis of lipids liquefied in presence of hydrogen show un-detectable peaks for oxygenated compounds such as organic acids, phenol, aldehydes and ketones (Table 4.6). On the other hand, the biocrude produced in absence of hydrogen shows large peaks corresponding to oxygenated compounds such as organic acids, phenol, aldehydes and ketones (Table 4.3). The absence of these peaks in the biocrude produced under hydrogen conditions suggests that de-oxygenation reactions such as hydro-deoxygenation or hydrodecarboxylation took place leading to removal of oxygen in form of CO_2 or H_2O and formation of hydrocarbons as illustrated in equation 5 below. The increase in hydrocarbon compounds witnessed from the GC-MS results (Table 4.6) confirms that such reactions led to the conversion of oxygenated compounds to hydrocarbons with loss of oxygen in form of water or CO_2.

$$R\text{-}OH + H_2 \longrightarrow R\text{-}H + H_2O \qquad (4.5)$$

The elemental analysis results (Table 4.5) also confirm the reduction in oxygen content of biocrude produced under hydrogen atmosphere. A high oxygen content lowers the energy content of the lipid by reducing the high heating value. Therefore, removal of oxygen improves the heating value of the biocrude oil. On the hand, addition of hydrogen

improves the heating value of the lipid, improves saturation of the hydrocarbons and facilitates the removal of nitrogen, sulphur and oxygen through hydrogenation reaction (Ramirez, Brown and Rainey, 2015).

Table 4. 6. Major Compounds identified from GCMS spectrum of biocrude from *Spirulina* HTL under 30-bar hydrogen in presence of different MNPs.

RT(min)	Compound Name	Relative area (wt. %)			
		Spirulina	Fe_3O_4	Ni/Fe_3O_4	Pd/ Fe_3O_4
11.04	Dodecane	*	*	*	5.5
14.588	4,6(1H)-Pyrimidine dione, 3,4,5,6-tetrahydro-2-imino-	4.4	*	*	*
19.967	Heptadecane	15	14.5	12.4	11.8
22.004	2-Hexadecene, 3,7,11,15-tetramethyl-, [R-[R*,R*-(E)]]-	4	4.1	4.4	3.7
22.181	2-Hexadecene, 3,7,11,15-tetramethyl-, [R-[R*,R*-(E)]]-	7.9	8.2	5.5	4.6
27.125	N-Methyldodecanamide	4.9	6.3	4.5	4
28.887	9-Octadecenamide, (Z)-	7.2	9.9	4	
	Others	56.6	57	69.2	75.9
Total (%)		100	100	100	100

** Very small peaks with area less than 4 % were left*

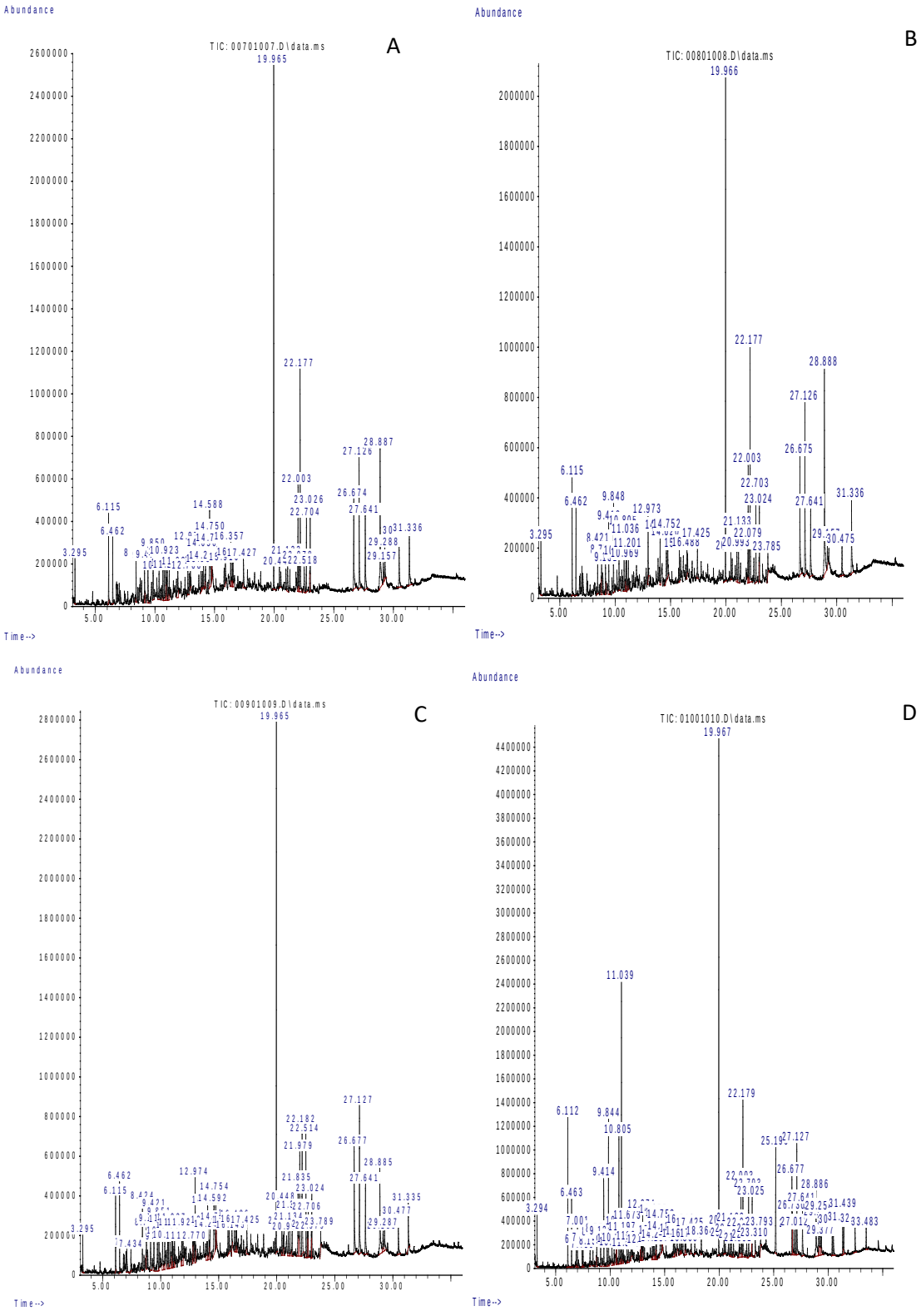

Figure 4. 17. HTL of spirulina under 30 bar hydrogen gas and different MNPs: A) only spirulina, B) Spirulina with magnetite, C) Ni ferrite, and D) Pd (0) magnetite.

4.4.5. Effect of HTL under acidic conditions on biocrude yield and composition

The effect of HTL under acidic conditions on biocrude yield and elemental composition was also investigated. In this project, the main objective was to investigate the effect of acidic conditions on removal of nitrogenated compounds from biocrude oil. Liquefaction was done in the presence of 5 wt. % sulphuric acid or 5 wt.% formic acid. Formic acid was chosen because it is a weak organic acid commonly found in biomass. The effect of acids on biocrude yield was also investigated (Figure 4.18). The yield of biocrude oil in absence of formic and sulphuric acid was higher than when the acids were present. The lowest yield was observed when 5 wt.% sulphuric acid was used. The reduction in biocrude yield is possibly due to the hydrolysis reactions between acids and proteins in which the C-N peptide bond in amino acids is broken down to produce carboxylic acid and NH_4^+ ions (Reitz et al., 1946). The NH_4^+ ions do not contribute to the biocrude yield since they are soluble in the aqueous phase resulting in reduced biocrude yield.

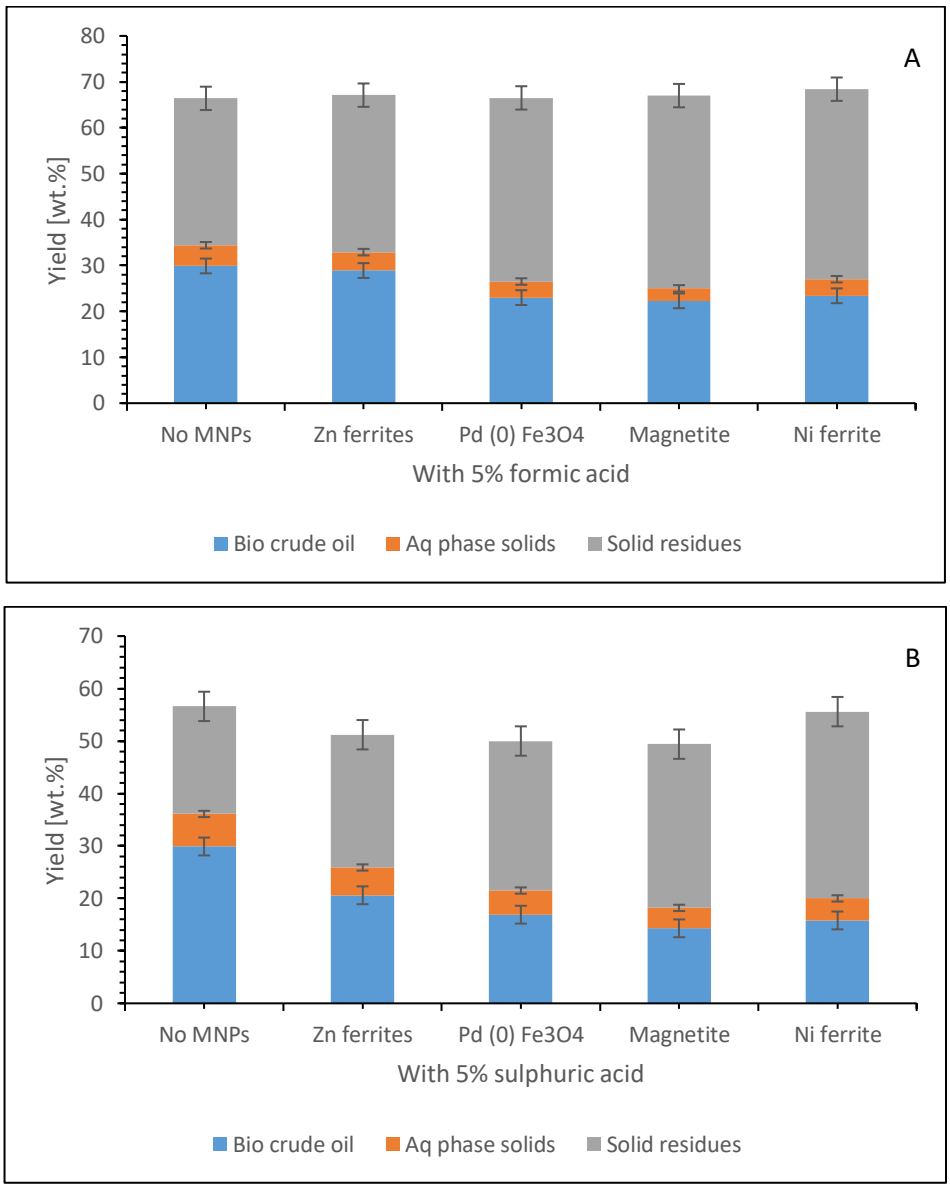

Figure 4. 18. Product yield after HTL of Spirulina in presence of different MNPs and A) formic acid and B) sulphuric acid at 320 °C for 60 minutes.

Table 4. 7. Elemental composition from biocrude from spirulina liquefaction in presence and absence of 5 wt. % formic and sulphuric acid at 320 °C for 60 minutes.

Biocrude	C (wt. %)	H (wt. %)	N (wt. %)	R_N%
Spirulina	46.3±0.06	6.65±0.00	10.3±0.06	0.00
No acid	71.9±0.06	9.2±0.04	7.50±0.11	27.18
With HCOOH	74.0±0.18	10.0±0.01	6.55±0.00	36.41
With H_2SO_4	74.28±0.00	10.6±0.06	1.66±0.07	83.88

***** R_N is nitrogen removal percentage.

This effect is more profound in presence of sulphuric acid than formic acid possibly due to its high acidity. This is confirmed by elemental analysis results in Table 4.7 which show a substantial reduction in the percentage composition of nitrogen content of biocrude oil by 83.9 wt. % when HTL was done in presence of sulphuric acid compared to 36.4 wt. % when formic acid was used. The nitrogen content reduced from 10.3 wt. % in Spirulina biomass to 7.5 wt. % in biocrude liquefied in absence of acids and to 1.66 wt. % in biocrude liquefied in presence of 5% sulphuric acid. This is the lowest reduction (83.9 wt. %) in nitrogen content from Spirulina liquefaction so far. The carbon and hydrogen content of biocrude oil was also higher when HTL was done under 5% sulphuric acid conditions. The hydrogen content increased from 6.65 wt. % in Spirulina biomass to 9.2 wt. % in biocrude produced in absence of acids and to 10.6 wt. % in biocrude produced in presence of sulphuric acid. This is the highest increase in hydrogen content of biocrude in this work. The high dissociation ability of sulphuric acid enables access to hydrogen ions used in reactions such as hydro-deoxygenation and hydrodecarboxylation resulting in the addition of hydrogen to organic acids and removal of oxygen in form of carbondioxide or water as explained earlier. The carbon content of biocrude increased from 46.3 wt. % in Spirulina biomass to 71.9 wt. % in biocrude produced in absence of acids and to 74.3 wt. % in biocrude produced in presence of 5% sulphuric acid. These results show that HTL in presence of mild sulphuric acid conditions can result in a substantial reduction in nitrogen

content and an increase in the hydrogen content of biocrude oil. This leads to improvement in quality of biocrude oil. However, this comes at the expense of reduction in the biocrude yield.

4.5. Conclusions

The aim of this Chapter was to explore the effect of liquefaction conditions on yield and chemical composition of biocrude oil with emphasis on deoxygenation and denitrogenation of the biocrude during the HTL process. This was done by varying the holding time, temperature, HTL under hydrogen conditions in presence and absence of MNPs and microalgae HTL in presence of 5 wt.% formic or sulphuric acid. In these studies, the optimum holding time for biocrude yield was 90 minutes at 307 ºC and 60 minutes at 320 ºC with a biocrude yield of 32.8 wt.% and 36.2 wt.% respectively. Increasing the holding time resulted in gradual increase in carbon and hydrogen content of biocrude and an overall reduction in the nitrogen, oxygen and sulphur content of biocrude. Liquefaction of microalgae under 30 bar hydrogen gas atmospheres resulted in the highest increase in biocrude yield compared to microalgae HTL in absence of hydrogen. Liquefaction under 5% sulphuric acid led to the highest reduction in nitrogen content of biocrude oil (83.9 wt. %) and the highest increase in hydrogen content of biocrude oil (10.6 wt.%). The biocrude yield did not increase significantly when microalgae HTL was done under acidic conditions. The improvement in biocrude quality through denitrogenation and deoxygenation came at the expense of a slight reduction in biocrude yield.

5. Extraction of lipids from magnetically separated microalgae using ionic liquids

Chapters 3 and 4 examined the processing of the whole microalgae cell to biocrude oil through the HTL process; the focus in Chapter 4 was to lower the N and O compounds from biocrude oil by investigation the effect of process conditions on biocrude composition and yield to improve biocrude quality. This Chapter presents the processing of part of the microalgae cell through lysis of the magnetically separated microalgae using ionic liquids (ILs) and the dissolution of lipids from the lysed cells into the hexane phase. The lipids were then transesterified to biodiesel. It combines magnetic separation of microalgae with IL extraction just as Chapter 3 and 4 combined magnetic separation of microalgae with HTL. It therefore bridges a gap in the literature on the extraction of lipids from magnetically separated microalgae. This could potentially lower the processing cost of biofuels from microalgae.

5.1. Abstract

In this work, the efficient extraction of lipids from magnetically separated microalgae using ionic liquids (ILs) and the recycling of magnetic nanoparticles (MNPs) and ILs was fully demonstrated for the first time. MNPs were used to separate microalgae from aqueous phase at a separation efficiency of 99%. The separated microalgae/MNPs slurry was subjected to IL treatment to lyse the microalgae cell membrane and efficiently extract lipids using hexane. The lysed cells were mixed with hexane for 2 hours to dissolve the extracted lipids. An extraction efficiency of 99% was achieved when ILs were used compared to 5% in absence of ILs. The extracted lipids were analysed using GC-MS, FT-IR and ^{1}H NMR. The MNPs were recovered from cell biomass by sonication in DI water and recycled to harvest more microalgae at a separation efficiency of 96%. TGA analysis of recovered MNPs confirmed absence of algal biomass on the particles. The ILs were also recycled and analysed using ^{1}HNMR, Mass spectrometry and FT-IR analysis. All these confirmed absence of structural alteration in the recovered IL. The effect of process conditions such as ratio of microalgae to IL, treatment time, water content of microalgae and temperature on extraction efficiency of lipids were also investigated. Recycling MNPs and ILs and extraction of essential compounds alongside microalgae lipids could be an economical alternative for biofuel processing from algae.

5.2. Introduction

The ever-increasing global energy demands with associated environmental impact from petroleum-derived chemicals have encouraged the development of alternative environmentally friendly energy sources such as biodiesel (Orr et al., 2015). Microalgae have the ability to convert sunlight and carbon dioxide into fats and lipids, which are a precursor for biodiesel production (Orr et al., 2015). They are also a source of many other essential compounds such as carotenoids, proteins and carbohydrates. They offer numerous advantages over current lipid crops as source of oil for biodiesel production. This is because there is no need of agricultural land for their cultivation; they can grow in wastelands and salty waters, they have a high productivity and photosynthetic conversion rate, and have no seasonal limitations so can grow all year round (Orr et al., 2015; Egesa, Chuck and Plucinski, 2017).

The use of microalgae as a source of lipids for biofuel production has limitations due to the costly harvesting step contributing to 25% of the overall processing cost for biofuel production (Safarik et al., 2016). In addition, the energy intensive and costly dewatering and drying steps and the cost prohibitive lipid extraction steps contribute to 30-50% of the overall cost of biofuel processing from micro-microalgae (Teixeira, 2012). These limitations arise due to the small size of microalgae cultivated in dilute aqueous solutions in very low concentrations, making harvesting and dewatering difficult and the presence of a cellulosic cell wall that is resistant to mechanical cell lysis preventing diffusion of solvents during lipid extraction (Jasvinder Singh and Gu, 2010; Orr et al., 2015). Because of these limitations, the production cost of biofuels is higher in comparison to petroleum derived fuels.

To lower the cost of microalgae harvesting, alternative microalgae separation techniques such as magnetic separation have been investigated. It was reported that magnetic separation can lower the cost of microalgae harvesting by 90% (Los-Alamos, 2012). Magnetic separation uses simple devises, it is not energy intensive, it is a fast process, the magnetic field is not destructive to microalgae cells and is easy to manipulate and recycle MNPs (Prochazkova, Safarik and Branyik, 2013; Egesa, Chuck and Plucinski, 2017). The current methods of microalgae harvesting e.g. centrifugation and screening are energy intensive while others like sedimentation are slow (Uduman et al., 2010). In magnetic separation, the MNPs are adsorbed on the microalgae cells by electrostatic interactions and in presence of a magnetic field, the microalgae/MNPs responds to magnetic force concentrating the cells and effecting separation *i.e.* microalgae are targeted directly for separation (Egesa, Chuck and Plucinski, 2017).

In this work, magnetic separation of microalgae was done and the microalgae/MNPs slurry was subjected to ionic liquid treatment to lyse (disrupt) microalgae cell walls and efficiently extract lipids. Extraction of microalgae lipids is commonly done using solvents (Jasvinder Singh and Gu, 2010; Halim et al., 2012). However, most solvents present health and safety challenges, for example hexane is the most used solvent to extract lipids due to its low polarity. Solvent extractions are also slow and time-consuming requiring heating the solvent at higher temperatures to increase the extraction efficiency. The use of large

quantities of solvent to increase extraction efficiency is also a bottleneck. This makes the process more costly and energy intensive (Medina et al., 1998; Orr et al., 2015). Low polarity solvents are also limited in the extraction of neutral lipids in the microalgae cell wall because of the association of neutral lipids with polar lipid protein complexes requiring greater force to break (Medina et al., 1998; Halim et al., 2012). High polarity solvents like methanol can be paired with low polarity solvents like hexane since they can disrupt these high energy complexes through hydrogen bond formation (Medina et al., 1998; Halim et al., 2012). However, this will result in extracted lipids containing many more polar and undesirable compounds like chlorophyll, phospholipids, and sterols, which may interfere with the transesterification process (Emilio Molina Grima, González and Giménez, 2013).

Therefore, alternative cell lysis and extraction techniques such as mechanical cell lysis were also investigated in the literature. However, the cellulosic cell wall in microalgae is resistant to mechanical cell lysis (Halim et al., 2012; Orr et al., 2015). Ball milling has been reported as the most effective mechanical cell lysis technique but it is ineffective in the extraction of lipids from *Chlorella vulgaris* and *Chlorophyte*, it also has a challenge of over-heating and it is not economical to scale up (Rahul Kapoore et al., 2018). In addition, biological cell lysis techniques have also been developed to mitigate the use of toxic solvents but they often contaminate the cell extract and can form artefacts during further downstream processing (Rahul Kapoore et al., 2018). Biological techniques using enzymes such as cellulases or pectinases are constrained by economics since enzymes are expensive and at times lack efficiency (Rahul Kapoore et al., 2018).

Due to the limitations of solvent, mechanical and biological cell lysis techniques as discussed above, it is prudent to develop cost effective and low energy cell lysis and extraction techniques. Therefore, ionic liquids are a promising option since many have recently been proven to lyse microalgae cells at room temperature (Plechkova and Seddon, 2008; Pinkert et al., 2009; Tadesse and Luque, 2011). They are called ‘green’ designer solvents due to their excellent properties since they are suitable solvents in many chemical applications (Pinkert et al., 2009). They are non-flammable substances, have very low vapour pressure and are thermally, electrochemically and mechanically stable due to their

strong ionic interaction (Earle et al., 2006). Their solvent properties such as melting point, viscosity and miscibility with other solvents can be tuned by the right design and combination of each ion since they possess discrete anions and cations (Wishart, 2009). Depending on their polarity, they are immiscible with water or organic solvents resulting into biphasic systems. ILs are capable of partially or completely dissolving lignin, cellulose or lingocellulosic biomass especially for imidazolium based ILs (Zavrel et al., 2009). This is due to their ability to act as hydrogen bond acceptors with limited capacity to donate hydrogen. ILs can dissolve biomass because they form hydrogen bonds between the anion and the hydroxyl groups of the cellulose. This results into lysis of the hydrogen bond crosslinking of the polysaccharide (Mazza et al., 2009). IL lysis of microalgae cells improves the recovery efficiency of lipids using solvents by increasing the interfacial area of solvent to cellular matrix for mass transfer (Orr et al., 2015). In addition, the use of ILs in wet microalgae biomass results in a reduced energy demand on the system (0.4 MJ kg^{-1}) compared to conventional solvent extraction processes, which consumes 4-9 MJ $kg.^{-1}$ (Teixeira, 2012). Furthermore, the use of ILs results in reduced solvent extraction time since the cellular components are exposed to the solvents after IL cell lysis.

In this work, a mixed culture of *Scenedesmus obliquus and Monoraphidium spp*/MNPs slurry was subjected to IL treatment to lyse/disrupt microalgae cells and to efficiently extract lipids. The cell lysis efficiency using ILs and the lipid extraction efficiency using hexane were determined. The MNPs and ILs were recycled. The aim is to extract lipids from magnetically separated microalgae using ionic liquids and to recycle both MNPs and ionic liquid. Achieving this aim should potentially lower the cost of biodiesel processing from microalgae. The objectives are to:

i) Magnetically separated microalgae at a separation efficiency above 95%.
ii) Lyse microalgae cells using ILs at a lysis efficiency of at least 90%.
iii) Extract microalgae lipids using ILs at an efficiency of at least 90%.
iv) Recycle MNPs after IL treatment for further microalgae separation.
v) Recycle ILs for further microalgae cell lysis and lipid extraction.
vi) Optimise IL lipid extraction conditions.

This will be the first report on extraction of lipids from magnetically separated microalgae using ILs and on recycling of MNPs after IL treatment of microalgae/MNPs. Achieving the above objectives will potentially lead to an efficient processing of biodiesel from microalgae. This could result in the cost of biodiesel being competitive in comparison to petroleum-derived fuels. Recycling ILs and MNPs suggests that this will be a truly green and sustainable process. In addition, this shows that IL extraction and magnetic separation can also be applied on mixed microalgae cultures. This would reduce the cost of keeping out unwanted microalgae species during cultivation.

5.3. Materials, methods and analytical techniques

5.3.1. Materials

All ILs used were purchased from Sigma Aldrich and had the following compositions: [Bmim][Cl] 98 wt.%, [Bmim][TSFI] 98 wt. %, [Bmim][HSO_4] 98 wt.%, thermomorphic IL was prepared in our laboratory and [Bmim][MeSO4] 95 wt.%. Hexane 99 wt. % and methanol 98 wt.% were also purchased from Sigma Aldrich UK and were used without further purification.

5.3.2. Methods

In Figure 5.1, the scheme illustrates the separation of microalgae from culture medium using MNPs, after separation, the microalgae/particle slurry was subjected to ILs treatment for lysis of the cell wall to release cellular compounds such as lipids, proteins and carbohydrates. Since the lipids are hydrophobic and the ILs are used are hydrophilic, the lipids float to the surface of the IL/microalgae mixture and are efficiently recovered by dissolving them in hexane as illustrated in Figure 5.3. The recovered lipids were transesterified to biodiesel, the ILs, microalgae biomass and MNPs were recovered as described in the next sections.

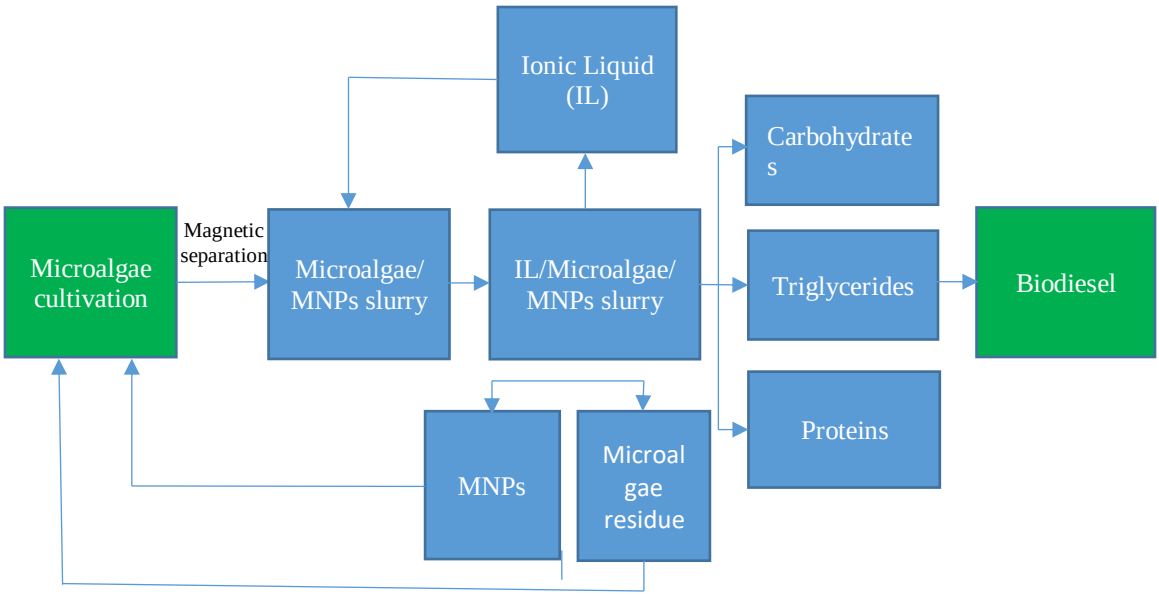

Figure 5. 1. Illustration of the IL lysis of magnetically separated microalgae and extraction of lipids from disrupted microalgae. M/sep is magnetic separation.

5.3.2.1. Microalgae cultivation

Scenedesmus obliquus/Monoraphidium spp. was cultivated in photobioreactors in the department of Chemical Engineering University of Bath UK. The details of cultivation conditions are elaborated in chapter 3 (Egesa, Chuck and Plucinski, 2017). The total lipid content in the *Scenedesmus obliquus/Monoraphidium spp.* biomass was determined using the Bligh and Dyer method (Bligh and Dyer, 1959). Spirulina powder was purchased from Bulk Powders Company and had a composition of 63 wt.% protein, 21 wt.% carbohydrates and 6 wt.% fats and the rest miscellaneous biochemical compounds.

5.3.2.2. Magnetic separation of microalgae

Magnetic separation of microalgae was done at an optimised pH4 according to the detailed procedure in Chapters 3. The separated microalgae/MNPs slurry with a water content of about 60-78 wt.% was subjected to IL treatment as detailed in the next section see also Figure 5.2.

5.3.2.3. Lysis of magnetically separated microalgae using IL

The microalgae/MNPs slurry (ratio of MNPs to microalgae 1:2 g/g, with a water content of 74.8 wt. % was mixed with an appropriate amount of IL in a ratio of 1:10 (microalgae: IL), the ILs were diluted with an equal amount of water. The IL/microalgae/MNPs mixture was stirred (100 rpm) at 65 ℃ for 18 hours to allow contact of microalgae cells with IL and to prevent settling of the cells. For the control, water was used instead of IL. After liberation of lipids, hexane (6 ml) was mixed with the IL/microalgae/MNPs mixture for 2 hours to dissolve lipids. The upper hexane layer containing lipids was recovered and hexane was evaporated (Figure 5.2 and 5.3). The yield of extracted lipids was calculated using equation 5.1.

$$Y\ (\%) = \frac{M\ (g)}{A\ (g)} \times 100\% \qquad [5.1]$$

Where: Y is yield of extracted lipids (%), M is mass of extracted lipids and A is dry mass of microalgae (without moisture and inorganic or ash content).

The total lipid content was determined using the conventional Bligh and Dyer method (Bligh and Dyer, 1959).

The extracted lipids were transesterified to biodiesel through acid catalysed transesterification according to the modified method described by Christie et al., (1973). Extracted lipids (10 mg) were redissolved in hexane (1 mL) and mixed with a 0.6M HCl in methanol solution (2ml). The solution was heated at 80 ºC for 2.5 hours under mixing (300 rpm). After cooling the reaction mixture, hexane (2 ml) was added to extract the fatty acid methyl esters (Christie, 1973). An internal standard (heptadecanoic acid (1.22 mg/ml) was added to the hexane extract and GC-MS analysis done to identify the fatty acid content of biodiesel. The fatty acid ester content was determined according to the method described by Coen Duvekot from Agilent technologies (Duvekot, 03/05/2019). In this method, the fatty acid ester content was expressed as a percentage mass fraction and calculated using equation 5.2.

$$L = \frac{AL)}{(\Sigma A) - AEI} \times 100\% \qquad [5.2]$$

Where: L is fatty acid methyl content, ΣA is total peak area from the FAME $C_{14:0}$ to $C_{24:1}$, AEI is peak area of methylheptadecanoate, and AL is peak area of the different methyl esters.

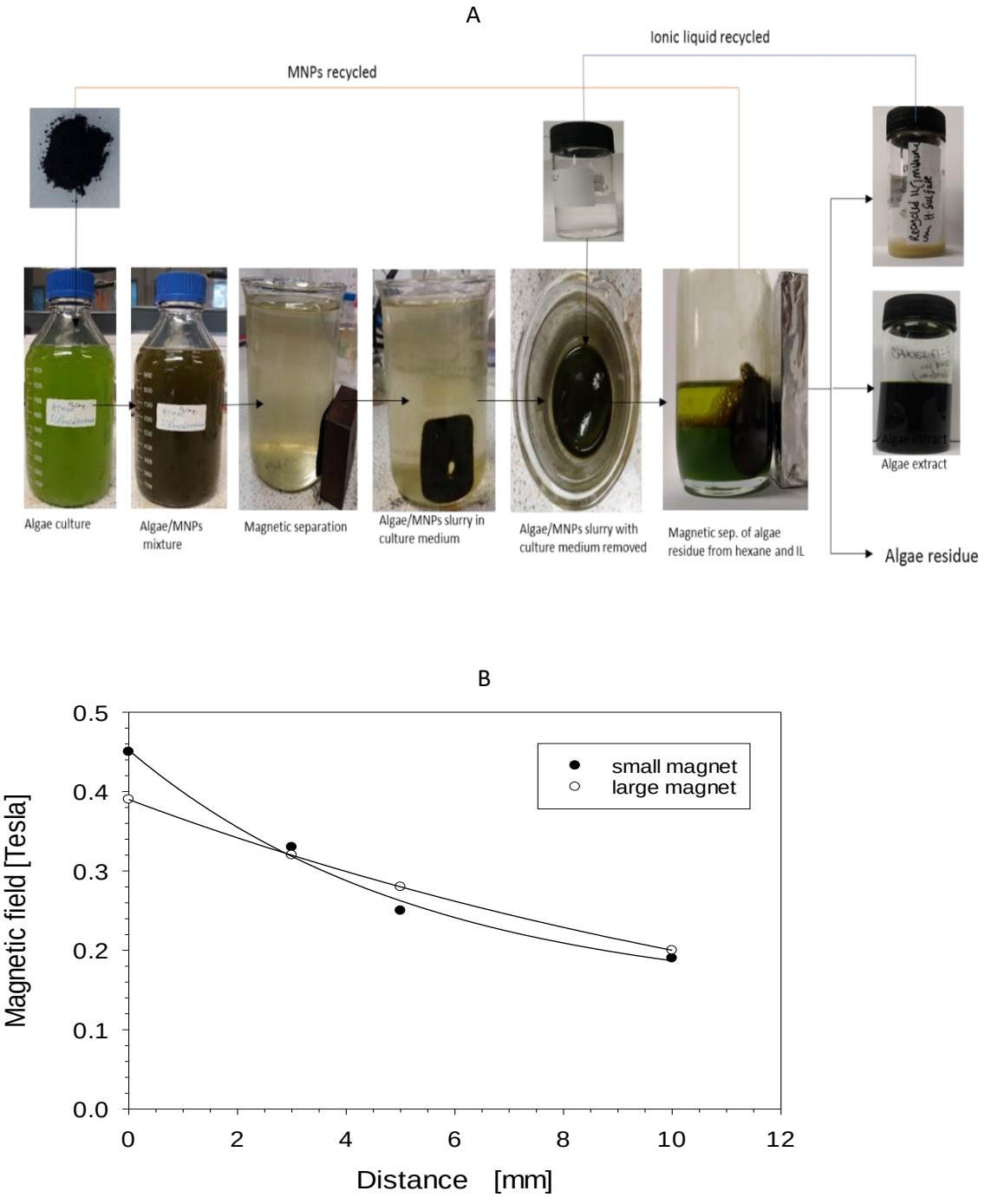

Figure 5. 2. A) Illustration of the magnetic separation of microalgae, IL extraction of lipids from magnetically separated microalgae and recycling of MNPs and ILs. B) Magnetic field strength against distance for the large and small magnet. The large magnet was used in this work.

5.3.2.4. Microalgae cell lysis

The efficiency of cell lysis by ILs on the microalgae was determined based on the percentage reduction in the total number of microalgae cells after IL treatment (Shankar et al., 2017). The cell count per ml was determined by dividing the total counts with the number of 4 x 4 grids counted and the result multiplied by 10^4. The cell count and the morphologies of the disrupted microalgae cells were observed by optical microscopy (EVOS FL) with samples mounted on the counting grids. The IL treated microalgae were diluted in water to precipitate the microalgae constituents and to give better visualization (Teixeira, 2012). The counting grid consisted of 10 slots of 4×4 grids and the volume above each 4×4 grid is 10^{-4}ml. The cell concentration per mL is given by equation 5.3.

$$\frac{\text{Counts}}{\text{ml}} = \left[\frac{\text{Total counts}}{\text{number of 4×4 grids counted}}\right] \times 10\text{^}4 \tag{5.3}$$

The percentage cell lysis was determined according to equation 5.4 (Shankar et al., 2017).

$$\text{cell lysis (\%)} = 100\left[1 - \frac{\text{T}}{\text{C}}\right] \tag{5.4}$$

Where T and C are number of cells per ml in treated sample and control respectively.

5.3.2.5. Recycling of MNPs

The MNPs/microalgae were extracted from the IL mixture using magnetic force (Figure 5.2 and 5.3), the magnetic field strength on the surface of the magnet varied between 0.4 to 0.43 Tesla (Figure 5.2.B). The microalgae MNPs mixture was in a 50 mL glass bottle with a thickness of about 4 mm. The separated MNPs/microalgae residue were suspended in DI water and sonicated for 30 minutes to weaken the attachment between microalgae and MNPs. This washing process was repeated three times to recover clean MNPs for recycling. The recovered MNPs were analysed by TGA to determine the extent of removal of microalgae biomass from MNPs. The separation efficiency of fresh and recovered MNPs was then compared. The microalgae biomass residue removed from MNPs was recovered from water by filtration using a filter paper and analysed using FT-IR to estimate changes in the main microalgae components such as proteins, lipids and carbohydrates.

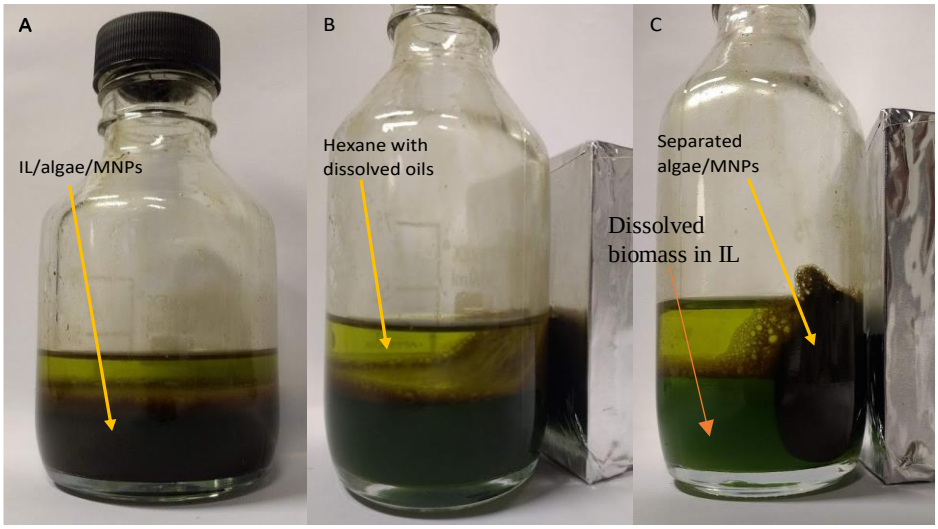

Figure 5. 3. Magnetic separation of microalgae after dissolving IL extracted lipids in the hexane phase (top). A) IL/microalgae/MNPs/hexane mixture before magnetic separation. B) Magnetic separation of microalgae/MNPs slurry from the mixture. C) After magnetic separation.

5.3.2.6. Recycling of ionic liquid

The ILs were recycled according to the method described by (Orr et al., 2015) by adding methanol (6 ml) to the IL mixture to precipitate dissolved biomass (Figure 5.3 green bottom phase). The green colour is for the biomass pigments such as chlorophyll, which dissolved in the hydrophilic IL. The IL/methanol mixture was then vacuum filtered with a fine porosity Buchner funnel, the residue was washed with methanol to recover any remaining IL. The IL was recovered by distilling off the methanol using a rotary evaporator operating at 60 °C under vacuum at a rotation speed of 150 rpm until there was no change in weight.

5.3.2.7. Effect of microalgae treatment conditions on the lipid yield

To determine the effect of IL treatment time on the yield of extracted lipids from *S. obliquus/Monoraphidium spp* and Spirulina (total fat content of 20.3 wt. % and 6.0 wt. % respectively), 2.5g ILs were mixed with 0.25 g of dry microalgae powder giving a ratio of 10:1. The microalgae/IL mixture was stirred mildly to improve the distribution of microalgae within the IL mixture at 65°C. After IL treatment, hexane (6.0 ml) was added to the mixture for 2 hours under mild mixing (200 rpm) to dissolve extracted lipids. The

upper hexane phase with dissolved lipids was transferred to a pre-weighed vail and evaporated using a rota-evaporator operated under vacuum conditions at a rotation speed of 20 rpm and temperature of 40 °C. After evaporation of hexane, the mass of extracted lipids was calculated from the difference in the masses of the vail with lipids and that of the empty vail. The yield of the bio-oils was calculated using equation 1.

The effect of water content of the reaction mixture on yield was determined by varying only the water content of microalgae from 0, 27.8, 42.4, 68.8, 74.6, 82.2 and 84.6 wt. % by adding water to 0.25g of dry microalgae powder. The wet microalgae were mixed with 2.5g of IL. The resulting mass fraction of water in the whole system (IL/microalgae mixture) was 0, 0.035, 0.067, 0.2, 0.267, 0.421 and 0.5 respectively. In many papers, authors only use the mass fraction of water in microalgae (Orr et al., 2015). All the other conditions were kept constant as described earlier.

The effect of ratio of IL to microalgae on the lipid yield was determined by treating microalgae at different mass ratios of IL to microalgae (0.5, 10,15 and 20 g/g) while keeping all other conditions constant as described in the preceding section. For the control experiment, water was used instead of IL. After treating microalgae with IL, the extracted lipid was dissolved in 6 ml of hexane and the lipid yield determined as described in section 5.3.2.3.

5.3.3. Analytical Techniques

5.3.3.1. GC-MS Analysis

Compounds in the extracted lipid were identified by GC-MS analysis on an Agilent Technologies GC system 7890A with triple-axis detector, 5975 network mass-selective detector, and Agilent JW scientific GC column. The column oven initial temperature was 100 °C, holding time was 5 minutes, raised to 250 °C at a rate of 5 °C min^{-1} and held for 15 minutes, total time was 35 minutes. The carrier gas was helium. The compounds were identified using a mass spectral library software.

5.3.3.2. ^{1}H NMR Analysis of ILs

^{1}H NMR analysis was done to confirm the structural integrity of the recycled ILs in comparison with fresh ILs. The spectra were recorded using a Bruker Avance III NMR

spectrometer operating at 500.13 MHz for ^{1}H. The probe used was a BBFO+ with three channels. Unless otherwise specified samples were analysed at 25 °C using standard Bruker pulse sequences (Topspin 2.1). ^{1}H spectra were acquired with a SW of 20 ppm, and 16 transients. Spectra were referenced using the residual solvent signal, at 7.26 ppm for ^{1}H.

5.3.3.3. FT-IR Analysis of microalgae lipids, biomass and ILs

FT-IR analysis was performed to further analyse extracted lipids based on their functional groups and to compare with the microalgae biomass before and after lipid extraction. It was also used to analyse and compare the functional groups in fresh and recycled ILs. Spectra were collected using a Frontier Fourier Transform Infrared Spectrometer (FTIR) (PerkinElmer, Seer Green, U.K.) with attached MIRacle single reflection attenuated total reflectance (ATR) sampling accessory (Pike technologies, Madison, WI, U.S.A.). 10 scans were collected using a $4cm^{-1}$ resolution in the range 400-600 cm^{-1}.

5.3.3.4. Mass spectral analysis of ILs

Mass spectral analysis was performed on fresh and recycled ILs to confirm that the recycled ILs maintained their structural integrity after IL treatment and extraction of microalgae lipids. This was done on an electrospray time-of-flight (MicrOTOF) mass spectrometer (Bruker Daltonik GmbH, Bremen, Germany), which was coupled to an Agilent 1100 HPLC stack (Agilent, Santa Clara, CA, United States) consisting of Agilent G1312A binary pump with G1329A auto-sampler and G1316A column oven.

5.3.3.5. TGA Analysis of MNPs

TGA analysis of fresh and recycled MNPs was performed to determine the extent of removal of microalgae biomass from used MNPs after sonication. The analysis was performed in nitrogen on a TG Setaram 92 microbalance. The ramp rate was 10 ºC min^{-1} from ambient temperature to 1000 ºC.

5.3.3.6. UV−vis measurement of optical density

To measure separation efficiency, optical density measurements were done on a UV−vis Cary series instrument JEM-1200 EX11 and separation efficiency calculated as explained in Chapter 3 and 4.

5.3.3.7. HR-TEM analysis of MNPs

In order to ascertain the surface morphology, size and particle distribution of MNPs, high-resolution transmission electron microscopy (TEM) was done. HR-TEM analysis was done as described earlier in chapters 3 and 4.

5.4. Results and Discussion

5.4.1. Main microalgae cell lysis/disruption techniques compared to ionic liquids

IL treatment was compared with other conventional microalgae cell lysis techniques such as microwave and sonication in order to justify the importance of ILs use in relation to other techniques. The microalgae used was a mixed culture of *S. obliquus and Monoraphidium spp*. The percentage cell lysis was estimated based on the reduction in the number of visible microalgae cells after treatment with different techniques. This gave an indication of the number of cells that lost structural integrity after IL treatment.

5.4.1.1. Lysis/disruption of microalgae cells using ILs

Five different ILs were used for microalgae lysis and lipid extraction. These include: 1-Ethyl-3-methylimidazolium hydrogen sulphate ([Bmim][HSO_4]), 1-butyl-3-methylimidazolium bis-imide ([BMIM][TFSI]), 1-butyl-3-methylimidazolium chloride ([Bmim][Cl]), 1-butyl-3-methylimidazolium methyl-sulphate [Bmim][$MeSO_4$] and Betainium bis(trifluoromethylsulfonyl) imide ([Hbet][Tf_2N]). In Figure 5.4, their chemical structures are shown. All the ILs used were hydrophilic and were chosen based on availability and some have rarely been used for microalgae lysis for example [BMIM][TFSI].

[Bmim][HSO4]

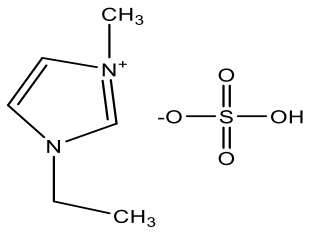

[Bmim][TFSI]

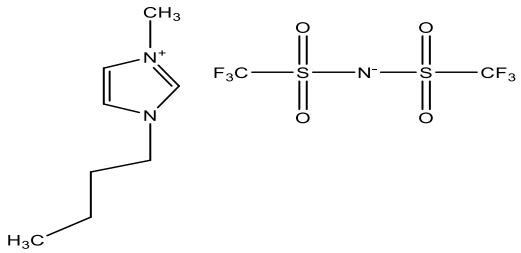

[Bmim][Cl]

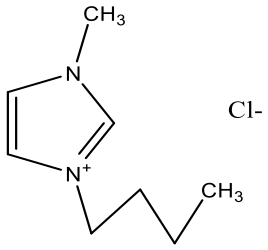

[Bmim][$MeSO_4$]

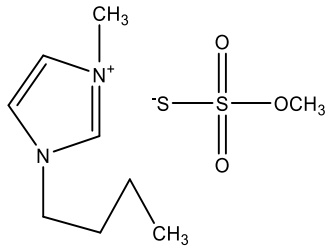

[Hbet][Tf_2N]

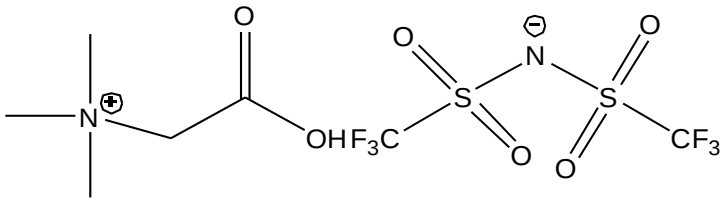

Figure 5. 4. Showing the chemical structures of the main ILs used for lysis and extraction of microalgae lipids

In Figure 5.5, the cell lysis using ILs was compared to the highest cell lysis under sonication and microwave treatment. Although these are different lysis techniques, the comparison is to give an insight in the potential of IL lysis in relation to conventional techniques. From this comparison, it is evident that ILs especially [Bmim][$MeSO_4$] exhibited the highest cell lysis compared to sonication and microwave treatment. Since ILs can lyse microalgae cells even at ambient temperature and in a wet environment, their application for cell lysis can potentially result in an energetically economical extraction of microalgae lipids for biofuel processing and for essential compounds. Application of conventional microalgae lysis techniques like sonication, microwaves and mechanical lysis is energy intensive, results in low percentage cell lysis compared to ILs (Shankar et

al., 2017) and some techniques like mechanical and solvent extraction work best with dry microalgae. Drying and lipid extraction costs amount to 90% of the total energy costs for the process (Lardon et al., 2009). If the drying step is eliminated 25% reduction in energy can be achieved (Gursong Yoo et al., 2012). In Figure 5.5, ILs cell lysis using wet and dry microalgae was compared. The water content for the wet microalgae was 74.6 wt. %. The percentage cell lysis from wet microalgae was generally higher compared to dry microalgae with exception of the control where hexane was used in absence of ILs. Similar findings were reported by Olkiewicz et al., (2015) in the recovery of lipids from wet *Nannochloropsis oculata* with a water content of 71.7 wt. % using a hydrated phosphonium chloride IL. It was reported that lipid yield increased by 16 wt. % when wet microalgae was used (Olkiewicz et al., 2015). Though the type of microalgae and IL used are different from this work, the trend is similar and the ILs used in both cases are hydrophilic.

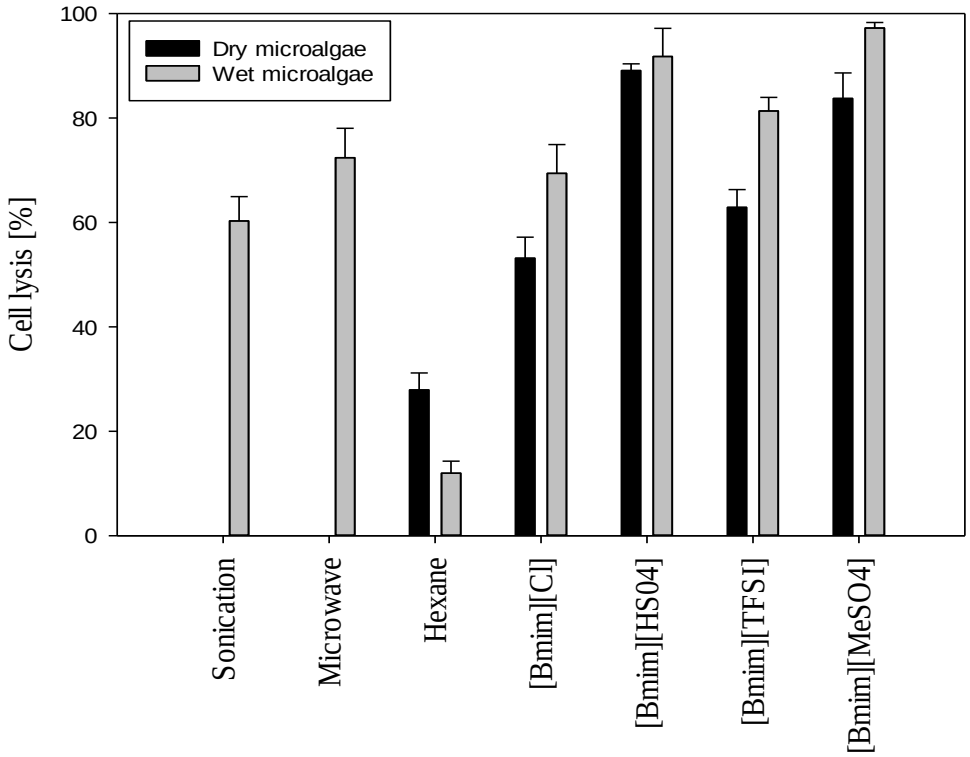

Figure 5. 5. Percentage microalgae cell lysis using sonication, microwave and different ionic liquids. The cell lysis was done at 65 °C for 18 hours. The lipids were dissolved in hexane after cell lysis.

In addition, Teixera., (2012) in the investigation on wet extraction of microalgae lipids using chloride based ILs, used microalgae with a water content of 90 wt. % and observed complete lysis of cells within 30 minutes of IL treatment (Teixeira, 2012). The treatment temperature was between 100 °C to 140 °C at a ratio of microalgae to IL of 1:20 (Teixeira, 2012). Furthermore, Fujita et al., (2013) reported the complete room temperature dissolution of wet marine microalgae with a water content of 95 wt. % within 30 minutes using [C2mim][MeO(H)PO2] (Fujita et al., 2013). Also, Orr et al., (2015) reported a high lipid recovery in the wet extraction of lipids from *chlorella vulgaris* with a water content of 75.0 wt % using [C2mim][EtSO4] with methanol in a ratio of 2:1 (Orr et al., 2015). Moreover according to Fujita at al., (2013), wet extraction of microalgae lipids using hydrophilic ILs is advantageous since the energy intensive drying step is avoided resulting in an energy efficient process (Fujita et al., 2013). The high microalgae lysis in wet biomass is due to the hydrolysis reactions that take place during the lysis process. According to Teixeira.,(2012) ILs dissolve both wet and dry biomass but complete dissolution takes place in wet biomass (Teixeira, 2012). This is due to the interaction between ILs and water to produce hydronium and hydroxide ions. The hydroxide anions donate electrons to the anchoring carbon on the polysaccharide chain. And the hydronium ion donates protons to the bare oxygen intermediate in the polysaccharide chain leading to breakage of the glyosidic bonds and hence increased cellular lysis.

In comparing the percentage cell lysis of the different ILs, it was observed that [Bmim][$MeSO_4$] resulted in the highest microalgae lysis (Figure 5.5). This is further confirmed by the microscopic images in Figure 5.6 which show complete dissolution of microalgae in [Bmim][$MeSO_4$] IL. While [Bmim][Cl] gave the lowest microalgae lysis. This is in agreement with the findings of (Sun-A Choi et al., 2014) where [Bmim][Cl] ILs were reported to have very low cell lysis and extraction efficiency. In addition, (Olkiewicz et al., 2015) also observed low cell lysis and lipid extraction when hydrated chloride based ILs were used to extract lipids from *N. oculata*. On the other hand, the high cell lysis associated with [Bmim][$MeSO_4$] is also in agreement with several literature where high lysis was observed even at room temperature (Young et al., 2010; Sun-A Choi et al., 2014; Orr et al., 2015).

The actual reason for such high cell lysis using [Bmim][$MeSO_4$] and the low cell lysis for the chloride based ILs is not yet clear since IL-cell membrane interaction are not yet clearly understood (Brian Yoo et al., 2016). But it is possible that the high Hildebrand solubility parameter (δ_H ($Mpa^{0.5}$)) of [Bmim][$MeSO_4$] (26.4) compared to that of [Bmim][Cl] (24.16) and other ionic liquids such as [Bmim][TFSI] (25.7) and [Hbet][Tf_2N] (25.8) facilitated the high cell solubilisation and lysis (Weerachanchai et al., 2012). The solubility parameter gives an indication of the strength of molecular interaction between interacting molecules (Swiderski et al., 2004).

The other possible reason is that the anions of [Bmim][MeSO4] are better hydrogen bond acceptors compared to the other ILs. Therefore they are better at dissolving biomass than the other ILs through hydrogen bonding (Zhao et al., 2002). The mechanism of cell wall solubilisation as described earlier, involves hydrogen bond formation between the IL anion and the hydroxyl groups in the polysaccharide chains of cellulose leading to breakage of the hydrogen bond cross linkages in the polysaccharide chain (Remsing et al., 2006). A comparison of the Kamlet-Taft parameters for these anions shows the β value of [Bmim][MeSO4] to be higher than the other ILs (0.66) (Ab Rani et al., 2011; Al Hattab, Ghaly and Hammoud, 2015). The values of α, β and π* in the Kamlet-Taft expression are a measure of the donating ability of hydrogen bonding, accepting ability of hydrogen bonding and the polarizability respectively (Fujita et al., 2013). ILs with a high β value have a substantial ability to dissolve cellulose (Fukaya et al., 2008; Fujita et al., 2013). The high β value for [Bmim][MeSO4] anion further confirms that it has a greater ability to dissolve the cellulose in the microalgae cell wall through hydrogen bonding causing greater cell lysis/solubilisation than other ILs. The complete cell lysis in Figure 5.6C corresponding to [Bmim][MeSO4] IL further confirms that complete dissolution of the microalgae was done when [Bmim][$MeSO_4$] was used.

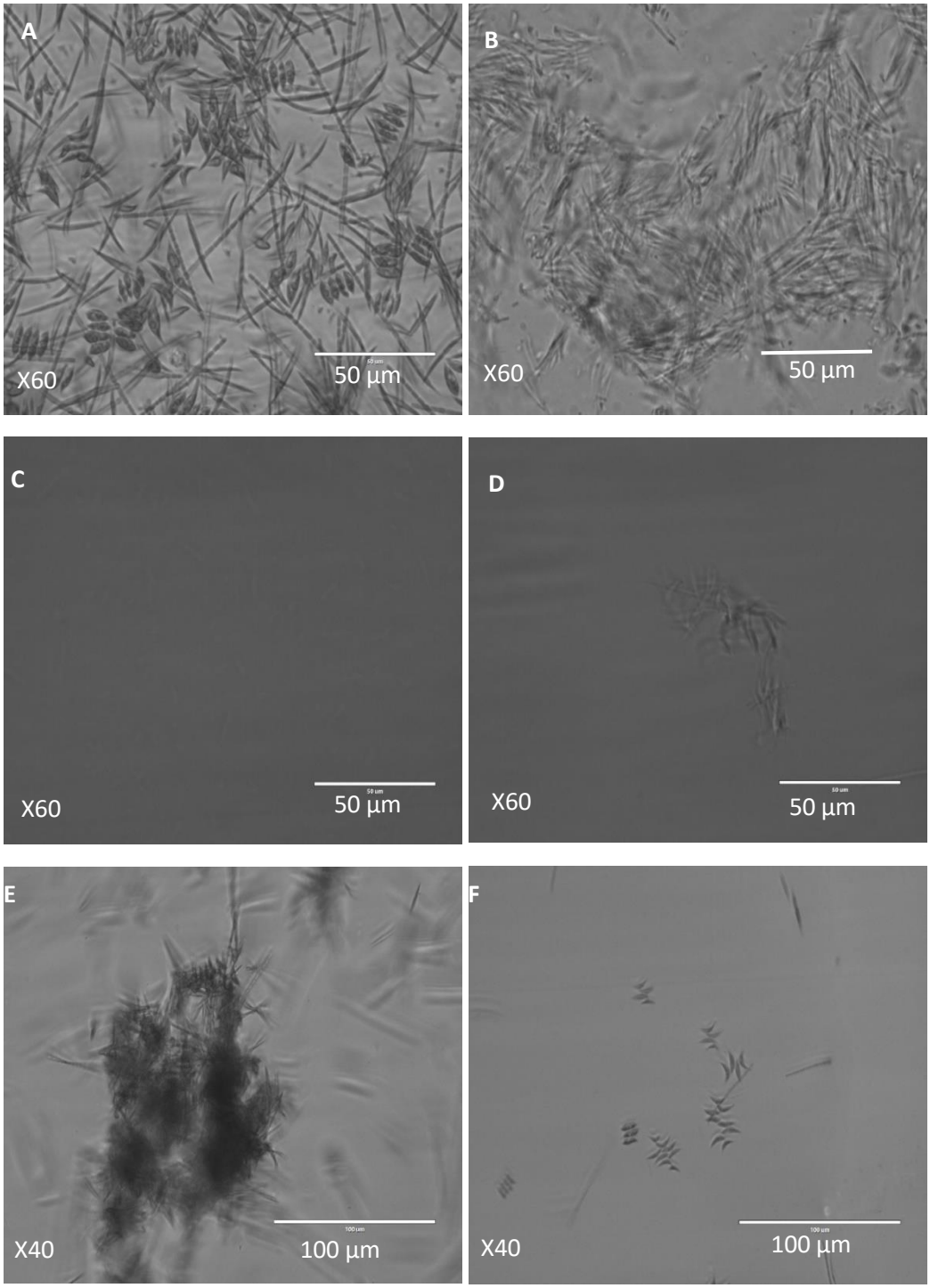

Figure 5. 6. Microscopic images of wet disrupted *Scenedesmus obliquus/Monoraphidium spp*) after lysis and lipid extraction using hexane at 65 °C for 18 hours. A) Untreated microalgae, B) treated with [Bmim][HSO_4] IL, C) treated with [Bmim][$MeSO_4$], D) treated with [Bmim][TSFI], E) microwave treatment for 60 seconds and F) sonication for 2 hours.

For the control experiment, the low microalgae lysis in wet environment under hexane treatment was due to water acting as a barrier to solvent extraction (Balasubramanian, Doan and Obbard, 2013). Therefore, drying of microalgae is important for efficient solvent extraction. The use of dry microalgae for solvent extraction results in a more energy intensive process that is less economical for large-scale applications.

5.4.1.2. Sonication treatment

Treatment of microalgae cells by sonication was done for 30, 60 and 120 minutes resulting in lysis efficiencies of 40.2, 55.7 and 60.3% respectively (Figure 5.7). This low lysis shows that sonication alone is not an efficient cell lysis technique but can be used in combination with other techniques like solvent extraction or IL extraction. These results are in close agreement with the findings of Shankar et al., (2017) where the lysis of C*hlorella sp* and *Chloroccocum* by sonication was done and the highest cell lysis of 70.74% after 40 minutes was achieved from *Chlorococcum sp* (Shankar et al., 2017). It was also noted that increase in sonication time did not have a significant effect on cell lysis efficiency. The slight difference in results with this work could be due to differences in strength of the sonication equipment or the difference in microalgae species. These results suggest that sonication alone is not so effective in disrupting microalgae cells and an increase in acoustic energy does not significantly lead to increased cell breakdown. The higher energy input used implies that it is a less economical process (Halim et al., 2012; Andrew K Lee, Lewis and Ashman, 2012).

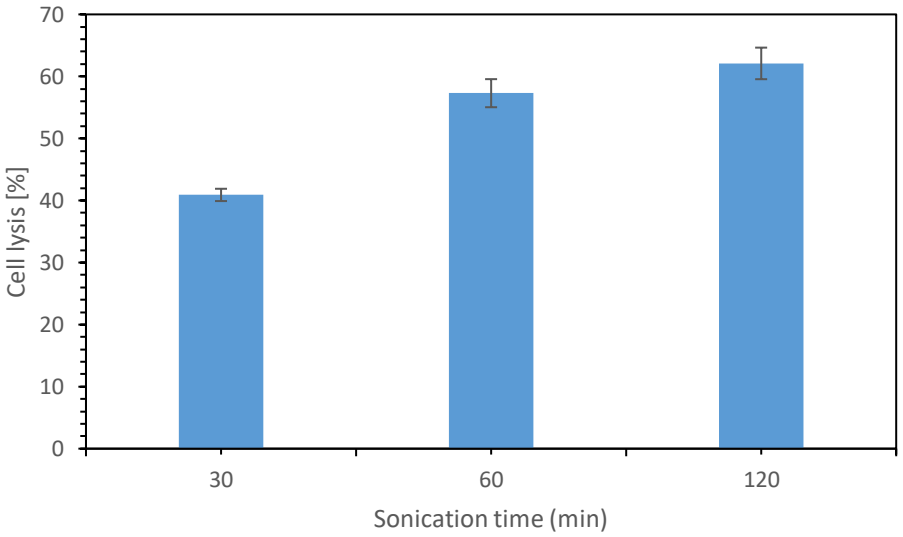

Figure 5. 7. Microalgae (*S. obliquus and Monoraphidium spp*) lysis at different sonication times

5.4.1.3. Microwave treatment

A conventional microwave operating at 700W was used to lyse microalgae cells from a mixed culture of *Scenedesmus obliquus*/*Monoraphidium spp.* Cell lysis was done for 60, 120, and 180 seconds giving lysis percentages of 56.3, 65.2 and 72.4 wt.% respectively (Figure 5.8). These results show that the extent of cell lysis was dependant on the time of microwave exposure. The highest lysis efficiency (at 120 minutes) was compared with IL and microwave lysis efficiencies (Figure 5.5). Shankar et al., (2017) did microalgae lysis using a conventional microwave operating at 700W and obtained the highest cell lysis of 74.75 wt. % after 180 seconds (Shankar et al., 2017). Microwave method has been reported as an effective way of disrupting and extracting microalgae lipids from *Chlorella*, *Chlorococcum* and *Botryococcus* (Jae-Yon Lee et al., 2010; Shankar et al., 2017).

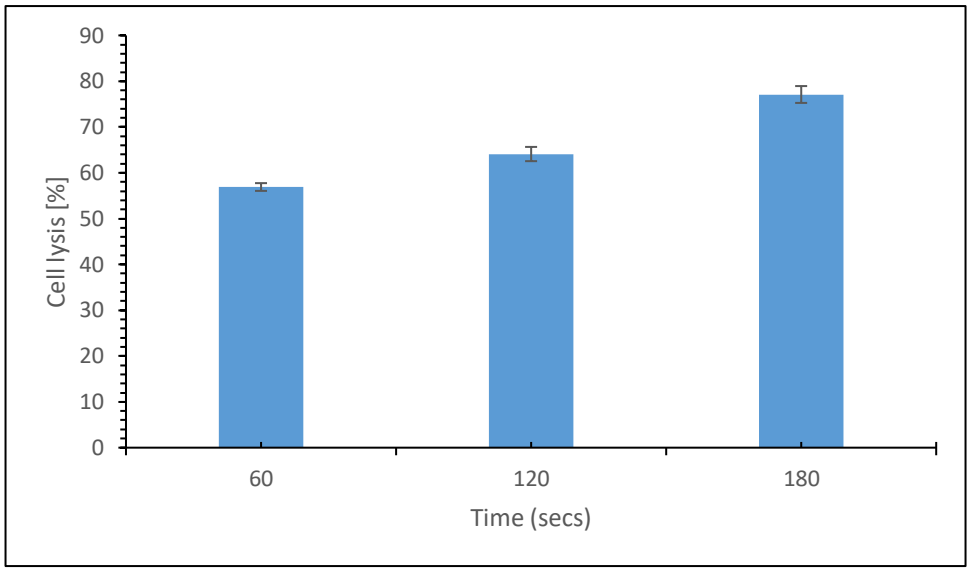

Figure 5. 8. Microalgae lysis (*S. obliquus and Monoraphidium spp*) efficiency using conventional microwave

The challenge with this procedure was that continual microwave treatment led to heating and drying of the microalgae culture. However better cell lysis can be achieved by using thermostatic microwave reactors which also prevent heating and drying of the culture medium (Bach et al., 2017; Shankar et al., 2017). Microwave lysis is a quick procedure however; it is energy intensive and may not be suitable for commercial applications due to the high-energy cost.

5.4.3. Recovery of microalgae lipids after IL treatment

After cell lysis using ILs, hexane was added to the IL/microalgae mixture to dissolve the extracted lipids and separate them from the mixture. The action of the IL was to lyse the cell wall so as to release the cellular content thereby improving the efficiency at which lipids are dissolved by hexane (Young et al., 2010). The lipid yield was determined gravimetrically after evaporating hexane. The total lipid content of *S.obliquus/Monoraphidium spp* was determined using the Bligh and Dyer method (Bligh and Dyer, 1959) and was found to be 20.3 wt.% and for spirulina 6 wt.% (determined by bulk powders- the Spirulina processing company). The extraction efficiency and the lipid yields corresponding to the different ILs were compared based on the total lipid content of the microalgae and the dry cell weight respectively (Figure 5.9).

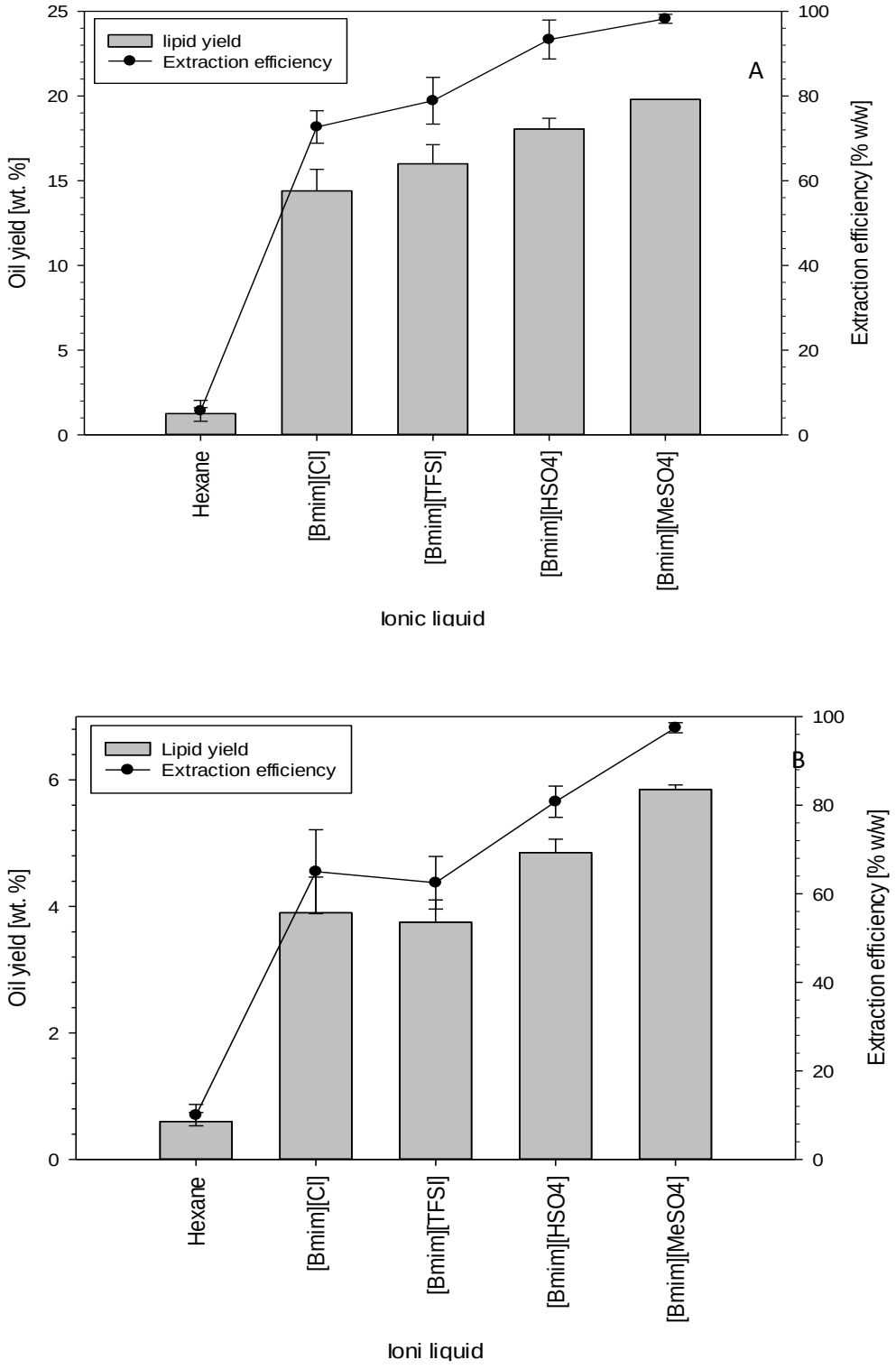

Figure 5. 9. Percentage yield and extraction efficiency of microalgae lipids after cell lysis using different ILs from wet microalgae at 65 ℃ for 18 hours. The lysed microalgae were mixed with hexane for 2 hrs to extract lipids. A) *Scenedesmus obliquus/Monoraphidium spp* and B) Spirulina.

It is evident that the highest lipid yield (20.1 wt. % and 5.85 w.%) and extraction efficiency (99% and 97%) for *S. obliquus/Monoraphidium spp* and Spirulina respectively were obtained when [Bmim][$MeSO_4$] was used. There are not many reports in literature comparing lipid yields of different ILs. However, some literature like Kim et al., (2013) reported on the use of [Bmim][$MeSO_4$] to extract lipids from *Chlorella vulgaris* and a yield of 4.7 wt. % dry cell weight was obtained; compared to 2.1 and 2.9 wt. % dry cell weight for the Soxhlet's and Bligh and Dyer methods respectively (Kim et al., 2013). This extraction was done under sonication conditions.

In addition, Gregory Young et al., (2010) used [Bmim][$MeSO_4$] as a co-solvent with methanol to extract lipids from *chlorella sp* and obtained lipid yields of 8.6 wt. % (Young et al., 2010). The extraction efficiency of [Bmim][$MeSO_4$] alone when tested on canola seeds was 13% compared to 11% for methanol (Young et al., 2010). A comparison of IL lysis and the extraction efficiency (Figures 5.5 and 5.9) clearly show a direct correlation between the extent of cellular lysis and the lipid extraction efficiency. Therefore, it can be concluded that the high extraction efficiency when [Bmim][$MeSO_4$] was used was due to it is high cell lysis ability. The high cell lysis resulted in increased exposure of cellular material to solvents hence increasing the contact between the solvent (hexane) and the cellular matrix for increased mass transfer (Orr et al., 2015). The increased extraction of lipids by the solvent resulted into increased yield of lipids extracted by hexane. On the other hand, for ILs like [Bmim][Cl] with lower cellular lysis and lipid yields, the reverse is true. Reduced cellular lysis leading to reduced contact area between solvent and cellular matrix resulting in reduced mass transfer to the solvents and hence reduced lipid yields and extraction efficiency. The low lipid yields observed when hexane was used in absence of ILs (Figure 5.9) also confirms this. The use of ILs for cell lysis and subsequent lipid extraction by hexane results in a reduction in the amount of solvents used to dissolve and extract the lipids. For example, in this work, only 6 mL of hexane were used to dissolve extracted lipids.

Typical solvent extractions like Bligh and Dyer method (Bligh and Dyer, 1959) that use a mixture of polar and non-polar solvents like tri-chloromethane and methanol in a 1:2 ratio can result in comparable high lipid yields. But they use large quantities of solvent

(45 cm^3 *i.e.* 30 cm^3 methanol and 15 cm^3 tri-chloromethane for 1g of microalgae) (Orr et al., 2015) and extract many polar compounds which act as impurities in the transesterification process hence lowering the yield of biodiesel. In addition, the use of ILs reduces the time needed for solvent extraction from 6 hours to only 1 to 2 hours like in this work and in some cases in literature to only 15-30 minutes but with low lipid yields (Orr et al., 2015). Furthermore, the use of limited amounts of hexane to dissolve lipids after cell lysis can be avoided if other techniques of separating ILs from the extracted lipids are applied. Since the extracted lipids are immiscible with the hydrophilic ILs used, they floated to the surface and could be recovered by centrifugation if they are in large amounts (Olkiewicz et al., 2015). However, the use of hexane can facilitate complete extraction of non-polar lipids to enable an accurate calculation of the lipid yield.

5.4.4. Characterisation of extracted lipids

These tests were carried out to confirm that the extracted compounds are lipids. The chemical composition of extracted lipids was analysed using GC-MS, ^{1}H NMR and FT-IR.

5.4.4.1. GC-MS Analysis of extracted lipids

Since the properties of biodiesel/ fatty acid methyl esters (FAME) strongly depend on its fatty acid composition, the extracted lipids from Spirulina and *S. obliquus*/*Monoraphidium spp* were first transesterified to fatty acid methyl esters through acid catalysed transesterification and the fatty acid profile of the FAME analysed using GC-MS (Figure 5.10, Table 5.1 and 5.2). More fatty acids were observed in the lipids extracted from *S. obliquus*/*Monoraphidium spp* compared to the lipids extracted from Spirulina (Table 5.1 and 5.2). This is possibly because of the dry Spirulina biomass used. Drying of Spirulina may have led to loss of some fatty acids. The *S. obliquus*/*Monoraphidium* spp were used as fresh microalgae magnetically harvested from culture medium without further processing. The other reason could be that the *S. obliquus*/*Monoraphidium spp* are a mixed microalgae culture, therefore contributing different types of fatty acids that may not be present in one microalgae type like Spirulina.

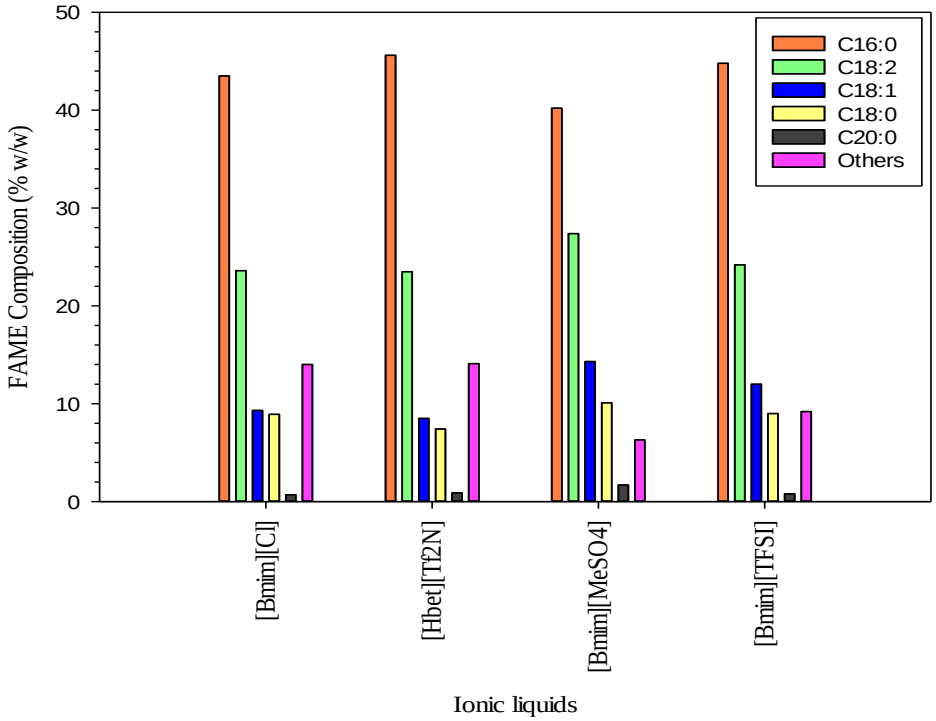

Figure 5. 10. Fatty acid profile of FAME from Spirulina lipids extracted using hexane after microalgae lysis using different ILs.

Table 5. 1. Fatty acid profile of biodiesel after transesterification of lipids extracted from Spirulina after lysis with different ionic liquids. The literature comparison (Olkiewicz et al., 2015) in the table is based on a different microalgae (*N. oculata*) and ionic liquid. Its purpose is to give an idea since better comparisons based on similar microalgae and ILs could not be found.

		FAME Composition (wt. %)				
RT (min)	Fatty acid chain	[Bmim][Cl]	[Hbet][Tf_2N]	[Bmim][MeSO4]	[Bmim][TFSI]	Literature [$P(CH_2OH)_4$]Cl
24.235	Hexadecanoic acid (C16:0)	43.5	45.6	40.2	44.8	21.3
26.461	Linoleic acid (C18:2)	23.6	23.5	27.4	24.2	25.3
26.518	Oleic acid (C18:1)	9.3	8.5	14.3	12	8.1
26.827	Octadecanoic acid (C18:0)	8.9	7.4	10.1	9	1.2
29.202	Eicosanoic acid (C20:3)	0.7	0.9	1.7	0.8	1.7
	Others	14	14.1	6.3	9.2	42.4
	Total (wt. %)	100	100	100	100	100

Table 5. 2. Fatty acid profile of biodiesel after transesterification of lipids extracted from *S. obliquus*/*Monoraphidium spp* after lysis with different ionic liquids. The literature comparison (Olkiewicz et al., 2015) in the table is based on a different microalgae (*N. oculata*) and ionic liquid. Its purpose is to give an idea since better comparisons based on similar microalgae and ILs could not be found.

		FAME Composition (wt. %)			
RT (min)	Fatty acid chain	[Bmim][HS]	[Bmim][TFSI]	[Hbet][Tf_2N]	Literature $[P(CH_2OH)_4]Cl$
11.493	Nonanoic acid (C9:0)	0.5	0.4	0.3	-
17.472	Nonanedioic acid (C10:0)	1.2	0.7	0.8	-
18.313	Octanoic acid, (C8:0)	15.1	20.7	13.6	-
20.322	Tetra-decanoic acid (C14:0)	2.1	2.0	3.4	5.0
23.263	Hexadecanoic acid (C16:0)	56.0	52	49.2	40.0
24.19	Pentadecanoic acid, (C15:0)	1.7	1.3	1.5	0.4
25.946	Octadecanoic acid (C18:0)	11.2	9.5	7.4	0.4
26.461	Linoleic acid (C18:2)	0.3	0.3	0.5	1.2
26.518	Oleic acid (C18:1)	0.3	0.2	0.4	2.3
27.199	Triacontanoic acid (C30:0)	1.1	0.8	0.9	-
	Others	10.4	12.1	22	50.7
	Total (wt. %)	100	100	100	100

From Figure 5.10, Table 5.1 and 5.2, it is evident that hexadecanoic/palmitic acid (C16:0) was the most dominant fatty acid in all the FAME samples from both Spirulina and *S. obliquus*/*Monoraphidium spp* lipids. Closely related findings from (Olkiewicz et al., 2015) also revealed a high content of hexadecanoic acid in the lipids extracted from other microalgae species such as *Chlorella vulgaris* and *Nannochloropsis oculata* using $[P(CH_2OH)_4]$ Cl at 24.3 and 14.49 wt. % respectively. Linoleic acid (C18:2) had the second highest content in the lipids extracted from Spirulina while in the lipids extracted from *S. obliquus*/*Monoraphidium spp*, it was present in low concentration (Table 5.1 and 5.2). Olkiewicz et al., (2015) reported high linoleic acid content in lipids extracted from *Chlorella vulgaris* (7.67 wt. %) compared to 1.43 wt. % in *Nannochloropsis oculata* (Olkiewicz et al., 2015). The third most dominant fatty acid from Spirulina lipids was oleic acid which was in very low concentrations in the lipids extracted from S. *obliquus*/*Monoraphidium spp* (Tables 5.1 and 5.2).

The lipids extracted from *S. obliquus*/*Monoraphidium spp* had substantial quantities of octanoic acid (C8:0) as the second most dominant fatty acid (Table 5.2). This however, was not present in the lipids extracted from spirulina (Table 5.1). Octadecanoic acid (C18:0) was also present in large quantities in the lipids extracted from *S. obliquus*/*Monoraphidium spp* and was the third dominant fatty acid (Table 5.2). While in Spirulina lipids, it was the fourth dominant fatty acid (Table 5.1). Several low molecular weight fatty acids such as octanoic acid (C8:0), nonanoic acid (C9:0), nonanedioic acid (C10:0) and tetra-decanoic acid (C14:0) present in the lipids extracted from *S. obliquus*/*Monoraphidium spp* are absent in the lipid extracted from Spirulina (Tables 5.1 and 5.2). This further suggests that their absence in Spirulina was due to evaporations during the drying of Spirulina biomass since they have low molecular weight. The lowest fatty acid chain from the lipids extracted from Spirulina powder is C16 (Table 5.1). The compounds classified under others were largely composed of non-saponifiable compounds majorly alkanes of which heptadecane was most dominant (over 50 wt. %).

It is worth noting that the oils extracted from microalgae consist of neutral lipids, polar lipids (phospholipids and glycol-lipids) and at times non-lipid compounds like carbohydrates and proteins which are extracted depending on the type of solvent used (Halim, Danquah and Webley, 2012; Olkiewicz et al., 2015). The neutral lipids are classified into saponifiable and non-saponifiable lipids. The saponifiables are lipids that contain an ester functional group and can be transesterified to biodiesel. They include acyl-glycerols and free fatty acids. The non-saponifiables do not contain an ester functional group and cannot be transesterified to biodiesel. They include hydrocarbons, ketones, pigments and sterols. On the other hand, polar lipids consist of glycolipids and complex phospholipids (Olkiewicz et al., 2015). Since only saponifiable lipids can be transesterified, there remains another percentage of lipids not transesterified (non-saponifiable lipids). The amount of non-saponifiables depends on the solvent used for extraction (Olkiewicz et al., 2015). In this work, since hexane a (non-polar solvent) was used to recover lipids after cell lysis, neutral lipids were largely recovered.

5.4.4.2. ^{1}H NMR Analysis of extracted Lipids

In addition to GC-MS chromatography, ^{1}H NMR spectrometry was also used to analyse, the lipids liberated using three different ILs (Figure 5.11). Signals characteristic of triglycerides composed of saturated and unsaturated long alkyl chain fatty acids were identified in all the spectra at around 4.1 ppm and 5.5 ppm. The signals corresponding to the functional group of esters (OCH_2, OCH) were identified between 3 to 4 pmm. Un-saturated bis allylic $(-CH=CH-CH2)_n$ identified around 2.4 ppm. Terminal (CH_3) and $(CH_2)_n$ for long fatty acid alkyl chain for both saturated and un-saturated fatty acids of triglycerides were identified around 0.5 t0 1.5 ppm. All these are also marked out in the spectra (Figure 5.11) (Sarpal et al., 2016).

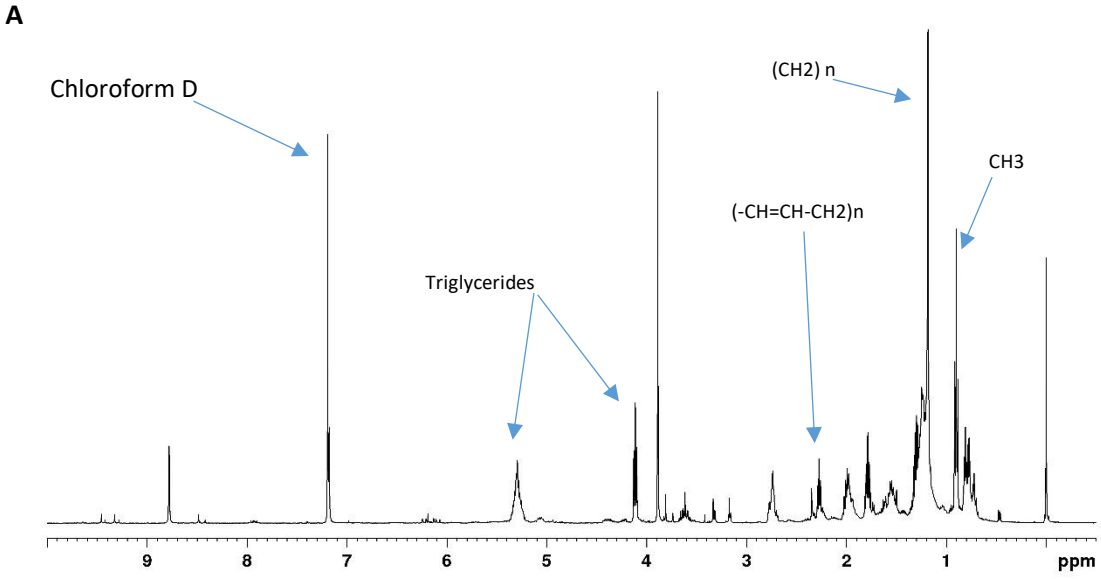

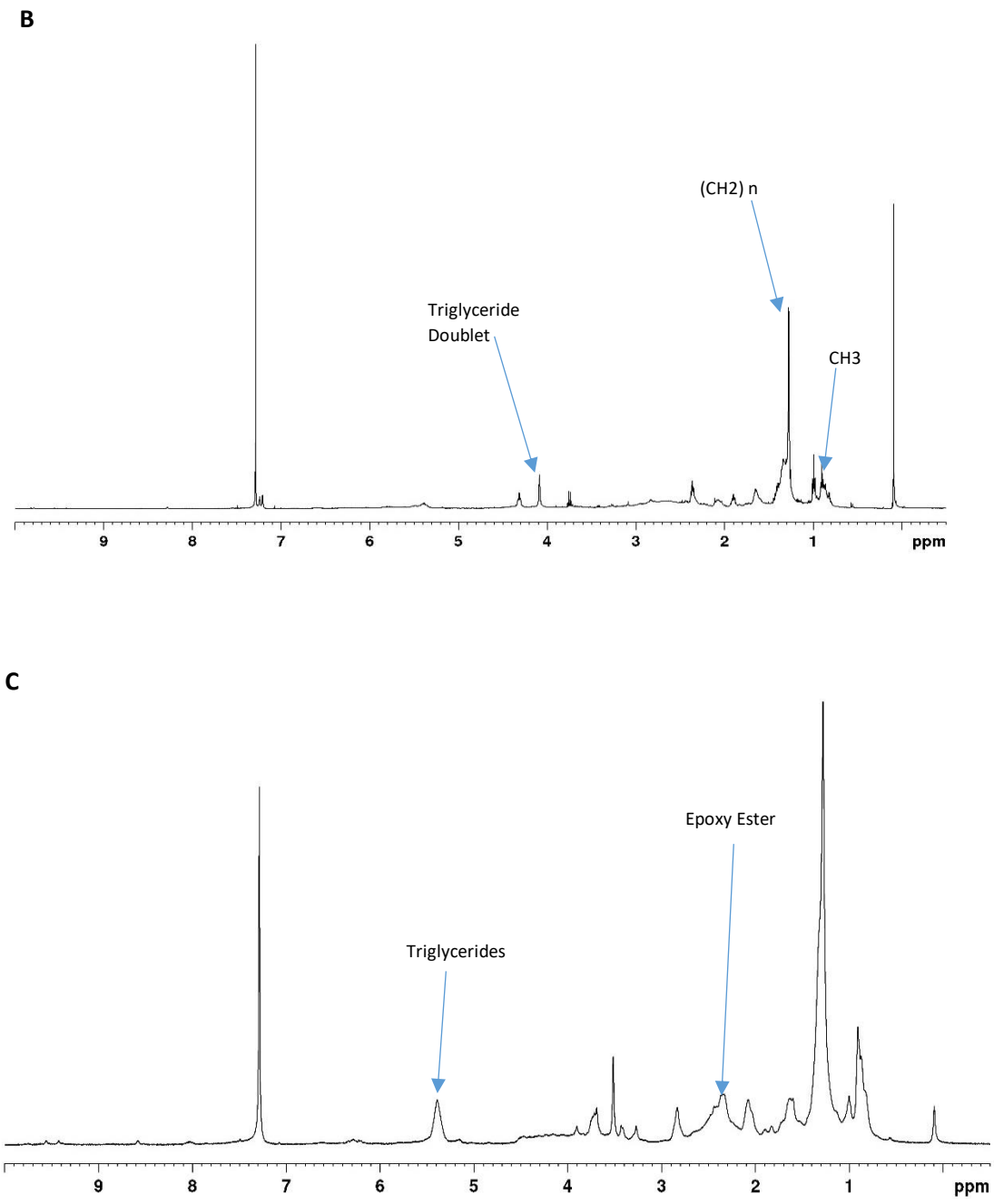

Figure 5. 11. ^{1}H NMR Spectra of lipids extracted from *S. obliquus/Monoraphidium spp* using different ionic liquids for lysis; A) [Bmim][TFSI], B) [Bmim][Cl], and C) [Bmim][HSO_4]. The identities of the lipids are according to the analysis made by (Sarpal et al., 2016).

All the ^{1}H NMR spectra showed that triglycerides were present in the extracted lipids in varying amounts depending on the type of IL used. Comparing the peak sizes in Figure

5.11.A, B and C, it is evident that there are more lipids extracted using [Bmim][TFSI] and [Bmim][HSO_4] compared to [Bmim][Cl] This agrees with the results on extraction efficiency (Figure 5.9).

5.4.4.3. FT-IR Analysis

In addition to GC-MS and ^{1}H NMR analysis, FT-IR analysis was also performed on extracted microalgae lipids, biomass residue and on the microalgae biomass before IL treatment and lipid extraction (Figure 5.12). The purpose of FT-IR analysis was to estimate changes in the main microalgae components i.e. proteins, lipids and carbohydrates. The IL used in cell lysis was [Bmim][$MeSO_4$] and the microalga was a mixed culture of *S. obliquus/Monoraphidium spp*. From Figure 5.12A, the FT-IR spectra of lipids extracted by hexane were compared with those of the microalgal residue after IL lysis. The spectra of extracted lipids gave absorption bands at 1710 cm^1 corresponding to the stretching vibrations of ester functional groups and between 2800-3000 cm^1 corresponding to the CH_3 and CH_2 stretching vibrations in the lipid acyl chain (Olkiewicz et al., 2015). For the biomass residue, bands 1000-1200 cm^1 was assigned to C-O and C-O-C groups of carbohydrates and 1500-1700 cm^{-1} to peptide amide groups of proteins (Pistorius, DeGrip and Egorova-Zachernyuk, 2009). In the lipid extract, the absorbance band corresponding to amides is invisible while in the algal residue it is clearly visible and large, suggesting that proteins are mostly present in the residue. This is also confirmed by GC-MS results that show less nitrogen compounds in the lipid extracts.

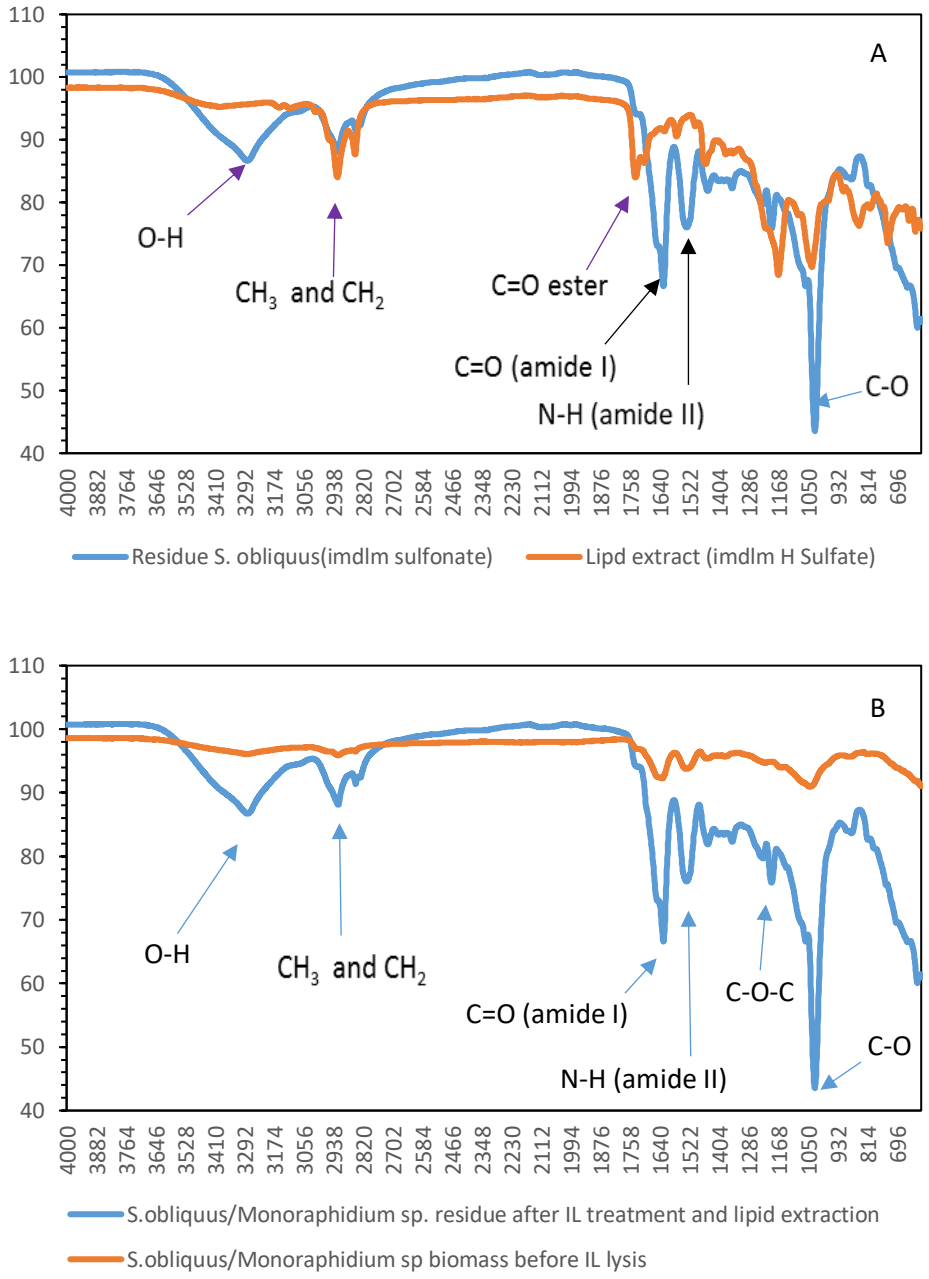

Figure 5. 12. FT-IR Spectra of *S. obliquus*/*Monoraphidium sp.* lipids extracted using ILs. A) Comparison of FTIR spectra of extracted lipids and the biomass. B) Comparison of the spectra of microalgae biomass and biomass residue after lysis and lipid extraction using [Bmim][TFSI].

In addition, the absorption band corresponding to carbohydrates (C-O) is more pronounced in the microalgal residue compared to the extracted lipids suggesting that carbohydrates are mostly present in the biomass residue. Furthermore, the band corresponding to esters C=O is clearly visible in the lipid extract and not present in the

biomass residue, suggesting that lipids were largely extracted out of the microalgae. According to this information, since carbohydrates and proteins are largely present in the biomass residue, it is therefore possible to extract proteins and carbohydrates alongside lipids in a single process. This can potentially result in a more economically viable processing of microalgae lipids using ionic liquids.

5.4.5. Recycling MNPs after IL lysis of microalgae

After magnetic separation of microalgae, the microalgae/MNPs slurry was subjected to IL treatment to lyse microalgae cells with subsequent extraction of lipids by hexane. The clean MNPs were then recovered from microalgae biomass by sonication in DI water as explained in the Method section. The recovered MNPs were dried and analysed by TGA to ascertain the extent of biomass removal (Figure 5.13). It is evident that the mass loss corresponding to microalgal biomass was approximately 11 mg for the pure microalgae sample while for the recycled MNPs there was no significant mass lose. The mass lose trend for the recycled MNPs is closely like that of the fresh MNPs. These results show that recovered MNPs were largely free of microalgal biomass. Sonication at higher pH (Figure 5.13) resulted in a substantial removal of biomass surrounding the MNPs possibly because of repulsion between the negative charge on the microalgae and the surrounding environment. Since the zeta potential around the MNPs is negative and the microalgae cells are also surrounded by a negative zeta potential, the difference in zeta potential between MNPs and microalgae cells is smaller resulting into repulsion and a reduced electrostatic interaction between MNPs and microalgae. The result is an improved biomass removal from the MNPs.

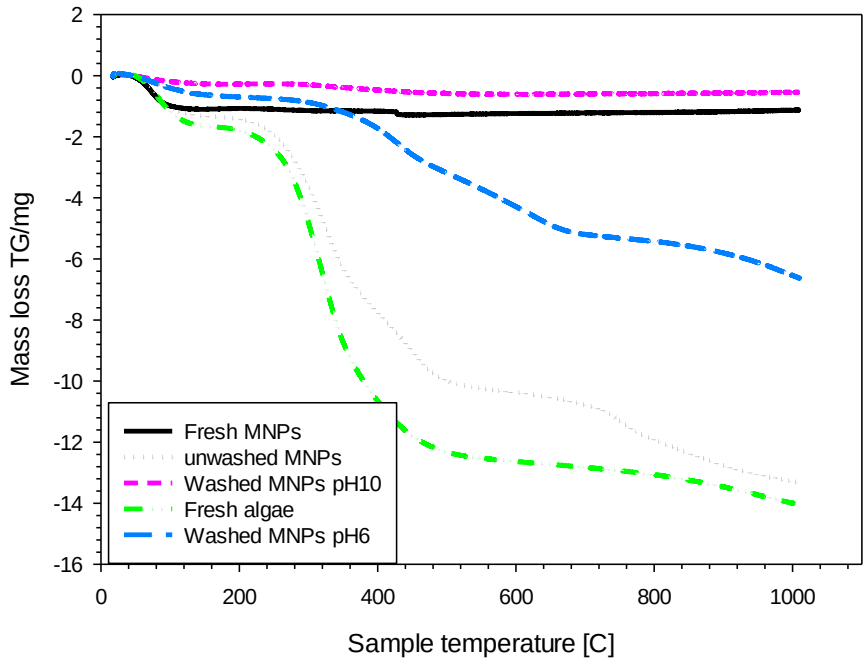

Figure 5. 13. TGA graphs of MNPs before and after IL treatment, comparing the weight losses of microalgae biomass attached on MNPs to the fresh MNPs and pure microalgae.

The recovered MNPs were recycled to further separate microalgae and the separation efficiency of the fresh and recycled MNPs was compared (Figure 5.14). In the first 12 minutes of magnetic separation, a substantial difference in the kinetics of separation of fresh and reused MNPs was observed, while after this time, the efficiencies of separation were comparable. The difference in kinetics was possibly due to aggregation of recycled MNPs after being subjected to IL treatment. The aggregation reduces the particle distribution on the surface of the algae cells resulting in reduced separation efficiency when magnetic force is applied. A separation efficiency of close to 96.6% at a separation time of 18 minutes was achieved when the recycled MNPs were used compared to about 98.6% for the fresh MNPs at the same separation time. This shows that MNPs can be effectively recycled after IL treatment to further separate microalgae from aqueous phase. In our previous work, presented in Chapter 3, we recycled MNPs after hydrothermal liquefaction of microalgae. This work is the second report on recycling MNPs but this time from the IL/microalgae mixture. The combination of magnetic separation of

microalgae with wet extraction using ILs could potentially result in an efficient processing of biofuels and essential compounds. According to the Los Alamos website, magnetic separation can lower the cost of microalgae harvesting by 90% (Los-Alamos, 2012) while wet extraction of microalgae lipids using ILs for microalgae lysis can eliminate the cost of microalgae drying and lower the cost of solvent extraction by 30-50% (Teixeira, 2012).

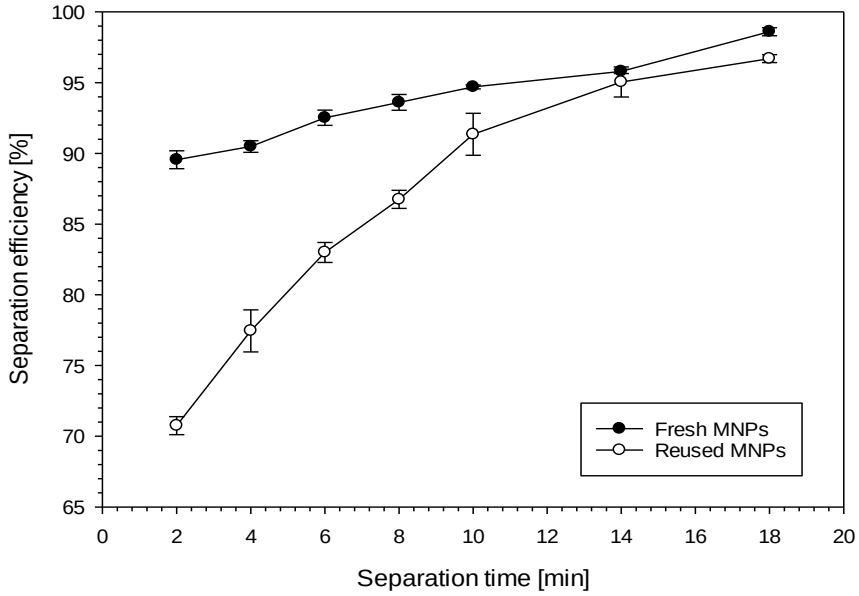

Figure 5. 14. Separation efficiency of fresh and re-used MNPs at pH 4 and varying separation time.

5.4.6. Recycling ILs after lipid extraction from microalgae

Since the use of ionic liquids may increase the cost of microalgae processing, the possibility of recycling them and their re-use for subsequent microalgae lipid extraction is paramount. In this work, different ILs were recycled and reused to lyse/solubilise microalgae and to extract liberated lipids from microalgae using hexane. The stability of some ILs after microalgae treatment was analysed using ^{1}H NMR (Figure 5.15), FT-IR (Figure 5.16 and 5.17) and mass spectroscopy (5.18, 5.19 and 5.20). In control experiments, hexane was used instead of ILs. In Figure 5.15, the ^{1}H NMR spectra of fresh and recycled IL ([Bmim][HSO_4]) were compared. Similar peaks can be observed for both the fresh and used IL indicating that the IL is stable even after microalgae treatment at

65°C for 18 hours. The peaks corresponding to water and residual methanol used as solvent are at 4.9 and 3.4 ppm respectively. The rest of the corresponding peaks are due to [Bmim][HSO_4] ionic liquid. The absence of additional peaks in the used IL is an indication that it did not decompose during the microalgae treatment process and can be recycled.

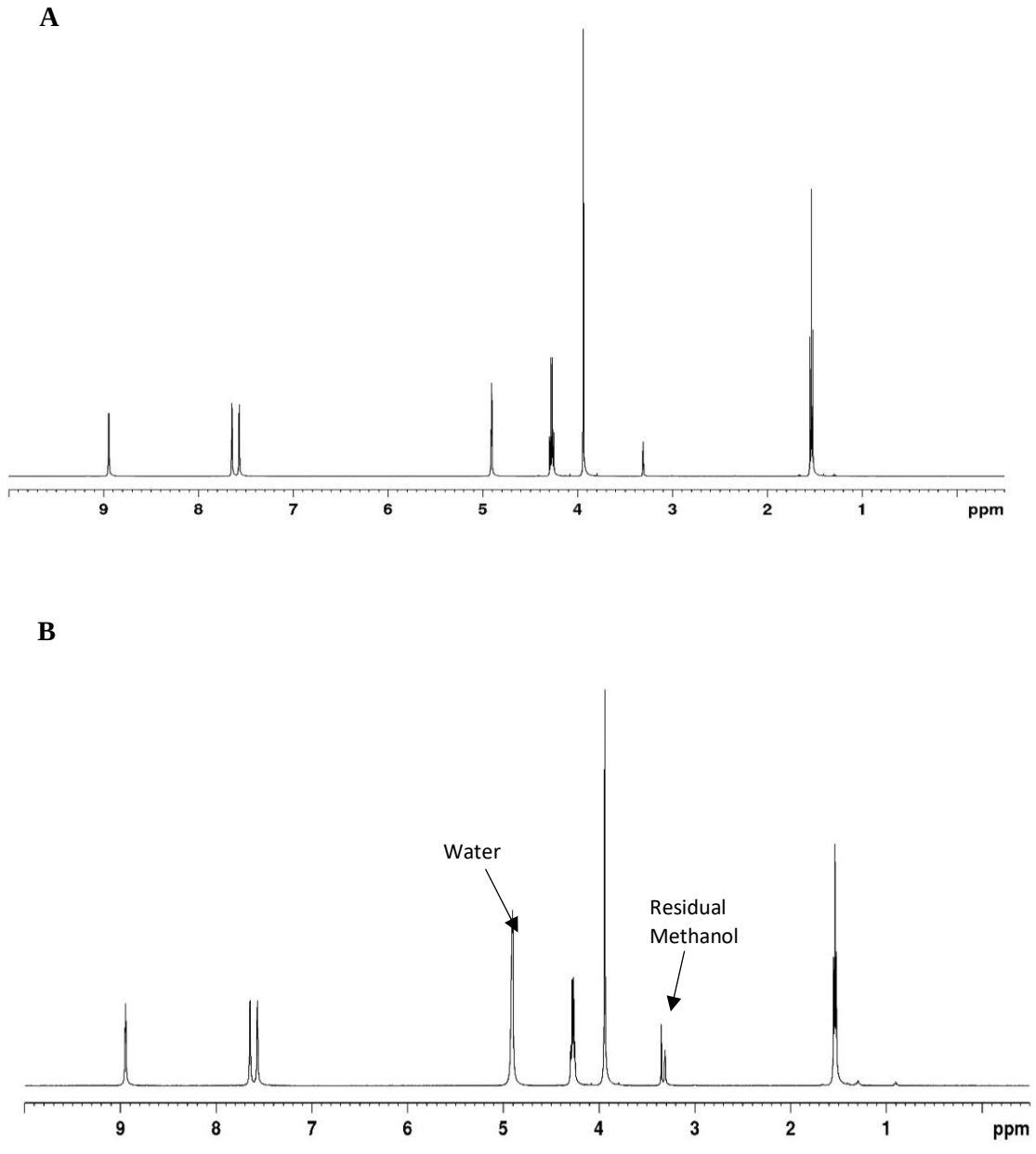

Figure 5. 15. ^{1}H NMR Spectra of one of fresh and recycled [Bmim][HSO_4] ILs. A) fresh and B) recycled IL.

In addition, FT-IR analysis of fresh and recycled ILs ([Bmim][HSO_4] and [Hbet][Tf_2N]) was also done (Figure 5.16 and 5.17). Similar absorption patterns are seen for both the fresh and recycled ILs. This in addition to ^{1}HNMR analysis confirms the stability of the recycled ILs.

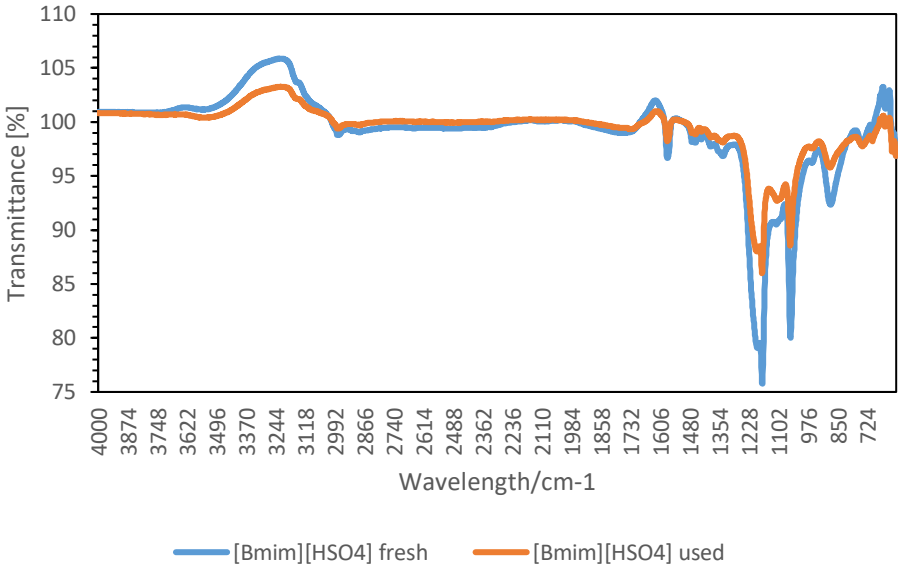

Figure 5. 16. FT-IR spectrum of fresh and used [Bmim][HSO_4] ionic liquids

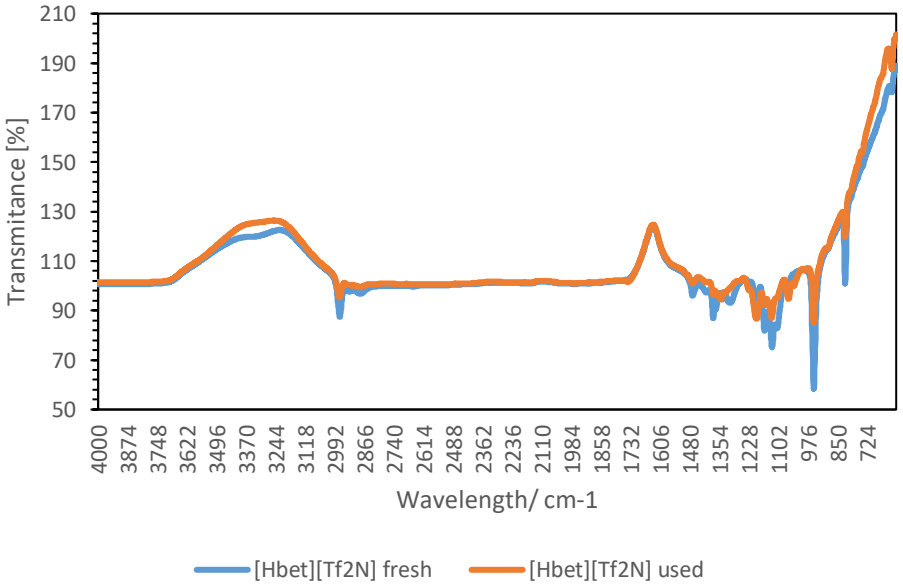

Figure 5. 17. FT-IR spectrum of fresh and used thermomorphic ionic liquid ([Hbet][Tf_2N])

To further ascertain the recyclability of the ILs, mass spectral analysis of fresh and recycled ILs ([Bmim][HSO_4], [Hbet][Tf_2N] and [Bmim][TSFI]) was also done. (Figures 5.18, 5.19 and 5.20). It is evident from the mass spectra that the fresh and recycled ILs largely show similar peaks further confirming that the recycled ILs did not lose their structural integrity after the microalgae lysis at 65 ℃ for 18 hours.

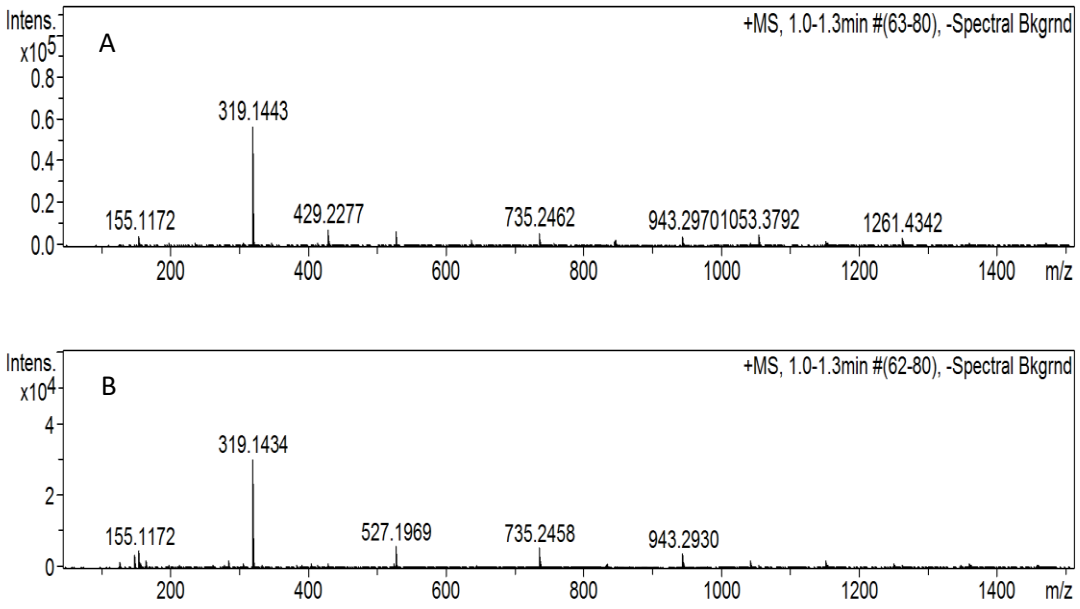

Figure 5. 18. Mass spectrum for [Bmim][HSO_4]: A and B correspond to fresh IL and used IL after microalgae extraction respectively.

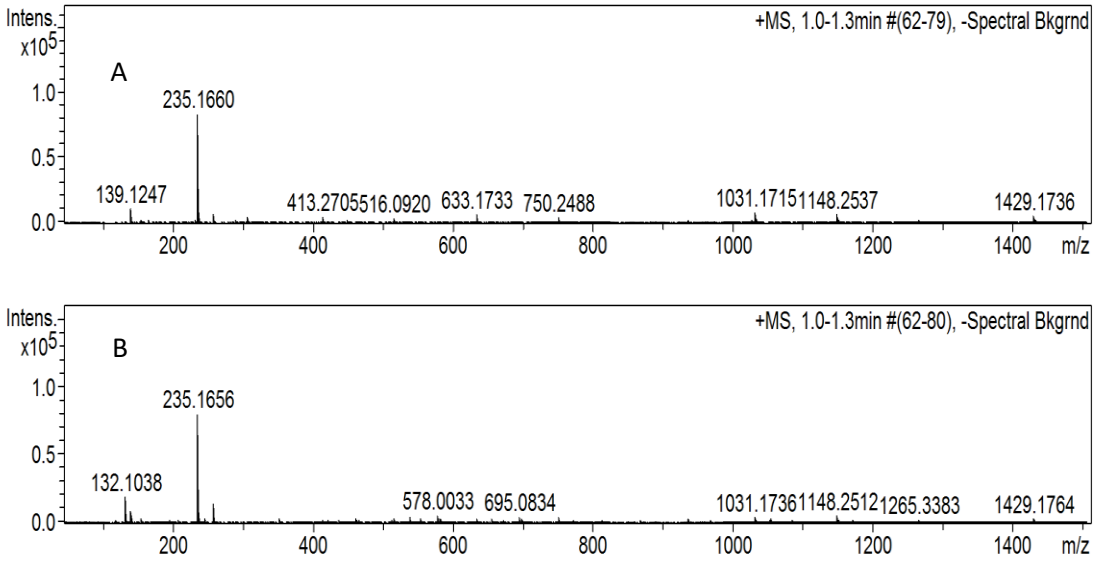

Figure 5. 19. Mass spectrum of [Hbet][Tf_2N] ionic liquids: A and B correspond to fresh and used IL after microalgae extraction respectively.

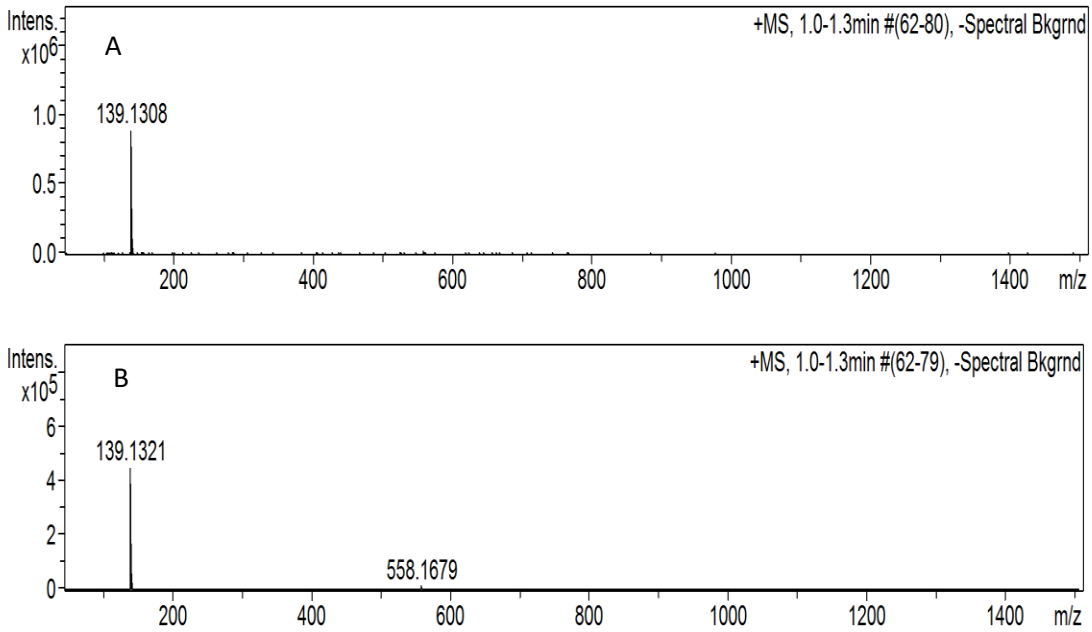

Figure 5. 20. Mass spectrum for [Bmim][TSFI]: A and B correspond to pure IL and used IL after treatment of *S. obliquus*/*Monoraphidium spp* respectively.

The recycled ILs were reused for microalgae treatment and their lysis efficiency was compared with that for fresh ILs. It is evident from Figure 5.21 that the extraction efficiency from recycled ILs was comparable to that of fresh ILs. This further confirms that ILs can be successfully recycled for further microalgae cell lysis and lipid extraction using hexane. In addition, it demonstrates the great potential of the IL cell lysis process that results in release of the microalgae lipids and the recycling of ILs. Recycling of ILs has also been demonstrated by Olkiewicz et al., (2015) where a phosphonium chloride IL was recycled up to four times (Olkiewicz et al., 2015). Since most ILs are expensive, recycling them can potentially result in a cost effective and sustainable processing of microalgae for production of biofuel and essential compounds.

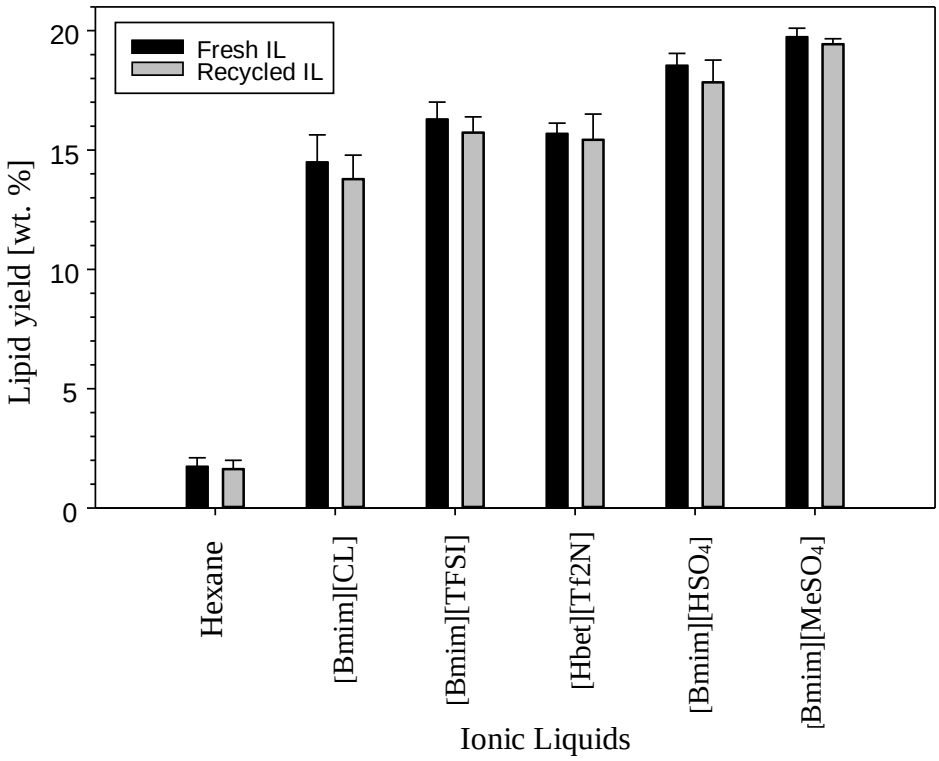

Figure 5. 21. Lipid yield of fresh and recycled ILs after lysis of microalgae at 65 °C for 18 hours, hexane was used to extract lipids from the microalgae/IL mixture in 2 hours.

5.4.7. Parameter evaluation of lysis conditions

To evaluate the yield of extracted lipids using ILs lysis, the treatment conditions such as lysis time, ratio of IL to microalgae, water content of microalgae and IL, lysis temperature and sonication time were evaluated. The IL used was [Bmim][$MeSO_4$] since it showed better cell lysis than other ILs. The microalgae used were a mixed of *S. obliquus/ Monoraphidium spp* and Spirulina.

5.4.7.1. Effect of lysis time on lipid yield

The lysis time was varied from 2 to 24 hours while the other conditions *e.g.* temperature and stirring speed was kept constant at 65 °C and 200 rpm respectively. From Figure 5.22 it is evident that two hours of lysis were not enough for effective cell disruption and

subsequent lipid extraction and a steady increase in lipid yield and extraction efficiency was observed. The low lipid yield at lower lysis time was possibly due to incomplete cell disruption while the high lipid yield at high lysis time was potentially due to more complete cell disruption. As explained earlier, the extent of cell disruption caused by IL lysis of microalgae is directly proportional to the extraction efficiency of microalgae lipids. Therefore, the longer the lysis time the greater the cell lysis and hence the higher the extraction efficiency leading to increase in lipid yield with time. A number of reports in literature use lysis time between 16-24 hours (Young et al., 2010; Olkiewicz et al., 2015; Orr et al., 2015; Shankar et al., 2017) while others use shorter times of up to 2 to 3 hours with sonication in some cases (Kim et al., 2013; Sun-A Choi et al., 2014).

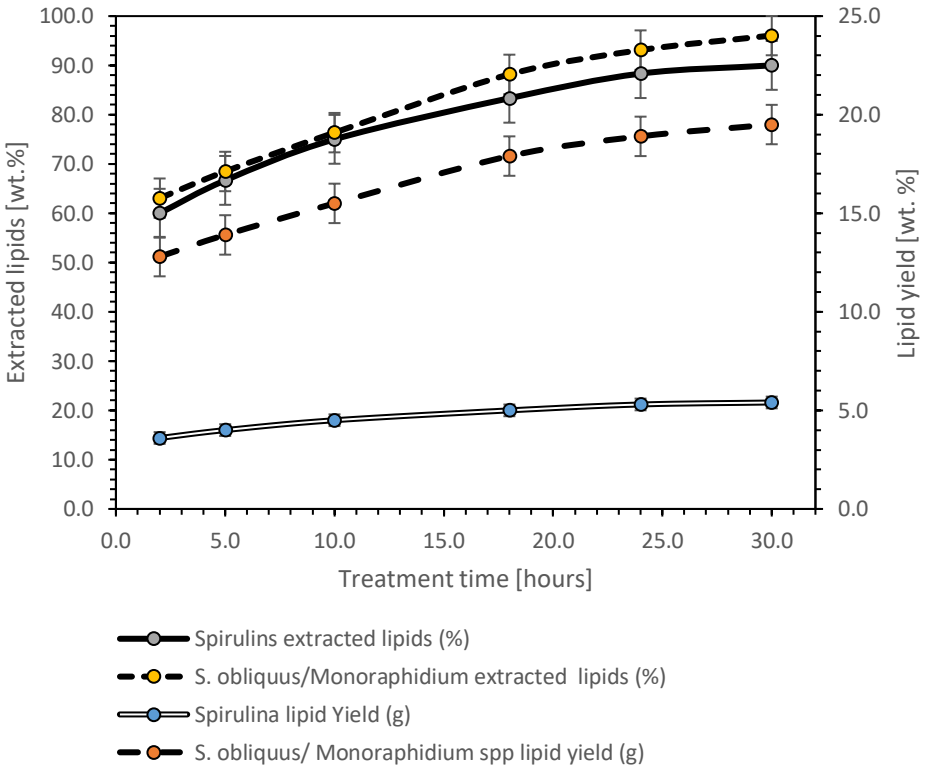

Figure 5. 22. Effect of IL treatment time on the yield of bio-oils from spirulina, after treatment of spirulina biomass at different times with the IL (methyl imidazolium sulphate and methyl imidazolium hydrogen sulphate water content 20 wt. %) at ambient temperature. The bio-oil was then extracted from IL/microalgae mixture using hexane for 2 h under mild mixing.

In some studies using [C2mim][EtSO4] ionic liquid, it was reported that treatment time between 2 to 17 hours did not have significant effect on the extraction efficiency of microalgae lipids (Orr et al., 2015). This shows that the optimum treatment time depends on the type of IL used. It is worth noting that the lysis time could be optimised when sonication was applied alongside IL treatment. The lysis time was reduced from 18 hours to only 2 hours with a considerably high lipid yield as illustrated in Figure 5. 27.

5.4.7.2. Effect of water content on lipid yield

To optimise the effect of water content of the system (microalgae, water, ILs) on lipid yield, the water mass fraction varied between 0 and 0.5. Two microalgae samples were used (*S. obliquus/ Monoraphidium spp* and Spirulina) and both gave similar trends of lipid yield and extraction efficiency as revealed in Figures 5.23 and 5.24. There was a gradual increase in lipid yield and extraction efficiency with increase in mass fraction of water in the system up to an optimum level (0.2 to 0.27). Then further increase in mass fraction of water led to a gradual reduction in lipid yield and extraction (Figure 5.16 and 5.17). The highest yield and extraction efficiency (98.5 wt. % and 20.0 wt. % respectively) from *S. obliquus/ Monoraphidium spp* were achieved at a microalgae water content of 0.27 g/g.

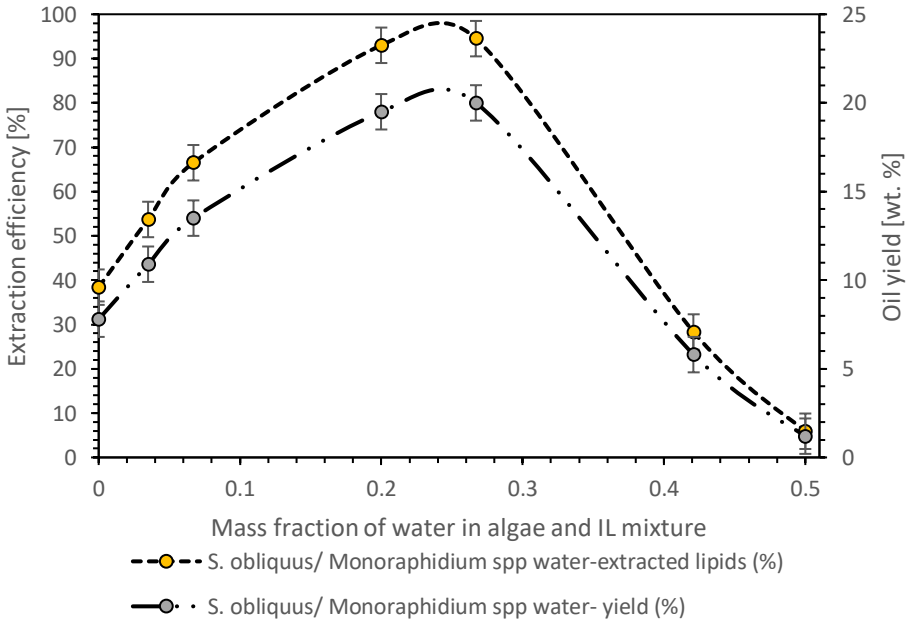

Figure 5. 23. Effect of water content on yield and extraction efficiency of lipids from *S. obliquus/ Monoraphidium spp*. Extraction time was 2 hours using hexane and IL ([Bmim] [$MeSO_4$]) treatment time was 18 h at room temperature.

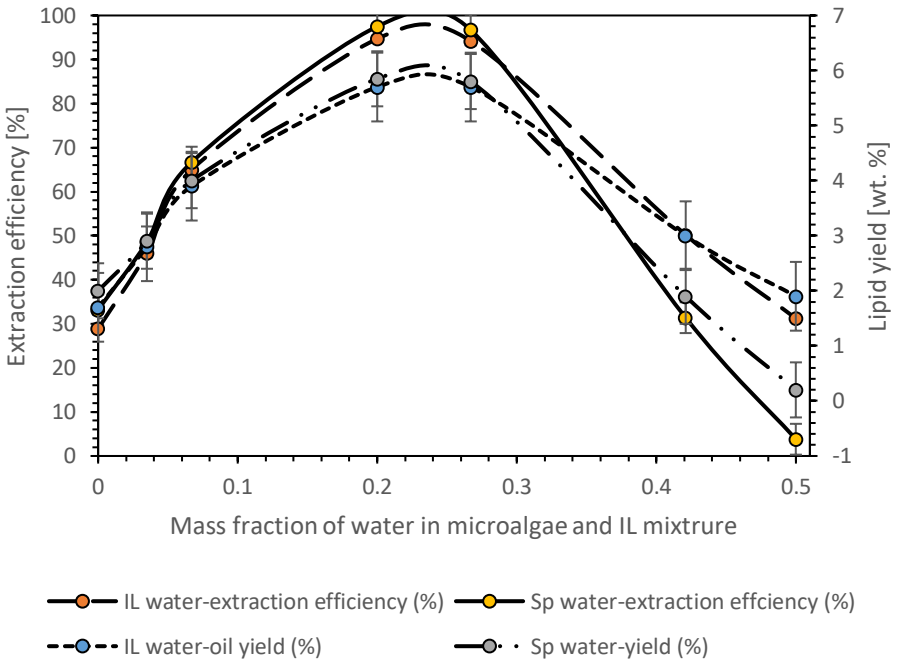

Figure 5. 24. Effect of water content on yield and extraction efficiency of lipids from Spirulina. Extraction time was 2 h using hexane and IL [Bmim][$MeSO_4$]) treatment time was 18 hrs at room temperature.

A maximum lipid yield and extraction efficiency was achieved at a microalgae water content between 0.2 and 0.27 g/g (Figures 5.23 and 5.24). For Spirulina, the highest extraction efficiency (97.5 wt. %) was observed at a water/system mass fraction of 0.2 g/g (68.8 wt. %), which was so close to the extraction efficiency of 96.7 wt. % at a mass fraction of 0.267 g/g (74.6 wt. %). Dry microalgae gave lower lipid yields and extraction efficiency in both cases while the highest mass fraction of water/system (0.5) gave the lowest lipid yield and extraction efficiency (Figure 5.23 and 5.24). (Orr et al., 2015) reported the highest lipid recovery at a microalgae water content of 75 wt. % using [C2mim] [EtSO4] ionic liquid to extract lipids from *Chlorella vulgaris*. They also observed a decreasing trend in extraction efficiency with increasing microalgae water content.

5.4.7.3. Effect of ratio of IL/microalgae on lipid yield

The effect of amount of ILs used on the yield of extracted lipids was determined by comparing the yield of extracted lipids at different mass ratio of IL to microalgae (0, 0.5, 10, 15 and 20). There was a steady increase in lipid yield and extraction efficiency with increasing ratio of IL to microalgae up to a peak level where the highest extraction efficiency for *S. obliquus* was 97 wt% and lipid yield was 19.7 wt.% at mass fraction of IL to microalgae of 13-15 (Figure 5.25). Beyond this mass fraction, there was a decreasing trend of lipid yield and extraction efficiency with further increase in mass fraction of IL to microalgae (Figure 5.25). The same trend in yield and extraction efficiency was observed with Spirulina.

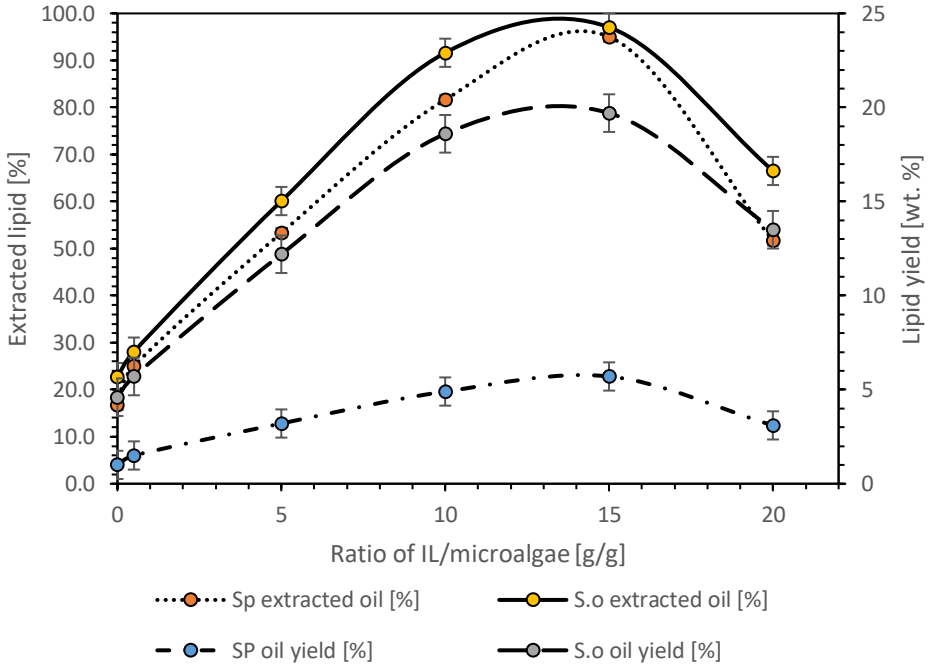

Figure 5. 25. Effect of ratio of IL ([Bmim][MeSO4]) /microalgae on yield of extracted bio lipids at ambient temperature and 18 h of extraction. The control was water/IL.

A similar trend was observed in literature for *Chlorella vulgaris* using [C2mim] [EtSO4] IL with methanol as a co-solvent. But in this case the highest lipid yield was reported at a mass ratio of IL to microalgae of 10:1 and any further increase in mass ratio led to reduction in lipid yield (Orr et al., 2015). The slight difference in ratios could be due to

use of different ILs, for example they used [C2mim] [EtSO4] with methanol. The synergetic effect of methanol in extraction of polar lipids could have resulted in reduction in the amount of IL needed to reach the optimum yield. In addition, the different microalgae species used could have led to difference in results too since the cell walls of some microalgae are more resistant to cell lysis than others. The lowest lipid yield and extraction efficiency was observed in the control experiment where water was used instead of IL. This confirms that ILs play an important role in cell lysis and the right ratio of IL to microalgae is needed to optimize the lipid yield and extraction efficiency.

5.4.7.4. Effect of temperature on lipid yield

The effect of temperature on lipid yield from *S. obliquus/Monoraphidium spp* was determined using [Bmim][Cl] and [Bmim][$MeSO_4$] ionic liquids at three different temperatures (25 ℃, 65 ℃ and 100 ℃). [Bmim][Cl] exhibited low lipid yield at ambient temperature and higher lipid yields at higher temperature (Figure 5.26). The increase in lipid yield with temperature for [Bmim][Cl] could have arisen from the reduction in viscosity of the IL at higher temperature. This led to better distribution of the microalgae in the IL resulting in increased cell lysis and extraction of lipids.

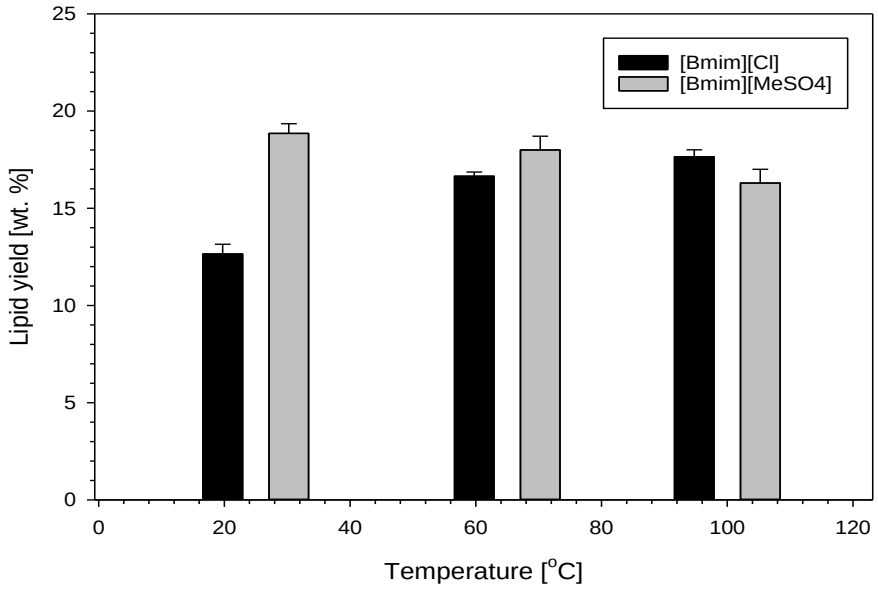

Figure 5. 26. Effect of treatment temperature of IL/ on yield of *S. obliquus/Monoraphidium spp* extracted lipids using [Bmim][Cl] and [Bmim][MeSO4] for treatment time of 18 hours and extraction time of 2 hours using hexane.

On the other hand, [Bmim][$MeSO_4$] a room temperature IL, exhibited a high lipid yield at ambient temperature (25 ℃) and an increase in temperature to 100 ℃ led to a slight reduction in lipid yield (Figure 5.26). The reduction in lipid yield with temperature is potentially due to the reduction in the Hildebrand's solubility parameter which has been reported to decrease with increase in temperature for several ILs (Weerachanchai et al., 2012). The decrease in Hildebrand's solubility parameters with increasing temperature indicates that there was a reduction in the strength of molecular interactions between the ILs and the interacting microalgae cells (Swiderski et al., 2004). This reduced interaction potentially results in reduced cell disruption/lysis of microalgae cells by the IL resulting in reduced lipid extraction efficiency and yield. Increase in temperature has also been reported to decrease the cohesive energy density of ILs (Weerachanchai et al., 2012). The other possibility is that the high lipid yield at ambient temperature for [Bmim][$MeSO_4$] ionic liquid could be due to its low viscosity at ambient temperature facilitating a better distribution of microalgae cells within the IL resulting in better cell lysis and extraction efficiency of lipids. Some studies have used [Bmim][$MeSO_4$] for room temperature extraction of lipids from *Chlorella vulgaris* giving substantially high lipid yields (Kim et al., 2013).

5.4.7.5. Effect of sonication on lipid yield

The effect of sonication of microalgae/water/ILs system on lipid yield in hexane extraction of *S. obliquus/ Monoraphidium spp* using [Bmim][Cl], [Bmim][HSO_4] and [Bmim][$MeSO_4$] was also investigated (Figure 5.27). Sonication enhanced the lipid yield for all ILs used. Lysis time was only 2 hours.

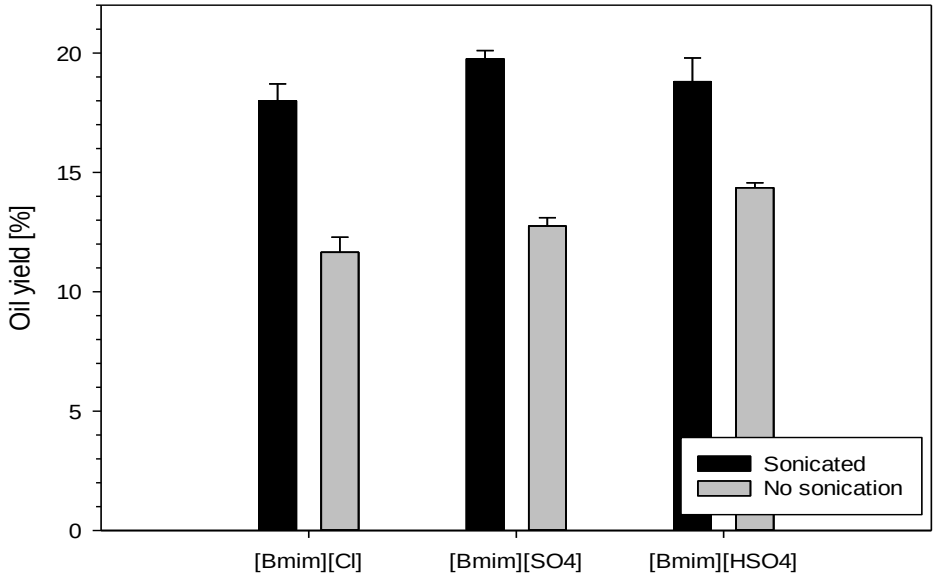

Figure 5. 27. Percentage yield of lipids extracted using different ionic liquids with hexane/methanol from magnetically separated *of S. obliquus/ Monoraphidium spp* at 65 °C for 2 hours under sonication and in absence of sonication.

The highest yield was registered while using [Bmim][MeSO4] followed by [Bmim][HSO_4] and the lowest yield was observed when [Bmim][Cl] was used. It is interesting to note that IL extraction under sonication conditions can result in high lipid yields at substantially lower lysis time of only 2 hours compared to the standard lysis time of 18h.

5.5. Conclusions

In this work, magnetic nanoparticles (MNPs) were used to separate microalgae from culture medium at a separation efficiency of 99%. The separated microalgae/MNPs slurry with a water content of 74.5% was mixed with ILs to liberate lipids from microalgae cells (lysis). After wet lipid extraction, the MNPs were magnetically separated from IL/microalgae biomass, dispersed in DI water, and sonicated. The recovered MNPs were then recycled to separate more microalgae from aqueous phase at a separation efficiency of 95 wt. %. The ILs were also successfully recycled after precipitating remaining biomass with methanol, filtering and evaporating the methanol and any dissolved water. The

percentage cell lysis (disruption), hexane extraction efficiency and lipid yield using different ILs was compared. [Bmim][$MeSO_4$] had the highest cell lysis and extraction efficiency (98% and 99% respectively). It also extracted a larger percentage of lipids at room temperature (97.8 wt.%). The extracted lipids using different ILs were transesterified to fatty acid methyl esters and their fatty acid profile was analysed using GC-MS. The fatty acid profile of biodiesel was like that obtained by conventional solvent extraction techniques. Hexadecanoic acid (C16:0) was the most dominant fatty acid in the lipids extracted from both Spirulina and of *S. obliquus/ Monoraphidium spp*. Other analytical techniques such as ^{1}H NMR, FT-IR, TGA and mass spectrometry were also used to analyse extracted lipids, fresh and recycled MNPs, fresh and recycled IL and microalgae biomass. The effect of treatment conditions like IL treatment time, water content, ratio of IL to microalgae treatment temperature and sonication time were also optimised.

Therefore, it was demonstrated for the first time the wet extraction of lipids from magnetically separated microalgae and recycling of both MNPs and IL for further microalgae separation and wet lipid extraction respectively. The combination of the two processes coupled with the recycling of MNPs and ILs could potentially result in an efficient processing of biofuels from microalgae resulting in a truly sustainable processing of biofuels and high value compounds. This could result in the lowering of the processing cost of microalgae for production of biofuels and high value compounds. Potentially culminating in biofuels being more competitive with petroleum-derived fuels.

5.6. Supporting Information

Efficient extraction of lipids from magnetically separated microalgae using ionic liquids

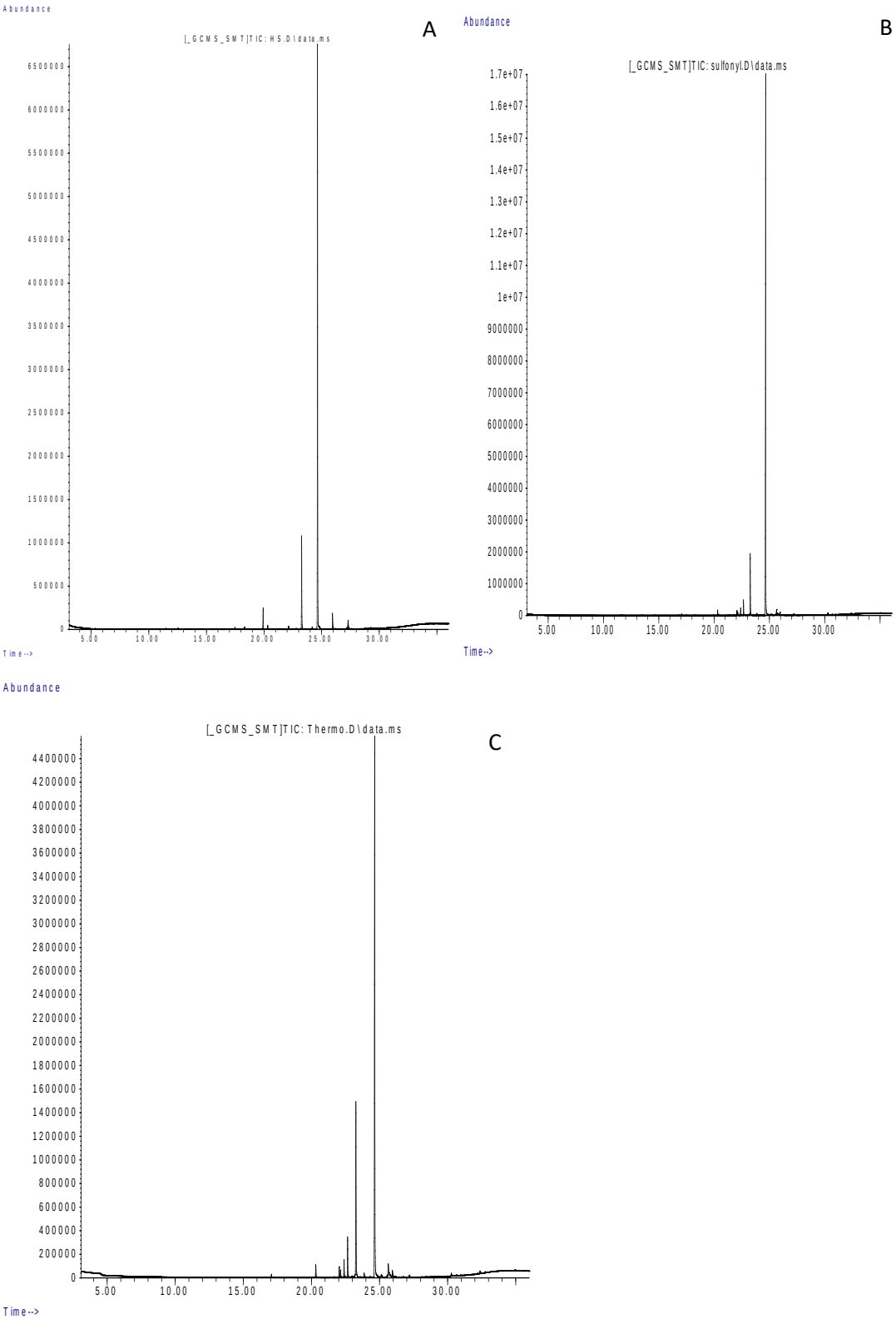

Figure S. 1. GCMS Chromatogram of FAME from transesterified lipids extracted from *S. obliquus*/*Monoraphidium spp* using different ILs: A) [Bmim][HSO_4], B) [Bmim][TFSI], C) [Hbet][Tf_2N].

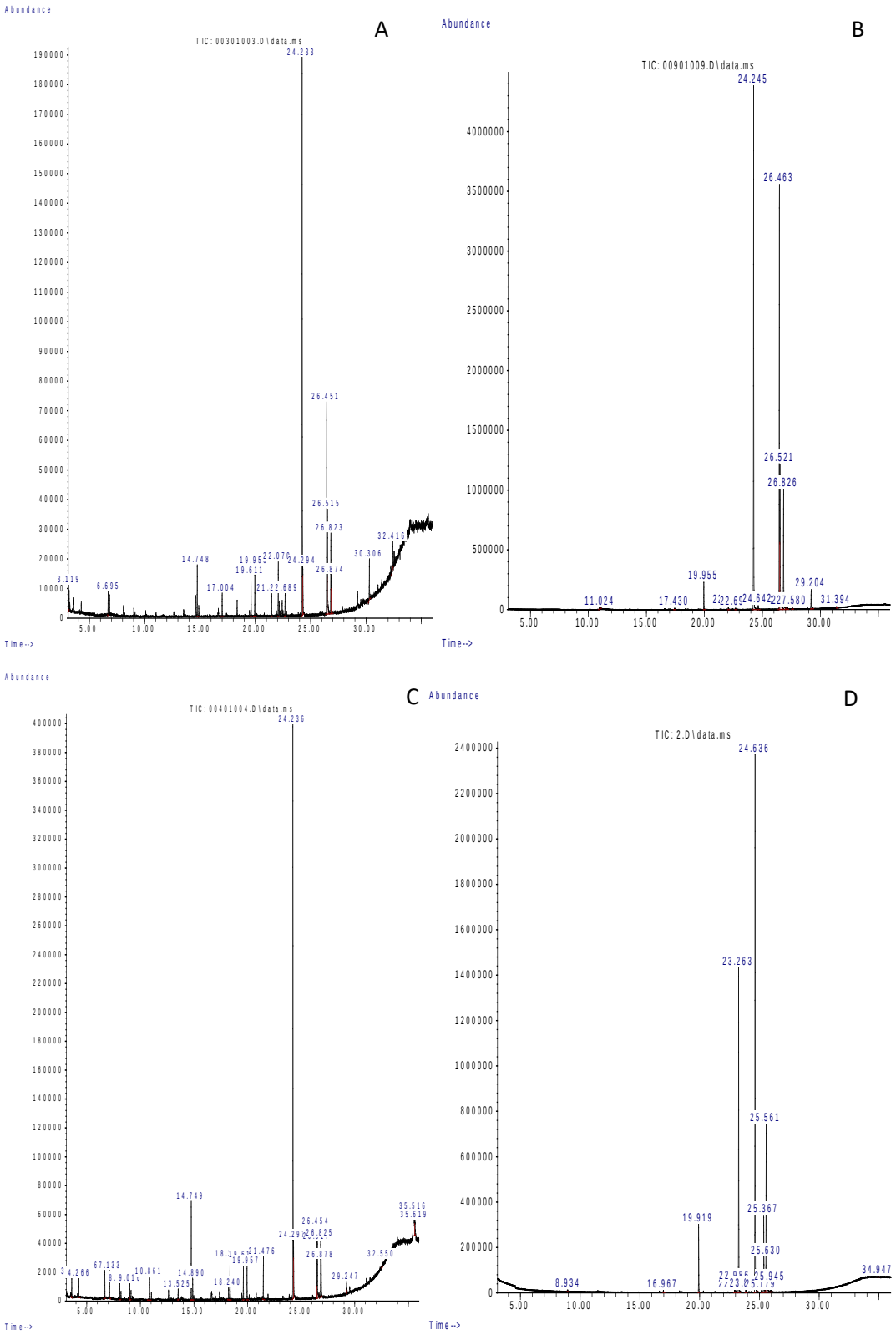

Figure S. 2. GCMS Chromatogram of FAME from transesterified lipids extracted from Spirulina using different ILs: A) [Bmim][Cl], B) [Bmim][$MeSO_4$], and C) [Hbet][Tf_2N] and D) [Bmim][TFSI].

6. Conclusions and future work

In this chapter, the summary, conclusions and proposed future work are presented.

6.1. Conclusions

In conclusion, the multifunctional application of MNPs for efficient microalgae separation and for catalytic hydrothermal liquefaction was demonstrated for the first time. MNPs were synthesised and used for magnetic separation of microalgae from culture medium at an optimised separation efficiency of 99%. The MNPs played a catalytic role by increasing the yield of bio-crude oil and reducing the N, O and S content. The MNPs were also recycled successfully to harvest more algae and to catalyse the HTL process. In addition, magnetically separated microalgae were also subjected to IL treatment for the first time to extract lipids. The MNPs and ILs were recycled for further microalgae separation and IL treatment respectively. The main findings from this work were as follows:

1. The characterization results confirmed that magnetite as well as different ferrite NPs were successfully synthesised. XRD results confirmed that the magnetite peaks correspond to the standard peaks. HR-TEM results revealed the hexagonal structure of MNPs with a size distribution ranging between 10-12 nm for the bare MNPs and 14-18 nm for the doped MNPs (ferrites). Elemental mapping revealed a uniform distribution of metal dopants on the surface of magnetite nanoparticles for all MNPs. UV-vis absorbance at 300 nm corresponded to the absorbance peak for MNPs.

2. Increasing the separation time from 2 minutes to 8 minutes led to an increase in the separation efficiency by 3%. While increasing the mass ratio of MNPs to microalgae from 0.5 to 1.0 led to an increase in the separation efficiency by 5% at pH 9.

3. HTL under Zn and Mg ferrites led to the highest increase in biocrude yield by 13.9 wt.%. According to GC-MS results, the percentage area of hydrocarbons and heptadecane increased by 26.6 and 27.8 wt.% respectively under Zn ferrite catalysed liquefaction. ^{1}H NMR analysis revealed that HTL in presence of Zn and Mg ferrites resulted in an increase of alkanes by 16 wt. %. Elemental analysis results revealed that HTL under MNPs resulted in an increase in the carbon content of biocrude oil by 1.1 wt.% and a reduction in the nitrogen, oxygen and sulphur content by 27.2, 21.1 and 75 wt. % respectively.

4. Recycled MNPs were still effective in microalgae separation resulting in a separation efficiency of 96.1 wt.% compared to 98.5 wt.% for the fresh ones. The biocrude yield increased by 7.0 and 8.7 wt.% for the recycled and fresh MNPs respectively.

5. There was a gradual increase in biocrude yield with holding time, the highest yield was 36.2 wt.% after 60 minutes. Further increase in holding time resulted in a reduction in biocrude yield to 18 wt.% after 120 minutes. The solid residue yield reduced gradually with increase in holding time from 40 wt. % after 15 minutes to 18 wt.% after 120 minutes. Liquefaction under 5% sulphuric acid led to the highest reduction in nitrogen content of biocrude oil (83.9 wt. %) and the highest hydrogen content of biocrude oil (10.6 wt. %). The biocrude yield did not increase significantly under acidic conditions.

6. [Bmim][$MeSO_4$] exhibited the highest microalgae lysis efficiency (over 95%) and [Bmim][Cl] the lowest (about 70%). The IL lysis was also compared with other cell lysis techniques such as sonication and microwave. The highest lysis efficiency with sonication was 60.3% while microwave was 78.4%. [Bmim][$MeSO_4$] exhibited the highest lipid yield (19.8 wt. %) and extraction efficiency (98.3%) while [Bmim][Cl] the lowest yield (15.4 wt. %) and extraction efficiency (72.7 wt. %). Hexadecanoic acids (C16:0) was the most abundant fatty acid (56 wt.%) in the fatty acid methyl esters from the extracted lipids. MNPs were still effective in microalgae separation after IL treatment. The SE of recycled MNPs was 96.6% compared to 98.6% for the fresh ones. Recycled ILs also exhibited an extraction efficiency comparable to the fresh ones. Extraction efficiency increased with IL treatment time. The highest extraction efficiency (97.5 wt.%) was achieved at a water content of 20 wt.%. The highest yield was observed at a ratio of IL to microalgae of 15. Lysis under sonication conditions led to an increase in the lipid yield by 8 wt. %.

6.2. Future work

This section discusses possible future work that can be done to extend or further improve work in this field.

6.2.1. Biosynthesis of MNPs and their application in microalgae separation

Synthesis of MNPs using biological methods such as use of plant extracts to reduce iron (III) and iron (II) chloride to MNPs can be explored as an economical, greener and environmentally friendly approach. This would further reduce the cost of manufacturing of MNPs and eventually the cost of biofuel processing. Bio-synthesised MNPs are also non-poisonous when applied to biological systems since they do not use toxic chemicals in their synthesis protocol. Plant extracts have been used to synthesise different kinds of nanoparticles such as silver and gold nanoparticles for different applications. More research needs to be done on the application of plant extracts to synthesis MNPs.

6.2.2. Wastewater treatment microalgae for biofuel production

In addition, to lower the cost of microalgae cultivation, it is essential to use microalgae from wastewater treatment streams for biofuel processing. This would cut the cost of nutrients since they use sewage waste as a nutrient source. The cost of pumping in air or CO_2 like in photo-bioreactors is also minimised since they use atmospheric air. The microalgae use is maximised since it will play two roles; to clean wastewater and to produce biofuels hence meeting two of the most challenging global issues namely: production of renewable and clean energy in form of biofuels and provision of clean and safe water.

6.2.3. Continuous magnetic separation and HTL

In this work, magnetic separation was done using batch experiments. Development of continuous magnetic separation processes can improve the processing volumes and reduce the amount of human labour invested in the batch operations. Continuous processes can easily be scaled up. The same applies to HTL processes; development of continuous HTL processes for microalgae may increase the feed volumes, improve biocrude yields and save time and human energy spent in the batch processes. The development of a process that combines continuous magnetic separation of microalgae and continuous HTL of the magnetically separated microalgae is one of the import future developments for this work. This would make the process more feasible for scaling up and commercialization. The other possibility is the development of a continuous magnetic separation process in

combination with continuous IL extraction of lipids from the magnetically separated microalgae. Continuous magnetic separation would be done as illustrated in Figure 6.1.

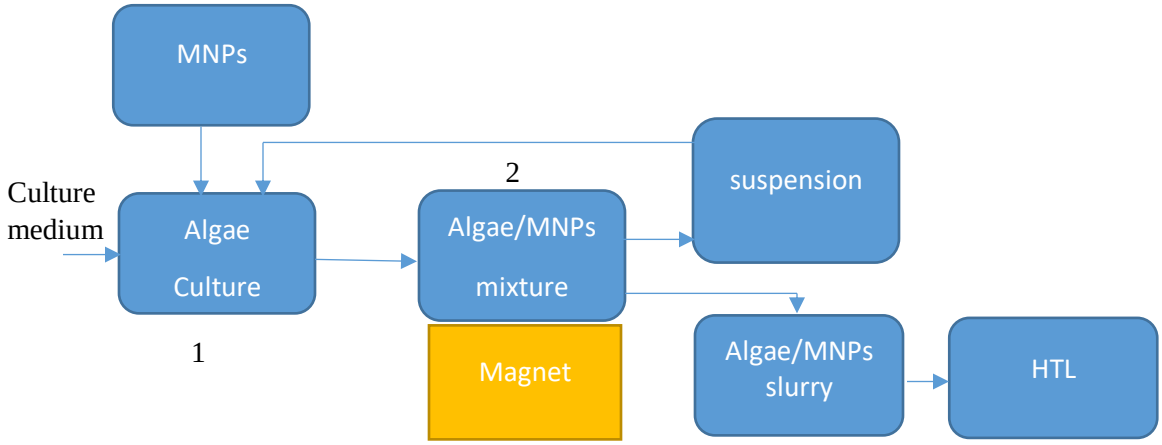

Figure 6. 1. Illustration of continuous magnetic separation of algae.

The culture medium is pumped into tank 1 where it is mechanically mixed with an appropriate amount of MNPs for a specified time for the MNPs to be adsorbed on the algae cells. Then, the algae/MNPs mixture is pumped to tank 2, where continuous magnetic separation takes place. Tank 2 has 2 outlets, one on top for the suspension (culture medium) and one at the bottom for the separated algae/particle slurry. The algae/particle slurry is pumped into the HTL reactor for catalytic HTL of separated algae to produce biocrude oil. The suspension is recycled for further algae cultivation since it contains nutrients.

6.2.4. Extraction of high value compounds alongside biofuel processing

The other potential area for future work is the extraction of high value products such as vitamins, proteins and carbohydrates alongside lipid extraction for biodiesel production and before HTL. Since biofuels are a low value product, extraction of high value compounds alongside biofuels can offset the high processing cost of biofuels and make them more competitive with petroleum-derived fuels. The extraction of high value products can be done in combination with HTL. In this case, the microalgae from which high value products were extracted is subjected to the HTL process to produce a biocrude

oil that can be refined to kerosene, diesel and gasoline. The extraction of proteins as a high value product prior to HTL reduces the nitrogen content of biocrude oil leading to improvement in the biocrude quality as well as benefitting from the protein product. The HTL process uses a wide variety of feedstock for biocrude production making it possible to use microalgae from which high value products are extracted.

6.2.5. Recycling of aqueous phase, gas phase and solid phase from HTL

The other potential area for future work is investigating the feasibility of recycling the gas phase from HTL of microalgae for microalgae cultivation. The gas phase from microalgae HTL is composed of over 98 wt.% CO_2 that is an essential carbon source for microalgae cultivation (S Raikova et al., 2016a). The future work would investigate the effect of this gas phase on microalgae growth comparing it with the usual CO_2 used. The other possibility is to investigate the recycling of the aqueous phase from HTL as a nutrient source for microalgae cultivation since it is rich in ammonia from the breakdown of proteins. It also contains other water-soluble nutrients (S Raikova et al., 2016a). The proposed work would investigate the effect of recycled aqueous phase on viability of microalgae in comparison to the typical culture medium. The other potential area is the possibility of using the solid residue from microalgae HTL as a fertilizer for crop production. Recycling the aqueous, gas and solid phase alongside biocrude oil production would potentially ensure an economical and sustainable processing of biofuels via the HTL route.

6.2.6. Improvement of biocrude quality

The biocrude produced in the HTL process contained a high nitrogen and oxygen content. The nitrogen compound was from the degradation of proteins that were present in high concentration in the Spirulina feedstock (63%). HTL under acidic conditions considerably reduced nitrogen content but further studies should be done on this since acid conditions may corrode reaction vessels. Further investigations in the denitrogenation and deoxygenation of the biocrude oil to make it suitable for use as a transportation fuel are needed. This can be done through development of HTL good catalysts or feed pre-treatment for example by first extracting protein before HTL to reduce the nitrogen content.

6.2.7. Magnetic heating of microalgae cells

It is known that radio frequency waves can heat superparamagnetic nanoparticles and cause them to disrupt cells. This technique can be applied to microalgae cells after magnetic separation to disrupt their cell walls and extract oils and high value compounds by dissolving them in appropriate solvents then evaporating solvents to retain the extracts. The MNPs can then be recycled for further microalgae separation and magnetic heating cell disruption.

References

Aaronson, S. and Dubinsky, Z., 1982. Mass production of microalgae. *Experientia*, 38(1), pp. 36-40.

Ab Rani, M., Brant, A., Crowhurst, L., Dolan, A., Lui, M., Hassan, N.H., Hallett, J., Hunt, P., Niedermeyer, H. and Perez-Arlandis, J., 2011. Understanding the polarity of ionic liquids. *Physical Chemistry Chemical Physics,* 13(37), pp. 16831-16840.

Adjaye, J.D., Sharma, R.K. and Bakhshi, N.N., 1992. Characterization and stability analysis of wood-derived bio-oil. *Fuel Processing Technology,* 31(3), pp. 241-256.

Akia, M., Yazdani, F., Motaee, E., Han, D. and Arandiyan, H., 2014. A review on conversion of biomass to biofuel by nanocatalysts. *Biofuel Research Journal,* 1(1), pp. 16-25.

Al Hattab, M., Ghaly, A. and Hammoud, A., 2015. Microalgae harvesting methods for industrial production of biodiesel: critical review and comparative analysis. *J Fundam Renew Energy Appl,* 5, p. 1000154.

Alamu, O., Waheed, M., Jekayinfa, S. and Akintola, T., 2007. Optimal transesterification duration for biodiesel production from Nigerian palm kernel oil. *Agricultural Engineering International: CIGR Journal*.

Ali, Y., Hanna, M.A. and Cuppett, S.L., 1995. Fuel properties of tallow and soybean oil esters. *Journal of the American Oil Chemists' Society,* 72(12), pp. 1557-1564.

Allnutt, F.T. and Kessler, B.A., 2015. Harvesting and downstream processing—and their economics. *Biomass and Biofuels from Microalgae.* Springer, pp. 289-310.

Amaro, H.M., Guedes, A.C. and Malcata, F.X., 2011. Advances and perspectives in using microalgae to produce biodiesel. *Applied energy,* 88(10), pp. 3402-3410.

Anastasakis, K. and Ross, A., 2011. Hydrothermal liquefaction of the brown macro-alga Laminaria saccharina: effect of reaction conditions on product distribution and composition. *Bioresource technology,* 102(7), pp. 4876-4883.

Aqua, V., 2019/01/19. Manifold photobioreactor.

Bach, Q.-V., Chen, W.-H., Lin, S.-C., Sheen, H.-K. and Chang, J.-S., 2017. Wet torrefaction of microalga Chlorella vulgaris ESP-31 with microwave-assisted heating. *Energy Conversion and Management,* 141, pp. 163-170.

Balasubramanian, R.K., Doan, T.T.Y. and Obbard, J.P., 2013. Factors affecting cellular lipid extraction from marine microalgae. *Chemical Engineering Journal,* 215, pp. 929-936.

Barreiro, D.L., Prins, W., Ronsse, F. and Brilman, W., 2013. Hydrothermal liquefaction (HTL) of microalgae for biofuel production: state of the art review and future prospects. *Biomass and Bioenergy,* 53, pp. 113-127.

Barreiro, D.L., Samorì, C., Terranella, G., Hornung, U., Kruse, A. and Prins, W., 2014. Assessing microalgae biorefinery routes for the production of biofuels via hydrothermal liquefaction. *Bioresource technology,* 174, pp. 256-265.

Barros, A.I., Gonçalves, A.L., Simões, M. and Pires, J.C., 2015. Harvesting techniques applied to microalgae: A review. *Renewable and Sustainable Energy Reviews,* 41, pp. 1489-1500.

Beer, L.L., Boyd, E.S., Peters, J.W. and Posewitz, M.C., 2009. Engineering algae for biohydrogen and biofuel production. *Current opinion in biotechnology,* 20(3), pp. 264-271.

Benemann, J. and Oswald, W., 1996. Systems and economic analysis of microalgae ponds for conversion of carbon dioxide to biomass (Final Report: Grant No. DEFG22 93PC93204). *Final report, Office of Scientific & Technical Information Technical Reports*.

Biller, P., Riley, R. and Ross, A., 2011. Catalytic hydrothermal processing of microalgae: decomposition and upgrading of lipids. *Bioresource technology*, 102(7), pp. 4841-4848.

Biller, P. and Ross, A., 2011. Potential yields and properties of oil from the hydrothermal liquefaction of microalgae with different biochemical content. *Bioresource technology,* 102(1), pp. 215-225.

Biofuelwatch, 2017/05. Biofuelwatch Responds to First Open Pond Testing of GMO algae. *Synbiowatch*.

Bitton, G., Fox, J. and Strickland, H., 1975. Removal of algae from Florida lakes by magnetic filtration. *Applied microbiology,* 30(6), pp. 905-908.

Bligh, E.G. and Dyer, W.J., 1959. A rapid method of total lipid extraction and purification. *Canadian journal of biochemistry and physiology*, 37(8), pp. 911-917.

Borowitzka, M., 1996. Closed algal photobioreactors: design considerations for large-scale systems. *Journal of Marine Biotechnology*, 4(4), pp. 185-191.
Borowitzka, M.A., 1999. Commercial production of microalgae: ponds, tanks, and fermenters. *Progress in industrial microbiology*. Elsevier, pp. 313-321.
Bos, R., Van der Mei, H.C. and Busscher, H.J., 1999. Physico-chemistry of initial microbial adhesive interactions–its mechanisms and methods for study. *FEMS microbiology reviews*, 23(2), pp. 179-230.
Brennan, L. and Owende, P., 2010. Biofuels from microalgae—a review of technologies for production, processing, and extractions of biofuels and co-products. *Renewable and sustainable energy reviews*, 14(2), pp. 557-577.
Brown, T.M., Duan, P. and Savage, P.E., 2010. Hydrothermal liquefaction and gasification of Nannochloropsis sp. *Energy & Fuels*, 24(6), pp. 3639-3646.
Bühler, W., Dinjus, E., Ederer, H., Kruse, A. and Mas, C., 2002. Ionic reactions and pyrolysis of glycerol as competing reaction pathways in near-and supercritical water. *The Journal of supercritical fluids*, 22(1), pp. 37-53.
Caporgno, M., Olkiewicz, M., Fortuny, A., Stüber, F., Fabregat, A., Font, J., Pruvost, J., Lepine, O., Legrand, J. and Bengoa, C., 2016a. Evaluation of different strategies to produce biofuels from Nannochloropsis oculata and Chlorella vulgaris. *Fuel Processing Technology*, 144, pp. 132-138.
Caporgno, M.P., Olkiewicz, M., Fortuny, A., Stüber, F., Fabregat, A., Font, J., Pruvost, J., Lepine, O., Legrand, J. and Bengoa, C., 2016b. Evaluation of different strategies to produce biofuels from Nannochloropsis oculata and Chlorella vulgaris. *Fuel Processing Technology*, 144, pp. 132-138.
Carvalho, A.P., Meireles, L.A. and Malcata, F.X., 2006. Microalgal reactors: a review of enclosed system designs and performances. *Biotechnology progress*, 22(6), pp. 1490-1506.
Center, I., 2006. Feasibility report, small scale biodiesel production. *Waste Management and Research Center*.
Cerff, M., Morweiser, M., Dillschneider, R., Michel, A., Menzel, K. and Posten, C., 2012. Harvesting fresh water and marine algae by magnetic separation: screening of

separation parameters and high gradient magnetic filtration. *Bioresource technology*, 118, pp. 289-295.

Chen, C.-Y., Yeh, K.-L., Aisyah, R., Lee, D.-J. and Chang, J.-S., 2011. Cultivation, photobioreactor design and harvesting of microalgae for biodiesel production: a critical review. *Bioresource technology,* 102(1), pp. 71-81.

Chen, F., Liu, Z., Li, D., Liu, C., Zheng, P. and Chen, S., 2012. Using ammonia for algae harvesting and as nutrient in subsequent cultures. *Bioresource technology,* 121, pp. 298-303.

Chen, Y., Zhao, N., Wu, Y., Wu, K., Wu, X., Liu, J. and Yang, M., 2016. Distributions of organic compounds to the products from hydrothermal liquefaction of microalgae. *Environmental Progress & Sustainable Energy*.

Chisti, Y., 2008. Biodiesel from microalgae beats bioethanol. *Trends in biotechnology,* 26(3), pp. 126-131.

Choi, H.-J., 2015. Optimization for Microalgae Harvesting Using Mg-Sericite Flocculant. *Journal of Korean Society on Water Environment,* 31(3), pp. 328-333.

Choi, S.-A., Oh, Y.-K., Jeong, M.-J., Kim, S.W., Lee, J.-S. and Park, J.-Y., 2014. Effects of ionic liquid mixtures on lipid extraction from Chlorella vulgaris. *Renewable Energy,* 65, pp. 169-174.

Choi, S., Lee, J., Kwon, D. and Cho, K., 2006. Settling characteristics of problem algae in the water treatment process. *Water Science and Technology,* 53(7), pp. 113-119.

Christensen, P.S., Peng, G.l., Vogel, F.d.r. and Iversen, B.B., 2014. Hydrothermal liquefaction of the microalgae Phaeodactylum tricornutum: impact of reaction conditions on product and elemental distribution. *Energy & Fuels,* 28(9), pp. 5792-5803.

Christenson, L. and Sims, R., 2011. Production and harvesting of microalgae for wastewater treatment, biofuels, and bioproducts. *Biotechnology advances,* 29(6), pp. 686-702.

Christie, W.W., 1973. *Lipid analysis.* Pergamon press Oxford.

CO2-earth, 2019. https://www.co2.earth/annual-ghg-index-aggi. Annual GHG Index (AGGI).

Cohen, E. and Arad, S.M., 1989. A closed system for outdoor cultivation of Porphyridium. *Biomass,* 18(1), pp. 59-67.

Costa, J.A.V. and De Morais, M.G., 2011. The role of biochemical engineering in the production of biofuels from microalgae. *Bioresource technology,* 102(1), pp. 2-9.
Dadyburjor, D.B., Stewart, W., Stiller, A., Stinespring, C., Wann, J.-P. and Zondlo, J., 1994. Disproportionated ferric sulfide catalysts for coal liquefaction: Iron-based catalysts for coal liquefaction. *Energy & fuels,* 8(1), pp. 19-24.
Danquah, M.K., Ang, L., Uduman, N., Moheimani, N. and Forde, G.M., 2009. Dewatering of microalgal culture for biodiesel production: exploring polymer flocculation and tangential flow filtration. *Journal of Chemical Technology & Biotechnology: International Research in Process, Environmental & Clean Technology,* 84(7), pp. 1078-1083.
Demirbas, A., 2009. Progress and recent trends in biodiesel fuels. *Energy conversion and management,* 50(1), pp. 14-34.
Demirbaş, A., 2000. Mechanisms of liquefaction and pyrolysis reactions of biomass. *Energy conversion and management,* 41(6), pp. 633-646.
Dote, Y., Sawayama, S., Inoue, S., Minowa, T. and Yokoyama, S.-y., 1994. Recovery of liquid fuel from hydrocarbon-rich microalgae by thermochemical liquefaction. *Fuel,* 73(12), pp. 1855-1857.
Duan, P. and Savage, P.E., 2010. Hydrothermal liquefaction of a microalga with heterogeneous catalysts. *Industrial & Engineering Chemistry Research,* 50(1), pp. 52-61.
Duan, P. and Savage, P.E., 2011. Catalytic hydrotreatment of crude algal bio-oil in supercritical water. *Applied Catalysis B: Environmental,* 104(1-2), pp. 136-143.
Duvekot, C., 03/05/2019. Determination of total FAME and linoleic acid methyl esters in biodiesel according to EN-14103.
Earle, M.J., Esperança, J.M., Gilea, M.A., Lopes, J.N.C., Rebelo, L.P., Magee, J.W., Seddon, K.R. and Widegren, J.A., 2006. The distillation and volatility of ionic liquids. *Nature,* 439(7078), p. 831.
Edenhofer, O., Pichs-Madruga, R., Sokona, Y., Seyboth, K., Matschoss, P., Kadner, S., Zwickel, T., Eickemeier, P., Hansen, G. and Schlömer, S., 2011. IPCC special report on renewable energy sources and climate change mitigation. *Prepared By Working Group*

III of the Intergovernmental Panel on Climate Change, Cambridge University Press, Cambridge, UK.

Eevera, T., Rajendran, K. and Saradha, S., 2009. Biodiesel production process optimization and characterization to assess the suitability of the product for varied environmental conditions. *Renewable Energy*, 34(3), pp. 762-765.

Egesa, D., Chuck, C.J. and Plucinski, P., 2017. Multifunctional role of magnetic nanoparticles in efficient microalgae separation and catalytic hydrothermal liquefaction. *ACS Sustainable Chemistry & Engineering*, 6(1), pp. 991-999.

Elliott, D.C., 2008. Catalytic hydrothermal gasification of biomass. *Biofuels, Bioproducts and Biorefining*, 2(3), pp. 254-265.

Elliott, D.C. and Sealock Jr, L.J., 1983. Aqueous catalyst systems for the water-gas shift reaction. 1. Comparative catalyst studies. *Industrial & engineering chemistry product research and development*, 22(3), pp. 426-431.

Faeth, J.L. and Savage, P.E., 2016. Effects of processing conditions on biocrude yields from fast hydrothermal liquefaction of microalgae. *Bioresource technology*, 206, pp. 290-293.

Fakhrullin, R.F., Shlykova, L.V., Zamaleeva, A.I., Nurgaliev, D.K., Osin, Y.N., García-Alonso, J. and Paunov, V.N., 2010. Interfacing living unicellular algae cells with biocompatible polyelectrolyte-stabilised magnetic nanoparticles. *Macromolecular bioscience*, 10(10), pp. 1257-1264.

Feris, L.A., Gallina, S.C.W., Rodrigues, R.T. and Rubio, J., 2000. Optimizing dissolved air flotation design system. *Brazilian Journal of Chemical Engineering*, 17(4-7), pp. 549-556.

Flottweg, 2019/01/18. Algae Harvesting and Oil Extraction Using the Separator and Sedicanter.

Freedman, B., Butterfield, R.O. and Pryde, E.H., 1986. Transesterification kinetics of soybean oil 1. *Journal of the American Oil Chemists' Society,* 63(10), pp. 1375-1380.

Freedman, B., Pryde, E. and Mounts, T., 1984. Variables affecting the yields of fatty esters from transesterified vegetable oils. *Journal of the American Oil Chemists Society*, 61(10), pp. 1638-1643.

Fujita, K., Kobayashi, D., Nakamura, N. and Ohno, H., 2013. Direct dissolution of wet and saliferous marine microalgae by polar ionic liquids without heating. *Enzyme and microbial technology,* 52(3), pp. 199-202.

Fukaya, Y., Hayashi, K., Wada, M. and Ohno, H., 2008. Cellulose dissolution with polar ionic liquids under mild conditions: required factors for anions. *Green Chemistry,* 10(1), pp. 44-46.

Garcia Alba, L., Torri, C., Samorì, C., van der Spek, J., Fabbri, D., Kersten, S.R. and Brilman, D.W., 2011. Hydrothermal treatment (HTT) of microalgae: evaluation of the process as conversion method in an algae biorefinery concept. *Energy & fuels,* 26(1), pp. 642-657.

Gong, M. and Bassi, A., 2016. Carotenoids from microalgae: a review of recent developments. *Biotechnology Advances,* 34(8), pp. 1396-1412.

Gorin, K.V., Sergeeva, Y.E., Butylin, V.V., Komova, A.V., Pojidaev, V.M., Badranova, G.U., Shapovalova, A.A., Konova, I.A. and Gotovtsev, P.M., 2015. Methods coagulation/flocculation and flocculation with ballast agent for effective harvesting of microalgae. *Bioresource technology,* 193, pp. 178-184.

Greenwell, H., Laurens, L., Shields, R., Lovitt, R. and Flynn, K., 2009. Placing microalgae on the biofuels priority list: a review of the technological challenges. *Journal of the royal society interface,* 7(46), pp. 703-726.

Grima, E.M., Belarbi, E.-H., Fernández, F.A., Medina, A.R. and Chisti, Y., 2003. Recovery of microalgal biomass and metabolites: process options and economics. *Biotechnology advances,* 20(7-8), pp. 491-515.

Grima, E.M., González, M.J.I. and Giménez, A.G., 2013. Solvent extraction for microalgae lipids. *Algae for biofuels and energy.* Springer, pp. 187-205.

Grima, E.M., Pérez, J.S., Camacho, F.G., Sánchez, J.G., Fernández, F.A. and Alonso, D.L., 1994. Outdoor culture of Isochrysis galbana ALII-4 in a closed tubular photobioreactor. *Journal of biotechnology,* 37(2), pp. 159-166.

Gudin, C., Bernard, A., Chaumont, D., Thepenier, C. and Hardy, T., 1984. Direct bioconversion of solar energy into organic chemicals. *World Biotech Rep,* 1, pp. 541-559.

Guo, Z., Lue, B.-M., Thomasen, K., Meyer, A.S. and Xu, X., 2007. Predictions of flavonoid solubility in ionic liquids by COSMO-RS: experimental verification, structural elucidation, and solvation characterization. *Green Chemistry*, 9(12), pp. 1362-1373.

Hadjoudja, S., Deluchat, V. and Baudu, M., 2010. Cell surface characterisation of Microcystis aeruginosa and Chlorella vulgaris. *Journal of colloid and interface science*, 342(2), pp. 293-299.

Halim, R., Danquah, M.K. and Webley, P.A., 2012. Extraction of oil from microalgae for biodiesel production: a review. *Biotechnology advances*, 30(3), pp. 709-732.

Halim, R., Gladman, B., Danquah, M.K. and Webley, P.A., 2011. Oil extraction from microalgae for biodiesel production. *Bioresource technology*, 102(1), pp. 178-185.

Halim, R., Harun, R., Danquah, M.K. and Webley, P.A., 2012. Microalgal cell disruption for biofuel development. *Applied Energy*, 91(1), pp. 116-121.

Hammerschmidt, A., Boukis, N., Hauer, E., Galla, U., Dinjus, E., Hitzmann, B., Larsen, T. and Nygaard, S.D., 2011. Catalytic conversion of waste biomass by hydrothermal treatment. *Fuel*, 90(2), pp. 555-562.

Hanotu, J., Bandulasena, H. and Zimmerman, W.B., 2012. Microflotation performance for algal separation. *Biotechnology and bioengineering*, 109(7), pp. 1663-1673.

Hariani, P.L., Faizal, M. and Setiabudidaya, D., 2013. Synthesis and properties of Fe3O4 nanoparticles by co-precipitation method to removal procion dye. *International Journal of Environmental Science and Development*, 4(3), p. 336.

Harun, R., Singh, M., Forde, G.M. and Danquah, M.K., 2010. Bioprocess engineering of microalgae to produce a variety of consumer products. *Renewable and Sustainable Energy Reviews*, 14(3), pp. 1037-1047.

Heasman, M., Diemar, J., O'connor, W., Sushames, T. and Foulkes, L., 2000. Development of extended shelf-life microalgae concentrate diets harvested by centrifugation for bivalve molluscs–a summary. *Aquaculture Research*, 31(8-9), pp. 637-659.

Henderson, R., Parsons, S.A. and Jefferson, B., 2008. The impact of algal properties and pre-oxidation on solid–liquid separation of algae. *Water research*, 42(8), pp. 1827-1845.

Herrada, R., Pérez–Corona, M., Shrestha, R., Pamukcu, S. and Bustos, E., 2014. 3. Electrokinetic remediation of polluted soil using nano-materials: Nano-iron case. *Evaluation of Electrochemical Reactors as a New Way to Environmental Protection,* 41.

Hillman, J.R., 2010. Sustainable Energy–Without the Hot Air. By DJC MacKay. Cambridge: IUT (2009), pp. 366.£ 19.99. ISBN 978-0-9544529-3-3. *Experimental Agriculture,* 46(1), pp. 117-117.

Ho, S.-H., Chen, W.-M. and Chang, J.-S., 2010. Scenedesmus obliquus CNW-N as a potential candidate for CO 2 mitigation and biodiesel production. *Bioresource Technology,* 101(22), pp. 8725-8730.

Horiuchi, J.-I., Ohba, I., Tada, K., Kobayashi, M., Kanno, T. and Kishimoto, M., 2003. Effective cell harvesting of the halotolerant microalga Dunaliella tertiolecta with pH control. *Journal of bioscience and bioengineering,* 95(4), pp. 412-415.

Hu, Y.-R., Wang, F., Wang, S.-K., Liu, C.-Z. and Guo, C., 2013. Efficient harvesting of marine microalgae Nannochloropsis maritima using magnetic nanoparticles. *Bioresource technology,* 138, pp. 387-390.

Huber, G.W., Iborra, S. and Corma, A., 2006. Synthesis of transportation fuels from biomass: chemistry, catalysts, and engineering. *Chemical reviews,* 106(9), pp. 4044-4098.

Javadli, R. and De Klerk, A., 2012. Desulfurization of heavy oil. *Applied Petrochemical Research,* 1(1-4), pp. 3-19.

Jazrawi, C., Biller, P., Ross, A.B., Montoya, A., Maschmeyer, T. and Haynes, B.S., 2013. Pilot plant testing of continuous hydrothermal liquefaction of microalgae. *Algal Research,* 2(3), pp. 268-277.

Jena, U., Das, K. and Kastner, J., 2011. Effect of operating conditions of thermochemical liquefaction on biocrude production from Spirulina platensis. *Bioresource technology,* 102(10), pp. 6221-6229.

Jena, U. and Das, K.C., 2009. *Production of biocrude oil from microalgae via thermochemical liquefaction process.* American Society of Agricultural and Biological Engineers.

Jestin-Fleury, N., 1994. International Energy Agency. World Energy Outlook. *Politique étrangère,* 59(59), pp. 564-565.

Kandpal, N., Sah, N., Loshali, R., Joshi, R. and Prasad, J., 2014. Co-precipitation method of synthesis and characterization of iron oxide nanoparticles.

Kapoore, R., Butler, T., Pandhal, J. and Vaidyanathan, S., 2018. Microwave-assisted extraction for microalgae: from biofuels to biorefinery. *Biology,* 7(1), p. 18.

Kapoore, R.V., 2014. *Mass spectrometry based hyphenated techniques for microalgal and mammalian metabolomics.* University of Sheffield.

Kates, M., 1972. *Techniques of Lipidology: Isolation Analysis and Identification.* North-Holland.

Kaur, M., Jain, P. and Singh, M., 2015. Studies on structural and magnetic properties of ternary cobalt magnesium zinc (CMZ) Co 0.6-x Mg x Zn 0.4 Fe 2 O 4 (x= 0.0, 0.2, 0.4, 0.6) ferrite nanoparticles. *Materials Chemistry and Physics,* 162, pp. 332-339.

Kim, Y.-H., Choi, Y.-K., Park, J., Lee, S., Yang, Y.-H., Kim, H.J., Park, T.-J., Kim, Y.H. and Lee, S.H., 2012. Ionic liquid-mediated extraction of lipids from algal biomass. *Bioresource technology,* 109, pp. 312-315.

Kim, Y.-H., Park, S., Kim, M.H., Choi, Y.-K., Yang, Y.-H., Kim, H.J., Kim, H., Kim, H.-S., Song, K.-G. and Lee, S.H., 2013. Ultrasound-assisted extraction of lipids from Chlorella vulgaris using [Bmim][MeSO4]. *Biomass and bioenergy,* 56, pp. 99-103.

Lardon, L., Helias, A., Sialve, B., Steyer, J.-P. and Bernard, O., 2009. Life-cycle assessment of biodiesel production from microalgae. ACS Publications.

Laska, U., Frost, C.G., Price, G.J. and Plucinski, P.K., 2009. Easy-separable magnetic nanoparticle-supported Pd catalysts: Kinetics, stability and catalyst re-use. *Journal of Catalysis,* 268(2), pp. 318-328.

Lee, A., Lewis, D., Kalaitzidis, T. and Ashman, P., 2016. Technical issues in the large-scale hydrothermal liquefaction of microalgal biomass to biocrude. *Current opinion in biotechnology,* 38, pp. 85-89.

Lee, A.K., Lewis, D.M. and Ashman, P.J., 2012. Disruption of microalgal cells for the extraction of lipids for biofuels: processes and specific energy requirements. *Biomass and bioenergy,* 46, pp. 89-101.

Lee, J.-Y., Yoo, C., Jun, S.-Y., Ahn, C.-Y. and Oh, H.-M., 2010. Comparison of several methods for effective lipid extraction from microalgae. *Bioresource technology,* 101(1), pp. S75-S77.

Leung, D. and Guo, Y., 2006. Transesterification of neat and used frying oil: optimization for biodiesel production. *Fuel processing technology*, 87(10), pp. 883-890.

Leung, D.Y., Wu, X. and Leung, M., 2010. A review on biodiesel production using catalyzed transesterification. *Applied energy*, 87(4), pp. 1083-1095.

Li, H., Hu, J., Zhang, Z., Wang, H., Ping, F., Zheng, C., Zhang, H. and He, Q., 2014a. Insight into the effect of hydrogenation on efficiency of hydrothermal liquefaction and physico-chemical properties of biocrude oil. *Bioresource technology*, 163, pp. 143-151.

Li, H., Liu, Z., Zhang, Y., Li, B., Lu, H., Duan, N., Liu, M., Zhu, Z. and Si, B., 2014b. Conversion efficiency and oil quality of low-lipid high-protein and high-lipid low-protein microalgae via hydrothermal liquefaction. *Bioresource technology*, 154, pp. 322-329.

Li, Z., Ma, J., Ruan, J. and Zhuang, X., 2019. Using Positively Charged Magnetic Nanoparticles to Capture Bacteria at Ultralow Concentration. *Nanoscale research letters*, 14(1), p. 195.

Lim, J.K., Chieh, D.C.J., Jalak, S.A., Toh, P.Y., Yasin, N.H.M., Ng, B.W. and Ahmad, A.L., 2012. Rapid magnetophoretic separation of microalgae. *Small*, 8(11), pp. 1683-1692.

Los-Alamos, 2012. http://www.lanl.gov/about/awards-achievements/rd100/2012.

Lv, Z., Wang, Q., Bin, Y., Huang, L., Zhang, R., Zhang, P. and Matsuo, M., 2015. Magnetic Behaviors of Mg-and Zn-Doped Fe3O4 Nanoparticles Estimated in Terms of Crystal Domain Size, Dielectric Response, and Application of Fe3O4/Carbon Nanotube Composites to Anodes for Lithium Ion Batteries. *The Journal of Physical Chemistry C*, 119(46), pp. 26128-26142.

Lyon, J.L., Fleming, D.A., Stone, M.B., Schiffer, P. and Williams, M.E., 2004. Synthesis of Fe oxide core/Au shell nanoparticles by iterative hydroxylamine seeding. *Nano Letters*, 4(4), pp. 719-723.

Ma, F. and Hanna, M.A., 1999. Biodiesel production: a review. *Bioresource technology*, 70(1), pp. 1-15.

Maiella, P. and Brill, T., 1998. Spectroscopy of Hydrothermal Reactions. 10. Evidence of Wall Effects in Decarboxylation Kinetics of 1.00 m HCO2X (X= H, Na) at 280− 330 C and 275 bar. *The Journal of Physical Chemistry A*, 102(29), pp. 5886-5891.

Makishima, S., Mizuno, M., Sato, N., Shinji, K., Suzuki, M., Nozaki, K., Takahashi, F., Kanda, T. and Amano, Y., 2009. Development of continuous flow type hydrothermal reactor for hemicellulose fraction recovery from corncob. *Bioresource technology,* 100(11), pp. 2842-2848.

Masojídek, J., Sergejevová, M., Rottnerová, K., Jirka, V., Korečko, J., Kopecký, J., Zaťková, I., Torzillo, G. and Štys, D., 2009. A two-stage solar photobioreactor for cultivation of microalgae based on solar concentrators. *Journal of applied phycology,* 21(1), pp. 55-63.

Mata, T.M., Martins, A.A. and Caetano, N.S., 2010. Microalgae for biodiesel production and other applications: a review. *Renewable and sustainable energy reviews,* 14(1), pp. 217-232.

Matsui, T.-o., Nishihara, A., Ueda, C., Ohtsuki, M., Ikenaga, N.-o. and Suzuki, T., 1997. Liquefaction of micro-algae with iron catalyst. *Fuel,* 76(11), pp. 1043-1048.

Mazza, M., Catana, D.-A., Vaca-Garcia, C. and Cecutti, C., 2009. Influence of water on the dissolution of cellulose in selected ionic liquids. *Cellulose,* 16(2), pp. 207-215.

Medina, A.R., Grima, E.M., Giménez, A.G. and González, M.I., 1998. Downstream processing of algal polyunsaturated fatty acids. *Biotechnology advances,* 16(3), pp. 517-580.

Melo, A.F., Luz, R.A., Iost, R.M., Nantes, I.L. and Crespilho, F.N., 2013. Highly stable magnetite modified with chitosan, ferrocene and enzyme for application in magneto-switchable bioelectrocatalysis. *Journal of the Brazilian Chemical Society,* 24(2), pp. 285-294.

Miao, W. and Chan, T.H., 2006. Ionic-liquid-supported synthesis: a novel liquid-phase strategy for organic synthesis. *Accounts of chemical research,* 39(12), pp. 897-908.

Milledge, J.J. and Heaven, S., 2013. A review of the harvesting of micro-algae for biofuel production. *Reviews in Environmental Science and Bio/Technology,* 12(2), pp. 165-178.

Minowa, T. and Sawayama, S., 1999. A novel microalgal system for energy production with nitrogen cycling. *Fuel,* 78(10), pp. 1213-1215.

Minowa, T., Yokoyama, S.-y., Kishimoto, M. and Okakura, T., 1995. Oil production from algal cells of Dunaliella tertiolecta by direct thermochemical liquefaction. *Fuel,* 74(12), pp. 1735-1738.

Mollah, M.Y., Morkovsky, P., Gomes, J.A., Kesmez, M., Parga, J. and Cocke, D.L., 2004. Fundamentals, present and future perspectives of electrocoagulation. *Journal of hazardous materials,* 114(1-3), pp. 199-210.

Moomaw, W., Yamba, F., Kamimoto, M., Maurice, L., Nyboer, J., Urama, K. and Weir, T., 2011. IPCC special report on renewable energy sources and climate change mitigation. *Edenhofer, O., Pichs-Madruga, R., Sokona, Y., Seyboth, K., Matschoss, P., Kadner, S., Zwickel, T., Eickemeier, P., Hansen, G., Schlömer, S., von Stechow, C., Eds*.

Morais, M.G.d., Martins, V.G., Steffens, D., Pranke, P. and da Costa, J.A.V., 2014. Biological applications of nanobiotechnology. *Journal of nanoscience and nanotechnology,* 14(1), pp. 1007-1017.

Morita, M., Watanabe, Y. and Saiki, H., 2000. Investigation of photobioreactor design for enhancing the photosynthetic productivity of microalgae. *Biotechnology and bioengineering,* 69(6), pp. 693-698.

Neveux, N., Yuen, A., Jazrawi, C., Magnusson, M., Haynes, B., Masters, A., Montoya, A., Paul, N., Maschmeyer, T. and De Nys, R., 2014a. Biocrude yield and productivity from the hydrothermal liquefaction of marine and freshwater green macroalgae. *Bioresource technology,* 155, pp. 334-341.

Neveux, N., Yuen, A., Jazrawi, C., Magnusson, M., Haynes, B., Masters, A., Montoya, A., Paul, N.A., Maschmeyer, T. and De Nys, R., 2014b. Biocrude yield and productivity from the hydrothermal liquefaction of marine and freshwater green macroalgae. *Bioresource technology,* 155, pp. 334-341.

Norsker, N.-H., Barbosa, M.J., Vermuë, M.H. and Wijffels, R.H., 2011. Microalgal production—a close look at the economics. *Biotechnology advances,* 29(1), pp. 24-27.

Ocfemia, K., Zhang, Y. and Funk, T., 2006. Hydrothermal processing of swine manure into oil using a continuous reactor system: Development and testing. *Transactions of the ASABE,* 49(2), pp. 533-541.

Olivier-Bourbigou, H. and Magna, L., 2002. Ionic liquids: perspectives for organic and catalytic reactions. *Journal of Molecular Catalysis A: Chemical,* 182, pp. 419-437.

Olkiewicz, M., Caporgno, M.P., Font, J., Legrand, J., Lepine, O., Plechkova, N.V., Pruvost, J., Seddon, K.R. and Bengoa, C., 2015. A novel recovery process for lipids from microalgæ for biodiesel production using a hydrated phosphonium ionic liquid. *Green chemistry,* 17(5), pp. 2813-2824.

Orr, V.C., Plechkova, N.V., Seddon, K.R. and Rehmann, L., 2015. Disruption and wet extraction of the microalgae Chlorella vulgaris using room-temperature ionic liquids. *ACS Sustainable Chemistry & Engineering,* 4(2), pp. 591-600.

Papazi, A., Makridis, P. and Divanach, P., 2010. Harvesting Chlorella minutissima using cell coagulants. *Journal of Applied Phycology,* 22(3), pp. 349-355.

Parks, G.A., 1965. The isoelectric points of solid oxides, solid hydroxides, and aqueous hydroxo complex systems. *Chemical Reviews,* 65(2), pp. 177-198.

Patel, B. and Hellgardt, K., 2015. Hydrothermal upgrading of algae paste in a continuous flow reactor. *Bioresource technology,* 191, pp. 460-468.

Patel, B., Tamburic, B., Zemichael, F.W., Dechatiwongse, P. and Hellgardt, K., 2012. Algal biofuels: a credible prospective? *ISRN Renewable Energy*, 2012.

Patil, V., Tran, K.-Q. and Giselrød, H.R., 2008. Towards sustainable production of biofuels from microalgae. *International journal of molecular sciences,* 9(7), pp. 1188-1195.

Pei, Y., Wang, J., Wu, K., Xuan, X. and Lu, X., 2009. Ionic liquid-based aqueous two-phase extraction of selected proteins. *Separation and Purification Technology,* 64(3), pp. 288-295.

Peterson, A.A., Vogel, F., Lachance, R.P., Fröling, M., Antal Jr, M.J. and Tester, J.W., 2008. Thermochemical biofuel production in hydrothermal media: a review of sub-and supercritical water technologies. *Energy & Environmental Science,* 1(1), pp. 32-65.

Petrusevski, B., Bolier, G., Van Breemen, A. and Alaerts, G., 1995. Tangential flow filtration: a method to concentrate freshwater algae. *Water Research,* 29(5), pp. 1419-1424.

Pinkert, A., Marsh, K.N., Pang, S. and Staiger, M.P., 2009. Ionic liquids and their interaction with cellulose. *Chemical reviews,* 109(12), pp. 6712-6728.

Pinto, A.C., Guarieiro, L.L., Rezende, M.J., Ribeiro, N.M., Torres, E.A., Lopes, W.A., Pereira, P.A.d.P. and Andrade, J.B.d., 2005. Biodiesel: an overview. *Journal of the Brazilian Chemical Society*, 16(6B), pp. 1313-1330.

Pires, J., Alvim-Ferraz, M., Martins, F. and Simões, M., 2012. Carbon dioxide capture from flue gases using microalgae: engineering aspects and biorefinery concept. *Renewable and Sustainable Energy Reviews*, 16(5), pp. 3043-3053.

Pistorius, A.M., DeGrip, W.J. and Egorova-Zachernyuk, T.A., 2009. Monitoring of biomass composition from microbiological sources by means of FT-IR spectroscopy. *Biotechnology and bioengineering*, 103(1), pp. 123-129.

Plechkova, N.V. and Seddon, K.R., 2008. Applications of ionic liquids in the chemical industry. *Chemical Society Reviews*, 37(1), pp. 123-150.

Posten, C., 2009. Design principles of photo-bioreactors for cultivation of microalgae. *Engineering in Life Sciences*, 9(3), pp. 165-177.

Pragya, N. and Pandey, K.K., 2016. Life cycle assessment of green diesel production from microalgae. *Renewable energy*, 86, pp. 623-632.

Pragya, N., Pandey, K.K. and Sahoo, P., 2013. A review on harvesting, oil extraction and biofuels production technologies from microalgae. *Renewable and Sustainable Energy Reviews*, 24, pp. 159-171.

Prochazkova, G., Podolova, N., Safarik, I., Zachleder, V. and Branyik, T., 2013. Physicochemical approach to freshwater microalgae harvesting with magnetic particles. *Colloids and Surfaces B: Biointerfaces*, 112, pp. 213-218.

Prochazkova, G., Safarik, I. and Branyik, T., 2013. Harvesting microalgae with microwave synthesized magnetic microparticles. *Bioresource technology*, 130, pp. 472-477.

Pugazhendhi, A., Shobana, S., Bakonyi, P., Nemestóthy, N., Xia, A. and Kumar, G., 2019. A review on chemical mechanism of microalgae flocculation via polymers. *Biotechnology Reports*, p. e00302.

Raikova, S., Le, C., Wagner, J., Ting, V. and Chuck, C., 2016a. Towards an Aviation Fuel Through the Hydrothermal Liquefaction of Algae. *Biofuels for Aviation.* Elsevier, pp. 217-239.

Raikova, S., Smith-Baedorf, H., Bransgrove, R., Barlow, O., Santomauro, F., Wagner, J.L., Allen, M.J., Bryan, C.G., Sapsford, D. and Chuck, C.J., 2016b. Assessing hydrothermal liquefaction for the production of bio-oil and enhanced metal recovery from microalgae cultivated on acid mine drainage. *Fuel Processing Technology,* 142, pp. 219-227.

Ramirez, J., Brown, R. and Rainey, T., 2015. A review of hydrothermal liquefaction bio-crude properties and prospects for upgrading to transportation fuels. *Energies,* 8(7), pp. 6765-6794.

Rawat, I., Kumar, R.R., Mutanda, T. and Bux, F., 2011. Dual role of microalgae: phycoremediation of domestic wastewater and biomass production for sustainable biofuels production. *Applied energy,* 88(10), pp. 3411-3424.

Reddy, H.K., Muppaneni, T., Ponnusamy, S., Sudasinghe, N., Pegallapati, A., Selvaratnam, T., Seger, M., Dungan, B., Nirmalakhandan, N. and Schaub, T., 2016. Temperature effect on hydrothermal liquefaction of Nannochloropsis gaditana and Chlorella sp. *Applied Energy,* 165, pp. 943-951.

Reddy, H.K., Muppaneni, T., Sun, Y., Li, Y., Ponnusamy, S., Patil, P.D., Dailey, P., Schaub, T., Holguin, F.O. and Dungan, B., 2014. Subcritical water extraction of lipids from wet algae for biodiesel production. *Fuel*, 133, pp. 73-81.

Reitz, H.C., Ferrel, R.E., Fraenkel-Conrat, H. and Olcott, H.S., 1946. Action of sulfating agents on proteins and model substances. I. Concentrated sulfuric acid. *Journal of the American Chemical Society,* 68(6), pp. 1024-1031.

Remsing, R.C., Swatloski, R.P., Rogers, R.D. and Moyna, G., 2006. Mechanism of cellulose dissolution in the ionic liquid 1-n-butyl-3-methylimidazolium chloride: a 13 C and 35/37 Cl NMR relaxation study on model systems. *Chemical Communications,* (12), pp. 1271-1273.

Richmond, A., Boussiba, S., Vonshak, A. and Kopel, R., 1993. A new tubular reactor for mass production of microalgae outdoors. *Journal of Applied Phycology,* 5(3), pp. 327-332.

Robles-Medina, A., González-Moreno, P., Esteban-Cerdán, L. and Molina-Grima, E., 2009. Biocatalysis: towards ever greener biodiesel production. *Biotechnology advances,* 27(4), pp. 398-408.

Rojas-Pérez, A., Diaz-Diestra, D., Frias-Flores, C.B., Beltran-Huarac, J., Das, K., Weiner, B.R., Morell, G. and Díaz-Vázquez, L.M., 2015. Catalytic effect of ultrananocrystalline Fe 3 O 4 on algal bio-crude production via HTL process. *Nanoscale*, 7(42), pp. 17664-17671.

Ross, A., Biller, P., Kubacki, M., Li, H., Lea-Langton, A. and Jones, J., 2010. Hydrothermal processing of microalgae using alkali and organic acids. *Fuel*, 89(9), pp. 2234-2243.

Rubio, J., Souza, M. and Smith, R., 2002. Overview of flotation as a wastewater treatment technique. *Minerals engineering*, 15(3), pp. 139-155.

Safari, J. and Zarnegar, Z., 2013. Immobilized ionic liquid on superparamagnetic nanoparticles as an effective catalyst for the synthesis of tetrasubstituted imidazoles under solvent-free conditions and microwave irradiation. *Comptes Rendus Chimie*, 16(10), pp. 920-928.

Safarik, I., Prochazkova, G., Pospiskova, K. and Branyik, T., 2015. Magnetically modified microalgae and their applications. *Critical reviews in biotechnology*, pp. 1-11.

Safarik, I., Prochazkova, G., Pospiskova, K. and Branyik, T., 2016. Magnetically modified microalgae and their applications. *Critical reviews in biotechnology*, 36(5), pp. 931-941.

Safarik, I., Sabatkova, Z. and Safarikova, M., 2008. Hydrogen peroxide removal with magnetically responsive Saccharomyces cerevisiae cells. *Journal of agricultural and food chemistry*, 56(17), pp. 7925-7928.

Salunkhe, A., Khot, V., Ruso, J. and Patil, S., 2015. Synthesis and magnetostructural studies of amine functionalized superparamagnetic iron oxide nanoparticles. *RSC Advances*, 5(24), pp. 18420-18428.

Sander, K. and Murthy, G.S., 2010. Life cycle analysis of algae biodiesel. *The International Journal of Life Cycle Assessment*, 15(7), pp. 704-714.

Santos, M., Seabra, A., Pelegrino, M. and Haddad, P., 2016. Synthesis, characterization and cytotoxicity of glutathione-and PEG-glutathione-superparamagnetic iron oxide nanoparticles for nitric oxide delivery. *Applied Surface Science*, 367, pp. 26-35.

Sarpal, A., Costa, I., Teixeira, C., Filocomo, D. and Candido, R., 2016. Investigation of Biodiesel Potential of Biomasses of Microalgaes Chlorella, Spirulina and Tetraselmis by NMR and GC-MS Techniques. *J Biotechnol Biomater,* 6(220), p. 2.

Schenk, P.M., Thomas-Hall, S.R., Stephens, E., Marx, U.C., Mussgnug, J.H., Posten, C., Kruse, O. and Hankamer, B., 2008. Second generation biofuels: high-efficiency microalgae for biodiesel production. *Bioenergy research,* 1(1), pp. 20-43.

Schuchardt, U., Sercheli, R. and Vargas, R.M., 1998. Transesterification of vegetable oils: a review. *Journal of the Brazilian Chemical Society,* 9(3), pp. 199-210.

Semerjian, L. and Ayoub, G., 2003. High-pH–magnesium coagulation–flocculation in wastewater treatment. *Advances in Environmental Research,* 7(2), pp. 389-403.

Shakya, R., Whelen, J., Adhikari, S., Mahadevan, R. and Neupane, S., 2015. Effect of temperature and Na 2 CO 3 catalyst on hydrothermal liquefaction of algae. *Algal Research,* 12, pp. 80-90.

Shankar, M., Chhotaray, P.K., Agrawal, A., Gardas, R.L., Tamilarasan, K. and Rajesh, M., 2017. Protic ionic liquid-assisted cell disruption and lipid extraction from fresh water Chlorella and Chlorococcum microalgae. *Algal Research,* 25, pp. 228-236.

Shelef, G., Sukenik, A. and Green, M., 1984. *Microalgae harvesting and processing: a literature review.*

Shi, W., Zhu, L., Chen, Q., Lu, J., Pan, G., Hu, L. and Yi, Q., 2017. Synergy of flocculation and flotation for microalgae harvesting using aluminium electrolysis. *Bioresource technology,* 233, pp. 127-133.

Show, K.-Y. and Lee, D.-J., 2013. *Biofuels from Algae: Chapter 9. Production of Biohydrogen from Microalgae.* Elsevier Inc. Chapters.

Singh, J. and Gu, S., 2010. Commercialization potential of microalgae for biofuels production. *Renewable and Sustainable Energy Reviews,* 14(9), pp. 2596-2610.

Singh, R., Bhaskar, T. and Balagurumurthy, B., 2015. Effect of solvent on the hydrothermal liquefaction of macro algae Ulva fasciata. *Process Safety and Environmental Protection,* 93, pp. 154-160.

Solomon, S., Qin, D., Manning, M., Averyt, K. and Marquis, M., 2007. *Climate change 2007-the physical science basis: Working group I contribution to the fourth assessment report of the IPCC.* Cambridge university press.

Soxhlet, F.v., 1879. Die gewichtsanalytische bestimmung des milchfettes. *Polytechnisches J,* 232, pp. 461-465.

Speight, J.G., 2015. *Fouling in refineries.* Gulf Professional Publishing.

Srokol, Z., Bouche, A.-G., van Estrik, A., Strik, R.C., Maschmeyer, T. and Peters, J.A., 2004. Hydrothermal upgrading of biomass to biofuel; studies on some monosaccharide model compounds. *Carbohydrate Research,* 339(10), pp. 1717-1726.

Sukenik, A. and Shelef, G., 1984. Algal autoflocculation—verification and proposed mechanism. *Biotechnology and bioengineering,* 26(2), pp. 142-147.

Swiderski, K., McLean, A., Gordon, C.M. and Vaughan, D.H., 2004. Estimates of internal energies of vaporisation of some room temperature ionic liquids. *Chemical Communications,* (19), pp. 2178-2179.

Tadesse, H. and Luque, R., 2011. Advances on biomass pretreatment using ionic liquids: an overview. *Energy & Environmental Science,* 4(10), pp. 3913-3929.

Tang, M., 2014. *Identifying opportunities to cultivate algae combined with wastewater recycling as a source of renewable energy in Southeast Asia.* Murdoch University.

Teixeira, R.E., 2012. Energy-efficient extraction of fuel and chemical feedstocks from algae. *Green chemistry,* 14(2), pp. 419-427.

Terry, K.L. and Raymond, L.P., 1985. System design for the autotrophic production of microalgae. *Enzyme and Microbial Technology,* 7(10), pp. 474-487.

Toh, P.Y., Ng, B.W., Ahmad, A.L., Chieh, D.C.J. and Lim, J., 2014a. Magnetophoretic separation of Chlorella sp.: role of cationic polymer binder. *Process Safety and Environmental Protection,* 92(6), pp. 515-521.

Toh, P.Y., Ng, B.W., Chong, C.H., Ahmad, A.L., Yang, J.-W., Derek, C.J.C. and Lim, J., 2014b. Magnetophoretic separation of microalgae: the role of nanoparticles and polymer binder in harvesting biofuel. *RSC Advances,* 4(8), pp. 4114-4121.

Toor, S.S., Rosendahl, L. and Rudolf, A., 2011. Hydrothermal liquefaction of biomass: a review of subcritical water technologies. *Energy,* 36(5), pp. 2328-2342.

Torri, C., Garcia Alba, L., Samori, C., Fabbri, D. and Brilman, D.W., 2012. Hydrothermal treatment (HTT) of microalgae: detailed molecular characterization of HTT oil in view of HTT mechanism elucidation. *Energy & Fuels,* 26(1), pp. 658-671.

Torzillo, G., Pushparaj, B., Bocci, F., Balloni, W., Materassi, R. and Florenzano, G., 1986. Production of Spirulina biomass in closed photobioreactors. *Biomass,* 11(1), pp. 61-74.

Tredici, M.R. and Zittelli, G.C., 1998. Efficiency of sunlight utilization: tubular versus flat photobioreactors. *Biotechnology and bioengineering,* 57(2), pp. 187-197.

Uduman, N., Qi, Y., Danquah, M.K., Forde, G.M. and Hoadley, A., 2010. Dewatering of microalgal cultures: a major bottleneck to algae-based fuels. *Journal of renewable and sustainable energy,* 2(1), p. 012701.

Ugwu, C., Aoyagi, H. and Uchiyama, H., 2008. Photobioreactors for mass cultivation of algae. *Bioresource technology,* 99(10), pp. 4021-4028.

Umdu, E.S., Tuncer, M. and Seker, E., 2009. Transesterification of Nannochloropsis oculata microalga's lipid to biodiesel on Al2O3 supported CaO and MgO catalysts. *Bioresource Technology,* 100(11), pp. 2828-2831.

Valdez, P.J., Dickinson, J.G. and Savage, P.E., 2011. Characterization of product fractions from hydrothermal liquefaction of Nannochloropsis sp. and the influence of solvents. *Energy & Fuels,* 25(7), pp. 3235-3243.

Valdez, P.J., Nelson, M.C., Wang, H.Y., Lin, X.N. and Savage, P.E., 2012. Hydrothermal liquefaction of Nannochloropsis sp.: Systematic study of process variables and analysis of the product fractions. *biomass and bioenergy,* 46, pp. 317-331.

Van Gerpen, J. and Dvorak, B., 2002. The effect of phosphorus level on the total glycerol and reaction yield of biodiesel, Bioenergy 2002. *The 10th Biennial Bioenergy Conference, Boise, ID*.

Vandamme, D., Foubert, I., Fraeye, I., Meesschaert, B. and Muylaert, K., 2012. Flocculation of Chlorella vulgaris induced by high pH: role of magnesium and calcium and practical implications. *Bioresource technology,* 105, pp. 114-119.

Vandamme, D., Foubert, I. and Muylaert, K., 2013. Flocculation as a low-cost method for harvesting microalgae for bulk biomass production. *Trends in biotechnology,* 31(4), pp. 233-239.

Vidal-Vidal, J., Rivas, J. and López-Quintela, M., 2006. Synthesis of monodisperse maghemite nanoparticles by the microemulsion method. *Colloids and Surfaces A: Physicochemical and Engineering Aspects,* 288(1-3), pp. 44-51.

Wagner, J., 2016. *Sustainable Biofuel Production via the Hydrothermal Liquefaction of Microalgae and*

Subsequent Bio-Oil Upgrading. (PhD), University of Bath. Available from: *https://bath-ac-primo.hosted.exlibrisgroup.com/primo-explore/fulldisplay?docid=44BAT_ALMA_DS2148235360002761&context=L&vid=44BAT_VU1&lang=en_US&search_scope=CSCOP_44BAT_DEEP&adaptor=Local%20Search%20Engine&tab=local&query=any,contains,Sustainable%20Biofuel%20Production%20via%20the%20Hydrothermal%20Liquefaction%20of%20Microalgae%20and&sortby=rank&pcAvailability=false*.

Wang, S.-K., Stiles, A.R., Guo, C. and Liu, C.-Z., 2015. Harvesting microalgae by magnetic separation: a review. *Algal Research*, 9, pp. 178-185.

Wang, S.-K., Wang, F., Hu, Y.-R., Stiles, A.R., Guo, C. and Liu, C.-Z., 2013. Magnetic flocculant for high efficiency harvesting of microalgal cells. *ACS applied materials & interfaces*, 6(1), pp. 109-115.

Watanabe, M., Iida, T. and Inomata, H., 2006. Decomposition of a long chain saturated fatty acid with some additives in hot compressed water. *Energy Conversion and Management*, 47(18–19), pp. 3344-3350.

Weerachanchai, P., Chen, Z., Leong, S.S.J., Chang, M.W. and Lee, J.-M., 2012. Hildebrand solubility parameters of ionic liquids: Effects of ionic liquid type, temperature and DMA fraction in ionic liquid. *Chemical engineering journal*, 213, pp. 356-362.

Wishart, J.F., 2009. Energy applications of ionic liquids. *Energy & Environmental Science*, 2(9), pp. 956-961.

Xu, D. and Savage, P.E., 2015. Effect of reaction time and algae loading on water-soluble and insoluble biocrude fractions from hydrothermal liquefaction of algae. *Algal Research*, 12, pp. 60-67.

Xu, L., Brilman, D.W.W., Withag, J.A., Brem, G. and Kersten, S., 2011a. Assessment of a dry and a wet route for the production of biofuels from microalgae: energy balance analysis. *Bioresource technology*, 102(8), pp. 5113-5122.

Xu, L., Guo, C., Wang, F., Zheng, S. and Liu, C.-Z., 2011b. A simple and rapid harvesting method for microalgae by in situ magnetic separation. *Bioresource technology,* 102(21), pp. 10047-10051.
Xu, Y., Fu, Y. and Zhang, D., 2017. Cost-effectiveness Analysis on Magnetic Harvesting of Algal Cells. *Materials Today: Proceedings,* 4(1), pp. 50-56.
Yadidia, R., Abeliovich, A. and Belfort, G., 1977. Algae removal by high gradient magnetic filtration. *Environmental Science & Technology,* 11(9), pp. 913-916.
Yang, Y., Feng, C., Inamori, Y. and Maekawa, T., 2004. Analysis of energy conversion characteristics in liquefaction of algae. *Resources, Conservation and Recycling,* 43(1), pp. 21-33.
Yavuz, C.T., Prakash, A., Mayo, J. and Colvin, V.L., 2009. Magnetic separations: from steel plants to biotechnology. *Chemical Engineering Science,* 64(10), pp. 2510-2521.
Yoo, B., Jing, B., Jones, S.E., Lamberti, G.A., Zhu, Y., Shah, J.K. and Maginn, E.J., 2016. Molecular mechanisms of ionic liquid cytotoxicity probed by an integrated experimental and computational approach. *Scientific reports,* 6, p. 19889.
Yoo, G., Park, W.-K., Kim, C.W., Choi, Y.-E. and Yang, J.-W., 2012. Direct lipid extraction from wet Chlamydomonas reinhardtii biomass using osmotic shock. *Bioresource technology,* 123, pp. 717-722.
Yoon, R. and Luttrell, G., 1989. The effect of bubble size on fine particle flotation. *Mineral Procesing and Extractive Metallurgy Review,* 5(1-4), pp. 101-122.
Young, G., Nippgen, F., Titterbrandt, S. and Cooney, M.J., 2010. Lipid extraction from biomass using co-solvent mixtures of ionic liquids and polar covalent molecules. *Separation and Purification Technology,* 72(1), pp. 118-121.
Yu, G., Zhang, Y., Schideman, L., Funk, T. and Wang, Z., 2011. Hydrothermal liquefaction of low lipid content microalgae into bio-crude oil. *Transactions of the ASABE,* 54(1), pp. 239-246.
Yu, J., Biller, P., Mamahkel, A., Klemmer, M., Becker, J., Glasius, M. and Iversen, B.B., 2017. Catalytic hydrotreatment of bio-crude produced from the hydrothermal liquefaction of aspen wood: a catalyst screening and parameter optimization study. *Sustainable Energy & Fuels,* 1(4), pp. 832-841.

Zavrel, M., Bross, D., Funke, M., Büchs, J. and Spiess, A.C., 2009. High-throughput screening for ionic liquids dissolving (ligno-) cellulose. *Bioresource technology,* 100(9), pp. 2580-2587.

Zenouzi, A., Ghobadian, B., Hejazi, M. and Rahnemoon, P., 2013. Harvesting of microalgae Dunaliella salina using electroflocculation. *Journal of Agricultural Science and Technology,* 15(5), pp. 879-887.

Zhang, X., Amendola, P., Hewson, J.C., Sommerfeld, M. and Hu, Q., 2012. Influence of growth phase on harvesting of Chlorella zofingiensis by dissolved air flotation. *Bioresource technology,* 116, pp. 477-484.

Zhang, Y., Dube, M., McLean, D. and Kates, M., 2003. Biodiesel production from waste cooking oil: 2. Economic assessment and sensitivity analysis. *Bioresource technology,* 90(3), pp. 229-240.

Zhao, D., Wu, M., Kou, Y. and Min, E., 2002. Ionic liquids: applications in catalysis. *Catalysis today,* 74(1-2), pp. 157-189.

Zhou, D., Zhang, L., Zhang, S., Fu, H. and Chen, J., 2010. Hydrothermal liquefaction of macroalgae Enteromorpha prolifera to bio-oil. *Energy & Fuels,* 24(7), pp. 4054-4061.

Zhou, W., Min, M., Hu, B., Ma, X., Liu, Y., Wang, Q., Shi, J., Chen, P. and Ruan, R., 2013. Filamentous fungi assisted bio-flocculation: a novel alternative technique for harvesting heterotrophic and autotrophic microalgal cells. *Separation and Purification Technology,* 107, pp. 158-165.

Zou, S., Wu, Y., Yang, M., Li, C. and Tong, J., 2009. Thermochemical catalytic liquefaction of the marine microalgae Dunaliella tertiolecta and characterization of bio-oils. *Energy & Fuels,* 23(7), pp. 3753-3758.

Zou, S., Wu, Y., Yang, M., Li, C. and Tong, J., 2010. Bio-oil production from sub-and supercritical water liquefaction of microalgae Dunaliella tertiolecta and related properties. *Energy & Environmental Science,* 3(8), pp. 1073-1078.

Appendix

Complete website references

Since the endnote software omitted the website addresses in the main reference section, these have been included below:

1. Website for open algae open pond photo www.synbiowatch.org/2017/05/biofuelwatch-responds-to-first-open-pond-testing-of-gmo-microalgae.

2. Website for the screening image https://www.waterra.com.au/cyanobacteria-manual/Chapter5.htm. Accessed on 05/12/2018.

3. Website for the centrifuge image www.flottweg.com/application. Accessed on 10/01/2018.

4. The Los Alamos website http://www.lanl.gov/about/awards-achievements/rd100/2012.php accessed October 25, 2017.